DISCHARGE MEASUREMENT IN TERMS OF PRESSURE DIFFERENCES AT BRIDGE PIERS

C Meyer • A Rooseboom • MJ Retief • GC Cloete

WRC Report No 980/3/00

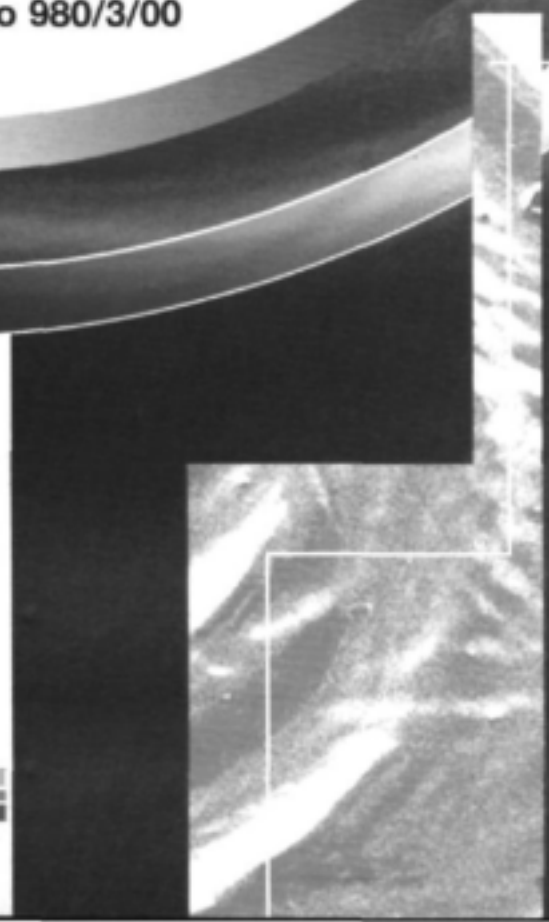

Water Research Commission

DISCHARGE MEASUREMENT IN TERMS OF PRESSURE DIFFERENCES AT BRIDGE PIERS

by

C Meyer, A Rooseboom, M J Retief & G C Cloete

SIGMA BETA
CONSULTING CIVIL ENGINEERS

WRC Report No. 980/3/00
ISBN: 1 86845 665 X

February 2002

PREFACE

This report is one of five which were produced under Water Research Commission contract No. 980, and which are listed below.

The first three reports contain results which may be regarded as conclusive, whilst the last two contain the results of exploratory research which may serve as the basis of further research.

WRC Report No. 980/1/00

The rating of compound sharp-crested weirs under modular and non-modular flow conditions.

WRC Report No. 980/2/00

The rating of sluicing flumes in combination with sharp-crested and Crump weirs under modular and non-modular flow conditions.

WRC Report No. 980/3/00

Discharge measurements in terms of pressure differences at bridge piers.

WRC Report No. 980/4/00

Flow gauging in rivers by means of natural controls.

WRC Report No. 980/5/00

The application of Doppler velocity meters in the measurement of open channel discharges.

EXECUTIVE SUMMARY:

This study entailed the successful investigation and evaluation of a new methodology for measuring high discharges passing through bridges. Pressure differences generated around bridge piers have been measured and related to discharges. These pressure differences are mainly functions of downstream flow conditions. The pressure differences have been converted into velocities by applying Newton's second law expressed in terms of the laws of conservation of energy, momentum, and of power.

The energy principle was re-evaluated following a previous study (*Retief* 1998) on a limited number of model pier combinations and flow conditions. Comparison of the energy approach with newly developed theories in terms of the momentum and power laws respectively led to the conclusion that the energy principle gave the best results. The question of applicability of the theory to different practical pier/stream width and length ratios as well as its validity under flow conditions commonly found under flood conditions required that additional laboratory tests be done.

The energy-based discharge equation was calibrated in terms of newly selected measuring points, different pier width and length ratios, as well as pier rotations for both super and sub-critical downstream conditions. According to the new tests performed at the Hydraulics Laboratory of the University of Stellenbosch on model piers, clear relationships were found between discharges and pressure differences measured *against* the pier. Calibration curves for practical flow measurement application were derived in terms of principal dimensionless parameters.

Following on the very positive results which were obtained in the laboratory, tests were also performed on a real bridge. Even though conditions at this bridge (across the Breede River) were far from ideal, very encouraging results were obtained. This methodology therefore holds much promise for application in practice.

ACKNOWLEDGEMENTS

The authors wish to thank the following members of the Steering Committee for their appreciated contributions to the project.

Mr. D S van der Merwe (Chairman)

Mr. H Maaren

Prof G R Basson

Prof A H M Görgens

Mr F P le Roux

Dr J Rossouw

Prof G G S Pegram

Dr M J Shand

Mr S van Biljon

Mr J van Heerden

Dr P Wessels

Mr O C E Hempel

Ms S Matthews

Ms U Wium

A special word of thanks is due to the Department of Water Affairs for their support and advice, particularly through the stimulating involvement of Dr P Wessels, as well as their inputs into the field tests.

Messrs M J Retief and G C Cloete made very important contributions to this study as undergraduate thesis students. Thanks are also due to the personnel in the workshops and Hydraulics Laboratory of the Civil Engineering Department at the University of Stellenbosch who assisted with implementing a successful test programme.

CONTENTS:

		Page number:
Preface		i
Executive Summary		ii
Acknowledgements		iii
List of contents		iv
List of figures		viii
List of tables		xii
List of photos		xiii
List of symbols		xvii
1.	Introduction	1
2.	Background	4
2.1	South African rivers	4
2.2	Occurrence and management of floods in South Africa	6
2.3	Criteria for new measuring techniques for South African conditions	11
3.	Flow measuring theory	12
3.1	Approach followed	12
3.2	Description of Retief Model	13
3.3	Introduction to flow measurement	16
3.4	Fundamental concepts related to flow measurement	17
	Newton's second law and the Law of Conservation of Mass	17
	Choice of control volumes in the analysis of pier flow	19
3.5	Continuity	20
	Derivation	20
	Application of the continuity equation	22
	Defining the geometry of a typical bridge pier	22
3.6	Energy Approach	23
	Derivation	23
	Water surface level differences at bridges in terms of the energy equation	27
	Energy transformation at a bridge pier	31

Conventional applications of the Energy equation for flow measurement: D'Aubuisson, Nagler and the "Bridge damming formula" 33
Application of the Energy equation in terms of measured pressures and water depths at bridge piers 41
Introduction, the Pitôt-tube theory 41
Theory 46
Results 48
3.7 Momentum Approach 49
Derivation 49
An overview of drag forces 52
Forces acting on bridge piers 56
Conventional applications of the Momentum equation with respect to flow measurement 57
Application of the Momentum principle in terms of measured pressures and water depths at bridge piers 59
Introduction 59
Theory 59
Results 61
3.8 Power Approach 63
Derivation 63
Application of the Power equation in terms of measured pressures and water depths at bridge piers 66
Introduction 66
Derivation 67
Power approach, another perspective 72
Establishing the relevant velocity associated with the pier drag force 75
Calibration of the "general flow rate equation" (power based) in terms of appropriate control volumes 80
Results 84
3.9 Summary of theories and results 85
3.10 Results in graph form, discussion 87

Energy 88
Power 92
Momentum 96

3.11 Conclusions and recommendations 100

4. Model tests and results 102

4.1 Model analysis and similarity study 102

4.2 Model tests in the laboratory 110

4.2.1 Introduction 110

4.2.2 Description of the laboratory lay-out used for the tests 112

4.2.3 Defining the configuration of the model piers and the arrangement of pressure measurement. 115

4.2.4 Defining the different flow conditions 120

4.2.5 Model tests on flow patterns around piers, pictorial record. 123

4.2.5.1 Parallel flow approaching pier 123

4.2.5.2 Non-parallel flow approaching pier 136

4.2.6 Defining the energy based discharge equation in terms of the new system of pressure measurements 139

4.2.7 Calibration of the energy based discharge equation (*equation 4.4*) for the different flows considered, *paragraph 4.2.4*. 143

4.2.7.1 Parallel approaching flow direction 144

4.2.7.2 Non-parallel approaching flow direction 146

4.3 Results in graph form and Conclusions 148

4.3.1 Parallel approaching flow direction 149

Conclusions and recommendations 165

4.3.2 Non-parallel approaching flow direction 167

Conclusions and recommendations 179

5. Overall conclusions and recommendations 181

6. References 182

Appendix A – Laboratory Results and coefficients – *Retief* data:
Energy Approach A.1–A.2
Momentum Approach A.1–A.2
Power Approach A.1–A.4

Appendix B - Energy Approach, Laboratory Data and calibrated coefficients - additional test:
32mm Short B.1 - B.3

32mm Medium	B.1 - B.3
32mm Long	B.1 - B.3
40mm Short	B.1 – B.3
40mm Medium	B.1 – B.3
40mm Long	B.1 – B.3
49mm Short	B.1 – B.3
49mm Medium	B.1 – B.3
49mm Long	B.1 – B.3
62mm Short	B.1 – B.3
62mm Medium	B.1 – B.3
62mm Long	B.1 – B.3
32mm Short 5 Deg.	B.1 – B.3
32mm Short 10 Deg.	B.1 – B.3
32mm Short 15 Deg.	B.1 – B.3
32mm Medium 5 Deg.	B.1 – B.3
32mm Medium 10 Deg	B.1 – B.3
32mm Medium 15 Deg	B.1 – B.3
32mm Long 5 Deg	B.1 - B.3
32mm Long 10 Deg.	B.1 – B.3
32mm Long 15 Deg.	B.1 – B.3

Appendix C - Field Tests C.1 - C.5

FIGURE:	*DESCRIPTION:*
Figure 3.1	Schematic side view of model pier set-up in the Hydraulics Laboratory, University of Stellenbosch
Figure 3.2	Schematic plan view of model pier set-up in the Hydraulics Laboratory, University of Stellenbosch
Figure 3.3	The three basic hydraulic laws, Continuity, Energy and Momentum
Figure 3.4	An extension on the three basic hydraulic laws, Power being added
Figure 3.5	Describing and defining the plan view of a typical pier lay-out
Figure 3.6	Typical open channel flow profile, taken between section 1 and section 2
Figure 3.7	Typical relationship between the flow depth and the specific energy for a rectangular section
Figure 3.8	Typical pier lay-out, the flow is approaching from the left
Figure 3.9	Flow depths vs. specific energy for two rectangular sections with widths B and b respectively
Figure 3.10	Theoretical potential and kinetic energy values upstream and within the contraction before damming takes place
Figure 3.11	Potential and kinetic energy values upstream and within the contraction with damming
Figure 3.12	Longitudinal section of a bridge pier under high discharges
Figure 3.13	Plan view of a typical pier lay-out
Figure 3.14	Measuring water surface level differences between upstream and downstream of a bridge
Figure 3.15	Water surface level differences between upstream and downstream of a bridge pier
Figure 3.16	A typical Pitôt-tube for measuring stream velocity; p_0 = dynamic or stagnation pressure, p_s = hydrostatic pressure, $h = p_0-p_s$ (*White*, 1986)

Figure 3.17 Typical flow lines around a bridge pier, p_0 = dynamic or stagnation pressure, p_s = hydrostatic pressure

Figure 3.18 The same flow set-up as shown in *figure 3.15*, pressure and pressure differences in terms of manometer levels and manometer level differences

Figure 3.19 A small particle with mass **dm** forms part of a fluid mass flowing from **section 1** to **section 2**

Figure 3.20 Flow lines around a bridge pier for the case of an ideal fluid

Figure 3.21 Flow lines around a bridge pier for the case of turbulent flow of a non-ideal fluid

Figure 3.22 Elemental forces acting on area **dA** of a typical pier; **p.dA** forms an angle of θ with the flow direction and τ.**dA** an angle of **(90-θ)**

Figure 3.23 A control volume for the application of the momentum equation; section A being the **inflow** section and section B the **outflow** section

Figure 3.24 Longitudinal flow section taken at a bridge pier; v = flow velocity, F = pier drag force, Δh = water level difference and L = length of the pier

Figure 3.25 Typical longitudinal flow pattern at a bridge pier, water flowing from left to right

Figure 3.26 Moving a boat through a fluid mass towards the left hand side in the sketch

Figure 3.27 Longitudinal section of pier for normal flow conditions

Figure 3.28 Longitudinal section of an idealised boat [having the same dimensions as the bridge pier] being dragged through a stationary mass of water; the pier moves to the left and water therefore flows to the right in the sketch

Figure 3.29 Defining the boundary lines of control volume ❶

Figure 3.30 Defining the boundary lines of control volume ❷

Figure 3.31 C_d-calibration curves , ENERGY approach

Figure 3.32 C_d-calibration curves, POWER approach

Figure 3.33 C_d-calibration curves, MOMENTUM approach

Figure 4.1 Typical flow element shown in three dimensions, x, y & z

Figure 4.2 Defining the sections for the new configuration of pressure measurements

Figure 4.3 Detail of pressure measurement positions at **A** and **B** at the upstream pier end (downstream lay-out similar)

Figure 4.4 Typical flow lines around the upstream end of a bridge pier, a convergence takes place when the width of flow changes from **B** to **(B-b_p)** where **b_p** depicts the pier width

Figure 4.5 Typical flow lines past a converging transition channel when the width of flow changes from **B** to **(B-b_p)** where **(B-b_p)** depicts the contracted width (analogous to flow entering between piers

Figure 4.6 C_d ; y_{UE}/y_{DS} ; Fr_{DS} – CALIBRATED COEFFICIENTS FOR B/b_p = 19 (32 mm), L/b_p = 6.9 (LONG)

Figure 4.7 C_d ; y_{UE}/y_{DS} ; Fr_{DS} – CALIBRATED COEFFICIENTS FOR B/b_p = 19 (32 mm), L/b_p = 5.6 (MEDIUM)

Figure 4.8 C_d ; y_{UE}/y_{DS} ; Fr_{DS} – CALIBRATED COEFFICIENTS FOR B/b_p = 19 (32 mm), L/b_p = 4.2 (SHORT)

Figure 4.9 C_d ; y_{UE}/y_{DS} ; Fr_{DS} – CALIBRATED COEFFICIENTS FOR B/b_p = 15.2 (40 mm), L/b_p = 6.9 (LONG)

Figure 4.10 C_d ; y_{UE}/y_{DS} ; Fr_{DS} – CALIBRATED COEFFICIENTS FOR B/b_p = 15.2 (40 mm), L/b_p = 5.6 (MEDIUM)

Figure 4.11 C_d ; y_{UE}/y_{DS} ; Fr_{DS} – CALIBRATED COEFFICIENTS FOR B/b_p = 15.2 (40 mm), L/b_p = 4.2 (SHORT)

Figure 4.12 C_d ; y_{UE}/y_{DS} ; Fr_{DS} – CALIBRATED COEFFICIENTS FOR B/b_p = 12.4 (49 mm), L/b_p = 6.9 (LONG)

Figure 4.13 C_d ; y_{UE}/y_{DS} ; Fr_{DS} – CALIBRATED COEFFICIENTS FOR B/b_p = 12.4 (49 mm), L/b_p = 5.6 (MEDIUM)

Figure 4.14 C_d ; y_{UE}/y_{DS} ; Fr_{DS} – CALIBRATED COEFFICIENTS FOR B/b_p = 12.4 (49 mm), L/b_p = 4.2 (SHORT)

Figure 4.15 C_d ; y_{UE}/y_{DS} ; Fr_{DS} – CALIBRATED COEFFICIENTS FOR B/b_p = 9.7 (62.5 mm), L/b_p = 6.9 (LONG)

Figure 4.16 C_d ; y_{UE}/y_{DS} ; Fr_{DS} – CALIBRATED COEFFICIENTS FOR B/b_p = 9.7 (62.5 mm), L/b_p = 5.6 (MEDIUM)

Figure 4.17 C_d ; y_{UE}/y_{DS} ; Fr_{DS} – CALIBRATED COEFFICIENTS FOR B/b_p = 9.7 (62.5 mm), L/b_p = 4.2 (SHORT)

Figure 4.18 C_d ; y_{UE}/y_{DS} ; Fr_{DS} – CALIBRATION CURVES ALL B/b_p and L/b_p combinations

Figure 4.19 C_d ; y_{UE}/y_{DS} ; Fr_{DS} – CALIBRATION CURVES ALL B/b_p and L/b_p combinations

Figure 4.20 C_d ; y_{UE}/y_{DS} ; Fr_{DS} – CALIBRATION CURVES FOR L/b_p = 6.9 (LONG), θ = 5 °, B/b_{p_eff} = 12.4

Figure 4.21 C_d ; y_{UE}/y_{DS} ; Fr_{DS} – CALIBRATION CURVES FOR L/b_p = 6.9 (LONG), θ = 10 °, B/b_{p_eff} = 9.4

Figure 4.22 C_d ; y_{UE}/y_{DS} ; Fr_{DS} – CALIBRATION CURVES FOR L/b_p = 6.9 (LONG), θ = 15 °, B/b_{p_eff} = 7.5

Figure 4.23 C_d ; y_{UE}/y_{DS} ; Fr_{DS} – CALIBRATION CURVES FOR L/b_p = 5.6 (MEDIUM), θ = 5 °, B/b_{p_eff} = 13.5

Figure 4.24 C_d ; y_{UE}/y_{DS} ; Fr_{DS} – CALIBRATION CURVES FOR L/b_p = 5.6 (MEDIUM), θ = 10 °, B/b_{p_eff} = 10.7

Figure 4.25 C_d ; y_{UE}/y_{DS} ; Fr_{DS} – CALIBRATION CURVES FOR L/b_p = 5.6 (MEDIUM), θ = 15 °, B/b_{p_eff} = 8.7

Figure 4.26 C_d ; y_{UE}/y_{DS} ; Fr_{DS} – CALIBRATION CURVES FOR L/b_p = 4.2 (SHORT), θ = 5 °, B/b_{p_eff} = 15.2

Figure 4.27 C_d ; y_{UE}/y_{DS} ; Fr_{DS} – CALIBRATION CURVES FOR L/b_p = 4.2 (SHORT), θ = 10 °, B/b_{p_eff} = 12.4

Figure 4.28 C_d ; y_{UE}/y_{DS} ; Fr_{DS} – CALIBRATION CURVES FOR L/b_p = 4.2 (SHORT), θ = 15 °, B/b_{p_eff} = 10.5

TABLE:	*DESCRIPTION:*
Table 3.1	Summary, a comparison between the continuity, energy, momentum and power entities.
Table 4.1	Calibrated C_d-values, parallel approaching flow, normal flow conditions downstream
Table 4.2	Calibrated C_d-values, parallel approaching flow, drowned flow conditions downstream
Table 4.3	Calibrated C_d-values, non-parallel approaching flow, normal flow conditions downstream
Table 4.4	Calibrated C_d-values, non-parallel approaching flow, drowned flow conditions downstream
Table 4.5	Non-parallel flow conditions where pressure US exceeds pressure UE (marked with crosses)

PHOTOS:	***DESCRIPTION:***
Photo 3.1	Wooden model pier used by Retief, defining the sections used by him and the corresponding pressure measuring points
Photo 3.2	A typical water surface profile at a bridge pier under flood conditions, Δh_1 showing the normal water surface level difference measured at bridge piers and Δh_2 the pressure difference obtained by measuring pressures next to the pier
Photo 4.1	Side view of glass flume used for testing the model piers, Hydraulics Laboratory University of Stellenbosch
Photo 4.2	Side view of glass flume used for testing the model piers, Hydraulics Laboratory University of Stellenbosch
Photo 4.3	Looking downstream at the glass flume used for testing the model piers, Hydraulics Laboratory University of Stellenbosch
Photo 4.4	Sluice at the end of the glass flume used for testing the model piers, Hydraulics Laboratory University of Stellenbosch
Photo 4.5	PVC 63 mm pier (SHORT) during a ±130 l/s test, normal flow conditions downstream etc.
Photo 4.6	Measured pressure heads inside manometer pipes during a test on a PVC 63 mm pier (SHORT) ,±130 l/s test, normal flow conditions downstream etc.
Photo 4.7	Defining sections 1,2,3 and 4 and measuring positions UE, US, DS and DE
Photo 4.8	Four different model pier widths of the model piers: A=63 mm (B/b_p=9.6), B=50 mm (B/b_p=12.2), C=40 mm (B/b_p=15.2), D=32 mm (B/b_p=19.0)
Photo 4.9	"Building blocks" of a typical PVC pier model. A=upstream end, B=extension for "MEDIUM" length, C=extension for "LONG" length, D=downstream end
Photo 4.10	Defining the rotation of the model pier. A=direction of approaching flow, B=long axis direction,θ=relative angle between A and B

Photo 4.11 Defining the effective pier width for non-parallel flow conditions, B = total flume width, B_{p_eff} = effective pier width and ($B-b_{p\_eff}$) the effective or net width of passing flow

Photo 4.12 Flow patterns past model pier, parallel approaching flow, B/b_p = 9.7, L/b_p = 6.9 (LONG), Q = ±130 l/s, normal flow conditions downstream

Photo 4.13 Flow patterns past model pier, parallel approaching flow, B/b_p = 9.7, L/b_p = 5.6 (MEDIUM), Q = ±130 l/s, normal flow conditions downstream

Photo 4.14 Flow patterns past model pier, parallel approaching flow, B/b_p = 9.7, L/b_p = 4.2 (SHORT), Q = ±130 l/s, normal flow conditions downstream

Photo 4.15 Flow patterns past model pier, parallel approaching flow, B/b_p = 12.2 , L/b_p = 6.9 (LONG), Q = ±130 l/s, normal flow conditions downstream

Photo 4.16 Flow patterns past model pier, parallel approaching flow, B/b_p = 12.2 , L/b_p = 5.6 (MEDIUM), Q = ±130 l/s, normal flow conditions downstream

Photo 4.17 Flow patterns past model pier, parallel approaching flow, B/b_p = 12.2 , L/b_p = 4.2 (SHORT), Q = ±130 l/s, normal flow conditions downstream

Photo 4.18 Flow patterns past model pier, parallel approaching flow, B/b_p = 15.2 , L/b_p = 6.9 (LONG), Q = ±130 l/s, normal flow conditions downstream

Photo 4.19 Flow patterns past model pier, parallel approaching flow, B/b_p = 15.2 , L/b_p = 5.6 (MEDIUM), Q = ±130 l/s, normal flow conditions downstream

Photo 4.20 Flow patterns past model pier, parallel approaching flow, B/b_p = 15.2 , L/b_p = 4.2 (SHORT), Q = ±130 l/s, normal flow conditions downstream

Photo 4.21 Flow patterns past model pier, parallel approaching flow, B/b_p = 19.0 , L/b_p = 6.9 (LONG), Q = ±130 l/s, normal flow conditions downstream

Photo 4.22 Flow patterns past model pier, parallel approaching flow, B/b_p = 19.0 , L/b_p = 5.6 (MEDIUM), Q = ±130 l/s, normal flow conditions downstream

Photo 4.23 Flow patterns past model pier, parallel approaching flow, B/b_p = 19.0 , L/b_p = 4.2 (SHORT), Q = ±130 l/s, normal flow conditions downstream

Photo 4.24 Flow patterns past model pier, parallel approaching flow, B/b_p = 9.7 , L/b_p = 6.9 (LONG), Q = ±130 l/s, drowned flow conditions downstream

Photo 4.25 Flow patterns past model pier, parallel approaching flow, B/b_p = 9.7 , L/b_p = 5.6 (MEDIUM), Q = ±130 l/s, drowned flow conditions downstream

Photo 4.26 Flow patterns past model pier, parallel approaching flow, B/b_p = 9.7 , L/b_p = 4.2 (SHORT), Q = ±130 l/s, drowned flow conditions downstream

Photo 4.27 Flow patterns past model pier, parallel approaching flow, B/b_p = 12.2 , L/b_p = 6.9 (LONG), Q = ±130 l/s, drowned flow conditions downstream

Photo 4.28 Flow patterns past model pier, parallel approaching flow, B/b_p = 12.2 , L/b_p = 5.6 (MEDIUM), Q = ±130 l/s, drowned flow conditions downstream

Photo 4.29 Flow patterns past model pier, parallel approaching flow, B/b_p = 12.2 , L/b_p = 4.2 (SHORT), Q = ±130 l/s, drowned flow conditions downstream

Photo 4.30 Flow patterns past model pier, parallel approaching flow, B/b_p = 15.2 , L/b_p = 6.9 (LONG), Q = ±130 l/s, drowned flow conditions downstream

Photo 4.31 Flow patterns past model pier, parallel approaching flow, B/b_p = 15.2 , L/b_p = 5.6 (MEDIUM), Q = ±130 l/s, drowned flow conditions downstream

Photo 4.32 Flow patterns past model pier, parallel approaching flow, B/b_p = 15.2 , L/b_p = 4.2 (SHORT), Q = ±130 l/s, drowned flow conditions downstream

Photo 4.33 Flow patterns past model pier, parallel approaching flow, B/b_p = 19.0 , L/b_p = 6.9 (LONG), Q = ±130 l/s, drowned flow conditions downstream

Photo 4.34 Flow patterns past model pier, parallel approaching flow, B/b_p = 19.0 , L/b_p = 5.6 (MEDIUM), Q = ±130 l/s, drowned flow conditions downstream

Photo 4.35 Flow patterns past model pier, parallel approaching flow, B/b_p = 19.0 , L/b_p = 4.2 (SHORT), Q = ±130 l/s, drowned flow conditions downstream

Photo 4.36 Flow patterns past model pier, non-parallel approaching flow, B/b_p = 19.0 , L/b_p = 4.2 (SHORT), θ = 15 degrees, "positive pier side" shown, Q = ±130 l/s, normal flow conditions downstream

Photo 4.37 Flow patterns past model pier, non-parallel approaching flow, B/b_p = 19.0 , L/b_p = 4.2 (SHORT), θ = 15 degrees, "negative (lee) pier side" shown, Q = ±130 l/s, normal flow conditions downstream

Photo 4.38 Flow patterns past model pier, non-parallel approaching flow, B/b_p = 19.0 , L/b_p = 4.2 (SHORT), θ = 15 degrees, "negative (lee) pier side" shown, Q = ±130 l/s, drowned flow conditions downstream

Photo 4.39 Flow patterns past model pier, non-parallel approaching flow, B/b_p = 19.0 , L/b_p = 4.2 (SHORT), θ = 15 degrees, "looking upstream" view, Q = ±130 l/s, normal flow conditions downstream

Photo 4.40 Manometer stand pipe readings for normal flow conditions and zero pier rotation

Photo 4.41 Manometer standing pipe readings for normal flow conditions and non-zero pier rotation

SYMBOL:	*DESCRIPTION:*
A	Area [m^2]
A^*	Plan or projected area [m^2]
ε_p	Potential energy [J]
ε_k	Kinetic energy [J]
κ	Kappa term – power correction factor [non dim]
Q	Flow rate [m^3/s]
Q_{50}	Peak flow rate with a 50 year return period
b	Width between piers [m]
B	Centreline distance for piers [m]
b_p	Pier width (maximum) [m]
s	Slope [m/m]
S_f	Energy slope [m/m]
S_0	Bed slope [m/m]
V	Volume [m^3]
v	Velocity [m/s]
v_{pier}	Theoretical velocity of the pier (special case) [m/s]
$v_{approach}$	Velocity of approaching fluid [m/s]
v_∞	Velocity of fluid far upstream of the pier [m/s]
C_d	Flow correction factor [non dim]
C_d^*	Drag coefficient [non dim]
q	Flow rate per unit width [m^2/s]
L	Length [m]
L_p	Pier length [m]

y	Flow depth [m]
d	Flow depth [m]
F	Force [N]
M	Momentum [N]
P	Power [W]
$\mathbf{H_0}$	Work line distance of a force taken from point 0
$\mathbf{M_0}$	Moment around point 0 [N.m]
$\mathbf{h_L}$	Transitional losses [m]
$\mathbf{h_f}$	Frictional losses [m]
g	Gravitational acceleration [m/s^2]
ρ	Rho, fluid density [kg/m^3]

ABBREVIATIONS:	*DESCRIPTION:*
DWAF	Department of Water Affiars and Forestry (RSA)
RMF	Regional Maximum Flood
MAR	Mean Annual Run-off
RSA	Republic of South Africa

1. *INTRODUCTION*

South Africa is a water poor country. It is thus of the utmost importance to measure the run-off from catchments as accurately as possible in order to quantify the country's water resources. The measurement of run-off is undertaken by the Department of Water Affairs and Forestry (DWAF) by using a network of flow gauging stations. These gauging stations are usually restricted to lower flows in terms of their capacity. Therefore, the measurement of high flows has become very important because most gauging stations can not cope with these flows. Being able to measure higher flows (floods), one will also be able to analyse and predict the occurrence of floods more accurately.

Therefore, in order to assure reliable continuous flow records, improved methods for measuring high discharges need to be found. The existing network of flow gauging stations on South African rivers consists mainly of compound gauging weirs. Most of these weirs become inaccurate when high discharges occur because they cannot be built large enough to cope with very high flows. These inaccuracies are mainly due to drowned conditions. The geometry of the gauging weir and the average energy slope taken across the weir become insufficient to prevent the sub-critical flow downstream from influencing the flow upstream i.e. of drowning the weir. The flow regime associated with drowned conditions is also known as non-modular flow. The calculation of the flow rate **Q** based on flow depths measured under drowned conditions tends to be quite inaccurate due to the fact that a control section with a unique relationship between depth and discharge no longer exists. Research is presently being done on the phenomenon of drowned conditions at gauging stations in a separate parallel study. Flow gauging under drowned conditions however remains problematic. It is also important to mention that weirs that are large enough to be able to measure the full range of flows become very expensive and often cause the inundation of large areas upstream of the weirs.

The accurate measurement of high discharges has several advantages and uses:

❶ For example – the *design* of a new dam. One of the most important design aspects in the design of a new dam is the flood analysis which forms part of the stability analysis of the dam wall. Flood analysis includes testing of the dam wall stability, as well as the determination of the capacity of the overflow section during flood events which directly affect the load on the wall. The safety aspect associated with downstream flooding (also when the dam wall would fail) is directly linked to high inflows. The quantification of these high inflows is therefore of great importance in order to perform reliable calculations in terms of safety.

❷ If a method for measuring high discharges more accurately can be found, one will be able to test the accuracy of hydrological models which describe the complex relationship between run-off as a function of precipitation and other input parameters. These models are subject to uncertainties due to the simplified assumptions that have to be made in order to compensate for the complex nature of the run-off process, as well as the limited availability of data on a regional scale. This implies that these models also need calibration – these models will therefore benefit from flow records that include more accurate higher discharge values.

❸ By quantifying high discharges accurately, the calculation of flood levels and potential damage can be made more accurately. This means for example that if the flow rate at a calibrated bridge upstream of a town or settlement exceeds the Q_{50} flood discharge, which has been used to determine the Q_{50} flood lines for the town/settlement, one will know with greater certainty when to evacuate people.

❹ The modelling of estuaries can also benefit from accurately measured high inflow discharges. Flushing (dilution of the salt concentration within the estuary) occurs mainly during high inflows of fresh water from the inland. By quantifying these high discharges, one can link the degree of flushing to specific inflows. The ability of predicting the flushing of an estuary in terms of inflows will enable ecologists to predict environmental and biological changes within the estuary with greater accuracy. In addition, knowing the

high inflow discharges will enable engineers to predict the extent to which a certain flood will breach the sand spit which separates the estuary from the ocean during low flow periods. These events can then be related to specific return periods.

- Given the possible ability of measuring high discharges accurately at existing bridges (the method being investigated in this report), one will be able to update the RMF-indices of Kovacs. This implies that having an extreme flood event and having the ability to measure the peak discharge accurately, adjustments to the RMF-index can be made if this flood has exceeded the historical Regional Maximum Flood as documented for the specific region.

This study has concentrated on the possible application of bridge piers as high discharge measuring structures by analysing flow patterns and flow characteristics around pier models for different flow conditions. The use of the fundamental laws of nature and "reasonable" simplified assumptions have led to a variety of possible mathematical models (Energy, Momentum and Power) which were investigated individually both in terms of their suitability and accuracy in terms of model description. Several theoretical approaches and models that appeared to have satisfied the criteria were eventually investigated in further detail.

The fundamental phenomenon on which the bridge pier concept is based, is the stagnation of flow at the upstream end of a bridge pier and the associated conversion of potential energy into kinetic energy from the stagnation point in the direction of the downstream end of the pier. The phenomenon of stagnation of fluids has been used with great success in velocity gauges for many years and forms the principle on which the Pitôt-tube velocity gauge works. The velocity of aeroplanes as well as water flowing under uniform conditions can be measured to an accuracy of about 1% by using this technique (*White* 1986). The theory of the Pitôt-tube will be discussed as an introduction to flow measuring theory in terms of the energy equation with specific reference to the application at bridge piers.

2. BACKGROUND:

(*Retief, M.J.*, 1998 –extended and amended)

2.1 SOUTH AFRICAN RIVERS:

South Africa is a relative dry country with an average annual rainfall of about 500 mm. This is much less than the world average of 860 mm. In addition, the temporal distribution of lower rainfalls in South Africa is such that, the run-off in rivers may be lower than average for periods of up to 10 years (*DWAF* 1986). It is for this reason that accurate knowledge about the discharge of water for use as well as for the temporary storage of floodwater is so important.

2.1.1 *Factors which are problematic for flow measurement in South Africa:*

- Climate:

Not only is the flow in South African rivers limited but also highly unsteady. In contrast, Europe for example is dependent for a major part of its river flows from the melting of snow in the mountain areas. The snow plays a dual role: gradually releasing water during the physical process of melting of the snow and secondly rain is trapped in the snow and released only when the snow starts to melt. In European countries the cause of flood events is usually the rapid melting of snow in which rain has been trapped (*"The Institution of Civil Engineers, London"*, 1966). This may happen when warmer weather follows a period of cold rainy weather.

The generally wetter climate of Europe contributes further to more steady and uniform flows in rivers than in South Africa. The flow characteristics of South

African rivers are much more unstable and unpredictable. Comparing the River Thames in England with the Limpopo River for example, a huge difference in variability of discharge is evident.

The South African climate is one of extreme events. Floods are usually associated with rainstorms, thunderstorms and tropical cyclones. In spite of the extreme events of floods, South Africa on average has a relatively dry climate with snow making very little contribution to run-off during or after the winter season. The run-off in rivers is very unsteady in South Africa due to the fact that there are large areas which are either summer or winter rainfall areas. This means that we do not have rain on a regular basis, but rather at random during a specific rainfall season. A further contribution to the unsteadiness of flow is the variation in rainfall durations and rainfall intensities, which is found on a country-wide scale. These large variations in flow depths make discharge measurement difficult.

❷ Sediment:

Sediment problems are experienced at conventional gauging stations especially in the following regions: Eastern Cape, Western Cape, Free State and Kwazulu Natal (*Rooseboom* 1992).

Sediment accumulation at existing flow gauging stations poses serious problems, especially during high discharges when flooding rivers carry heavy loads of sediment. (*Rossouw. et al,* 1998) deal with the design and maintenance of flow gauging stations on sediment carrying rivers in South Africa.

❸ Labour and financial problems:

A shortage of personnel and funds contributes further to the flow-measuring problem. Sufficient skilled human power is usually not available during flood

events– this is due to the vast areas which are usually affected by floods and the short time span during which most floods occur. Field trips are however undertaken during floods to measure flow depths, flow velocities etc. in order to collect flood data. Unfortunately, gauging stations are often inaccessible during these times posing a logistical problem to physical flow measurements.

- Vandalism:

This has become a major problem in certain parts of South Africa and contributes to incomplete flow records. Measures need to be taken in order to safeguard measuring equipment at flow gauging stations which contribute to high maintenance costs.

2.2 *OCCURRENCE AND MANAGEMENT OF FLOODS IN SOUTH AFRICA:*

As mentioned earlier, South Africa experiences large variations in river run-off. These varying floods are important both in terms of their destructive abilities as well as their contribution to the mean annual run-off (MAR).

2.2.1 Defining a flood:

A flood can be defined as an event during which the water surface in a river rises to such an extent that the river is no longer flowing only in the main channel, but also fills the floodplains on the sides, therefore rising above the normal flow boundaries. From the point of view of hydrology (*Rooseboom*, 1985): *"a flood is a wave that progresses along a watercourse and causes changes in water level, discharge, flow velocity and water surface slope all along the course".*

2.2.2 *The nature of floods:*

Floods in South Africa can be quite destructive. Recent examples are the 1998 floods along the Orange River and the floods in Natal during September 1987 (*Du Plessis*, 1989).

Other examples, which illustrate the nature of southern African floods, are the flood events that were associated with the tropical cyclone "Domoina" (*Retief*, 1998). "Domoina" was first noticed on 17 January 1984 on satellite photos and 10 days later it started to move towards the Mozambique coast and from there further inland over the African continent. During the 5 days that followed, heavy rains fell over southern Mozambique, Mpumalanga, Swaziland and the northern parts of Kwazulu-Natal. More than 10 000 people were directly affected by the floods and more than 200 lives were lost during the events. In South Africa alone more than R100 million's damage was caused to communication installations, the agricultural sector and nature reserves.

2.2.3 *Methods for flow measurement presently used in the R.S.A.:*

Due to the lack of better and more efficient measuring methods for very high flows, as well as the problems of accessibility of gauging stations during flood events, the past practice of the DWAF was to wait for a flood to subside before flood levels were determined (*Herschy*, 1978). Maximum flow depths were taken up to the highest levels of scouring and debris accumulation afterwards.

Methods, which are generally used in South Africa for high flow measurement, include the slope-area method and the bridge contraction method. These methods are used in conjunction with flow measurement data from gauging stations and reservoir spillways. Standard gauging stations are usually unable to measure high flows as they become drowned which means that a control section ceases to exist

and the calculation of flow rates as functions of upstream water depths therefore becomes inaccurate.

❶ Slope Area method:

This method is used most frequently. It is based on the assumption that the flow is uniform (cross-sections' geometry relatively constant) for the reach where flow measurement is being undertaken. This method assumes that the flow depth is a function of the average bed slope s_o, bed roughness (Manning **n-value** or Chezy **C-value**) and cross sectional geometry and is not influenced by control sections and/or obstructions elsewhere along the river. The maximum water levels that have been reached during the flood are determined and by using the Manning or Chezy equation for steady uniform open channel flow, the average flow velocities can be calculated. From the velocities and information on the cross sections the flow rate can then be calculated. The equations of Manning and Chezy are well known and can be found in any hydraulics handbook.

The following problems were found using the Slope Area method:

❶ The calculated flow rate **Q** is very sensitive to the energy slope and small errors made with the energy slope may result in large variations in the flow rate. The assumption of uniform flows implies that the energy slope S_f is taken as the same as the bed slope S_o which is not always correct especially if accelerating flow is present.

❷ The bed roughness, which is used as a parameter in the open channel flow equations, is typically taken as the k-value of the irregular bed as found after the flood has passed. Recent research (*Rooseboom, Le Grange,* 2000) has shown that the bed roughness (k-value) in sand-bedded rivers is totally different during the flood event compared to after the flood event. The reason for this is that deformation of sand beds occurs when flows pass over

them, especially during high flows. The formation of bed forms of several metres in height is quite possible during large floods. This means that the estimation of bed roughness according to the bed profile after a flood can lead to the under-estimation of bed roughness (Manning **n-value** or Chezy **C-value**).

❷ Bridge contraction method:

This method is based on the fact that flows approaching a bridge experience contraction due to the bridgeheads and undergo an associated drop in water surface level upon passing through the bridge openings. The flow equation for calculating the flow rate can be determined by using the continuity law as well as the energy equation of *Bernoulli*. This method cannot be used reliably at most South African bridges because the drops in surface levels are too small to measure with sufficient accuracy.

2.2.4 Other flow measuring techniques:

Increased use is being made in South Africa of stream gauging. This involves the measurement of flows through near uniform river reaches and the derivation of stage-discharge relationships. OTT Southern Africa (Pty) Ltd is supplying the equipment which is currently being used for velocity measurements. The equipment consists mainly of a heavy elongated fin-shaped instrument with a propeller directed in the upstream direction. This instrument is supported by a cable that runs across a river and the instrument can be lowered into the stream. The instrument is sometimes lowered to a level that corresponds to **0.4** times the flow depth (measured from the riverbed). The reason for this is that the average velocity of an open channel stream is approximately equal to the velocity found at a distance of **0.4D** above the riverbed, where **D** is the total depth of flow at a specific location. The flow of the water drives the propeller and by doing a simple calculation that correlates the revolutions per unit time with the velocity, local velocities within the stream can be calculated. By taking these measured

velocities as being representative of their associated area elements and multiplying them with their elemental areas, one can obtain the flow rate for each elemental area. By adding these flow rates, one can obtain a relatively accurate estimation of the total flow rate. To allow for the deformation of sand beds, the area of the cross section should reflect conditions during the flood event and not after the flood event. More accurate results are obtained by measuring velocities at different levels. A bridge is also a convenient structure from which velocity measurements can be performed at representative points across the flow sections perpendicular to the flow direction although velocity distribution may differ from that in open channels and be more complex.

The cost of a calibration as described above is about R 80 000. This cost includes the installation as well as the maintenance of the cableway. A conventional gauging station costs at least R 250 000 (1998 prices).

This method provides us with an additional flow measuring technique which can be used to test the accuracy of newly proposed methods.

Advantages of stream gauging:

1. This method does not require the building of a large structure.
2. There is no damming or deceleration of the flow velocity as in the case of a gauging weir. This means that sediment build-up may not be a problem.

Disadvantages of stream gauging:

1. It is quite expensive at a cost of around R80 000 (1998) per calibration.
2. The cableway, if inappropriately sited, can be easily damaged or dragged along by larger debris (bridges can be used to support the velocity meters)

❸ Vandalism poses a serious problem for both the cableway and the measuring equipment.

❹ The velocity meter needs a minimum depth of about one meter to be able to register properly.

Stream gauging is the preferred method of calibration of flow gauging stations in most countries, particularly where river flows do not vary greatly.

2.3 *CRITERIA FOR NEW MEASURING TECHNIQUES FOR SOUTH AFRICAN CONDITIONS:*

Given the problems that have been experienced in the past with flow measurements during floods, a list of guidelines that will assist in the development of new measuring methods and techniques can be drawn up (*Lotriet, Rooseboom,* 1995):

❶ It is important to note the large variation in flow rates in typical South African rivers. A new system of flood measurement should therefore provide reliable and continuous flow records over a large spectrum of flows.

❷ The system should be less susceptible to sediment problems than the existing gauging weirs found in South Africa.

❸ South African rivers cross international boundaries and the proposed system should therefore comply with international standards.

❹ New methods should be economical and if possible not require the construction of additional structures but rather be incorporated in existing structures.

❺ Maintenance of structures should be a minimum.

❻ The system should be sturdy to resist the forces of nature and vandalism.

3. FLOW MEASURING THEORY:

3.1 APPROACH FOLLOWED:

The main aim of this investigation was to determine whether pressure differences at bridge piers could be related to discharges. *Retief* (1998) showed that the energy principle combined with the stagnation phenomenon did work for a limited number of model pier combinations. The energy principle was re-evaluated as a first step in the development of new theories to describe the pier pressure/discharge relationship.

This chapter describes a fundamental investigation undertaken in order to study the processes of energy, momentum and power conversion within set boundaries of a stream that incorporates an obstruction in the form of a bridge pier. Theoretical trends were analysed with the help of the basic laws of nature that are applicable to the hydraulic field. These theories were subsequently tested using laboratory data gathered by *Retief, (*1998*)* (covered in *sections 3.4, 3.5, 3.6, 3.7, 3.8* and summarised in *section 3.9*).

The re-evaluation of the energy based discharge equation, as well as the evaluation of the momentum and power based discharge equations (new theories, covered in *sections 3.7* and *section 3.8* respectively), led to promising conclusions and recommendations (*section 3.11*). These conclusions and recommendations helped with the identification of additional tests needed in order to investigate and answer problems and questions that arose from results based on *Retief's* (1998) data.

Additional tests performed during July/August 2000 (covered in *chapter 4*) at the Hydraulics Laboratory of the University of Stellenbosch helped to develop a better understanding of the process of pressure conversion at bridge piers and calibrated curves could be established according to the energy based theory for discharge measurement.

3.2 *MODEL DESCRIPTION - Retief:*

Figure 3.1 is a schematic representation of the laboratory lay-out used by *Retief* (1998) for his tests on model piers. These tests were performed at the Hydraulics Laboratory of the University of Stellenbosch. The glass flume that was used to simulate the prototype "river" or "channel" was flume number 3 in the laboratory with a width of 609 mm. Water was supplied via a 300 mm diameter pipe. This pipe is connected to a constant head tank to ensure constant discharge during the tests. Perforated blocks installed at the entrance of the flume ensured smooth inflow to the model.

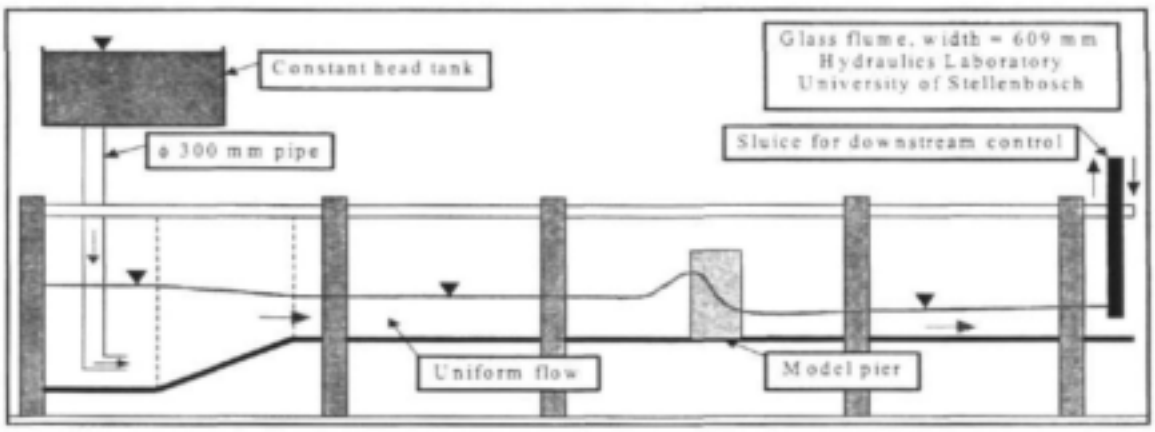

***Figure 3.1**: Schematic side view of model pier set-up in the Hydraulics Laboratory, University of Stellenbosch*

The mathematical models that will be derived in *sections 3.6* to *3.8* were calibrated using model data. Scale models of the real structure (prototype) were constructed from wood (*photo 3.1, p.16*) and tested in order to investigate flow conditions around bridge piers.

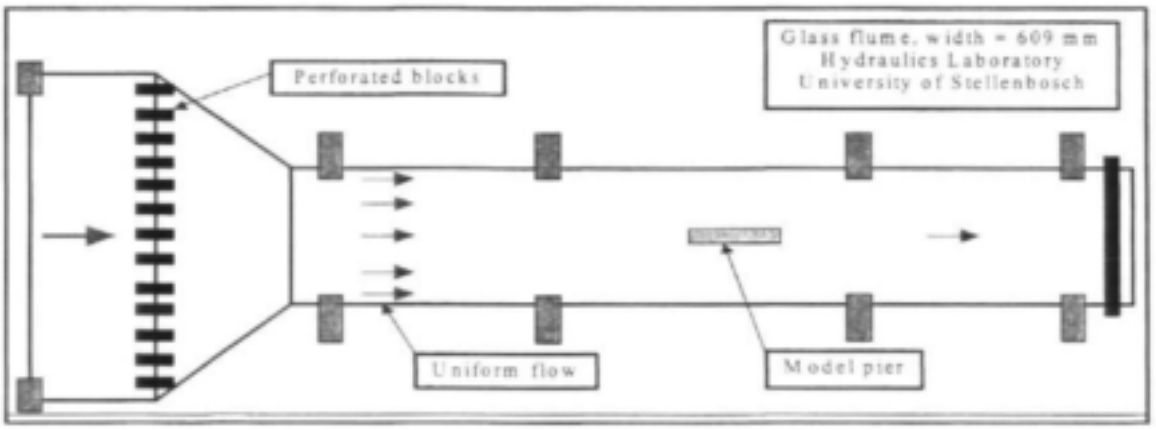

***Figure 3.2**: Schematic plan view of model pier set-up in the Hydraulics Laboratory, University of Stellenbosch*

Discharge measurement was done with a 213.0 mm orifice disc installed inside the 300 mm diameter pipe. The difference in water pressure upstream and downstream of the measuring disc was measured with a water/mercury manometer. From the pressure differences the discharge was calculated using the following equation:

$$Q = C_d a_1 \sqrt{\frac{2gh}{k^2 - 1}}$$

where **C_d = coefficient of discharge = 0.61** and

$$k = \frac{a_1}{a_2}$$

a_1 = pipe diameter and **a_2 = diameter of disc opening**

In order to have been able to test different ratios of channel width to pier width ($\mathbf{B/b_p}$), three different pier widths were used by *Retief*. Each pier was constructed with three horizontal holes for measuring pressures (**A**, **B** and **C** in *photo 3.1, p.16*), a hole in the front, a hole on the side (in the middle) and a hole at the downstream pier end. Three vertical shafts within the model were used to measure water levels (pressures) by connecting them to clear cylinders ensuring more stable water surfaces in order to increase the accuracy of measurement.

The different piers were placed symmetrically within the glass flume and were fixed to the flume floor to prevent movement during tests.

Three different flow conditions were investigated by *Retief*, viz: "Normal flows", "Debris flows" and "Sluice controlled flows". The "Normal flows" refer to flow conditions where a control section (critical depth) is found within the pier length. "Debris flows" refer to flow conditions where the effects of the accumulation of debris at the upstream end of the pier on the flow conditions were investigated. "Sluice controlled flows" refer to drowned flow conditions downstream of the pier.

For the "Normal flows" and "Debris flows", water depths were measured 900 mm upstream of the upstream pier end (*section 1, photo 3.1*), at the upstream end (*section 2, corresponds to pressure measuring at A*), at the middle of the pier (*section 3, corresponds to pressure measured at B*), at the downstream end (*section 4, corresponds to pressure measured at C*) and 4570 mm downstream from the downstream end of the pier (*section 5*) near to the sluice controlling the downstream conditions. For the "Sluice controlled flows", water depths were measured at the same positions but instead of measuring the downstream depth at 4570 mm, it was measured closer, viz. 700 mm downstream of **section 4**. The following picture shows one of the wooden model piers that was used in *Retief's* study. According to the pressure measuring configuration used

for the wooden piers, the following sections were defined accordingly and are shown as dotted lines:

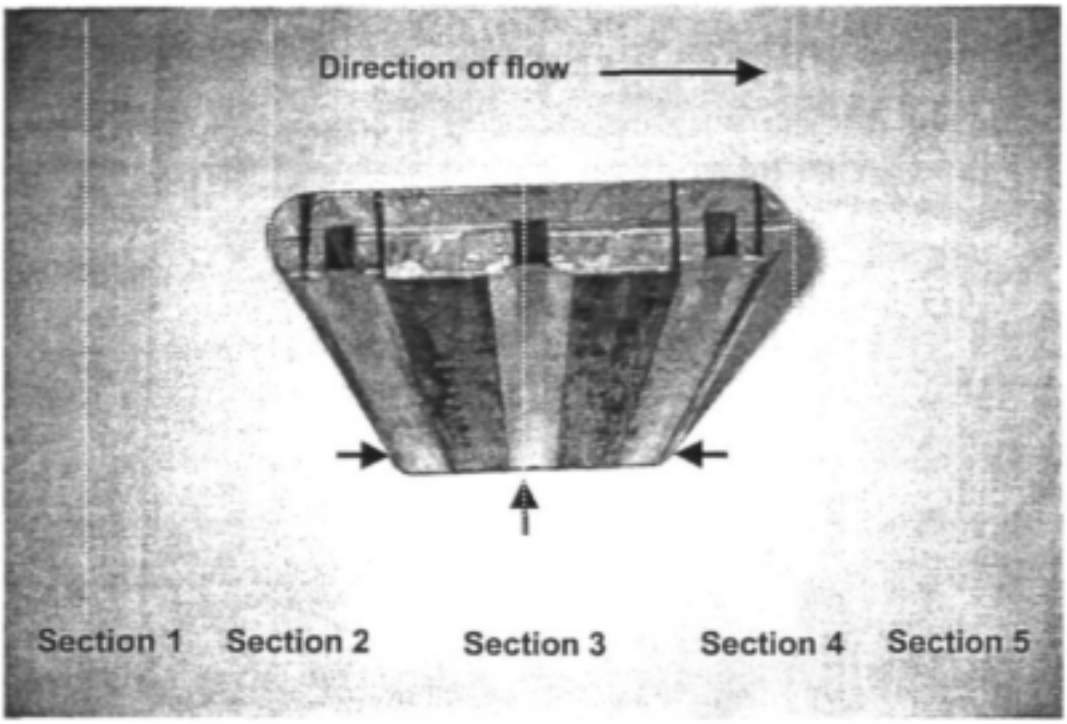

***Photo 3.1**: Wooden model pier used by Retief, defining the sections used by him and the corresponding pressure measuring points*

The discharge equations derived in *sections 3.6, 3.7* and *3.8* were calibrated using the data collected by *Retief* and the results of these fundamentally based equations are therefore applicable to a model pier set-up as has been described in *figure 3.1, figure 3.2 and photo 3.1.*

3.3 INTRODUCTION TO FLOW MEASUREMENT:

The typical problems engineers usually face with open channel flow is either of the following (*Rooseboom* 1985):

❶ "Given the flow rate, determine the flow depth in the channel"

❷ "Given the flow depth in the channel, determine the flow rate"

The first problem is typically a design problem and is most commonly being encountered by water engineers. Using either the Manning or Chezy equation for steady uniform open channel flow, one can determine the flow depths for a given discharge if the bed roughness and bed levels are known. These calculations usually form part of a water surface profile analysis.

The second stated problem forms the basis of this report, i.e. the measurement problem. Measurement here refers to the calculation of velocity as a function of measurable flow characteristics in order to estimate the flow rate. By measuring flow depths and pressure differences and applying the energy and continuity laws, one can calculate theoretical velocity values and by compensating for energy losses, accurate results can be obtained.

3.4 FUNDAMENTAL HYDRAULIC CONCEPTS RELATED TO FLOW-MEASUREMENT:

Newton's Second Law and the Law of Conservation of Mass:

There are two fundamental laws of nature which are used by civil engineers working in the water field – variations and combinations of these two laws are commonly used when tackling hydraulic problems.

These two laws are basically: "The Law of the Conservation of Mass" and "Newton II". It will be shown that Newton II can be rewritten to indicate that force equals momentum change.

The following laws are used in different combinations in the field of hydraulics in order to analyse a wide range of problems:

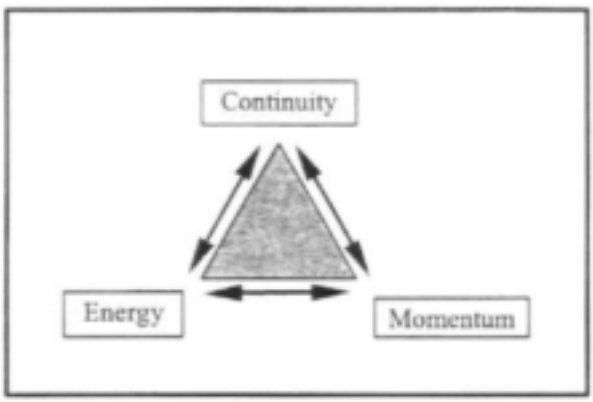

***Figure 3.3**: The three basic hydraulic laws, Continuity, Energy and Momentum*

An extension (*figure 3.4*) of the three laws has been proposed by *Rooseboom (*1992) by the introduction of Power Theory, in which he proved on a theoretical basis that the *Von Karman* coefficient nearly equals **0.4**. The arrows in the sketch below imply that different combinations of these laws may be used in calculations.

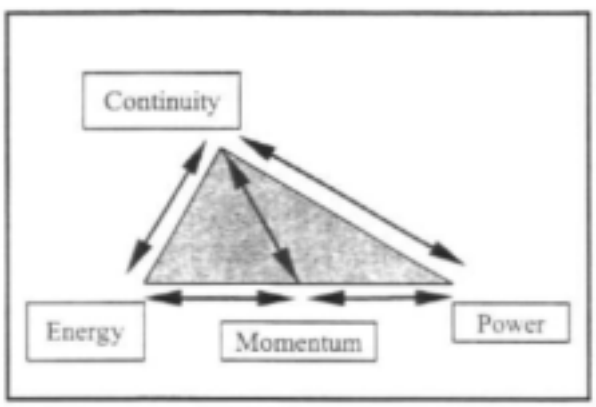

***Figure 3.4**: An extension on the three basic hydraulic laws, Power being added*

In the sketch above a forth law, namely the Conservation of Power, has been introduced. It is further important to note that these four laws are not all independent. Any combination of two laws that include continuity forms an independent combination. This implies that the combination of the Energy, Momentum and Power Laws do not constitute an independent set. The reason for this will be shown later to be the fact that all three of these laws can be derived from Newton's second law.

The continuity law represents "*The Law of the Conservation of Mass*" whilst the Energy, Momentum and Power Laws can all be derived by using different integration manipulations of Newton's second law.

The derivation of these four laws will be performed next for clarity. Consider firstly the choice of hydraulic configurations being used in the derivation of equations based on these laws.

Choice of control volumes in the analysis of pier flow:

The selection of configurations for the application of the 4 laws depends firstly on which of the 4 laws is being applied. The Energy equation is applicable along a continuous streamline whilst the Momentum equation applies to an enclosed control volume. The Power equation also requires a control volume for application purposes.

The choice depends secondly on where uniformity of flow exists. A section where the velocity or depth varies across the width is not suitable as an enclosing section for use with the Momentum or Power Laws.

A third consideration which influences the selection of sections is the location of large transitional losses. By using **section 4** rather that **section 5** for instance in (*Figure 3.5, p.23)*, uncertainties concerning the transitional losses occurring within the control volume can be drastically reduced. By doing this, more stable coefficients (resulting from the calibration process) were found.

Taking a section at the upstream end of the pier ensures greater water level differences and consequently more accurate measurements. **Section 2** (next to the upstream end of the pier) was not suitable due to the non-uniform flow conditions across the section.

3.5 CONTINUITY:

Derivation:

The Law of Conservation of Mass states (*Serway* 1982): "Matter is neither created nor destroyed" That is, the mass of the system before a process equals the mass of the system after the process.

Consider a system where the flow of water is continuous as it moves from point p_{in} to point p_{out} enclosed by isolating boundaries. The enclosed volume between p_{in} and p_{out} forms the control volume. The system can be either pipe flow or open channel flow.

Assuming that no mass is stored between points p_{in} and p_{out} in the system, there will be no volume change within if we assumed water to be incompressible for the purposes of this study. The above-mentioned assumption leads to the following derivation:

Definitions of symbols:

m_{in}: mass entering the system [kg]

m_{out}: mass exiting the system [kg]

ρ : mass density of the fluid [kg/m^3]

V_{in}: volume entering the system [m^3]

V_{out}: volume exiting the system [m^3]

$^{dx}/_{dt}$: time derivative with respect to variable x [non dim]

Mass entering the system = mass leaving the system

$$\Rightarrow \quad \textit{mass in}\,(m_{in}) = \textit{mass out}\,(m_{out})$$

Taking the time derivative on both sides:

$$\Rightarrow \quad \frac{d}{dt}(m_{in}) = \frac{d}{dt}(m_{out})$$

$$\Rightarrow \quad \frac{d}{dt}(\rho V_{in}) = \frac{d}{dt}(\rho V_{out})$$

The density is constant (incompressible fluid):

$$\Rightarrow \quad \frac{d}{dt}(V_{in}) = \frac{d}{dt}(V_{out})$$

$$\Rightarrow \quad Q_{in} = Q_{out} \qquad \textit{(Equation 3.1)}$$

Equation 3.1 is known as the continuity equation for application in fluid mechanics.

Applications of the continuity equation:

The continuity equation is used as a "primary tool" together with the Energy, Momentum and Power equations in solving hydraulic problems. The continuity equation links flow depths and velocities. In order to use the continuity equation in this study, it is necessary to describe the flow region in the vicinity of the pier as well as possible. This description will be used throughout *chapter 3* and is discussed in more detail in the following paragraph "*Defining the geometry of a typical bridge lay-out*".

Defining the geometry of a typical bridge pier lay-out:

This study entailed the investigation of flow patterns around isolated bridge piers under high flow conditions. This was done in order to determine whether piers could be used as flow measuring structures. The term "isolated pier" in this context refers to a pier where the flow conditions upstream and downstream are uniform across the width of flow. This condition is approached at long bridges where span lengths are constant and where flow conditions are the same for the different openings. The theories that were developed were based on the assumption of isolated piers. It was further assumed that the bed around the pier is horizontal for at least the length of the pier.

For application of the Energy, Momentum and Power equations, specific control volumes were considered as part of the theoretical approach. In order to ensure consistency in the definition of sections and points defining the possible control volumes, the following plan view of a typical pier lay-out was used.

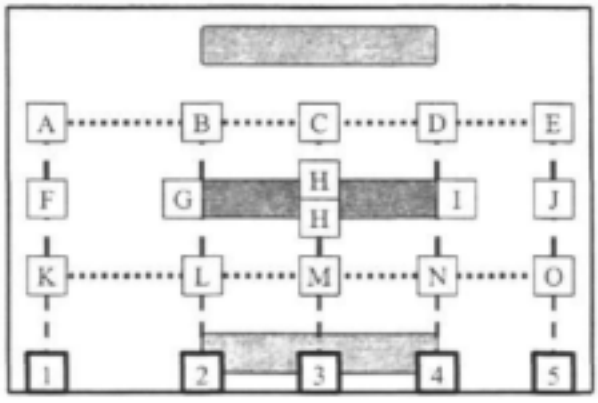

***Figure 3.5**: Describing and defining the plan view of a typical pier lay-out*

The numbering system depicted above is followed throughout chapter 3 (except for *p.33* to *p.40* where *figure 3.12*'s configuration, taken from *Webber* (1971)is used). Please note that when there are references to the pier width ($\mathbf{b_p}$), it always denotes the maximum dimension of the pier measured at right angles to the long axis of the pier. The distance between piers (**B**) is measured from centre to centre.

3.6 ENERGY APPROACH:

Derivation:

Newton's second law states *Serway* (1982): "The time rate of change of momentum of a body is equal to the resultant force acting on the body. If the mass of the body is constant, the net force equals the product of the mass and the acceleration."

Definitions of symbols:

a: Acceleration of the particle [m/s^2]

m: Mass of the body [kg]

F_{res}: Resultant force acting upon a system [N]

v: Velocity of flow [m/s]

s: Distance [m]

dx: Small increment in variable x [dim of x]

$^{dx}/_{dt}$: Time derivative with respect to variable x [non dim]

$U_{1\text{-}2}$: Work done between sections 1 and 2 (positive work is defined as work related to movement from section 1 toward section 2) [N]

$$a \propto F_{res}$$

$$a \propto \frac{1}{m}$$

$$\Rightarrow \quad a = \frac{F_{res}}{m}$$

$$\Rightarrow \quad F_{res} = ma \qquad \textit{(Equation 3.2)}$$

Note the following manipulation that is introduced:

$$a = \frac{dv}{dt} = \frac{dv}{ds}\frac{ds}{dt}$$

$$\Rightarrow \quad a.ds = dv\left(\frac{ds}{dt}\right)$$

$$\Rightarrow \quad F_{res} = ma = m\frac{v.dv}{ds}$$

$$\Rightarrow \quad F_{res}.ds = mv.dv$$

$$\int_{s_1}^{s_2} F_{res}.ds = \int_{v_1}^{v_2} mv.dv \qquad \textit{(Equation 3.3)}$$

$$\Rightarrow \quad F_{res}\left(s_2 - s_1\right) = \frac{m\left(v_2^{\,2} - v_1^{\,2}\right)}{2}$$

$$\Rightarrow \frac{mv_1^2}{2} + U_{1\text{-}2} = \frac{mv_2^2}{2} \qquad \textit{(Equation 3.4)}$$

The term $U_{1\text{-}2}$ represents the work done between points **1** and **2**. This term may also be seen as a differential potential energy value which is equal to the water surface level difference in terms of open channel flow (which is being studied here).

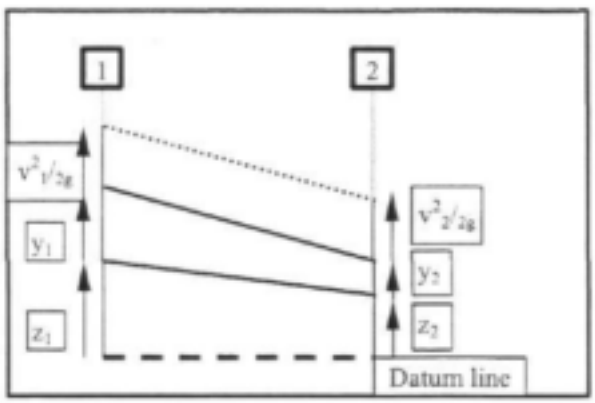

***Figure 3.6**: Typical open channel flow profile, taken between section 1 and section 2*

Consider a flow line along the surface as represented by the upper solid line in *figure 3.6*. The potential energy value at the surface at **section 1** equals $\varepsilon_{p1} = mg(y_1+z_1)$ and at **section 2** the value is $\varepsilon_{p2} = mg(y_2+z_2)$, measured relative to the dotted datum line.

Substitute $U_{1\text{-}2}$ with its differential definition in terms of the potential energy, viz. $U_{1\text{-}2} = \varepsilon_{p1} - \varepsilon_{p2}$. The reason why it is defined in this fashion comes from the definition of **g**, the earth's acceleration. If the unit gravitational force performs positive work it implies that the object on which the force is being exerted moves in the same direction in which the acceleration **g** works. This implies that positive work is associated with the movement of an object from a state of higher potential energy to a state of lower potential energy. Take for example an apple falling freely from a tree. The dominating force exerted on the apple is the gravitational force. The result of this force is a movement in a downward

direction, therefore resulting in a positive amount of work being done. Note that the term $\varepsilon_{p1} - \varepsilon_{p2}$ will therefore be positive because the apple has lost potential energy falling from **position 1** (up in the tree) to **position 2** (at any state during the free fall).

The work done between points **1** and **2**, $U_{1\text{-}2}$, takes on the following definition:

$$U_{1\text{-}2} = mgy_1 + mgz_1 - (mgy_2 + mgz_2) \qquad \textit{(Equation 3.5)}$$

Substitute $U_{1\text{-}2}$ (as defined in *equation 3.5*) into *equation 3.4*:

$$\Rightarrow \quad \frac{mv_1^2}{2} - mgy_2 - mgz_2 = \frac{mv_2^2}{2} - mgy_1 - mgz_1$$

$$\Rightarrow \quad \frac{mv_1^2}{2} + mgy_1 + mgz_1 = \frac{mv_2^2}{2} + mgy_2 + mgz_2$$

For the application of this equation in the Hydraulics field, all terms are expressed per unit volume of fluid. Divide by $W = mg$:

$$\Rightarrow \quad \frac{v_1^2}{2g} + y_1 + z_1 = \frac{v_2^2}{2g} + y_2 + z_2 \qquad \textit{(Equation 3.6)}$$

Equation 3.6 is known as the Bernoulli energy equation for the conservation of energy. Note that the friction and transitional loss terms do not appear on the right hand side of the equation. The reason for this is that these were ignored in the above derivation for simplicity.

The total energy equation can be obtained by adding the loss terms to the right hand side of *equation 3.6* and introducing a factor which compensates for the assumption of constant velocity across the section, namely the Coriolis coefficient α. The Coriolis coefficient has been taken as being = 1 throughout the text.

$$\Rightarrow \quad \frac{\alpha \bar{v}_1^{\,2}}{2g} + y_1 + z_1 = \frac{\alpha \bar{v}_2^{\,2}}{2g} + y_2 + z_2 + \sum h_{L_{1-2}} + h_{f_{1-2}} \qquad \textit{(Equation 3.7)}$$

The term $\Sigma h_{L1\text{-}2}$ represents the sum of all the transitional losses that occur between sections **1** and **2** whilst $h_{f1\text{-}2}$ represents the frictional loss between the same two sections. It should be clear that the Law of Conservation of Energy implies that there is a continuous exchange of potential energy ε_p and kinetic energy ε_k and that losses are associated with this process. It is the variation in relative magnitudes of $v^2/2g$ and $(z+y)$ that represents the energy exchange process.

Water surface level differences at bridges in terms of the energy equation:

The tol energy head at a point in open channel flow according to Bernoulli can be written as follows:

$$H \equiv \textit{total energy}\,[\textit{head in m water}]$$

$$H = y + \frac{v^2}{2g} + z \qquad \textit{(Equation 3.8)}$$

where **y** represents the flow depth, $v^2/2g$ the kinetic energy component and **z** the absolute height relative to a chosen datum level.

If we define $E_s = y + v^2/2g$ as the specific energy head, or in other words as the energy head component of **H** (total energy) that excludes **z**, E_s represents the energy head of the stream relative to the bed. By using E_s throughout our work where channels are prismatic in shape, calculations and the representation by means of graphs can be simplified.

The graphs in *figure 3.7 and figure 3.9* show the relationship of **y** vs. E_s for a specific flow rate and specific channel shape, taken to be rectangular in both cases:

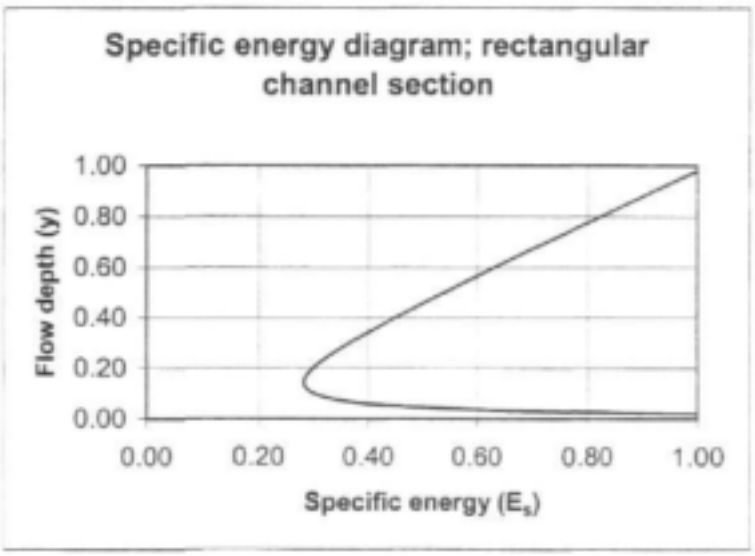

Figure 3.7: *Typical relationship between the flow depth and the specific energy for a rectangular section*

The value of E_s changes according to the flow depth **y**. If the flow depth reaches a critical value, that is $y = y_c$, the specific energy takes on a minimum value, $E_s = E_c$. It is quite clear from the graph that two different flow depths may be associated with a specific value of E_s. This means that the flow may be either subcritical or supercritical for the same value of E_s and quite different values for flow depths and velocities are possible.

Consider the following plan figure (showing a typical lay-out of bridge piers), as well as *figure 3.9,* in order to understand the change in water surface levels as water enters the space between the piers.

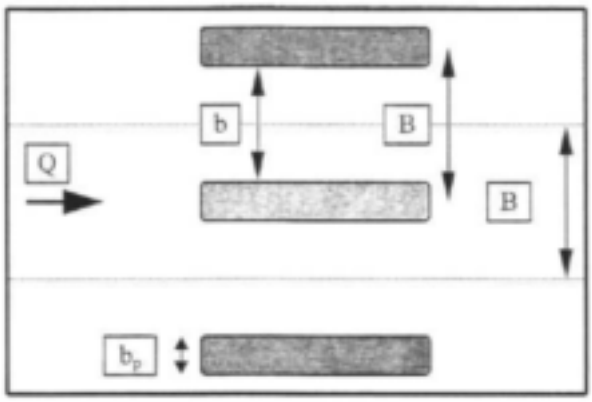

***Figure 3.8**: Typical pier lay-out, the flow is approaching from the left*

The distance between bridge pier centres is equal to **B** and this is also the representative width of approaching flow associated with each pier. The distance between piers in the contraction is equal to **b** and the width of each pier equals $\mathbf{b_p}$. The flow rate across width **B** is defined as **Q** as shown in the sketch. The total flow rate $\mathbf{Q_{tot}}$ can be calculated as the sum of **Q's**, or: $\Sigma\mathbf{Q}$. (According to convention flow will be towards the right in most figures.)

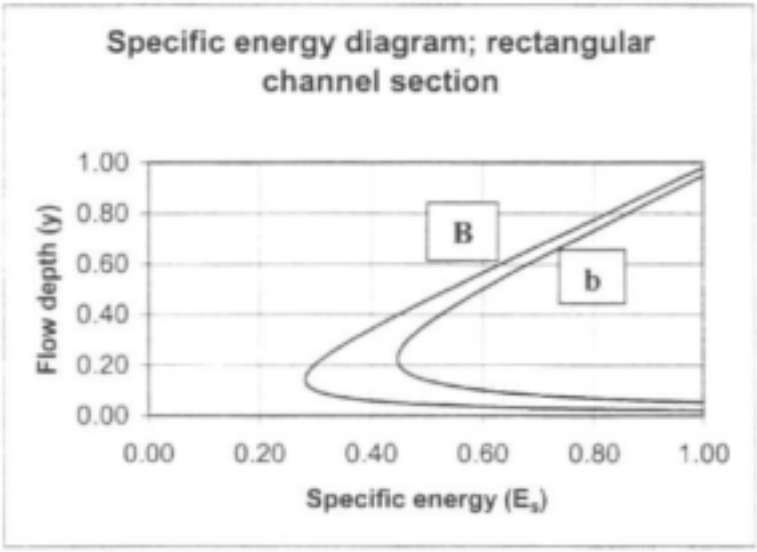

***Figure 3.9**: Flow depths vs. specific energy for two rectangular sections with widths B and b respectively*

It is important to note that the **y** vs. $\mathbf{E_s}$ relationship in *figure 3.9* is a function of the channel width. If we assume for the time being that both the approaching flow as well as the flow within the contraction are subcritical (which is often the case with high flows), one may explain the drop in water surface level in terms of energy principles. Assuming no energy losses (this assumption is justifiable because the energy losses occur mainly as transitional losses downstream of the pier) and constant specific energy head before and within the contraction (represented by the B and b curves respectively in *Figure 3.9)* it is evident from the graph that the flow depths have to differ (red lines). The depth associated with the **B** width is greater than that for the **b** width. The velocities must differ if the flow depths differ whilst water will flow slower upstream of the pier and faster within the contraction. This inter-relationship between depth and velocity makes it possible to measure pressure or depth differences around bridge structures and to convert these values into velocities. The conventional flow measuring method at bridges (bridge contraction method) is based on average depths and velocities and works on the same principle as a Venturi flume.

This study entailed the measurement of water pressures around a bridge pier. Due to stagnation the water at the upstream end of the pier is almost stationary, the specific energy value E_s here is virtually equal to the flow depth value as the velocity is almost zero. Within the contraction the E_s-value is made up of a smaller depth and a larger velocity head. Larger pressure or depth differences exist close to the pier as compared to the averaged values further upstream and downstream used in the conventional approach as followed by *d'Aubuisson* for instance *Webber* (1971).

Energy transformation at a bridge pier:

High flow rates past bridge piers are usually associated with damming upstream of the bridge and a consequent drop in water levels as the flow moves into the constriction between the piers. This has been discussed in detail in the previous section.

The conservation of the total energy head implies that the sum total of potential ε_p and kinetic ε_k energies stays the same if we ignore the losses as a first assumption and this may be used to explain the energy transformation associated with high flows around bridge piers.

It is a fact that an elemental particle of fluid at a fixed section and fixed values of flow rate **Q** and cross section (area **A** or width **B**) can not have a lower specific energy head than the critical specific energy head. For a given high flow rate **Q** it may happen that the specific energy of the approaching stream is lower than the critical specific energy associated with the same **Q** and reduced width ($B-b_p$), which is the width of the contraction. The only way in which the given discharge can pass through the constriction and at the same time satisfy the energy equation, is by increasing the approaching stream's energy head. This energy head must be larger than the specific energy value in the contraction, if losses are to be taken into account, or equal to the specific energy in the contraction, for the case of no losses.

In this case the upstream water level rises, resulting in a higher potential energy head. The kinetic energy head decreases at the same time because the flow rate **Q** stays the same while the cross sectional flow area **A** increases resulting in a decreased flow velocity **v** upstream. The result is an increase in energy head. This energy head increase (by means of a rise in water level) will continue until enough head has been built up to provide the critical energy head in the contraction. *Figure 3.10* shows the energy situation without damming; the solid line represents the water surface and the dotted line the energy line.

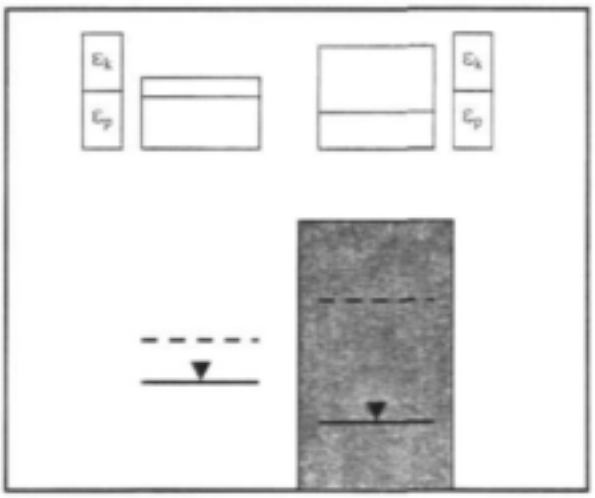

***Figure 3.10**: Theoretical potential and kinetic energy values upstream and within the contraction before damming takes place*

The relative contributions of kinetic and potential energy heads are represented by the ε_k and ε_p and blue rectangles respectively. It is evident that the sum totals of the energy components differ and they represent an unbalanced energy system.

Consider the same flow situation with enough damming to ensure a balance between the upstream and downstream energy heads.

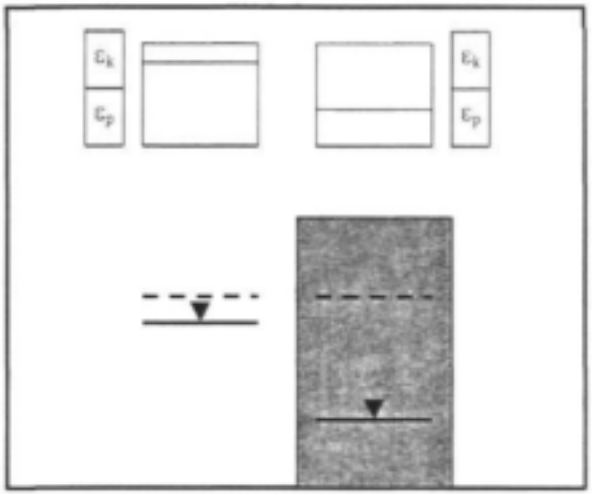

***Figure 3.11**: Potential and kinetic energy values upstream and within the contraction with damming*

Energy heads are now balanced as can be seen in *figure 3.11*. The sum totals of energy heads upstream and downstream of the bridge are the same.

Conventional applications of the Energy Equation for Flow Measurement: D'Aubuisson, Nagler and the "Bridge damming formula":

The method of *d'Aubuisson* (covered in *Webber* (1971)) is a classical example of a method which can be used for calculating flow rates at bridges in terms of average water surface levels upstream and downstream of bridges. The equation of *d'Aubuisson* was originally developed for calculating damming at bridges and can be derived as follows according to *Webber*, (1971).

Consider the following longitudinal section of a bridge pier (*figure 3.12*) and plan view (*figure 3.13*).

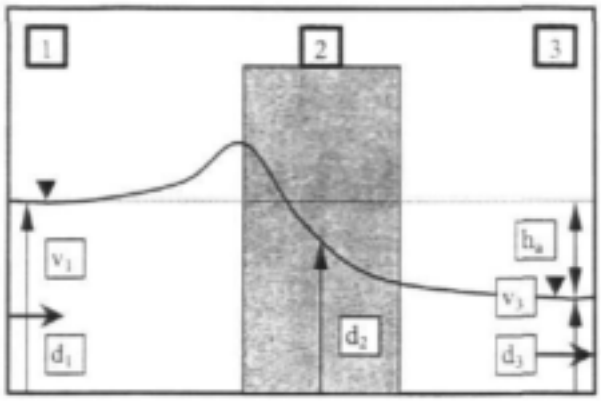

***Figure 3.12**: Longitudinal section of a bridge pier under high discharges*

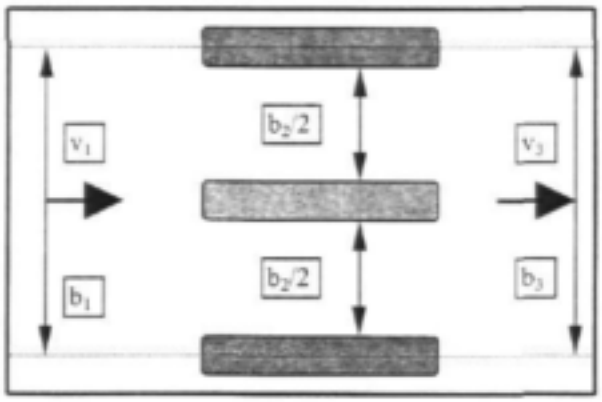

***Figure 3.13:** Plan view of a typical pier lay-out*

Bernoulli's energy equation can be applied between sections **1**,**2** and **3**, that is sections taken upstream, within the contraction, and downstream of the piers.

From *Bernoulli's* energy equation we have:

$$H_1 = H_2 + (\text{energy losses})_{1\text{-}2}$$

Also...

$$H_1 = H_3 + (\text{energy losses})_{1\text{-}3}$$

Expressing the energy heads in terms of specific energy ($E_s = H–z$) and assuming a horizontal bed:

$E_1 = E_2 + (energy\ losses)_{1\text{-}2}$

$$\Rightarrow \quad d_1 + \frac{v_1^2}{2g} = d_2 + \frac{v_2^2}{2g} + h_{L_{1\text{-}2}} \qquad \textit{(Equation 3.9)}$$

$$and \quad d_1 + \frac{v_1^2}{2g} = d_3 + \frac{v_3^2}{2g} + h_{L_{1\text{-}3}}$$

$$\Rightarrow \quad d_1 + \frac{v_1^2}{2g} = d_3 + \frac{v_3^2}{2g} + h_{L_{1\text{-}2}} + h_{L_{2\text{-}3}} \qquad \textit{(Equation 3.10)}$$

where $\mathbf{h_{L1\text{-}2}}$ primarily represents the contraction loss and $\mathbf{h_{L2\text{-}3}}$ the divergence loss.

The simplified assumption which is now made by *d'Aubuisson* is that the recovery of kinetic energy (ε_k) in the form of potential energy (ε_p) between sections 2 and 3 is negligible. This can be justified by the fact that such recovery is typically small, thus $\mathbf{d_2=d_3}$. The divergence energy loss thus equals:

$$h_{L_{2\text{-}3}} = \frac{v_2^2 - v_3^2}{2g}$$

Without recovery of ε_p, thus:

$$h_e = d_1 - d_3 = \frac{v_2^2}{2g} - \frac{v_1^2}{2g} + h_{L_{1\text{-}2}}$$

And from the continuity equation:

$$v_2 = \frac{Q}{A_2} = \frac{Q}{b_2 d_2} = \frac{Q}{b_3 d_3}$$

Therefore:

$$h_e = \frac{1}{2g}\left[\frac{Q^2}{b_2^2 d_3^2} - v_1^2\right] + h_{L_{1-2}}$$

$$\Rightarrow \quad 2g(h_e - h_{L_{1-2}}) = \frac{Q^2}{b_2^2 d_3^2} - v_1^2$$

$$\Rightarrow \quad \frac{Q^2}{b_2^2 d_3^2} = 2g(h_e - h_{L_{1-2}}) + v_1^2$$

$$\Rightarrow \quad Q = b_2 d_3 \sqrt{2g(h_e - h_{L_{1-2}}) + v_1^2} \qquad \textit{(Equation 3.11)}$$

C_d is defined as a flow correction factor that compensates for the loss $H_{L1\text{-}2}$ as well as other simplifying assumptions.

Therefore:

$$Q = C_d b_2 d_3 \sqrt{2gh_e + v_1^2} = C_d b_2 d_3 \sqrt{2g(d_1 - d_3) + v_1^2} \qquad \textit{(Equation 3.12)}$$

This equation has been in use for a long time and provides good results for long bridges, i.e. bridges which are long enough for piers to be considered as "isolated". Isolated piers

are defined as piers for which flow lines are not influenced by the effect of bridgeheads or neighbouring piers.

Nagler (*Webber*, 1971), also developed a formula. In the derivation of his equation he made provision for the recovery of potential energy providing very accurate results for cases with low turbulence.

According to *Basson's* (1990) work on damming at bridges, *Bradley* summarised the studies of *Liu, Bradley* and *Plate* (1957) on damming at bridges and called it "Hydraulics of Bridge Waterways" (University of Stellenbosch Department of Transport 1973). In this text he provides the general equation for calculating the height of dam upstream of a bridge:

Definitions of symbols:

h_1^*: Total increase in upstream depth [m].

K^*: Total damming coefficient [non dim].

α_1: Kinetic energy coefficient at section 1 [non dim] (*figure 3.12*)

α_2: Kinetic energy coefficient at section 2 [non dim] (*figure 3.12*)

A_{n2}: Cross-sectional area in the contraction measured below the normal water surface level [m^2].

$v_{n2} = Q/A_{n2}$

A_3: Cross-sectional area at section 3 (*figure 3.12*)

A_1: Cross-sectional area at section 1 (*figure 3.12*)

The formula reads (*figure 3.12* configuration):

$$h_1^* = K\alpha_2 \frac{v_{n2}^2}{2g} + \alpha_1\left(\left(\frac{A_{n2}}{A_3}\right)^2 - \left(\frac{A_{n2}}{A_1}\right)^2\right)\frac{v_{n2}^2}{2g} \qquad \textit{(Equation 3.13)}$$

By replacing v_{n2} with Q/A_{n2} in *equation 3.13* and because h_1^* is basically equal to $(d_1 - d_3)$ in *figure 3.12*, *equation 3.13* can be rewritten in order to express Q as a function of h_1^* or $(d_1 - d_3)$. This energy based equation is basically the same as those of *D'Aubuisson* and Nagler for Q is written as a function of water surface level differences measured *upstream* and *downstream* of a bridge.

Flood events in South Africa typically go hand in hand with high velocities and associated large fluctuations in water surface levels due to wave action. This also makes the above-mentioned bridge damming formulas (*D'Aubuisson*, *Nagler* and the general equation from "*The Hydraulics of Bridge Waterways*") inaccurate for discharge measurement purposes, given the relatively small differences in averaged water depths upstream and downstream of a bridge.

The unsuitability of the bridge damming formulas for accurate discharge measurement due to the small differences in averaged water depths can be explained as follows:

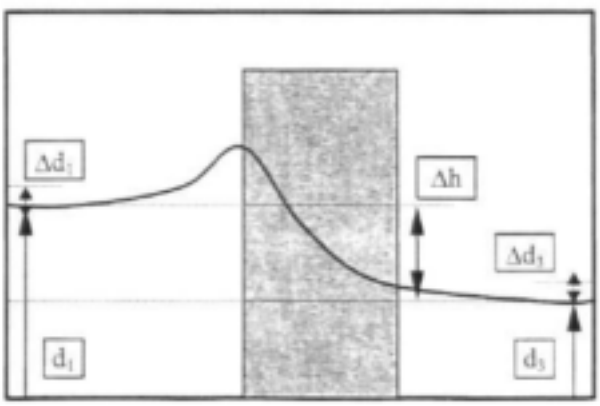

Figure 3.14: *Measuring water surface level differences between upstream and downstream of a bridge*

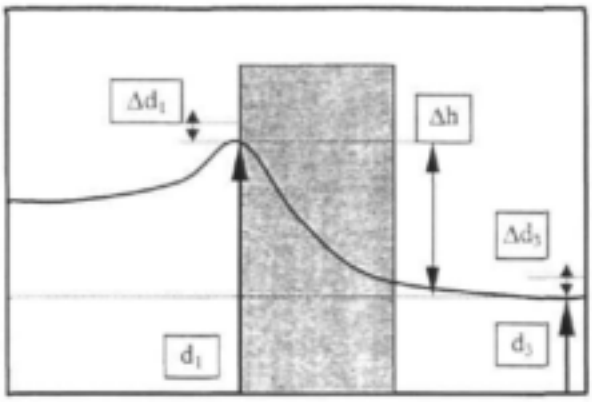

***Figure 3.15**: Water surface level differences between upstream and downstream of a bridge pier*

Sections **1 and 3** in *figure 3.14* and *figure 3.15* indicate positions where water levels are measured. *Figure 3.14* depicts the conventional system of defining water depths upstream and downstream of a bridge (*d'Aubuisson*, *Nagler* and the "*The Hydraulics of Bridge Waterways*" equations) whilst *figure 3.15* depicts the difference in water surface elevations between the upstream and downstream ends of a pier.

The flow rate **Q** is a function of $\Delta h = d_1 - d_3$ (this follows later from the Pitôt-tube theory). By expressing the error made in **Δh** as a function of "measurement errors in depths d_1 **and** d_3", we can calculate the error made in the calculation of **Q**. By expressing the error made in **Δh** for both configurations (*figure 3.14 and figure 3.15*), it can be shown that the latter method gives more accurate results than the other.

Consider the following definition for the error in **Δh**:

$$ERROR\ in\ \Delta h\ as\ \%\ of\ \Delta h = \frac{error\ in\ \Delta h}{correct\ value\ of\ \Delta h\ value} * \frac{100}{1}$$

$$\Rightarrow \quad ERROR = \frac{\Delta h - \left[\left(d_1 - \Delta d_1\right) - \left(d_3 - \Delta d_3\right)\right]}{correct\ \Delta h\ value} * \frac{100}{1}$$

$$\Rightarrow \quad ERROR = \frac{\Delta h - [(d_1 - \Delta d_1) - (d_3 - \Delta d_3)]}{\Delta h} * \frac{100}{1}$$

$$\Rightarrow \quad ERROR = \frac{\Delta h - [d_1 - d_3 + \Delta d_3 - \Delta d_1]}{\Delta h} * \frac{100}{1}$$

$$\Rightarrow \quad ERROR = \frac{\Delta h - \Delta h - (\Delta d_3 - \Delta d_1)}{\Delta h} * \frac{100}{1}$$

$$\Rightarrow \quad ERROR = \frac{\Delta d_1 - \Delta d_3}{\Delta h} * \frac{100}{1}$$

$$\Rightarrow \quad ERROR = \frac{\Delta d_1 - \Delta d_3}{d_1 - d_3} * \frac{100}{1} \qquad \textit{(Equation 3.14)}$$

Let us assume that the variations in the water surface level will cause the same measurement errors Δd_1 and Δd_3 for the two flow measuring configurations. It is now evident from *equation 3.14* that the error made in Δh and also the error in the flow rate **Q** will be greater for the measuring configuration shown in *figure 3.14*. The reason for this is that a smaller water surface level difference (Δh) is observed for the same value of ($\Delta d_1 - \Delta d_3$) in the *figure 3.14-configuration*. It is for this reason that the configuration in *figure 3.15* has been adopted.

The above discussion can be summarised by the detail in *photo 3.2*. Note that Δh_1 depicts the normal water surface level difference used by methods such as *D'Aubuisson*, *Nagler* and the "*Bridge damming formula*" being measured by the two water level recorders shown on *photo 3.2*. By measuring the water surface level difference next to the pier (Δh_2) it is possible to obtain a larger water surface level difference and therefore better accuracy.

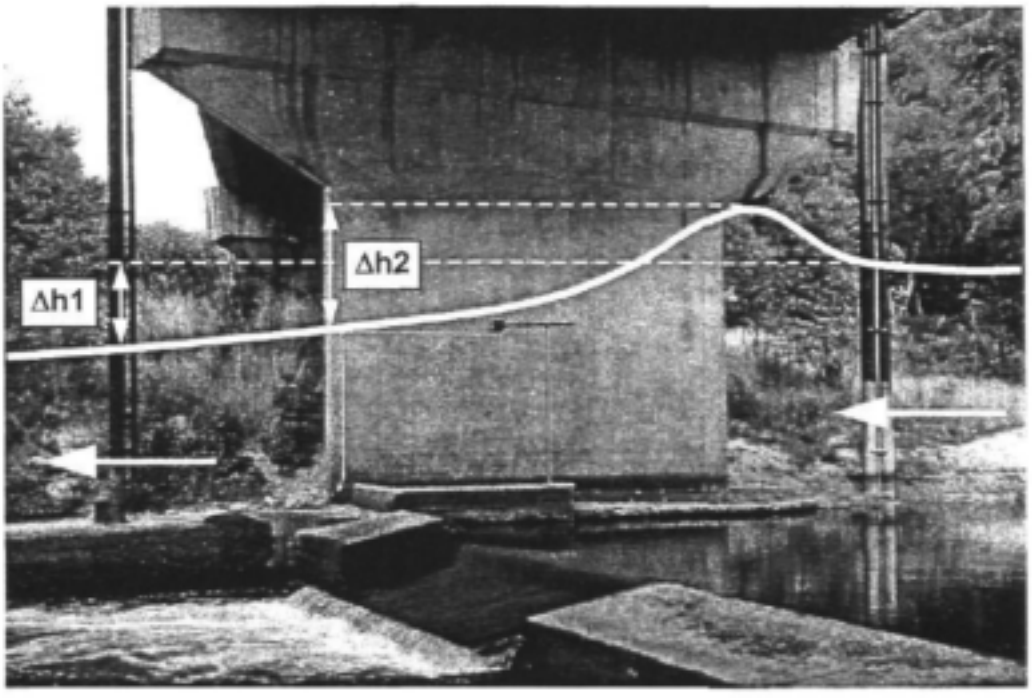

***Photo 3.2**: A typical water surface profile at a bridge pier during flood conditions, Δh_1 showing the normal water surface level difference measured at bridge piers and Δh_2 the pressure difference obtained by measuring pressures next to the pier*

Such an approach is not only more accurate, but is at the same time also fundamentally sound because it is based on the fact that water becomes stationary at the stagnation point upstream of a pier making a reliable estimate of the flow velocity possible here.

Application of the Energy equation in terms of measured pressures and water depths at bridge piers:

***Introduction, the Pitôt tube theory** (White,*1986**):**

Flow measurement at bridges based on the measurement of pressures around piers relies on the existence of a stagnation point. A measuring device which has long been in use to measure flow velocities and which is based on the principle of conservation of energy

between a stagnation point and flow elsewhere, has prompted investigations into the possible use of a pier for flow measurement. The instrument or measuring device is called a Pitôt-tube. The principle on which the Pitôt-tube works and the analogies between this simple measuring device and a pier as flow measuring device are set out in the following paragraphs.

A typical layout of a Pitôt-tube is depicted in *figure 3.16* (lay-outs differ but they all work on the same principle):

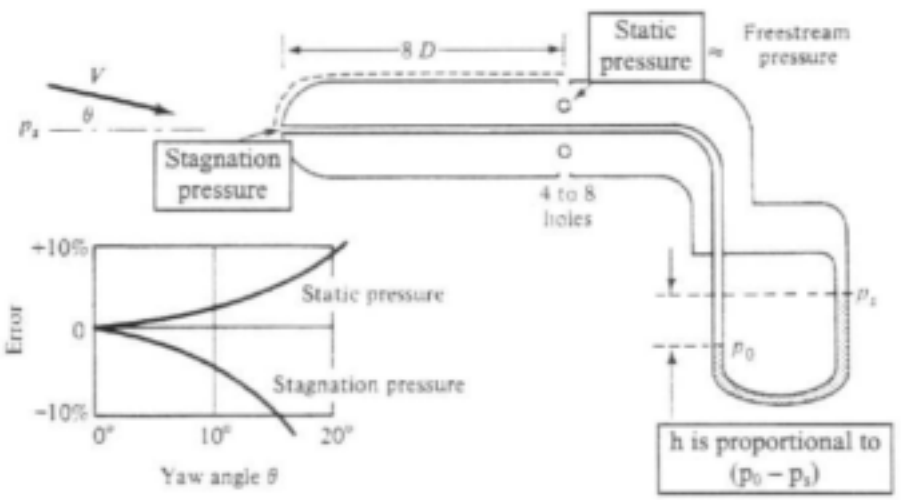

Figure 3.16: *A typical Pitôt-tube for measuring stream velocity; p_0 = dynamic or stagnation pressure, p_s = hydrostatic pressure, $h = p_0 - p_s$ (White, 1986)*

The *Pitôt*-tube essentially measures the difference between the dynamic (stagnation pressure) and hydrostatic pressure along a streamline. Note that $\mathbf{p_0}$ represents the dynamic or stagnation pressure and $\mathbf{p_s}$ the hydrostatic pressure or free flow pressure. On the side of the *Pitôt*-tube there are holes to measure the static pressure $\mathbf{p_0}$. As liquid inside the tube is stagnant, the approaching liquid will be decelerated to zero velocity. The pressure at this opening represents the dynamic or stagnation pressure $\mathbf{p_0}$. The

pressures p_0 and p_s are not measured separately but the difference between them is recorded by using the manometer as shown in *figure 3.16*.

Energy losses for flow past the Pitôt-tube are small and *Bernoulli's* energy equation therefore gives accurate results.

For incompressible fluids along a stream line (broken line in *figure 3.16*) with small energy losses:

$$\frac{p_s}{\rho g} + \frac{v_s^2}{2g} + z_s \approx \frac{p_o}{\rho g} + \frac{v_o^2}{2g} + z_o \qquad \textit{(Equation 3.15)}$$

By taking a horizontal streamline $z_0 = z_s$, *equation 3.15* can be simplified giving the following result:

$$v_s = \sqrt{\left[\frac{2(p_o - p_s)}{\rho}\right]} \qquad \textit{(Equation 3.16)}$$

Where v_0 has been taken as ≈ 0

This equation is known as the *Pitôt*-formula and is named after a French Engineer who developed the instrument in 1732 (*White*, 1986).

There is a resemblance between a *Pitôt*-tube and a bridge pier:

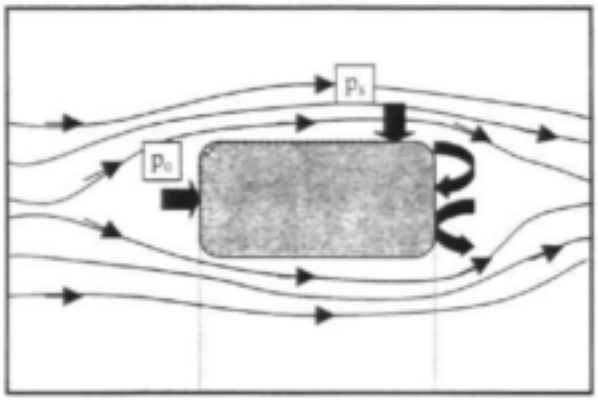

***Figure 3.17**: Typical flow lines around a bridge pier, p_0 ≡ dynamic or stagnation pressure, p_s ≡ hydrostatic pressure*

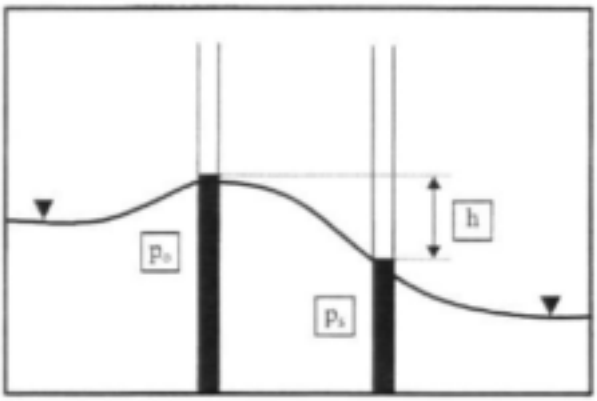

***Figure 3.18**: The same flow set-up as shown in figure 3.17, pressure and pressure differences in terms of manometer levels and manometer level differences*

Applying Bernoulli's energy equation for open channel flow along the dotted line (between the straight arrows) in *figure 3.17* and assuming that water may be regarded as incompressible in this case:

$$y_0 + \frac{v_0^2}{2g} + z_0 = y_s + \frac{v_s^2}{2g} + z_s \qquad \textit{(Equation 3.17)}$$

Adopting a horizontal river bed alongside the bridge pier, the term ($z_s - z_0$) will be zero and y_0 and y_s are the flow depths. We also assume that only small frictional and transitional losses occur over the short distance between points "**0**" and "**s**". This assumption is justifiable as the transitional losses occur mainly downstream of the pier and friction losses are small. The positioning of point "**s**" is upstream of the downstream end of the pier, i.e. upstream of the region where the main transitional losses occur in break-away eddies.

A stagnation point exists at the pier head and $v_s \approx 0$. *Equation 3.17* becomes:

$$y_0 + 0 = y_s + \frac{v_s^2}{2g}$$

$$\Rightarrow \; v_s^2 = 2g(y_0 - y_s)$$

$$\Rightarrow \; v_s = \sqrt{2g(y_0 - y_s)}$$

with

$$\left(y_0 = \frac{p_0}{\gamma} \; \textit{and} \; y_s = \frac{p_s}{\gamma} \right)$$

(Equation 3.18)

The pressure distribution in open channel flow is hydrostatic if flow is either uniform or stagnant, therefore:

$$p = \rho g y$$

$$\Rightarrow \; y = \frac{p}{\rho g}$$

Substitute **y** as defined above into *equation 3.18*:

$$\Rightarrow \; v_s \approx \sqrt{\frac{2g}{\rho g}(p_0 - p_s)}$$

$$\Rightarrow \quad v_s \approx \sqrt{\frac{2(p_s - p_s)}{\rho}} \qquad \textit{(Equation 3.19)}$$

This equation corresponds with the previous equation for the Pitôt-tube (*equation 3.16*).

This relationship forms the basis of flow measurement by means of pressure recordings alongside bridge piers based on the ***energy principle***.

Theory (Application of the Energy equation in terms of measured pressures and water depths at bridge piers):

The following approach uses the energy equation express the flow rate **Q** in terms of measurable flow variables in the vicinity of the pier.

Consider the energy equation of *Bernoulli*:

$$\frac{\alpha \bar{v}_1^{\,2}}{2g} + y_1 + z_1 = \frac{\alpha \bar{v}_2^{\,2}}{2g} + y_2 + z_2 + \sum h_{L_{1\text{-}2}} + h_{f_{1\text{-}2}} \qquad \textit{(Equation 3.20)}$$

This equation is applicable along any streamline. By applying this equation between points **F** and **G** and **G** and **I** (*figure 3.5*) respectively, we end up with two possible flow rate equations in terms of flow variables at sections **1, 2** and **4** (*figure 3.5*).

Consider firstly a flow line taken between **F** and **G**. By ignoring frictional losses since the distance is very short, the term $\Sigma h_{f1\text{-}2}$ (*equation 3.20*) can be eliminated:

$$\frac{\alpha \bar{v}_F^{\,2}}{2g} + y_F + z_F = \frac{\alpha \bar{v}_G^{\,2}}{2g} + y_G + z_G + h_{L_{F-G}} \qquad \textit{(Equation 3.21)}$$

h_{LF-G} represents the transitional losses between positions **F** and **G**.

Assuming a horizontal bed around the pier, i.e.:

$z_F = z_G$

Substituting $z_F = z_G$, *equation 3.21* simplifies to:

$$\frac{\alpha \bar{v}_F^{\,2}}{2g} + y_F = \frac{\alpha \bar{v}_G^{\,2}}{2g} + y_G + h_{L_{F-G}} \qquad \textit{(Equation 3.22)}$$

A stagnation point forms at **G** where the water is decelerated to zero velocity next to the upstream head of the pier. We can therefore set:

$v_G \approx 0$

$$\Rightarrow \frac{v_G^{\,2}}{2g} \approx 0$$

$$\Rightarrow \frac{\alpha \bar{v}_F^{\,2}}{2g} + y_F = y_G + h_{L_{F-G}}$$

$$\Rightarrow v_F^{\,2} = \tfrac{2g}{\alpha}\left[\left(y_G - y_F\right) + h_{L_{F-G}}\right]$$

$$\Rightarrow v_F = \sqrt{\tfrac{2g}{\alpha}\left[\left(y_G - y_F\right) + h_{L_{F-G}}\right]} \qquad \textit{(Equation 3.23)}$$

Applying the continuity equation to **section 1** at **F** (*figure 3.5*):

$$Q = \bar{v}_1 A_1 = \bar{v}_F A_F = \bar{v}_F B y_F$$

This implies that we assume a uniform flow depth over the width at **section 1** and therefore also uniform velocity. This is a reasonable assumption for the flow at **section 1** has not yet experienced any contraction. Using the energy and continuity results together:

$$v_F = \frac{Q}{B_F y_F} = \sqrt{\tfrac{2g}{\alpha}\left[(y_G - y_F) + h_{L_{F-G}}\right]}$$

$$\Rightarrow Q = B_F y_F \sqrt{\tfrac{2g}{\alpha}\left[(y_G - y_F) + h_{L_{F-G}}\right]} = C_d B_F y_F \sqrt{\tfrac{2g}{\alpha}\left[(y_G - y_F)\right]} \qquad \textit{(Equation 3.24)}$$

The **C_d-value** is known as a flow correction factor and compensates for transitional losses and simplified assumptions made in the energy based model.

By considering secondly a streamline along **GI** we find exactly the same form of equation as *equation 3.24*, but in terms of flow characteristics at **G** and **I** (*figure 3.5*).

$$Q = C_d B_I y_I \sqrt{\tfrac{2g}{\alpha}\left[(y_G - y_I)\right]} \qquad \textit{(Equation 3.25)}$$

Results (Energy based flow rate equation):

Both *equation 3.24* and *equation 3.25* (preferred) were calibrated using model data and very good results were obtained in terms of **C_d**-values. The data used for the calibration

process were obtained from tests done by *Retief* (1998) in the Hydraulics Laboratory at the University of Stellenbosch.

The energy-based theory is simple and gives good results within a narrow accuracy band. C_d-values varied from **0.89** to **1.03** for the "normal flows" (control forming within the pier opening), it varied from **0.95** to **1.04** for the case of debris accumulation and varied from **0.82** to **0.97** for drowned conditions. This means that the purely theoretical flow rates differed from the real flow rates by a maximum value of **11%** for the supercritical flows, **5%** with debris accumulation and **18%** for drowned conditions. Refer to *section 3.9* for graphs based on the energy theory applied to *Retief's* data. Refer to Appendix A "Energy Approach" for the laboratory data and results.

3.7 MOMENTUM APPROACH:

Derivation:

Newton's second law has been linked in the previous section to "*The Law of the Conservation of Energy*" which has been used to find a flow rate equation in terms of flow variables for the pier flow lay-out. In this section the Law of Conservation of Momentum is considered in order to find a flow rate equation. It will be shown that this law also originates from Newton's second law.

Definitions of symbols:

a: Acceleration of the particle [m/s^2]

m: Mass of the particle [kg]

F_{res}: Resultant force acting upon as system [N]

v: Velocity of flow [m/s]

dx: Small increment in variable x [dim of x]

$^{dx}/_{dt}$: Time derivative with respect to variable x [non dim]

$I_{1\text{-}2}$: Impulse transferred to a particle within a time equal to t_2-t_1 [kg.m/s]

M: Momentum [kg.m/s]

$$F_{res} = ma$$

$$\Rightarrow F_{res} = m\frac{dv}{dt}$$

$$\Rightarrow F_{res}.dt = m.dv$$

$$\Rightarrow \left(\sum dF\right)dt = m.dv$$

$$\Rightarrow \int_{t_1}^{t_2}\left(\sum dF\right)dt = \int_{v_1}^{v_2} m.dv$$

$$\Rightarrow \quad Impulse \equiv I = mv_2 - mv_1 = m\Delta v \qquad \textit{(Equation 3.26)}$$

$$\Rightarrow \quad I_{1\text{-}2} = M_2 - M_1$$

Note that the **$I_{1\text{-}2}$-term** (**I** = force multiplied by time) represents an impulse. *Equation 3.26* basically states that if an impulse **$I_{1\text{-}2}$** is transferred to an object with constant mass **m**, it will give rise to a change in velocity **Δv** over a short time interval **$\Delta t = t_2 - t_1$**.

This result is known as the principle of linear impulse and momentum. Momentum is defined as the product of mass and velocity with units of [**kg.m/s**].

The Law of Conservation of Momentum can be described for fluid mechanics as follows (*Hibbeler*, 1992):

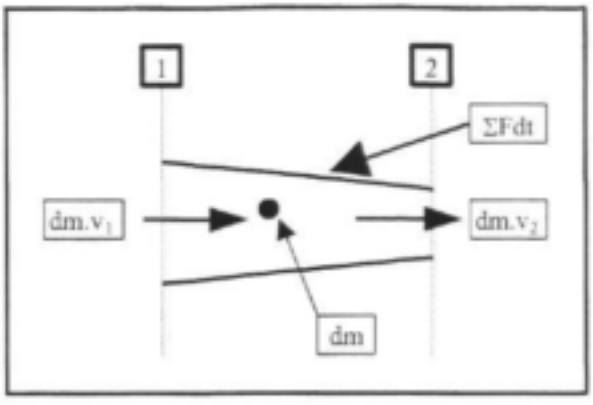

Figure 3.19**: A small particle with mass* **dm** *forms part of a fluid mass flowing from* ***section 1 *to* ***section 2***

Starting with the principle of linear impulse and momentum:

$$M_1 + I_{1\text{-}2} = M_2$$

$$\Rightarrow dm.v_1 + m\bar{v} + \sum F_{1\text{-}2}.dt = dm.v_2 + m\bar{v}$$

$$\Rightarrow \sum F_{1\text{-}2}.dt = dm.v_2 - dm.v_1$$

$$\Rightarrow \sum F_{1\text{-}2} = \frac{dm}{dt}(v_2 - v_1)$$

$$\Rightarrow F_{res} = \frac{d}{dt}(m)(v_2 - v_1)$$

$$\Rightarrow F_{res} = \frac{d}{dt}(\rho V)(v_2 - v_1)$$

$$\Rightarrow F_{res} = \rho Q(v_2 - v_1)$$

$$\Rightarrow F_{res} = \rho Q v_2 - \rho Q v_1 = \rho Q v_{out} - \rho Q v_{in} \qquad \textit{(Equation 3.27)}$$

Equation 3.27 is known as the momentum equation in fluid mechanics. Note that reference is made to a momentum equation even though the terms have units of force. The reason is that the equation is based on momentum principles, or the change in momentum with time.

An overview of drag forces (*Webber*, 1971):

This study focused on the flow patterns around a bridge pier in order to determine the possibility of using it as a flow measuring structure. One possible approach is to use drag force theory considering a liquid and a stationary object (in our case) which experience relative movement.

The bridge pier exercises a force on the passing stream. According to Newton's Third Law (**N III**) the liquid will also exercise a force of the same magnitude but opposite in direction on the bridge pier.

Drag forces are observed in everyday life. Take for example a boat in a river. If it were not for an anchor holding the boat in position, the boat would drift off in the flow direction. If the boat was to be anchored, which force was to cause the tensile stress in the anchor rope? It should be a force that originates from the flowing current which acts upon the boat and is then transferred to the anchor rope. This force acting on the boat is nothing else but a drag force – this is pure evidence of the existence of drag forces exerted by flowing currents on objects.

Consider the plan view of a bridge pier in *figure 3.20* and *figure 3.21*:

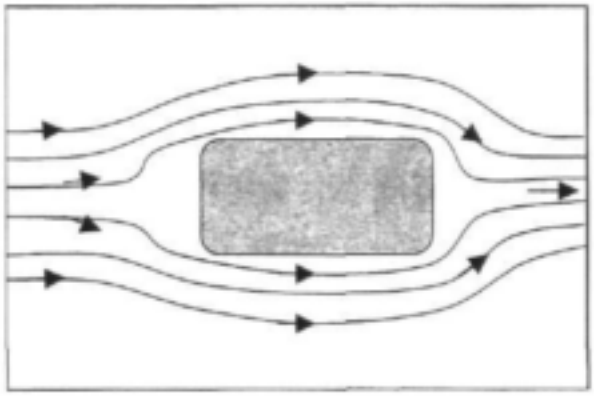

***Figure 3.20**: Flow lines around a bridge pier for the case of an ideal fluid*

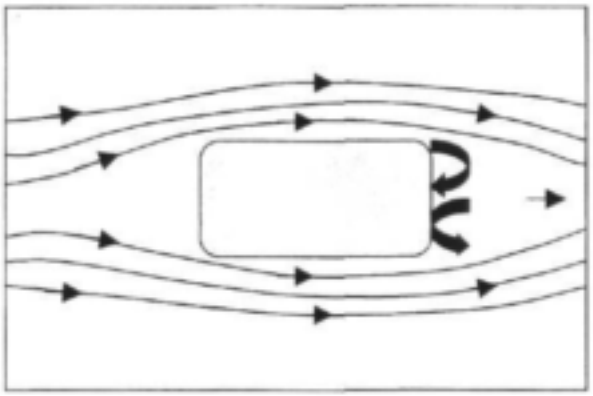

***Figure 3.21:** Flow lines around a bridge pier for the case of turbulent flow of a non-ideal fluid*

For an ideal fluid (*figure 3.20*), no viscous drag forces exist. In addition to this the symmetrical arrangement of flow lines implies that the effective force due to pressure differences will be zero and this being the only force, the drag force will be zero.

For the case of turbulent flow (*figure 3.21*), which is typically found in rivers, we find that the symmetrical flow pattern becomes disturbed. The flow lines break away from the surface near the downstream end of the pier and rotating eddies start forming. A reduction in the pressure force acting on the downstream end of the pier results and we find an unbalanced system in terms of upstream and downstream forces acting on the pier. This pressure difference forms the main contribution to the total drag force

experienced by blunt piers. Consider *figure 3.22* showing the forces acting on a typical pier:

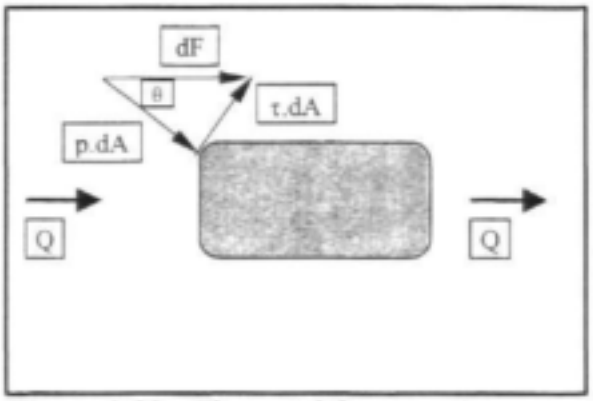

Figure 3.22: *Elemental forces acting on area* **dA** *of a typ*ical pier; **p.dA** forms an angle of θ with the flow direction and **τ.dA** an angle of **(90-θ)**

The forces acting on a small elementary area **dA** of the pier can be split into two components, a force **p.dA** normal to the surface and a shear force **τ.dA** working in a tangential direction to the pier surface. Taking both forces' components in a direction parallel to the flow direction and summing them, the resultant force **dF** follows:

$$dF = p\cos(\theta)dA + \tau\sin(\theta)dA$$

Integrating **dF** around the pier:

$$F = \int p\cos(\theta)dA + \int \tau\cos(\theta)dA$$
$$\Rightarrow F = F_p + F_s \qquad \textit{(Equation 3.28)}$$

The force **F** is the total drag force and is the sum of $\mathbf{F_p}$, the pressure drag force or form drag force and $\mathbf{F_s}$, the surface drag force or skin friction drag force. The relative contributions of these two forces depend mainly on the shape and size of the obstruction

within the flowing stream. It is clear that a blunt object will give rise to strong eddy formation at the downstream end leading to a larger contribution of F_p than of F_s. On the other hand, one will find that a streamlined obstruction orientated with its longest axis parallel to the flow direction will experience a much greater contribution of F_s than of F_p.

A streamlined "aerofoil" is the most effective shape to ensure a minimum drag force. This shape would be ideal for a pier seen from a hydraulic resistance point of view, but due to structural and aesthetical considerations only a limited amount of streamlining is possible in general.

The drag coefficient C_d^* represents the ratio of the true drag force relative to the dynamic force:

$$C_d^* = \frac{F}{\frac{1}{2}\rho v^2 A} \qquad \textit{(Equation 3.29)}$$

Note that v represents the relative velocity and A the projected area of the object measured in a plane perpendicular to the flow direction. The direct measurement of the drag force is usually done in wind tunnels, canals, towing tanks etc.

The form drag F_p can be determined by measuring the pressures along the surface of an obstruction with a stream of water or air flowing past. Integrating over the total surface area yields the form drag. The surface drag F_s can be determined if the total drag F and form drag F_p are known, from:

$$F = F_p + F_s \qquad \textit{(Equation 3.30)}$$

Large contributions to **F** in the form of $\mathbf{F_p}$ go hand in hand with large transitional energy losses. $\mathbf{F_p}$ is usually associated with eddying motion leeward of the obstruction. Eddies are associated with changes in both the direction and the magnitude of the flow velocity and give rise to transitional energy losses which occur mainly downstream of the pier.

Forces acting on bridge piers:

The typical design problem constitutes the calculation of forces in the flow direction that will have an impact on the structure under investigation. These forces can be calculated using the following equation:

$$F = \tfrac{1}{2} C_d^{*} \rho L v^2 y \qquad \textit{(Equation 3.31)}$$

Definitions of symbols:

F: drag force on the pier [N]

C_d^{*}: drag coefficient (*equation 3.29*) [non dim]

ρ: mass density of fluid under investigation [kg/m^3]

L: length of the obstruction [m]

v: velocity of fluid [m/s]

y: height to which flow dams up at the upstream side of the obstruction [m]

It is clear from *equation 3.31* that for calculating **F**, the velocity **v** should be known, therefore, the flow rate **Q** needs to be known - whether estimated from measurements or calculated.

Conventional applications of the Momentum equation with respect to flow measurement

It is interesting to note that the Momentum equation is not often used to measure flow rates. It is normally used to calculate forces on bridge piers knowing the flow rate. *Basson's* (1990) study made use of the Momentum equation in order to calculate forces on bridges during high flows and knowing the forces he was able to calculate the drag coefficients from the general drag formula. The following are typical formulae for calculating the drag forces on bridge piers and could be used in conjunction with the Momentum equation to calculate the respective drag coefficients (when the flow rate is known) or to calculate the flow rate when accurate values of drag coefficients are known.

The following formulae were taken form *Basson's* (1990) work on damming at bridges and can all be used to calculate the forces acting on bridge piers.

The Ontario format:

$$F = \frac{\rho C_D A v^2}{2} \qquad \textit{(Equation 3.32)}$$

Definitions of symbols:

F: The force exerted on the bridge pier [N].

A: Projected pier area perpendicular to the flow direction [m^2].

C_D: Drag coefficient according to the pier shape: Rectangular (C_D = 1.4); Rounded (C_D = 0.7); Sharp nose (C_D = 0.8); Debris accumulating around a rectangular pier (C_D = 1.4) [non dim].

ρ: Mass density of water [1000 kg/m^3]

v: Flow velocity [m/s]

The South African format:

$$F = KA_4 v^2 \qquad \textit{(Equation 3.33)}$$

Definitions of symbols:

F: The force exerted on the bridge pier [kN].

A_4: Projected pier area perpendicular to the flow direction [m^2].

K: Coefficient which is a function of the pier shape [non dim].

v: Flow velocity [m/s]

The Apelt&Isaacs format:

$$F = C\rho v^2 y \frac{L}{2} \qquad \textit{(Equation 3.34)}$$

Definitions of symbols:

F: The force exerted on the bridge pier [N]

L: Length or diameter of pier [m]

C: Coefficient of drag [non dim]

v: Approach flow velocity [m/s]

ρ: Mass density of water [1000 kg/m^3]

The general drag force equation:

$$F = \rho \frac{A_p}{2} v_{n\perp N}{}^2 C_D \qquad \textit{(Equation 3.35)}$$

Definitions of symbols:

F: The force exerted on the bridge pier [N]

C_D: Hydrodynamic drag coefficient [non dim]

v_{n2N}: Approach flow velocity [m/s]

ρ: Mass density of water [1000 kg/m^3]

A_p: Projected pier area in line with the flow direction, taken to be bounded by the upstream water surface level [m^2]

Application of the Momentum principle in terms of measured pressures and water depths at bridge piers:

Introduction:

A formula is sought which can express the flow rate in terms of measurable flow parameters at bridge piers by applying the fundamental laws of fluid mechanics. In this section we focus on the application of the Momentum equation in order to find a formula for **Q**.

Theory (Application of the Momentum principle in terms of measured pressures and water depths at bridge piers):

The Momentum equation is applicable to a control volume and not to a streamline as is the case with the energy equation. A suitable control volume should be enclosed by sections where the velocity and depth do not change across each section. Such sections were earlier identified as sections **1**, **3**, **4** and **5** (*figure 3.5*). **Section 2** does not comply with the criteria for a suitable section due to the damming around the pier and the variation in water depth over the width. Section **5** is situated downstream of the pier. Between **section 4** and **section 5** large eddies form implying high transitional energy

losses, as well as momentum transfer and this section has therefore not been used as a control volume boundary. Only sections **1**, **3** and **4** were identified as being suitable. To ensure measurable water level differences, the **1-3** and **1-4** combinations of sections were selected.

The derivation of the Momentum based flow rate equation follows the same steps for each of the two combinations and therefore only the **1-3** combination's derivation is shown.

The momentum equation states:

$$F_{res} = \sum F = \rho Q v_{leaving} - \rho Q v_{entering} \qquad \textit{(Equation 3.36)}$$

The **1-3** combination corresponds to control volume **ACMK** (refer to *figure 3.5*). The resultant force $\mathbf{F_{res}}$ is made up of the two hydrostatic forces acting at **sections 1** and **3** as well as the drag force due to the pier, therefore:

$$\tfrac{1}{2}\rho g y_1^{\,2} B_1^{\,2} - \tfrac{1}{2}\rho g y_3^{\,2} B_3^{\,2} - F_{pier} = \rho Q v_3 - \rho Q v_1$$

$$\Rightarrow \tfrac{1}{2}\rho g y_1 B_1^{\,2} - \tfrac{1}{2}\rho g y_3 B_3^{\,2} - \tfrac{1}{2}\rho C_d^{\,*} A v_1^{\,2} = \rho Q v_3 - \rho Q v_1 \qquad \textit{(Equation 3.37)}$$

The "general drag force equation" ($\mathbf{F = {}^1/_2\rho C_d^{\,*} A v^2}$), as discussed in the previous section (*p.56* and *p.58*) is used to represent the pier force $\mathbf{F_{pier}}$ in *equation 3.37*.

From the continuity law:

$$Q = v_1 y_1 B_1 = v_3 y_3 B_3$$

$$\Rightarrow v_1 = \frac{Q}{y_1 B_3} \text{ en } v_3 = \frac{Q}{y_3 B_3}$$

Substitute these terms into *equation 3.37* :

$$\tfrac{1}{2}\rho g y_1^{\,2} B_1 - \tfrac{1}{2}\rho g y_3^{\,2} B_3 - \tfrac{1}{2}\rho C_d^{\,*} A\left[\frac{Q^2}{y_1^{\,2} B_1^{\,2}}\right] = \rho Q\left[\frac{Q}{y_3 B_3}\right] - \rho Q\left[\frac{Q}{y_1 B_1}\right]$$

After simplification:

$$Q = C_d \sqrt{\frac{\tfrac{1}{2} g\left(y_1^{\,2} B_1 - y_3^{\,2} B_3\right)}{\left(\frac{1}{y_3 B_3} - \frac{1}{y_1 B_1} + \frac{C_d^{\,*} A^*}{2 y_1^{\,2} B_1^{\,2}}\right)}}$$ for the **1-3** combination of sections **or**

$$Q = C_d \sqrt{\frac{\tfrac{1}{2} g\left(y_1^{\,2} B_1 - y_4^{\,2} B_4\right)}{\left(\frac{1}{y_4 B_4} - \frac{1}{y_1 B_1} + \frac{C_d^{\,*} A^*}{2 y_1^{\,2} B_1^{\,2}}\right)}}$$ for the **1-4** combination of sections *(Equations 3.38)*

Note that $\mathbf{C_d^*}$ is the drag coefficient and $\mathbf{C_d}$ the flow correction factor. $\mathbf{C_d}$ represents the ratio between the real flow rate and the theoretical flow rate compensating for transitional losses.

Results:

Retief's data were used to calibrate *equation 3.38*. A drag coefficient of $\mathbf{C_d^* = 0.7}$ was used as recommended by the *Ontario Bridge Design Code* for the pier shape (bull nose) to which *Basson* (1992) refers in his work on hydraulic forces on bridges. He suggested that larger values for $\mathbf{C_d^*}$ of up to **3** could possibly apply. The results of the laboratory

tests confirmed this. During the calibration process the value of C_d^* for each model pier (1-4 section combination only) was determined in order to see whether this value changes with the pier width and with flow rate. In order to calculate C_d^*, the value of C_d was set equal to one. C_d^* values varied from **3** to **7** confirming the potential underestimation of the drag force on bridge piers for high flows.

The goal with the calibration process was to see whether stable **C_d-coefficients** could be found in order to use *equation 3.38* as a reliable flow rate equation. As the flow rate is not greatly dependent on the drag force (and therefore on C_d^*), a **C_d^*-value** of **0.7** was adopted for the bull-nose shaped pier. The **C_d^*-value** was therefore fixed and the calibration process merely required the calculation of the **C_d-value** for each respective flow rate.

It was surprising to note that the **C_d-values** did not vary much and were close to unity (especially for the **30 mm** pier). This implies firstly that the flow rate is not very sensitive to the drag force and therefore to the **C_d^*-value** in terms of the Momentum based theory (if the drag force is defined in terms of the upstream velocity). Secondly, the Momentum theory proves to work well even if a constant **C_d^*-value** is assumed, and can therefore be used to calculate the flow rate with relatively good accuracy.

The flow rate according to laboratory data has been overestimated by *equation 3.38* and errors varied between **+9%** and **+19%** (constant **C_d^*-value** assumed) for supercritical flows where a control section occurred within the pier length.

One of the drawbacks of the momentum based flow equation is the fact that the flow rate **Q** is defined in terms of depths y_1 and y_4 whilst in practice y_2 and y_4 will be measured.

The **1-3** combination gave **C_d-values** that varied from **0.78** to **1.09** whilst the **1-4** combination of sections gave values of C_d from **0.81** to **0.90**. The **1-4** combination was identified as the most suitable configuration to use in order to obtain the least variable

C_d-coefficients. The **C_d-values** for the condition with debris varied from **0.80** to **0.98** and for the drowned conditions from **0.50** to **0.87**. Refer to Appendix A "Momentum Approach" for the laboratory data and results.

3.8 POWER APPROACH:

Derivation:

In the previous section the momentum equation was derived from **Newton II**. It was also shown that a flow rate equation could be derived using the Law of the Conservation of Momentum. In this section the focus is transferred to the concept of the time derivative of work. **Newton II** will again be used to show that the Power Law originates from it. A flow rate equation based on the Power Law is also derived.

Power is defined as the rate at which work is performed:

Definitions of symbols:

P: Power [N.m/s = Watt]

W: Work [J]

t: time [s]

F: Force [N]

v: Velocity of flow [m/s]

dx: Small increment in variable x [dim of x]

$^{dx}/_{dt}$: Time derivative with respect to variable x [non dim]

ε_k: Kinetic energy at a specific section [J = N.m]

ε_p: Potential energy at a specific section [J = N.m]

$$P = \frac{work}{time} = \frac{W}{t} = \frac{dW}{dt} \qquad \textit{(Equation 3.39)}$$

$$\Rightarrow \quad P = \int dP = \int\left(\frac{dW}{dt}\right)$$

We define work as the product of force and distance viz. **W = Fs**:

$$\Rightarrow \quad P = \int \frac{d(Fs)}{dt} = F\int \frac{ds}{dt} = F\int dv = F.v$$

The equation for the Conservation of Power can be derived from the basic energy equation which originates from Newton's second law.

$$\varepsilon_{p_1} + \varepsilon_{k_1} + \sum U_{1\text{-}2} = \varepsilon_{p_2} + \varepsilon_{k_2} \qquad \textit{(Equation 3.40)}$$

$$\Rightarrow \sum U_{1\text{-}2} = \left(\varepsilon_{p_2} - \varepsilon_{p_1}\right) + \left(\varepsilon_{k_2} - \varepsilon_{k_1}\right)$$

Take the time derivative on both sides:

$$\Rightarrow \quad \frac{d}{dt}\left(\sum U_{1\text{-}2}\right) = \frac{d\left(\Delta\varepsilon_p\right)}{dt} + \frac{d\left(\Delta\varepsilon_k\right)}{dt} \qquad \textit{(Equation 3.41)}$$

Equation 3.41 implies that the "*net power*" of a system represents the rate at which potential energy ε_p changes between sections **1** and **2** plus the rate at which the kinetic energy ε_k changes between the same two sections.

Take the example of a ship moving at a constant velocity **v** along a horizontal trajectory.

Applying *equation 3.41* to our example problem and writing the left-hand side in terms of parameters describing movements, we find the following (note that LHS = Left hand side of *equation 3.41*):

Definitions of symbols:

LHS:	Left Hand Side of *equation 3.41* [N.m/s = Watt]
RHS:	Right Hand Side of *equation 3.41* [N.m/s = Watt]
F_i:	Force associated with a specific action, mechanical, friction etc. [N]
F_{res}:	Resultant force, resultant of forces ΣF_i [N]
v:	Velocity of the ship relative to the water mass [m/s]
$U_{1\text{-}2}$:	Work performed by the resultant force $\mathbf{F_{res}}$ from **point 1** to **point 2** [J]
m:	Mass of the ship [kg]
g:	Unit gravitational force [m/s^2]
h:	Vertical distance measured from a specific datum line [m]
mgh:	General product for potential energy [J]
$^1/_2mv^2$:	General product for kinetic energy [J]

$$LHS = \frac{d}{dt}\left(\sum U_{1-2}\right) = \frac{d}{dt}\left[F_{ship\_engine}.v - F_{air\ resistance}.v - F_{water\_resistance}.v \pm F_{motor}.v\right] = \frac{d}{dt}\left[F_{res}.v\right]$$

The right hand side of the equation may be written as follows:

$$RHS = \frac{d\left(mgh_2 - mgh_1\right)}{dt} + \frac{d\left(\frac{mv_2^2}{2} - \frac{mv_1^2}{2}\right)}{dt} = \frac{d\left(mgh - mgh\right)}{dt} + \frac{d\left(\frac{mv^2}{2} - \frac{mv^2}{2}\right)}{dt} = \frac{d(0)}{dt} = 0$$

The right hand side of *equation 3.41* equals zero as can be seen above. For the equation to hold, the left-hand side needs to be zero too, this means the net power should be zero. This is indeed true because the ship moves at a constant velocity and therefore experiences no acceleration. This is true because there are no unbalanced forces resulting

in a zero resultant force. A zero resultant force implies zero net work and therefore zero net power. This agrees with the zero RHS of the equation. Therefore, this simple example shows that the net power (time derivative of the work done by the net or resultant force) equals the rate of change in kinetic energy plus the rate of change in potential energy.

Application of the Power equation in terms of measured pressures and water depths at bridge piers:

Introduction:

The following equation states "*The law of the conservation of power*". It was derived earlier on and was shown to be a time derivative of the total energy equation. In this section the power equation will be used to show its application in terms of pressures at bridge piers for the measurement of flow rates.

Consider the power equation as derived earlier:

$$\frac{d}{dt}\left[\sum U_{1\text{-}2}\right]=\frac{d}{dt}\left(\Delta\varepsilon_{p}\right)+\frac{d}{dt}\left(\Delta\varepsilon_{k}\right) \qquad \textit{(Equation 3.42)}$$

This equation states that the change in power between section **1** and **2** as depicted in terms of the change in potential and kinetic energy (**RHS** of *equation 3.42*), should equal the change in power between the same two sections, generated by the resultant force acting upon the system under investigation. The resultant and dominating force has been identified as the total drag force on the pier.

The impact of secondary forces as contributors to the resultant force has been ignored in the power approach for they are of much smaller value than the total drag force.

Derivation (Application of the Power equation in terms of measured pressures and flow depths at bridge piers):

Rewriting *equation 3.42* in terms of drag power:

$$\Rightarrow \quad \kappa P_{pier\ drag} = \frac{d(\Delta\varepsilon_p)}{dt} + \frac{d(\Delta\varepsilon_k)}{dt} \qquad \textit{(Equation 3.43)}$$

Define the potential energy ε_p as follows:

$$\varepsilon_p = mgy$$

$$\Rightarrow \quad \Delta\varepsilon_p = mg\Delta y$$

$$\Rightarrow \frac{d}{dt}(\Delta\varepsilon_p) = \Delta\frac{d}{dt}(mgy) = \Delta\left[gy\frac{d}{dt}m\right]$$

$$\Rightarrow \frac{d}{dt}(\Delta\varepsilon_p) = \Delta\left(gy\rho\frac{dV}{dt}\right) = \Delta(\rho gyQ) = \rho gQ\Delta y \qquad \textit{(Equation 3.44)}$$

Define the kinetic energy ε_k as follows:

$$\varepsilon_k = \tfrac{1}{2}mv^2$$

$$\Rightarrow \quad \Delta\varepsilon_k = \tfrac{1}{2}m\Delta(v^2)$$

$$\Rightarrow \quad \frac{d}{dt}(\Delta\varepsilon_k) = \Delta\frac{d}{dt}\left(\tfrac{1}{2}mv^2\right) = \Delta\left(\tfrac{1}{2}v^2\frac{dm}{dt}\right)$$

$$\Rightarrow \frac{d}{dt}(\Delta\varepsilon_k) = \Delta\left(\tfrac{1}{2}v^2\frac{d}{dt}(\rho V)\right)$$

$$\Rightarrow \frac{d}{dt}(\Delta\varepsilon_k) = \Delta\left(\tfrac{1}{2}\rho v^2 Q\right) = \tfrac{1}{2}\rho Q\Delta v^2 \qquad \textit{(Equation 3.45)}$$

Substitute the time derivative terms into *equation 3.43*:

$$\Rightarrow \quad \kappa P_{pier\ drag} = \rho g Q\Delta y + \tfrac{1}{2}\rho Q\Delta\left(v^2\right) \qquad \textit{(Equation 3.46)}$$

The drag force on the pier can be described in terms of the momentum equation, the force being defined in terms of the momentum equation. Suppose sections **A** and **B** are such that they enclose a control volume and comply with criteria for the application of the momentum equation. We define the drag force (as referred to in terms of pier drag power) as follows:

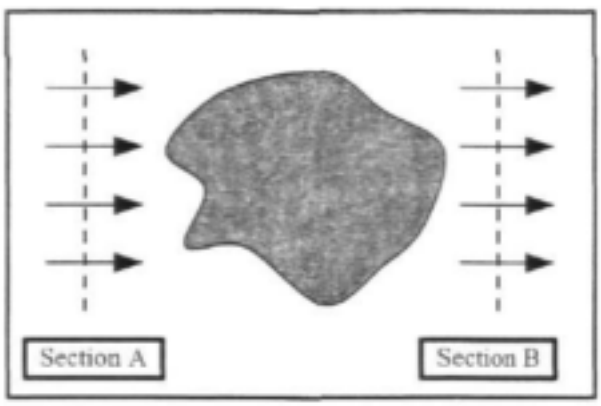

Figure 3.23: *A control volume for the application of the momentum equation; section A being the* ***inflow*** *section and section B the* ***outflow*** *section*

The following derivation relates to *figure 3.23*:

$$\sum F = F_{res} = \rho Q v_{leaving} - \rho Q v_{entering}$$

$$\Rightarrow \quad \tfrac{1}{2}\rho g y_A^{\,2} B_A - \tfrac{1}{2}\rho g y_B^{\,2} B_B - F_{pier} = \rho Q v_B - \rho Q v_A$$

$$\Rightarrow \quad F_{pier} = \tfrac{1}{2}\rho g\left(y_A^{\,2} B_A - y_B^{\,2} B_B\right) - \rho Q\left(v_B - v_A\right) \qquad \textit{(Equation 3.47)}$$

By expressing the drag force on the pier in terms of flow conditions at sections **A** and **B**, the applied power associated with the total drag force as a function of water depths and velocities can now be determined. Note the following definition:

$$Power \equiv P = \frac{dW}{dt}$$

$$and\ W = Fs$$

$$\Rightarrow \quad P = \frac{d(Fs)}{dt} = F\frac{ds}{dt} = Fv$$

The power associated with the total drag force can be expressed as the product of the drag force and the applicable relative flow velocity. The significant flow velocity and the associated section where this velocity is found, will be treated later. If we consolidate all the applicable definitions concerning the power approach, it is possible to derive a flow rate equation:

Substitute $\mathbf{F_{pier\ drag}}$ (*equation 3.47*) into *equation 3.46*:

$$\Rightarrow \quad \kappa\left[\tfrac{1}{2}\rho g\left(y_A^{\,2} B_A - y_B^{\,2} B_B\right) - \rho Q\left(v_B - v_A\right)\right] v = \rho g Q\left(y_B - y_A\right) + \tfrac{1}{2}\rho Q\left(v_B^{\,2} - v_A^{\,2}\right)$$

(Equation 3.48)

From the continuity law:

$$Q = vA = vyB$$

In terms of **sections A** and **B**:

$$Q = v_A y_A B_A = v_B y_B B_B \qquad \textit{(Equation 3.49)}$$

Rewriting *equation 3.49* with v_A and v_B as subjects respectively:

$$v_A = \frac{Q}{y_A B_A}; \quad v_B = \frac{Q}{y_B B_B} \qquad \textit{(Equation 3.50)}$$

Replace v_A, v_B and v in *equation 3.50* with their respective definitions:

$$\Rightarrow \quad \kappa\left[\tfrac{1}{2}\rho g\left(y_A^{\,2}B_A - y_B^{\,2}B_B\right) - \rho Q^2\left(\tfrac{1}{y_B B_B} - \tfrac{1}{y_A B_A}\right)\right]\tfrac{Q}{yB} = \rho g Q\left(y_B - y_A\right) + \tfrac{1}{2}\rho Q\left(\tfrac{Q^2}{y_B^{\,2}B_B^{\,2}} - \tfrac{Q^2}{y_A^{\,2}B_A^{\,2}}\right)$$

(Equation 3.51)

Divide *equation 3.51* by **Q** (we eliminate the root **Q = 0** from the **3rd degree** polynomial, an answer which is irrelevant to our study):

$$\Rightarrow \quad \kappa\left[\tfrac{1}{2}\rho g\left(y_A^{\,2}B_A - y_B^{\,2}B_B\right) - \rho Q^2\left(\tfrac{1}{y_B B_B} - \tfrac{1}{y_A B_A}\right)\right]\tfrac{1}{yB} = \rho g\left(y_B - y_A\right) + \tfrac{1}{2}\rho\left(\tfrac{Q^2}{y_B^{\,2}B_B^{\,2}} - \tfrac{Q^2}{y_A^{\,2}B_A^{\,2}}\right)$$

Simplifying:

$$Q^2\left[\frac{\kappa g}{\beta}\left(\frac{1}{y_B B_B}-\frac{1}{y_A B_A}\right)+\frac{1}{2}\left(\frac{1}{y_B^2 B_B^2}-\frac{1}{y_A^2 B_A^2}\right)\right]=g\left(y_A-y_B\right)+\frac{\kappa g}{2\beta}\left(y_A^2 B_A-y_B^2 B_B\right)$$

Rewriting **Q** as the subject:

$$Q=\sqrt{\frac{g\left(y_A-y_B\right)+\frac{\kappa g}{2\beta}\left(y_A^2 B_A-y_B^2 B_B\right)}{\frac{\kappa}{\beta}\left(\frac{1}{y_B B_B}-\frac{1}{y_A B_A}\right)+\frac{1}{2}\left(\frac{1}{y_B^2 B_B^2}-\frac{1}{y_A^2 B_A^2}\right)}} \qquad \textit{(Equation 3.52)}$$

The term **κ** (**kappa**) is a power correction factor. Calibration of *equation 3.52* using the laboratory data of *Retief* (1998) mentioned earlier, resulted in quite favourable results in terms of **kappa** (**kappa** being nearly 1 for the higher flows) values.

Rewriting *equation 3.52* into a more conventional discharge equation format requires the elimination of the power correction factor (kappa term) and the introduction of a flow correction factor $\mathbf{C_d}$. The following equation results:

$$Q=C_d Q_{theoretical} \qquad \textit{(Equation 3.53)}$$

$$\Rightarrow \quad Q=C_d\sqrt{\frac{g\left(y_A-y_B\right)+\frac{\beta}{2\kappa}\left(y_A^2 B_A-y_B^2 B_B\right)}{\frac{1}{\kappa\beta}\left(\frac{1}{y_B B_B}-\frac{1}{y_A B_A}\right)+\frac{1}{2}\left(\frac{1}{y_B^2 B_B^2}-\frac{1}{y_A^2 B_A^2}\right)}} \qquad \textit{(Equation 3.54)}$$

Calibrating this equation resulted in favourable $\mathbf{C_d}$-values as they did not vary much. The results will be discussed later on.

Units:

It can be shown that all the terms in *equation 3.48* have units of power and that the equation is dimensionally homogeneous:

$$\frac{d}{dt}(\Delta\varepsilon_p) = \rho g Q \Delta y = \left[\frac{kg}{m^3}\right]\left[\frac{m}{s^2}\right]\left[\frac{m^3}{s}\right]\left[m\right] = \left[\frac{kg \cdot m^2}{s^3}\right] \qquad \textit{(Equation 3.55)}$$

$$\frac{d}{dt}(\Delta\varepsilon_k) = \tfrac{1}{2}\rho Q \Delta v^2 = \left[\frac{kg}{m^3}\right]\left[\frac{m^3}{s}\right]\left[\frac{m^2}{s^2}\right] = \left[\frac{kg \cdot m^2}{s^3}\right] \qquad \textit{(Equation 3.56)}$$

It can be poven that the power term associated with the pier force also possesses units of power, viz:

$$Fv = \tfrac{1}{2}\rho g y^2 Bv + \rho Q v^2 = \left[\frac{kg}{m^3}\right]\left[\frac{m}{s^2}\right]\left[\frac{m^2}{1}\right]\left[\frac{m}{1}\right]\left[\frac{m}{s}\right] + \left[\frac{kg}{m^3}\right]\left[\frac{m^3}{s}\right]\left[\frac{m^2}{s^2}\right] = \left[\frac{kg \cdot m^2}{s^3}\right] \qquad \textit{(Equation 3.57)}$$

It has been shown above that all the relevant terms in the power equation do possess the units of power.

$$P = \frac{work}{time} = \frac{force.distance}{time} = \frac{mass.acceleration.distance}{time}$$

$$\Rightarrow P = \frac{\left[\frac{kg}{1}\right]\left[\frac{m}{s^2}\right]\left[\frac{m}{1}\right]}{\left[\frac{s}{1}\right]} = \left[\frac{kg \cdot m^2}{s^3}\right] = [Watt] \qquad \textit{(Equation 3.58)}$$

The power equation is therefore dimensionally homogeneous with units of Watts (W).

Power approach, another perspective:

The following fundamental approach consisted of the balancing of power terms. It included finding expressions for available power and applied power and applying them to a control volume. The available and applied power should be the same for a steady system and the terms were therefore equated.

Consider *figure 3.24* showing the applicable parameters describing the available and applied power.

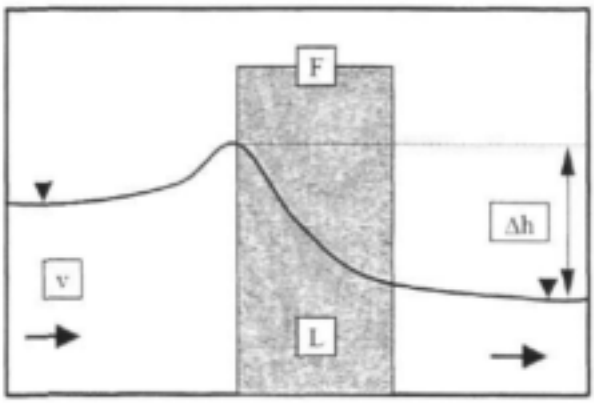

Figure 3.24: *Longitudinal flow section taken at a bridge pier; v ≡ flow velocity, F ≡ pier drag force, Δh ≡ water level difference and L ≡ length of the pier*

The power made available per unit volume according to *Rooseboom*, (1992) is:

$$P_{available} = \rho g s v \qquad \textit{(Equation 3.59)}$$

where **s = slope**.

$P_{available}$ is expressed in terms of a control volume with the upstream section taken to be **section 2** and downstream section to be **section 4** and centrelines between piers to be the boundaries on the sides (*figure 3.5*):

$$P_{available} = \rho g s v(AL) \qquad \textit{(Equation 3.60)}$$

Note that **A** represents the average flow area within the control volume and **L** the length of the control volume. According to the continuity law, **Q = vA**, substituting it into *equation 3.60*:

$$\Rightarrow P_{available} = \rho g s Q L \qquad \textit{(Equation 3.61)}$$

Define the energy slope as the average slope between sections **2** and **4** (describing the control volume, *figure 3.5*):

$$s = \frac{\Delta h}{L}$$

$$\Rightarrow P_{available} = \rho g \left[\frac{\Delta h}{L}\right] Q L = \rho g \Delta h Q = \rho g Q \Delta y \qquad \textit{(Equation 3.62)}$$

The applied power is made up of the power associated with overcoming friction as well as eddies that are kept in motion. Since most eddies are eliminated from our control volume due to our choice of downstream section (i.e. section **4** rather than section **5**) and the fact that the pier drag force dominates, the term $\mathbf{P_{eddies}}$ may be eliminated in the following equation.

$$\Rightarrow P_{applied} = P_{eddies} + P_{drag\ force}$$

$$\Rightarrow P_{applied} = \overline{\tau\left(\frac{dv}{dy}\right)} A L + F v$$

$$\Rightarrow P_{applied} \approx F v \qquad \textit{(Equation 3.63)}$$

Since a power balance always exists.

$\Rightarrow P_{available} = P_{applied}$ (based on the total volume, i.e. the control volume)

(Equation 3.64)

Substituting the relevant definitions into *equation 3.64*:

$$\rho g Q \Delta y = Fv \qquad \textit{(Equation 3.65)}$$

Equation 3.65 is similar to the power result found earlier under the paragraph "***Derivation***". The only difference is that *equation 3.65* lacks the following term:

$$\tfrac{1}{2}\rho Q \Delta v^2$$

The reason why this term is missing from *equation 3.65* follows directly from the assumption of uniform flow implying a constant energy slope between **section 2** and **section 4**, i.e. taking $s = \Delta h/L$. This implied that the velocities were assumed to be the same ($v_2 = v_4$) and resulted therefore in the Δv^2-term in $^1/_2\rho Q \Delta v^2$ to be zero – because $\Delta(v^2) = v_2^2 - v_4^2$.

Although the assumptions which led to *equation 3.65* may have been "too simplified", a similar power equation was found just by reasoning and thinking fundamentally in terms of power conservation.

Establishing the relevant velocity associated with the pier drag force:

Boat analogy:

The motivation for the use of the power approach was the analogy that exists between a bridge pier and a boat i.e. that the flow around a pier may be seen to be analogous to a boat being pulled through water. Consider the following figures:

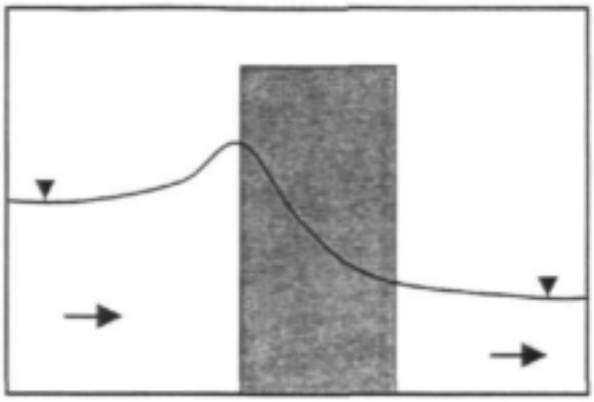

Figure 3.25: *Typical longitudinal flow pattern at a bridge pier, water flowing from left to right*

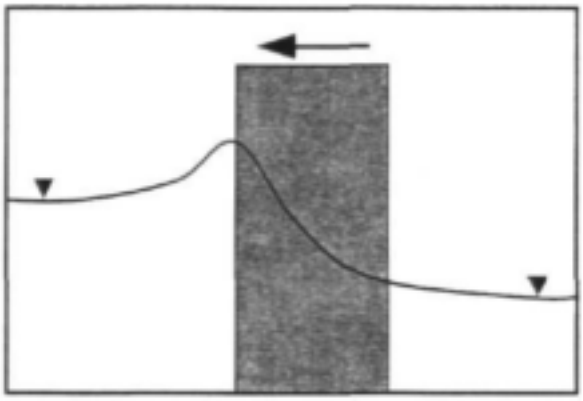

Figure 3.26*: Moving a boat through a fluid mass towards the left hand side in the sketch*

The flow around a pier (*figure 3.25*) can be visualised as the movement of an idealised boat through stationary water (*figure 3.26*). The drag force that was referred to earlier, is therefore analogous to the force needed to move the boat through a stagnant water mass at a constant velocity.

The fact that a boat would require a force to be displaced within a fluid, emphasises the fact that a certain amount of power is required to maintain its movement (an amount of power is therefore also associated with the continuous flow of water around a pier). This force, which is equal but opposite in direction to the drag force, causes dissipation of an amount of power. By quantifying the change in power within the defined control volume, in terms of potential and kinetic energy changes and the drag force, the **C_d-value** can be obtained. With **C_d** known, the flow rate becomes the only unknown

variable and is therefore quantifiable in terms of measurable flow parameters around the bridge pier. The only unknown term in the rewritten equation (with **Q** as the subject) is the "applicable velocity" which is associated with the pier drag force.

The boat analogy helped us to explain the "applicable velocity", or in other words, the velocity at which the pier drag force is transferred. Assume a flow rate **Q** past a pier reaching equilibrium as the water accelerates around the pier and returns to the normal flow condition downstream. Now: "At which velocity should a boat (analogous to the pier) be dragged through a stationary mass of fluid in order to obtain the same flow conditions as defined above, i.e. the same amount of damming upstream of the pier, the same acceleration around the pier as well as the same draw-down at the downstream end?" This is not an easy question, but can be resolved by considering the relative velocity between the pier and the oncoming flow.

Consider the real situation: The pier is fixed to the bed and a stream approaching at velocity $\mathbf{v}_\infty$ flows around the pier.

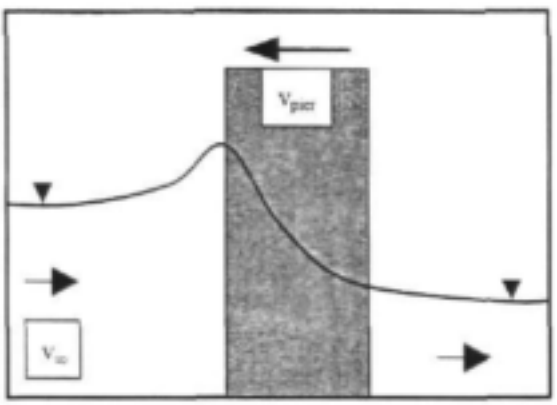

***Figure 3.27**: Longitudinal section of pier for normal flow conditions*

The following variables and their values are applicable to *figure 3.27*:

$v_{pier} = 0$; $v_{approaching\ flow} = v_{\infty}$

The relative velocity between pier and the approaching flow is defined as:

$$v_{relative} = v_{pier} - v_{approaching\ flow} = 0 - v_{\infty} = v_{\infty}$$

This implies that if the observer was to move with the oncoming flow the pier would have seemed to move to the left in *figure 3.27* at a velocity of v_{∞}.

Consider the boat analogy now. An idealised boat with the same dimensions as the bridge pier (*figure 3.27*) is pulled towards the left in *figure 3.28* within an endless "ocean" of stationary water. The water depth before movement starts equals the oncoming flow depth in *figure 3.27.*:

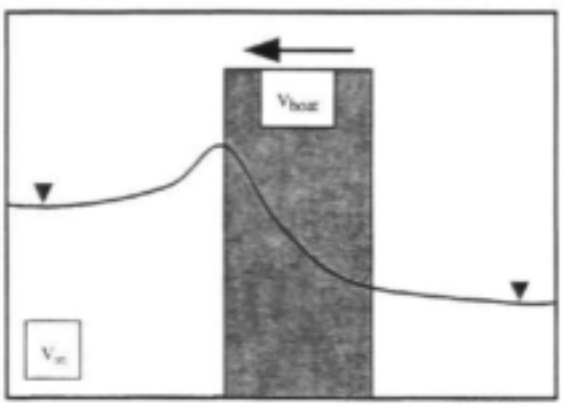

Figure 3.28: *Longitudinal section of an idealised boat [having the same dimensions as the bridge pier] being dragged through a stationary mass of water; the pier moves to the left and water flows therefore to the right in the sketch*

The following variables and their values are applicable to *figure 3.28*:

$v_{boat} = unknown$; $v_{approach} = 0$

The relative velocity between the boat and the approaching flow should be the same for the two conditions (real phenomenon (*figure 3.27)* and analogy (*figure 3.28*)) to assure that the analogy represents the correct simulation of the real phenomenon.

The relative velocity between steady pier flow and the idealised boat is defined as follows:

$$v_{relative} = v_{boat} - v_{\infty} = v_{boat} - 0 = v_{boat}$$

The relative velocity for the real situation and the analogy should be the same to ensure the same relative velocity in both the real situation and the analogy.

$$\Rightarrow v_{relative} = v_{boat} = -v_{\infty}$$

This implies that the boat needs to be moved with a velocity of v_{∞} in a direction opposite to the normal flow direction (the negative sign indicates this) in order to ensure the same hydraulic result found with the real phenomenon.

Thus, the "applicable velocity" at which the pier needs to be moved in terms of our analogy should equal the approach velocity. The approach velocity is therefore the correct velocity to use in conjunction with the pier drag force to ensure the correct value of drag power.

The approach velocity is per definition the average velocity found in **section 1** (defined earlier). By equating the applicable velocity (for the pier drag force) to the **velocity at 1** (section 1), the power based discharge equation can now be calibrated.

Define: B = **B**; v = $\mathbf{v_\infty = v_1}$; y = y_∞ = $\mathbf{y_1}$ to obtain the following "general discharge equation" (power based):

$$Q = C_d \sqrt{\frac{g\left(y_A - y_B\right) + \frac{\rho}{2\beta}\left(y_A^{\,2}B_A - y_B^{\,2}B_B\right)}{\frac{1}{\beta}\left(\frac{1}{y_B B_B} - \frac{1}{y_A B_A}\right) + \frac{1}{2}\left(\frac{1}{y_B^{\,2}B_B^{\,2}} - \frac{1}{y_A^{\,2}B_A^{\,2}}\right)}} \qquad \textit{(Equation 3.66)}$$

By defining the geometry of sections **A** and **B**, the $\mathbf{C_d}$**-valu** can be calibrated accordingly:

Calibration of the power based "general flow rate equation" (equation 3.66) in terms of appropriate control volumes:

The power based discharge equation [$\mathbf{Q = f(y'^s, B'^s, v'^s)}$] has been defined in general terms for the application between an upstream (**section A**) and a downstream section (**section B**) up to now. In order to have been able to calibrate the **Q**-equation, it was necessary to define a proper control volume in terms of any two of the following sections: **1,2,3,4** and/or **5**. The velocity which relates the pier drag force to the pier drag power has already been discussed and was taken as $\mathbf{v_\infty = v_1}$, the average velocity at section **1**.

There are basically only two control volumes that have been identified as being suitable for the application of the power equation. The most important consideration that influenced our decision was the uniformity of water depth and velocity as required at the boundary sections describing the control volume. It was assumed that **Q = vBy** (flow rate equals velocity times width times depth) which means that constant depths and constant velocities across the two boundary sections were assumed.

The two control volumes referred to are discussed separately:

Control volume ❶:

Sections were defined in the following manner for this control volume. The upstream section was taken as **section 1** and the downstream section as **section 3** (this section is halfway between **section 2** and **section 4** in terms of the pier length). Note that the lines AE and KO bound control volume ❶ on either side (*figure 3.5*).

The following plan view of a typical pier set-up shows the geometry for control volume ❶:

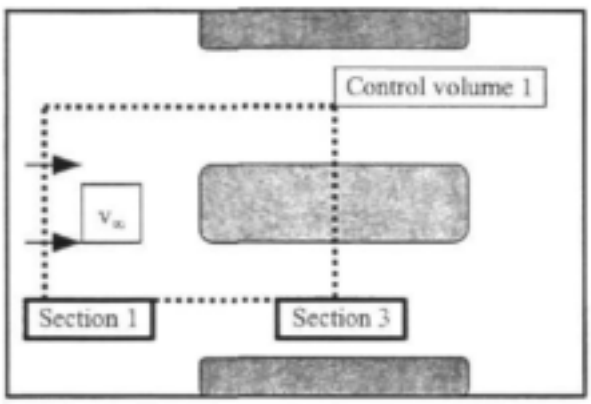

***Figure 3.29**: Defining the boundary lines of control volume* ❶

The general flow rate equation (power based) is (note that $v_\infty = v_1$):

$$Q = C_d \sqrt{\frac{g\left(y_{in} - y_{out}\right) + \frac{1}{2}\frac{r}{y_1 B_1}\left(y_{up}{}^2 B_{in} - y_{out}{}^2 B_{out}\right)}{\frac{1}{y_1 B_1}\left(\frac{1}{y_{out} B_{out}} - \frac{1}{y_{in} B_{in}}\right) + \frac{1}{2}\left(\frac{1}{y_{out}{}^2 B_{out}{}^2} - \frac{1}{y_{in}{}^2 B_{in}{}^2}\right)}}$$ *(Equation 3.67)*

Now substitute y_{out} with y_3, B_{out} with B_3, y_{in}, with y_1 and B_{in} with B_1:

$$\Rightarrow Q = C_d \sqrt{\frac{g(y_1 - y_3) + \frac{1}{2}\frac{r}{y_1 B_1}\left(y_1^2 B_1 - y_3^2 B_3\right)}{\frac{1}{y_1 B_1}\left(\frac{1}{y_3 B_3} - \frac{1}{y_1 B_1}\right) + \frac{1}{2}\left(\frac{1}{y_3^2 B_3^2} - \frac{1}{y_1^2 B_1^2}\right)}}$$

$$\Rightarrow Q = C_d \sqrt{\frac{g\left[(y_1 - y_3) + \frac{1}{2}\left(y_1 - \frac{y_3^2 B_3}{y_1 B_1}\right)\right]}{\frac{1}{y_1 B_1}\left(\frac{1}{y_3 B_3} - \frac{1}{y_1 B_1}\right) + \frac{1}{2}\left(\frac{1}{y_3 B_3} - \frac{1}{y_1 B_1}\right)\left(\frac{1}{y_3 B_3} + \frac{1}{y_1 B_1}\right)}}$$

$$\Rightarrow Q = C_d \sqrt{\frac{g\left[(y_1 - y_3) + \frac{1}{2}\left(y_1 - \frac{y_3^2 B_3}{y_1 B_1}\right)\right]}{\left(\frac{1}{y_3 B_3} - \frac{1}{y_1 B_1}\right)\left[\frac{1}{y_1 B_1} + \frac{1}{2}\left(\frac{1}{y_3 B_3} + \frac{1}{y_1 B_1}\right)\right]}}$$

(Equation 3.68)

Note $B_3 = (B - b_p)$ and $B_1 = B$.

Control volume ❷:

For this control volume we take **sections 1** and **4** as the boundary lines. **Section 1** is taken again as the upstream section and **section 4** as the downstream one. Lines **AE** and **KO** (*figure 3.5*) bound control volume ❷ on the sides

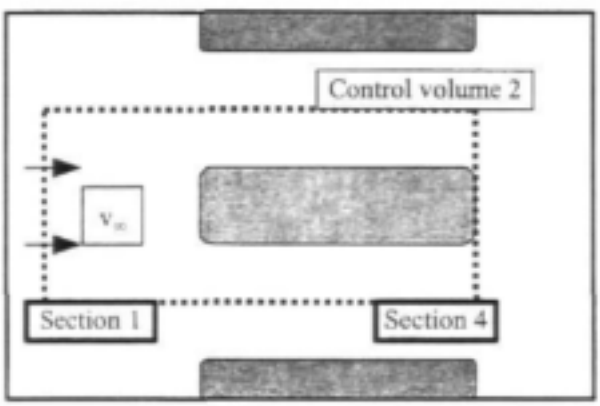

***Figure 3.30**: Defining the boundary lines of control volume ❷*

The general discharge equation (from power concepts) reads:

$$Q = C_d \sqrt{\frac{g(y_{in} - y_{out}) + \frac{1}{2}\frac{r}{y_1 B_1}\left(y_{in}^2 B_{in} - y_{out}^2 B_{out}\right)}{\frac{1}{y_1 B_1}\left(\frac{1}{y_{out} B_{out}} - \frac{1}{y_{in} B_{in}}\right) + \frac{1}{2}\left(\frac{1}{y_{out}^2 B_{out}^2} - \frac{1}{y_{in}^2 B_{in}^2}\right)}}$$

Now substitute y_{out} with y_4, B_{out} with B_4, y_{in} with y_1 and B_{in} with B_1:

$$\Rightarrow Q = C_d \sqrt{\frac{g(y_1 - y_4) + \frac{1}{2}\frac{\varepsilon}{y_1 B_1}\left(y_1^2 B_1 - y_4^2 B_4\right)}{\frac{1}{y_1 B_1}\left(\frac{1}{y_4 B_4} - \frac{1}{y_1 B_1}\right) + \frac{1}{2}\left(\frac{1}{y_4^2 B_4^2} - \frac{1}{y_1^2 B_1^2}\right)}} \qquad \textit{(Equation 3.69)}$$

Note $B_1 = B_4 = B$:

$$\Rightarrow Q = C_d \sqrt{\frac{g\left[(y_1 - y_4) + \frac{1}{2}\left(y_1 - \frac{y_4^2}{y_1}\right)\right]}{\frac{1}{B^2}\left[\left(\frac{1}{y_1 y_4} - \frac{1}{y_1^2}\right) + \frac{1}{2}\left(\frac{1}{y_4^2} - \frac{1}{y_1^2}\right)\right]}} \qquad \textit{(Equation 3.70)}$$

Simplifying and then multiplying above and below the line (within the square root sign) with $2y_1^2y_4^2$:

$$\Rightarrow Q = C_d \sqrt{\frac{gB^2\left[y_1 - y_4 + \frac{1}{2}y_1 - \frac{1}{2}\frac{y_4^2}{y_1}\right]}{\left[\frac{1}{y_1 y_4} - \frac{1}{y_1^2} + \frac{1}{2}\frac{1}{y_4^2} - \frac{1}{2}\frac{1}{y_1^2}\right]}}$$

$$\Rightarrow Q = C_d B\sqrt{g}\sqrt{\frac{\left[2y_1^3y_4^2 - 2y_1^2y_4^3 + y_1^3y_4^2 - y_1y_4^4\right]}{\left[2y_1y_4 - 2y_4^2 + y_1^2 - y_4^2\right]}}$$

$$\Rightarrow Q = C_d B\sqrt{g}\sqrt{\frac{y_1y_4^2(3y_1 + y_4)(y_1 - y_4)}{(y_1 + 3y_4)(y_1 - y_4)}}$$

$$\Rightarrow Q = C_d B y_4\sqrt{gy_1}\sqrt{\frac{(3y_1 + y_4)}{(y_1 + 3y_4)}}$$

After simplification we end up with the following simple result:

$$Q = C_d B y_4\sqrt{gy_1\varepsilon} \qquad \textit{(Equation 3.71)}$$

where $\varepsilon = \frac{(3y_1 + y_4)}{(y_1 + 3y_4)}$

This shows that the discharge per unit (**q = Q/B**) width is a function of the square root of the upstream depth (y_1), the downstream depth (y_4), the gravitational acceleration (**g**) and the ratio ε defined above.

Results:

Calibrating *equations 3.68* and *3.70* resulted in **C_d-values** ranging from **0.8** to **0.9** on average. The variation in **C_d-values** was low, implying a consistent model description. Both equations (control volume ❶ and control volume ❷) gave consistent **C_d-values** but *equation 3.70's* results showed that control volume ❷ performed slightly better in terms of stable coefficients and is therefore preferred. For control volume ❷ the **C_d-values** ranged from **0.79** to **0.92** for the "Normal flows", from **0.79** to **0.99** for the "Debris flows" and from **0.43** to **0.86** for the "Drowned flows". Refer to Appendix A "Power Approach" for detail on the laboratory data and results.

A final choice:

The power equation applied to control volume ❷ was adopted as the best alternative to the energy equation and momentum equation as a method for accurate calculation of the discharge **Q** as a function of flow parameters around a bridge pier. The power equation is much the same as the momentum equation in terms of the selection of the upstream enclosing section for the control volume. The power based **Q-function** is also a function of y_1 (like the **momentum based** one) where y_2 will be measured in practice. This problem needs to be addressed when deciding to use the power based discharge equation in practise.

3.9 *SUMMARY OF THEORIES, RESULTS:*

The following table provides an overall summary of the alternative fundamental approaches which have been discussed in the previous paragraphs. The aim of presenting the detail of the approaches in a comparative fashion is to give the reader an understanding of which approaches should be appropriate in the study and which not and where they are applicable and where not (*figure 3.5*).

Comparison between the four fundamental hydraulic laws

	LAWS			
	Continuity	Energy	Momentum	Power
Symbol used	Q	E	M	P
Fundamental origin of the entity	Law of conservation of mass	Newton II	Newton II	Newton II
Vector or Scalar function	Scalar	Scalar	Vector	Scalar
Applicable domain	Control volume	Stream line	Control volume	Control volume
Boundary values	In terms of cross-sectional data	In terms of point data	In terms of cross-sectional data	In terms of cross-sectional data
Requirements at the boundaries	Uniform conditions at sections	Points should be on the streamline	Uniform conditions at sections	Uniform conditions at sections
Point data (qualifications)	n.a.	Points should be adjacent to the stream line	n.a.	n.a.

	LAWS			
	Continuity	Energy	Momentum	Power
Symbol used	Q	E	M	P

Section:	Applicational suitability at sections 1,2,3,4 and 5			
Section 1 (with uniform flow approaching)	Well suitable for application	n.a.	Well suitable for application	Well suitable for application
Section 2 (upstream end of the pier)	Not suitable for application	n.a.	Not suitable for application	Not suitable for application
Section 3 (half-way in terms of the pier length)	Well suitable for application	n.a.	Well suitable for application	Well suitable for application
Section 4 (at the downstream end of the pier)	Less suitable for application	n.a.	Less suitable for application	Less suitable for application
Section 5 (further down-stream of the pier)	Well suitable for application	n.a.	Well suitable for application	Well suitable for application

Streamlines:	Applicational suitability of streamlines FG, GI, IJ and AE			
Between F & G	n.a.	Well suitable for application	n.a.	n.a.
Between G & I	n.a.	Well suitable for application	n.a.	n.a.
Between I & J	n.a.	Less suitable for application	n.a.	n.a.
Between A & E	n.a.	Well suitable for application	n.a.	n.a.

Time dependency (rate of change)	Yes (Rate of change in volume)	No	Yes (Rate of change in momentum)	Yes (Rate of change of energy)

	LAWS			
	Continuity	Energy	Momentum	Power
Symbol used	Q	E	M	P
Function of v^n (value of n)	v^1 (one)	v^2 (two)	v^2 (two)	v^3 (three)
Units (comment)	m^3/s (cumec)	m (meter water)	$kg.m/s^2$ (Newton)	$kg.m^2/s^3$ (Watt)
The implication of a negative sign in the results	Not possible	Not possible	The direction is opposite to that assumed	Not possible
Results (Cd-values) based on data by *Retief* (1998)				
Normal Debris Drowned	n.a.	**0.89-1.03** **0.95-1.04** **0.82-0.97**	**0.81 - 0.91** **0.86 - 0.90** **0.50 - 0.87**	**0. 79- 0.92** **0.79 – 0.99** **0.43 - 0.86**
* These flow conditions were only investigated for one pier width.				

Table 3.1

3.10 RESULTS IN GRAPH FORM, DISCUSSION:

The energy approach gave very good results (variability of **C_d-values** small) and was therefore developed further in terms of dimensionless ratios which were presented in graph form. The momentum and power approaches gave reasonably good results for the supercritical flow conditions but could not match the energy theory's stable coefficients for the whole flow range. *Figure 3.31* shows the calibration curves (energy approach) in terms of dimensionless parameters **Fr_4** (**Froude number** at *section 4, photo 3.1*) and **H/y_4** (note **$H = y_2$**) and *figures 3.32* and *3.33* show the calibrated **C_d-curves** (power and momentum approaches respectively) in terms of dimensionless parameters **Fr_4** (**Froude number** at *section 4, photo 3.1*) **$y_{upstream}/y_4$** (note **$y_{upstream} = y_1$**).

Using the ENERGY approach:

In order to present the results of the energy based discharge equation in a meaningful way, it was necessary to rewrite the equation in terms of dimensionless parameters:

Consider the energy based discharge equation given as *equation 3.25* earlier on:

Definitions of symbols:

Q: Flow rate [m^3/s]

C_d: Discharge coefficient compensating for transitional losses [non dim]

B: Representative width of oncoming flow for each bridge pier [m]

y: Flow depth [m]

α: Coriolis coefficient compensating for assumption of constant velocities [non dim], taken to be **1** throughout the text

v: Velocity of flow [m/s]

g: Unit gravitational force [m/s^2]

H: Energy head at the upstream end of the pier [m]

F_n: Froude number at section i [non dim]

$$Q = C_d B_i y_i \sqrt{\tfrac{2g}{\alpha}\left[(y_0 - y_i)\right]}$$

Rewriting it with velocity as subject by using the continuity law:

$$v_i = C_d \sqrt{\tfrac{2g}{\alpha}\left[(y_0 - y_i)\right]} \qquad \textit{(Equation 3.72)}$$

Squaring both sides of *equation 3.72* and manipulating as follows:

$$v_1^2 = C_d^2 \frac{2g}{\alpha}(y_G - y_1) \quad or \quad v_4^2 = C_d^2 \frac{2g}{\alpha}(y_2 - y_4)$$

Let $y_2 = H$, where H represents the stagnation head (hydrostatic + kinetic energy component):

$$\Rightarrow \quad v_4^2 = C_d^2 \frac{2g}{\alpha}(H - y_4)$$

$$\Rightarrow \quad \frac{v_4^2}{2gy_4} = \frac{C_d^2}{\alpha}\left(\frac{H}{y_4} - 1\right)$$

$$\Rightarrow \quad \tfrac{1}{2}F_{r4}^2 = \frac{C_d^2}{\alpha}\left(\frac{H}{y_4} - 1\right) \qquad \textit{(Equation 3.73)}$$

where F_{r4} denotes the Froude number at section 4.

Rewriting *equation 3.73* with C_d as the subject:

$$\Rightarrow \quad C_d^2 = \frac{\alpha F_{r_4}^2}{2\left(\frac{H}{y_4} - 1\right)}$$

$$\Rightarrow \quad C_d = \frac{F_{r_4}}{\sqrt{\frac{2}{\alpha}}\sqrt{\left(\frac{H}{y_4} - 1\right)}} \qquad \textit{(Equation 3.74)}$$

taking $\alpha = 1$

$$\Rightarrow \quad C_d = \frac{kF_{r_4}}{\sqrt{\left(\frac{H}{y_4} - 1\right)}} \quad \text{where k is a constant.}$$

Equation 3.74 indicates that a square root relationship should exist between the discharge coefficient $\mathbf{C_d}$ and the Froude number at the downstream end of the pier for a constant ratio of stagnation head **H** upstream to downstream depth $\mathbf{y_4}$ taken at **section 4** (*figure 3.5*) at the pier. This was confirmed by the model data (*figure 3.31*).

CALIBRATION CURVES

ENERGY APPROACH, C_d-value as a function of Froude number (Fr_4) and depth ratio (H/y_4)

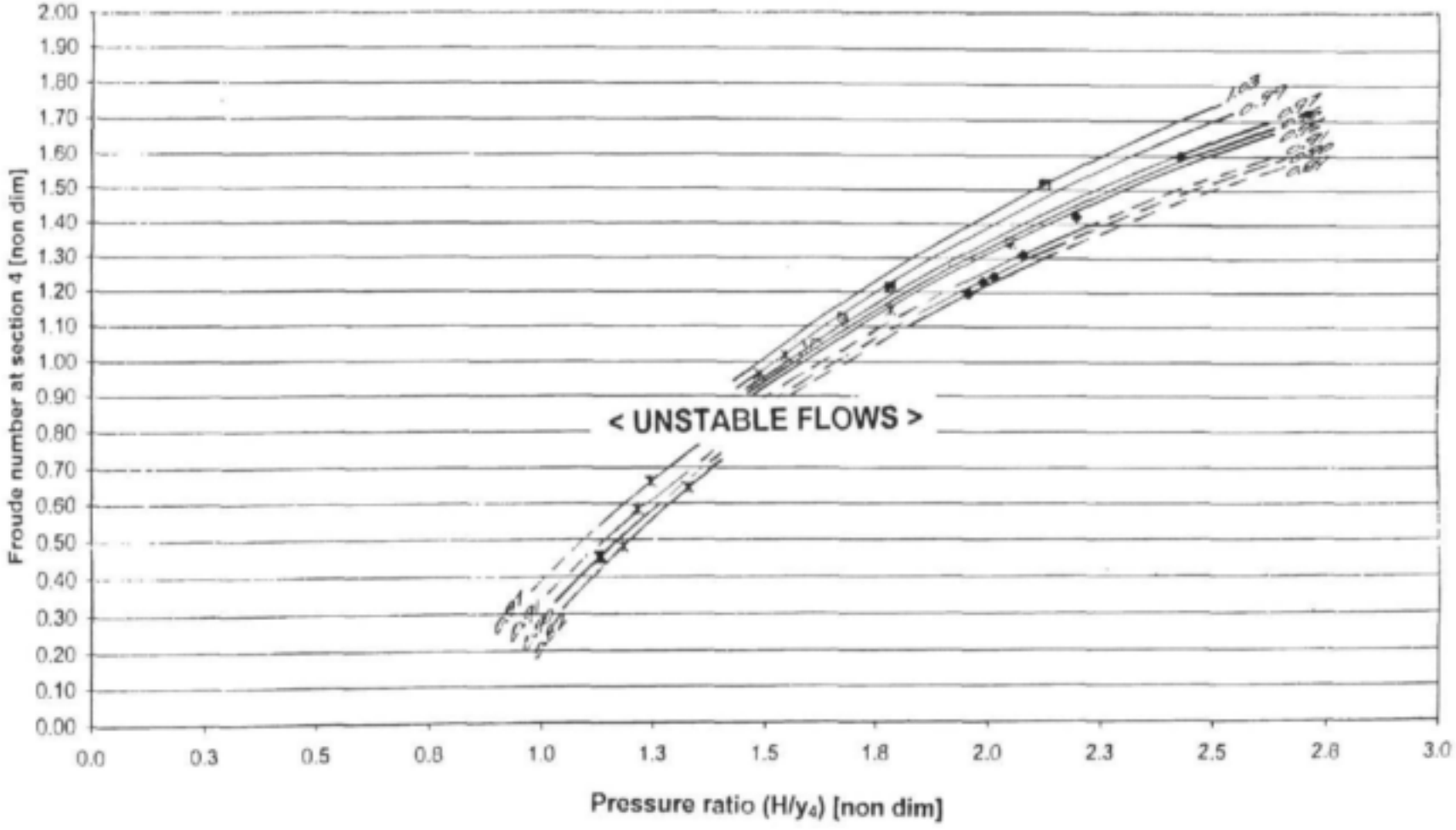

(Figure 3.31)

The following points are considered to be important:

❶ More data points were available for supercritical downstream conditions and this enabled the drawing of lines for this condition with greater accuracy. It is evident from the data points that for the supercritical condition, **C_d-values** closer to **1** were found. This implies that transitional losses tend to be small when we have a control section forming within the pier length. **C_d-values** close to **1** also reflect a more accurate representation of the real phenomenon.

❷ The uncertainty in flow parameters shown by the results for the condition of Froude numbers near to unity, is quite common for the transition region between subcritical and supercritical flow.

❸ The best results were obtained for condition of supercritical flow at the downstream end of the pier. For these conditions **C_d-values** close to **1** were found. Favourable conditions (**C_d** being close to **1**) are represented by high **Froude** numbers at the downstream end as well as high **H/y_4** values (large pressure differences along the pier).

Using the POWER approach:

The calibrated **C_d-values** of the discharge equation (power based) are presented as functions of dimensionless parameters. By rewriting the discharge equation a functional relationship could be established.

Definitions of symbols:

Q: Flow rate [m^3/s]

C_d: Discharge coefficient compensating for transitional losses [non dim]

B: Representative width of oncoming flow for each bridge pier [m]

y: Flow depth [m]

v: Velocity of flow [m/s]

g: Unit gravitational force [m/s^2]

H: Energy head at the upstream end of the pier [m]

F_{ri}: Froude number at section i [non dim]

Consider the power based discharge equation derived as *equation 3.71*:

$$Q = C_d B y_4 \sqrt{g y_1} \sqrt{\frac{(3y_1 + y_4)}{(y_1 + 3y_4)}}$$

Eliminating the $\varepsilon = \frac{(3y_1 + y_4)}{(y_1 + 3y_4)}$ term above in order to simplify the complex equation and then rewriting with velocity as subject by using the continuity law:

$$\Rightarrow \quad \frac{Q}{B y_4} = C_d \sqrt{g y_1}$$

$$\Rightarrow \quad v_4 = C_d \sqrt{g y_1} \qquad \textit{(Equation 3.75)}$$

Divide both sides by $(gy_4)^{0.5}$:

$$\Rightarrow \quad \frac{v_4}{\sqrt{g y_4}} = C_d \frac{\sqrt{y_1}}{\sqrt{y_4}}$$

$$\Rightarrow \quad F_{r_4} = C_d \frac{\sqrt{y_1}}{\sqrt{y_4}} \qquad \textit{(Equation 3.76)}$$

Rewriting with C_d as the subject of the equation:

$$\Rightarrow \quad C_d = \frac{F_{r_4}\sqrt{y_4}}{\sqrt{y_1}} = \frac{F_{r_4}}{\sqrt{\frac{y_1}{y_4}}} \qquad \textit{(Equation 3.77)}$$

Equation 3.77 indicates that a square root relationship exists between the **Froude number** at **section 4** and the pressure ratio y_1/y_4 for constant **C_d-values**. This was confirmed by the model data (*figure 3.32*).

In practice the $y_{upstream}$ value cannot be measured accurately, it is only the pressure heads y_2 (upstream end of the pier) and y_4 (downstream end of the pier) that are measured. This problem needs to be kept in mind when deciding between discharge theories.

The following points are considered to be important:

❶ **C_d-value** curves in the **$Fr_4 > 1$** region (supercritical downstream conditions, normal flows) show a definite trend as a function of Fr_4 and $y_{upstream}/y_4$ and corresponds well with the theoretical function: $Fr_4 = f(y_1/y_4)^{0.5}$.

❷ Drowned conditions are not reflected well by this power based theory resulting in **C_d-values** varying from **0.44** to **0.94.** There is therefore much uncertainty about the validity of the **C_d-curves** for the condition of drowned flow and the limited amount of data points available underline the uncertainty.

❸ The gap in data reflects the uncertainty in calibrated data for the range of **Froude numbers 0.8** to **1.0**. This uncertainty was to be expected due to unstable flow condition in the transitional region between subcritical and supercritical flow.

CALIBRATION CURVES

POWER APPROACH, C_d-value as a function of Froude number (Fr_4) and depth ratio ($y_{upstream}/y_4$)

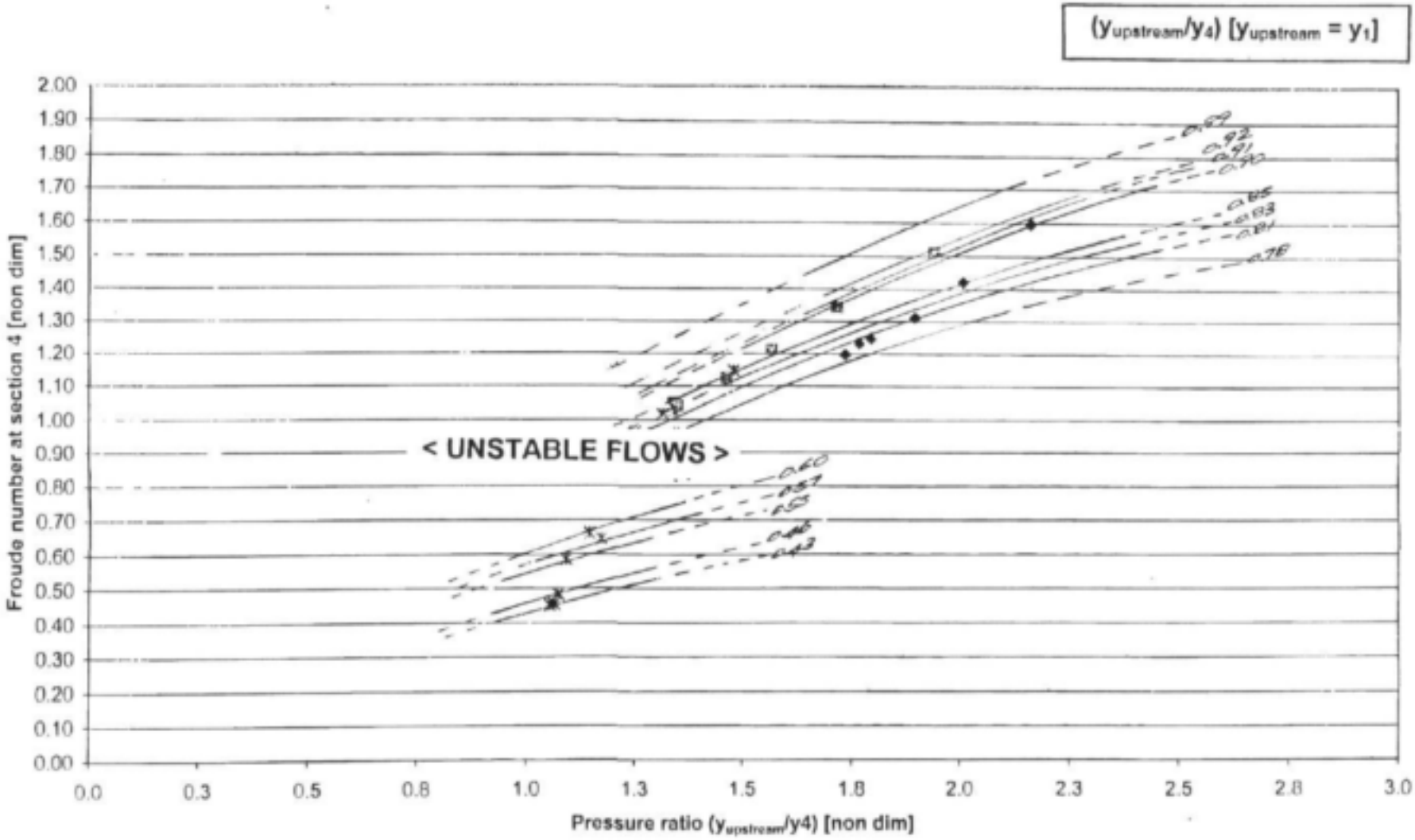

(Figure 3.32)

Using the MOMENTUM approach:

The calibrated **C_d-values** for the discharge equation (momentum based) are presented as functions of dimensionless parameters. This equation (*equation 3.38*) was too complex (it incorporated the $^1/_2\rho C_d{}^* Av^2$ term for example) to rewrite in terms of simple dimensionless parameters as was possible with the energy and power based discharge equations. In order to overcome this, it was assumed that the three fundamental approaches (energy, momentum and power) with their common base (**Newton II**) should more or less lead to the same relationship between dimensionless parameters. This was already seen for the energy and power approaches as both could be rewritten in terms of the same dimensionless parameters. It was therefore decided to express the discharge coefficient C_d in the momentum equation in terms of the same dimensionless parameters that were determined for the other two fundamental equations. Therefore, C_d was expressed in terms of the **Froude** number F_{r4} measured at the pier end as well as the ratio $y_{upstream}/y_4$ which is the ratio between upstream depth and the depth at the downstream pier end. Note that $y_{upstream}$ was used as in the power approach because the momentum based equation was based on the same control volume used in the power approach.

Definitions of symbols:

Q: Flow rate [m^3/s]

C_d: Discharge coefficient compensating for transitional losses [non dim]

B_i: Representative width at section i of oncoming flow for each bridge pier [m]

y: Flow depth [m]

v: Velocity of flow [m/s]

g: Unit gravitational force [m/s^2]

F_{ri}: Froude number at section i [non dim]

Consider the momentum based discharge equation derived as *equation 3.38* (**1-4** sectional combination, thus in terms of the better configuration: **section 1** and **section 4**):

$$Q_w = C_d \sqrt{\frac{\frac{1}{2} g \left(y_1^{\,2} B_1 - y_4^{\,2} B_4 \right)}{\left(\frac{1}{y_4 B_4} - \frac{1}{y_1 B_1} + \frac{C_d^{\,2} A^2}{2 y_1^{\,2} B_1^{\,2}} \right)}}$$

As was described above, the **C_d-value** in the above mentioned equation was expressed in terms of dimensionless parameters found by rewriting the flow rate equations based on the other two fundamental approaches (energy and power), viz:

$$C_d = f\left(F_{r_4}, \frac{y_{upstream}}{y_4} \right)$$

In practice the **$y_{upstream}$** value cannot be measured accurately, it is only the pressure heads **y_2** (upstream end of the pier) and **y_4** (downstream end of the pier) that are measured next to or along the pier length. This problem needs to be resolved if the momentum based discharge equation is to be used for flow measuring and only pressures next to the pier are being measured.

<u>The following points are considered to be important:</u>

- A rather clear trend of **C_d-curves** in terms of **Fr_4** (**Froude number** at **section 4**) and **y_1/y_4** values for the region **$Fr_4 > 1$** is evident from *figure 3.33*. This implies that the momentum based discharge equation describes the normal flow condition (supercritical downstream conditions) rather well with **C_d-values** varying very little.

❷ The drowned condition ($Fr_4 < 1$) is not described satisfactory by this theory, **C_d-values** varied from **0.50** to **0.87** implying inadequate description of the real phenomena. Data for the drowned condition were also limited and there is therefore much uncertainty about the validity of **C_d-curves** for the drowned condition.

❸ Uncertainty in the **Froude number** range **0.8** to **1.0** was again evident but to be expected for the transitional region.

CALIBRATION CURVES

MOMENTUM APPROACH, C_d-value as a function of Froude number (Fr_4) and depth ratio ($y_{upstream}/y_4$)

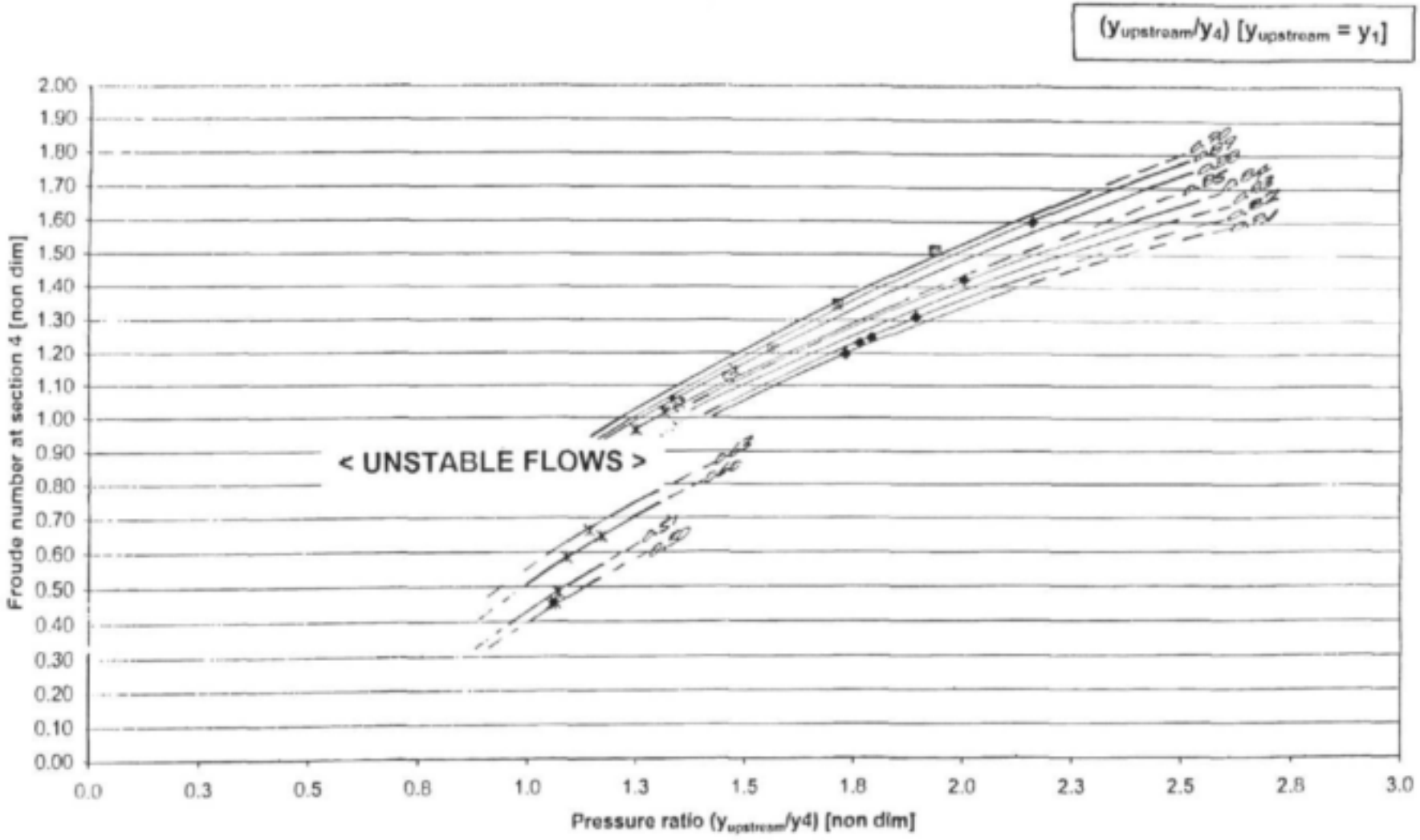

(Figure 3.33)

3.11 CONCLUSIONS AND RECOMMENDATIONS:

Calibrating the Energy, Momentum and Power based discharge theories with data collected by *Retief*, the following conclusions and recommendations are made:

i) The energy based model gave the best results (least variability in **C_d-values**, *table 3.1*) for the whole flow spectrum (supercritical & drowned flow conditions).

ii) The power and momentum based discharge theories described the drowned flow condition with less accuracy (**C_d-values** unstable, *table 3.1*) than the supercritical flow condition (control forming). This is also evident from the calibration curves, *figure 3.32* and *figure 3.33* respectively.

iii) It was realised that the energy based equation would work better in practise for it requires the measurement of pressures next to the pier only – therefore no need to measure water depths upstream of the pier as required by the momentum and power based models.

iv) It was not possible to measure a representative flow depth at the downstream end. The flow depth measured at **point C** (*photo 3.1*) was not a representative depth over the width of flow and an additional flow measuring point was therefore needed. Results in terms of pressure measurement at the middle of the pier (over the length) showed to be unsatisfactory (*Retief's* data) and pressure measurement was of little value here.

v) It is recommended that more realistic ratio's of **B/b_p** (flow width/pier width) should be considered during additional model pier tests. The **90 mm** pier tested by *Retief* gave a **B/b_p** ratio of **6.67** which is not often found in practice. The other ratio's considered by *Retief* were more representative and could be used again combined with a new pressure measuring configuration.

vi) The effect of changing the pier length should be considered. The piers tested by *Retief* all had a L/b_p (pier length/pier width) ratio of **5.56**. Different L/b_p ratio's are therefore recommended for further tests on model piers.

vii) Although the ideal flow pattern at bridge piers in terms of stable coefficients would be parallel flow approaching the pier, the effect of non-parallel flow approaching the pier should be considered. In practice it may be difficult to find a bridge with perfect zero pier rotation in terms of approaching flow and the relative rotation between pier and approaching flow directions may even change with discharge.

viii) The configuration of pressure measurement was to be changed in order to accommodate pressure measurement along the pier for non-parallel flow conditions as well as to measure a more representative flow depth at the downstream end. It is therefore recommended that two flow measuring points be added to the side of the pier, one at the upstream head and one at the downstream head. These are both to be positioned as close as possible to the pier end in order to be able to measure the maximum pressure difference over the length of the pier.

ix) Drowned conditions experienced at the downstream end of the pier should be investigated in detail. More tests on drowned conditions (which occur mainly during flood events) should be performed including more combinations of B/b_p, L/b_p and pier rotations.

x) Calibration curves should be constructed in order to present **C_d-values** as functions of dimensionless parameters in order to calculate discharges according to measured pressures at bridge piers.

4. MODEL TESTS AND RESULTS:

4.1 MODEL ANALYSIS AND SIMILARITY STUDY

Model analysis:

The mathematical models that were derived earlier in the text (refer to *chapter 3*) were calibrated using model data. Scale models of real structures (called prototypes) were tested to investigate flow conditions around piers. Results obtained from such model tests may not necessarily be applicable to the prototypes for example, due to inaccurate scaling of bed roughness or inappropriate scale distortions.

A brief discussion of similarity, which is very important for any model analysis, is therefore appropriate.

Similarity:

To assure perfect similarity between model and prototype, all relevant dimensionless hydraulic parameters should have the same values in both model and prototype. If this is true, the ratios between forces and momentum components within the model equal those in the prototype. This results in fluid elements being accelerated similarly in both model and prototype and therefore ensuring a true copy of the real phenomenon.

Considering all possible forces acting within the model boundaries during the modelling process is not necessary. Only the dominant forces need to be considered. Therefore, the first step in modelling the prototype structure is the identification of the most important or dominant forces.

The gravitational force is almost always of great importance. Froude similarity is necessary to ensure the correct ratio of momentum to gravitational force for both the model and the prototype.

Shear forces are not dominant forces except when conditions of low Reynolds numbers hold and viscous forces start to dominate, therefore Reynolds similarity is not important in normal models of bridge piers.

The following similarities exist:

1. Geometric similarity
2. Dynamic similarity
3. Kinematic similarity

Geometric similarity:

Geometric similarity implies that the model looks exactly like the prototype except that the model dimensions are proportionally smaller. This implies that the ratios between lengths and widths and heights should be the same in both the model and in the prototype in a so-called undistorted model. Because of the three-dimensional nature of flows around bridge piers, pier models need to be undistorted.

Dynamic similarity:

Dynamic similarity incorporates Froude similarity which is discussed later on.

Dynamic similarity refers to the similarity of forces as expressed through dimensionless ratios of momentum and force for example the ratio between momentum and the gravitational force, viscous shear force or the surface tension force. These ratios include Froude, Weber and Reynolds numbers. This study concerns mainly turbulent flows around piers and therefore Reynolds similarity is not required. Weber similarity is also not applicable. On the other hand, Froude similarity is of utmost importance as is evident from the section on *Froude similarity* below.

Kinematic similarity:

Kinematic similarity concerns the "steady even motion of fluids" and is usually automatically satisfied if dynamic similarity holds.

Froude similarity:

In turbulent open channel flow, which is the most important field of model studies for civil engineers, a very important requirement in terms of similarity is that the Froude numbers should be the same in both the model and the prototype. The Froude number has the following definition:

$$F_r \equiv \frac{Momentum}{Gravitational\ force}$$

The F_r-number also represents a ratio of kinetic energy to potential energy, viz:

$$F_r = f\left(\frac{\varepsilon_k}{\varepsilon_p}\right) \Rightarrow \quad F_r = f\left(\frac{\frac{1}{2}mv^2}{mgy}\right)$$

For our model, being an open channel flow model, in addition to geometrical similarity (which should be aimed for at all times), it is also essential to ensure Froude similarity i.e. ensuring the same Froude numbers in both the model and in the prototype.

One way to ensure Froude similarity is to use the correct scaling laws when determining the dimensions of the model. These scaling laws can be derived from basic scale ratios that are related to the Froude number.

The scale ratio can be determined as follows (*Rooseboom*, 1992).

For Froude similarity:

$$F_{r_p} = F_{r_m}$$

$$\Rightarrow \frac{v_p}{\sqrt{g_p y_p}} = \frac{v_m}{\sqrt{g_m y_m}} \qquad \textit{(Equation 4.1)}$$

$$\Rightarrow \frac{v_p}{v_m} = \sqrt{\frac{y_p}{y_m}} \qquad \textit{(Equation 4.2)}$$

$$\Rightarrow n_v = \sqrt{n_y}$$

Note that there are two traditional definitions for the Froude number, viz.:

$$F_r = \frac{v^2}{gy} \qquad \textit{(Equation 4.3)}$$

And also the square root of *equation 4.3*:

$$F_r = \frac{v}{\sqrt{gy}} \qquad \textit{(Equation 4.4)}$$

The definition according to *equation 4.3* is more appropriate than according to *equation 4.4*. Consider the following sketch and derivation in order to explain this statement.

Consider a flow element as shown in *figure 4.1*:

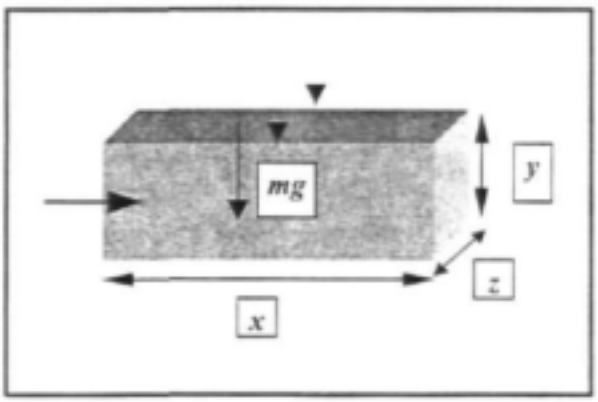

Figure 4.1: *Typical flow element shown in three dimensions, x, y & z*

The Froude number has been defined as being the ratio of momentum to the gravitational force, therefore:

The following definitions hold:

F_r: Froude number [non dim]

ρ: Mass density of the fluid [kg/m^3]

Q: Discharge [m^3/s]

v: Velocity of flow [m/s]

m: Mass of fluid or fluid particle [kg]

g: Unit gravitational force [m/s^2]

x: Horizontal dimension, flow element [m]

y: Vertical dimension, flow element [m]

z: Horizontal dimension, flow element [m]

$$F_r = \frac{Momentum}{Gravitational\ force} = \frac{\rho Q v}{mg}$$

$$\Rightarrow \quad F = \frac{\rho\left(\frac{V}{t}\right)v}{\rho V g} = \frac{\rho\left(\frac{xyz}{t}\right)v}{\rho(xyz)g} = \frac{xzv^2}{xyzg} = \frac{v^2}{gy}$$

which is in line with the definition of *equation 4.3*.

An investigation of Froude similarity results in a remarkable outcome, being the following: "Geometrical similarity in a model automatically ensures Froude similarity for equilibrium flow conditions in terms of hydraulic roughness".

This can be proven as follows for open channel uniform flow:

Say for instance a representative model is built of a river reach (prototype). The model is undistorted (vertical scale ratio equals horizontal scale ratio). The roughness has also been scaled accordingly. Geometric similarity holds:

Chezy's energy equation for open channel uniform flow, is used to represent the relationship between velocity and channel characteristics.

The following definitions hold:

v: Velocity of flow

g: Unit gravitational force [m/s^2]

R: Hydraulic radius (= A/P, = [flow area]/[wetted perimeter]) [m]

S_f: Energy slope [m/m]

S_o: Bed slope [m/m]

k: Absolute roughness [m]

y: Flow depth, vertical [m]

x_m: Parameter x in the model [dim of x]

x_p: Parameter x in the prototype [dim of x]

$$v = 5.75\sqrt{g}\,log\left(\frac{12R}{k}\right)\sqrt{RS_f} \qquad \textit{(Equation 4.5)}$$

For a wide river the hydraulic radius R ≈ y, the average flow depth:

$$\Rightarrow v = 5.75\sqrt{g}\,log\left(\frac{12y}{k}\right)\sqrt{yS_f}$$

$$\Rightarrow \frac{v}{\sqrt{gy}} = 5.75\,log\left(\frac{12y}{k}\right)\sqrt{S_f}$$

The same roughness-depth ratio has been applied, therefore:

$$\left(\frac{y}{k}\right)_p = \left(\frac{y}{k}\right)_m \qquad \textit{(Equation 4.6)}$$

Geometrical similarity holds, therefore the bed slopes are equal and from the uniform flow assumption the energy gradients are equal, viz:

$$(s_0)_p = (s_0)_m \Rightarrow (s_f)_p = (s_f)_m$$

Consolidating, the following equality holds:

$$5.75 log\left(\frac{12y}{k}\right)_p \sqrt{(s_f)_p} = 5.75 log\left(\frac{12y}{k}\right)_m \sqrt{(s_f)_m}$$

$$\Rightarrow \left(\frac{v}{\sqrt{gy}}\right)_p = \left(\frac{v}{\sqrt{gy}}\right)_m$$

$$\Rightarrow (F_r)_p = (F_r)_m$$

Therefore, Froude similarity holds, or in other words, the Froude number takes on the same value in both the model and in the prototype.

Summary:

1. Firstly, if Froude similarity holds, and a model is either a scaled up or scaled down version of the prototype, the gravitational force (which dominates in open channel flow) will ensure the same acceleration pattern in both the model and the prototype.
2. Secondly, the results obtained from a Froude resistance model are directly applicable and can be extrapolated to prototype results. This means the prototype will respond in the same manner as the model if the depth-roughness ratios are kept the same.

4.2 MODEL TESTS IN THE LABORATORY:

4.2.1 Introduction:

Model tests performed by *Retief* (1998) provided data for three model piers. From the calibration of the newly developed discharge equations using *Retief's*, data it proved that all three fundamental approaches (Energy, Momentum and Power) could be calibrated accurately, the Energy approach for the whole spectrum of flows and the other two theories for the "Normal flows" (supercritical downstream conditions) specifically. It was therefore shown that the Energy (whole flow spectrum), Momentum and Power approaches could be used to measure flows (momentum and power only for "Normal flows") at bridge piers in terms of measured pressures at and in the vicinity of the pier and that the pier approach may therefore be of great value to measure floods at prototype piers.

Because the momentum and power based discharge equations are based on the flow patterns within a control volume and the control volume needs to be bounded by constant depth sections, it was necessary to use **section 1** (*photo 3.1*) as the upstream enclosing section in order to have a constant flow depth across the width, as well as to include the pier within the control volume boundaries. The coefficients based on the Momentum and Power approaches were therefore determined in terms of the flow depth at **section 1** (*photo 3.1*). It is therefore important to note that if the momentum and power based discharge equations are to be used, the upstream flow depth **section 1** (*photo 3.1*) need to be known. This implies therefore that the Momentum and Power approaches cannot be used if pressures are measured against the pier only. Because of practical problems associated with the measurement of pressures upstream of piers, a system which only requires pressure measurements against piers is preferable.

The *energy equation*, based on pier pressures only, was therefore investigated in more detail in terms of different flow conditions, different ratios of channel width to pier width ($\mathbf{B/b_p}$) and pier length to pier width ($\mathbf{L/b_p}$), as well as different pier orientations relative to the direction of the oncoming flow in order to estimate the applicability of the energy theory to a wider flow regime. It was found that some of the ratio's describing the width of the pier relative to the width of the approaching stream in *Retief's* study were not representative of typical prototype ratios and additional tests on **4** different $\mathbf{b_p/B}$ (pier width / stream width) ratio's were conducted, these ratio's being more representative of those found in practice. The ratio describing the width of the pier relative to the length of the pier was also investigated. This was done because in the tests conducted by *Retief* a $\mathbf{L_p/b_p}$ ratio of **5.56** only was used. *Retief's* work included only a very brief reference to drowned pier flow conditions, i.e. sub-critical flow conditions. It was therefore decided that additional tests should be done for both supercritical and sub-critical downstream conditions.

The energy equation was expressed in terms of the pressure at a measuring position near the downstream end and this necessitated the introduction of an additional position for measuring the pressures along the pier. Please refer to *paragraph 4.2.3* for more detail on the pressure measuring configuration.

In conclusion, the aim of these additional laboratory tests was to determine whether the energy based discharge equation is applicable to a wide variety of practical bridge pier lay-outs combined with different flow conditions typically found under flood conditions. The following paragraphs cover the laboratory tests whilst the laboratory data can be found in the Appendices.

4.2.2 *Description of the laboratory lay-out used for the test:*

Photo 4.1 shows a side view of the laboratory lay-out used for the additional tests referred to in 4.2.1.

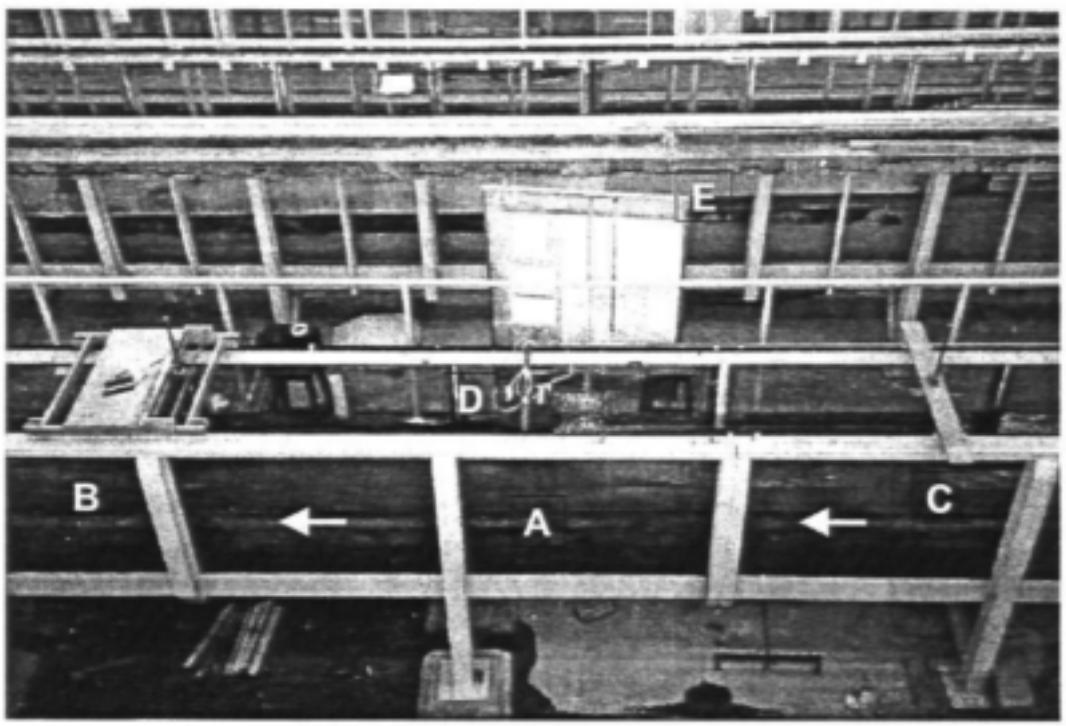

Photo 4.1: *Side view of glass flume used for testing the model piers, Hydraulics Laboratory, University of Stellenbosch*

Note that the lay-out is similar to that used by *Retief*. A glass flume (**A,** *photo .1*) of **609 mm** width was used to test the pier models. The bed slope was fixed at a very slight slope of **0.0025 m/m** over about **75 %** of the flume length and increased near the end in order to ensure supercritical conditions downstream during some of the tests. Downstream flow depths were registered from a moving trolly (**B**) and upstream by means of a measuring needle fixed to a portable frame (**C**). The position of the pier (**D**) is shown in *photo 4.1* and the arrows indicate the direction of flow. Manometer pipes

fixed to a wooden stand (**E**) were used to measure pressures at four points alongside the pier. The manometer pipes are shown in *photo 4.2*:

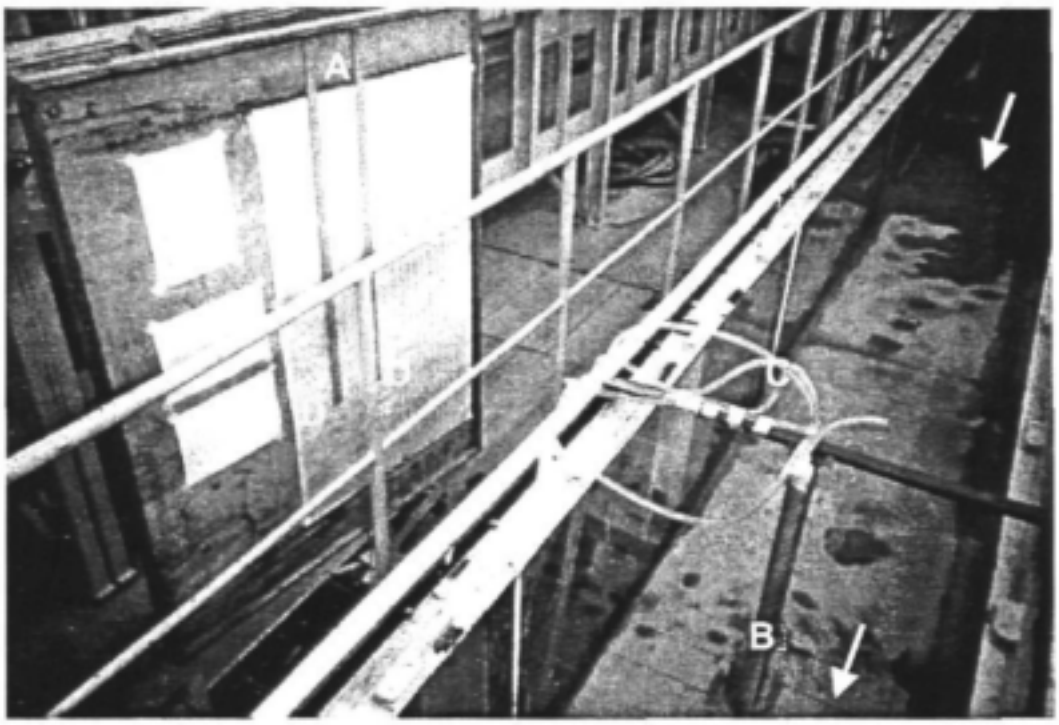

Photo 4.2: *Side view of glass flume used for testing the model piers, Hydraulics Laboratory, University of Stellenbosch*

Photo 4.2 shows the 4 manometer stand pipes (**A**) fixed to the wooden stand. These are connected to the pressure measuring points on the model pier (**B**) via flexible clear tubing (**C**). The water levels registered in the manometer pipes therefore correspond to the pressures alongside the pier. The manometer pipes were installed in such a way that the reading (in mm) on the adjacent scales (**D**) corresponded to the heads at the four points on the pier measured relative to the head of the furthest upstream pressure point (**position UE**, *figure 4.2, section 4.2.3*). The arrows show the direction of flow.

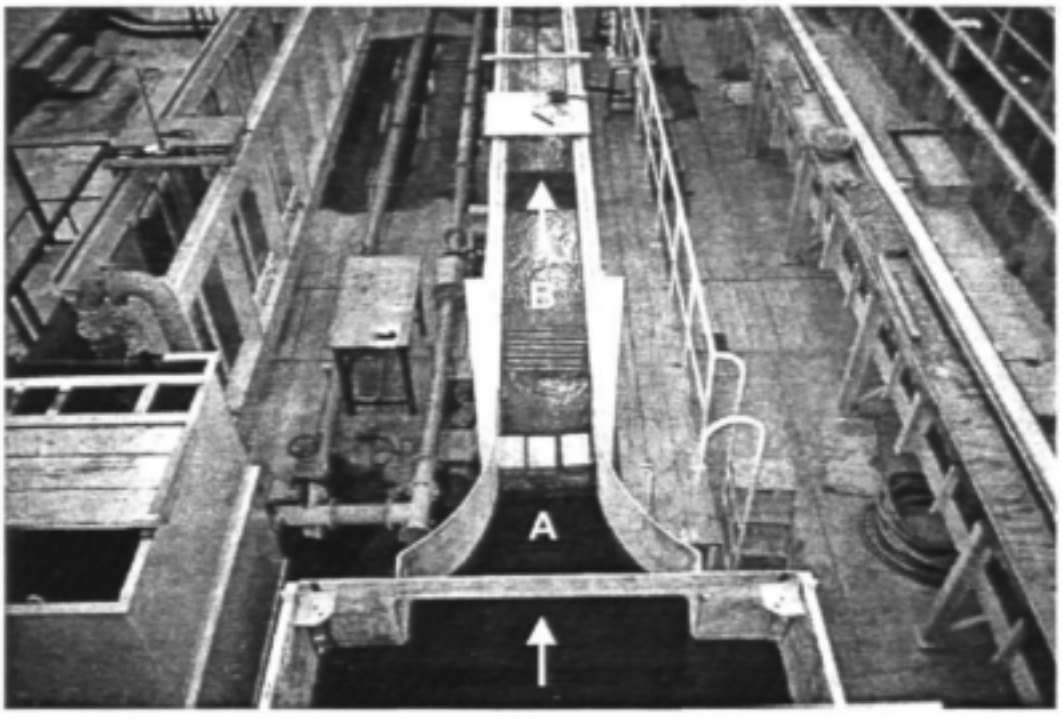

***Photo 4.3**: Looking downstream at the glass flume used for testing the model piers, Hydraulics Laboratory, University of Stellenbosch*

Photo 4.3 shows a downstream view of the upstream part of the glass flume with the baffle blocks (**A**) and wave dampener (**B**). The arrows indicate the direction of flow.

In order to simulate drowned conditions downstream of the pier, it was necessary to raise the tail water level. This was done by fixing a gate to the end of the flume. By adjusting its height the tail water could be raised or lowered accordingly. *Photo 4.4* shows the gate.

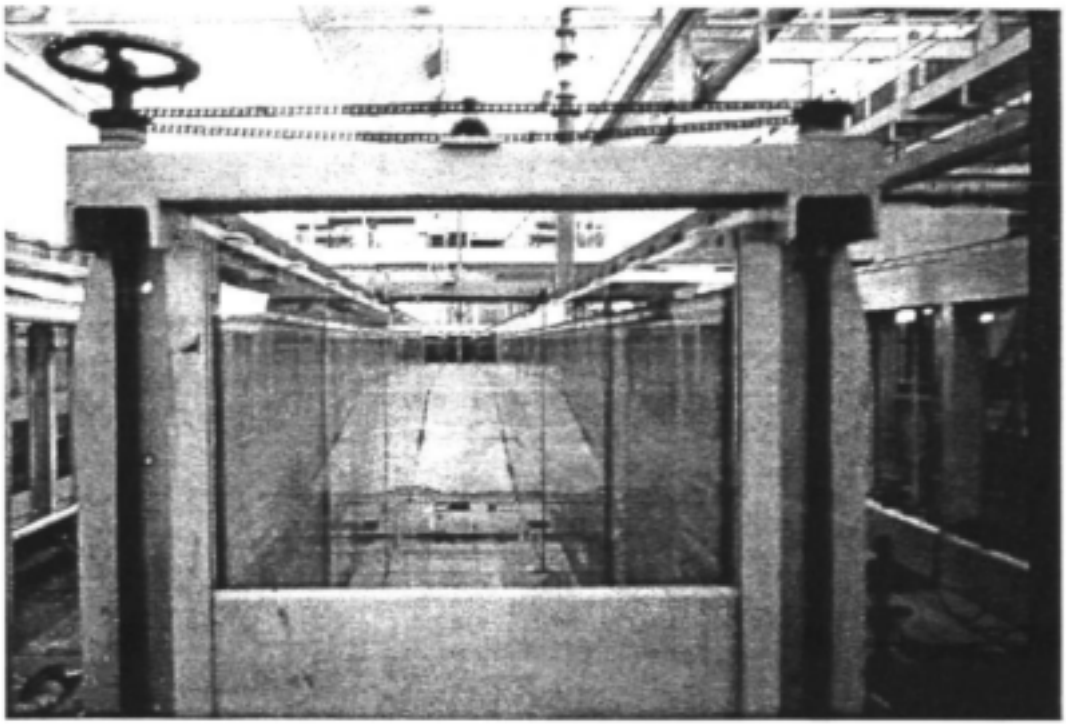

Photo 4.4: *Gate at the end of the glass flume used for testing the model piers, Hydraulics Laboratory, University of Stellenbosch*

4.2.3 Defining the configuration of the model piers and the arrangement of pressure measurement:

Optimisation of the energy based discharge equation for the above-mentioned flow conditions necessitated changing the pressure measuring configuration. In order to change the pressure measuring configuration and at the same time introduce additional measuring points, it was decided to construct new model piers from PVC. These model piers were made from hollow sections which could be joined as "building blocks" so as to form different combinations of lengths and widths. The advantage of these piers being hollow was that the water which accumulated "within" the pier ensured more stable water surface levels within the manometer pipes. The following changes were made to the pressure measuring configuration - note that **4** different positions along the pier surface were identified for calibration of the discharge formulae.

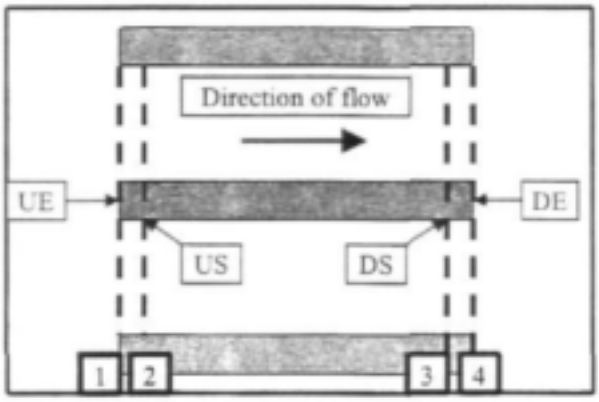

***Figure 4.)**: Defining the sections for the new configuration of pressure measurements*

❶ The pressure at the upstream end of the pier (**position UE,** *figure 4.2* or *photo 4.5*) was still measured as was done by *Retief*. This pressure represents the stagnation pressure, an important parameter in the energy based discharge equation.

❷ In addition to the pressure measurement at the face of the upstream end, the hydrostatic pressure on the side of the pier (**position US,** *figure 4.2* or *photo 4.5*) was measured. This pressure was measured at the upstream end of the pier where the curve of the semi-circular head joins the straight side of the pier.

❸ The third and fourth positions of pressure measurement (**positions DS and DE**, *figure 4.2* or *photo 4.5*) were used at equivalent positions to those mentioned above but at the downstream end of the pier. *Retief* used the **DE-position** (**section 4**) for pressure measuring during his tests. This was found to be unsatisfactory at high discharges for the pressure (depth) at **DE** is not representative of the total flow width due to the formation of eddies and draw-down of the water surface. This phenomenon was also observed during the model tests on the PVC piers as illustrated by the following two photos (*photo 4.5* and *photo 4.6*):

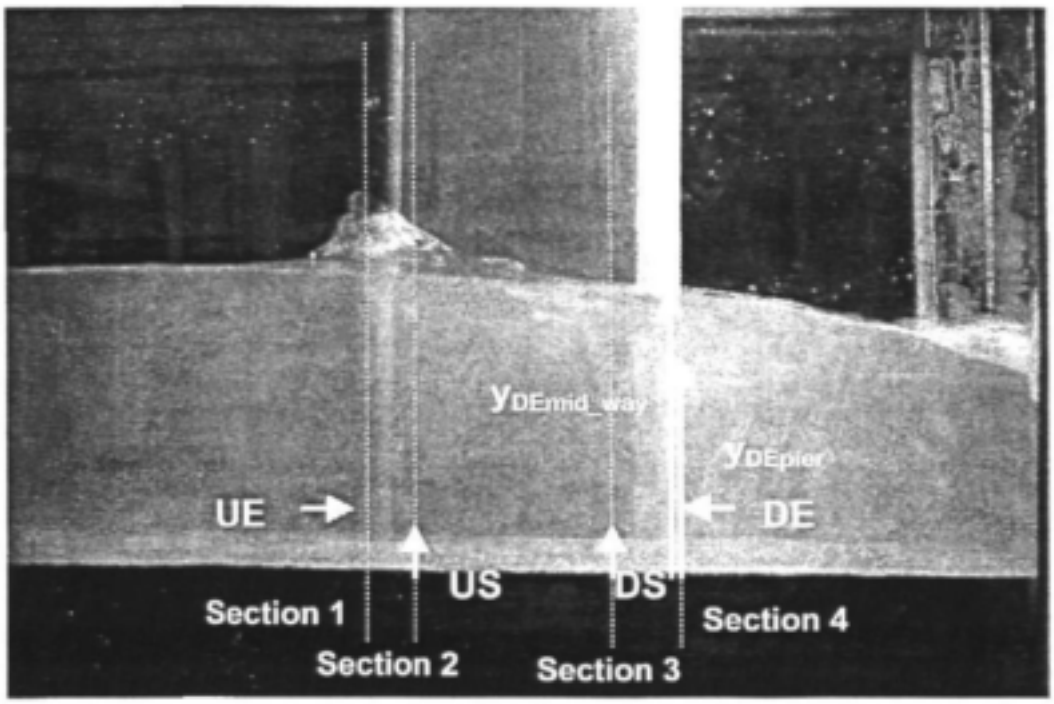

***Photo 4.5**: PVC 63 mm pier (SHORT) during a ±130 l/s test, supercritical flow conditions downstream etc.*

Note that the flow depth at **section DE** at the pier (y_{DEpier}) is much less than the flow depth at the same cross section but midway between two piers, i.e. flow depth $y_{DEmid\text{-}way}$. y_{DEpier} is therefore not representative of flow across **section DE. Section 3** and pressure point **DS** were therefore introduced in order to obtain a downstream water depth that would be more representative of the flow depth across the width between neighbouring piers. The differences in head are reflected by the manometer readings shown in *photo 4.6*. The water surfaces within the manometer pipes correspond to the flow depths at sections **UE, US, DS** and **DE** respectively as seen in *photo 4.5*.

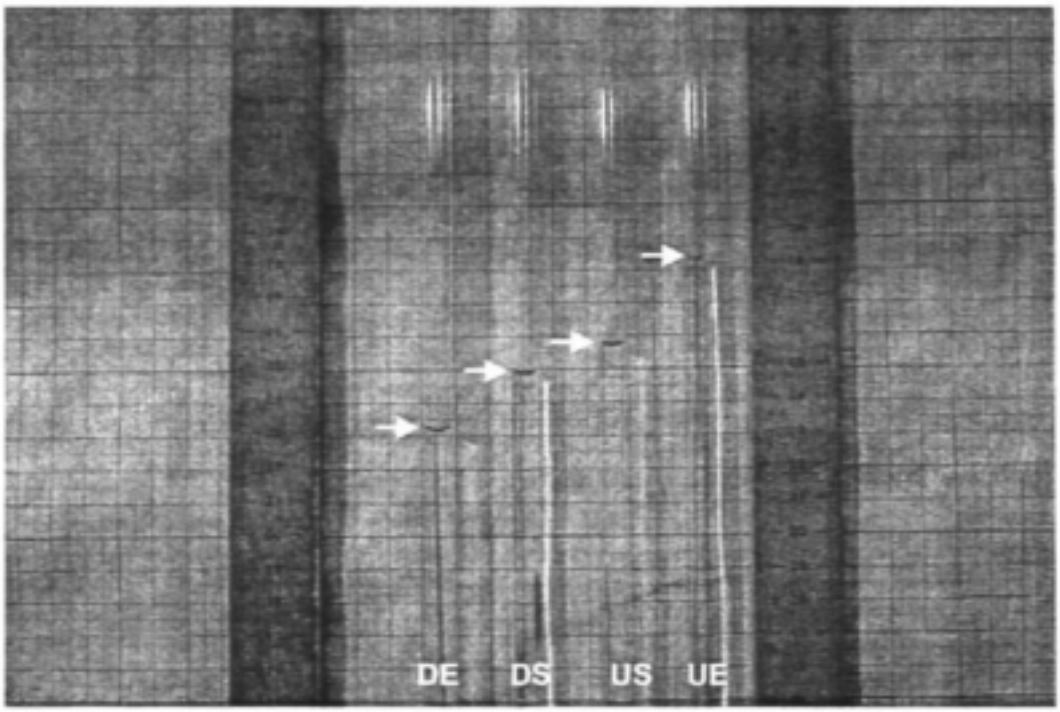

***Photo 4.6**: Measured pressure heads inside manometer pipes during a test on a PVC 63 mm pier (SHORT) ,±130 l/s test, supercritical flow conditions downstream etc.*

The water surface level in manometer **pipe DE** corresponds to the depth y_{DEpier} and is much lower than the depth y_{DEmid_way} which is found within the contraction.

Although measuring **position DS** was introduced, **position DE** was kept for use under drowned conditions where the pressure or depth becomes more representative of that across the flow width.

Figure 4.3 shows details of the pressure measuring lay-out at the upstream and downstream ends of the pier:

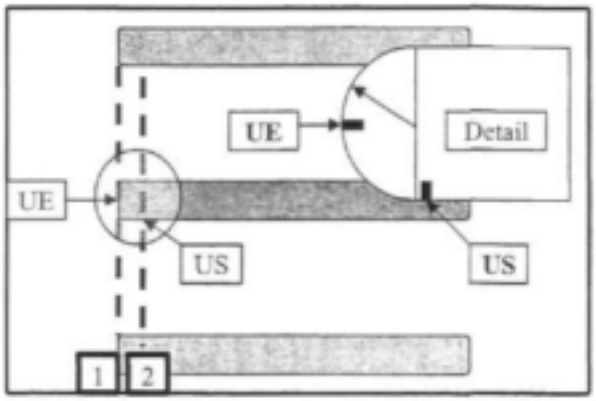

Figure 4.3: *Detail of pressure measurement positions at* **A** *and* **B** *at the upstream pier end (downstream lay-out similar)*

Photo 4.7 combines the details mentioned above.

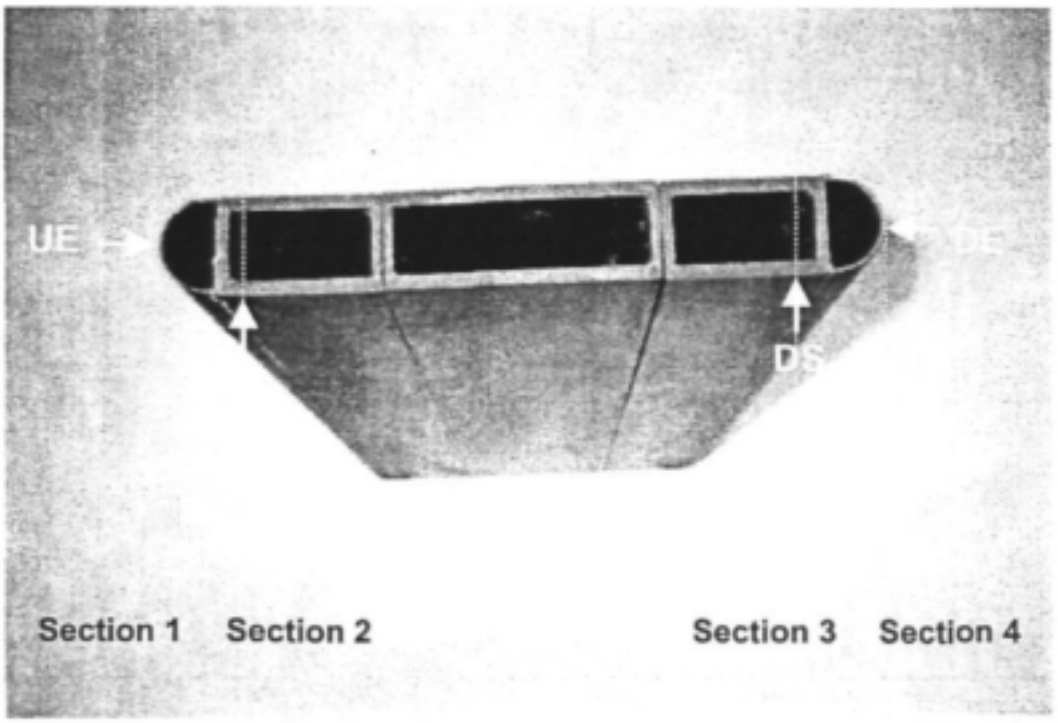

Photo 4.7: *Defining sections 1,2,3 and 4 and measuring positions UE, US, DS and DE*

4.2.4 Defining the different flow conditions:

The following flow conditions were investigated:

- Flow approaching the pier in line with the pier under non-drowned conditions, as well as drowned flow conditions downstream (supercritical vs. sub-critical conditions) for bull-nose shaped piers with different **B/b_p** ratios. The bull-nose shape is very common at existing bridges in the RSA and an estimated 80% of piers are of this shape for construction and hydraulic reasons. Pressure measuring was done according to the lay-out shown in *figure 4.3*. Four different **B/b_p** ratios were tested, they were: **9.7, 12.2, 15.2** and **19.0**. *Photo 4.8* shows the different pier widths that were used in the 609 mm wide flume in the laboratory:

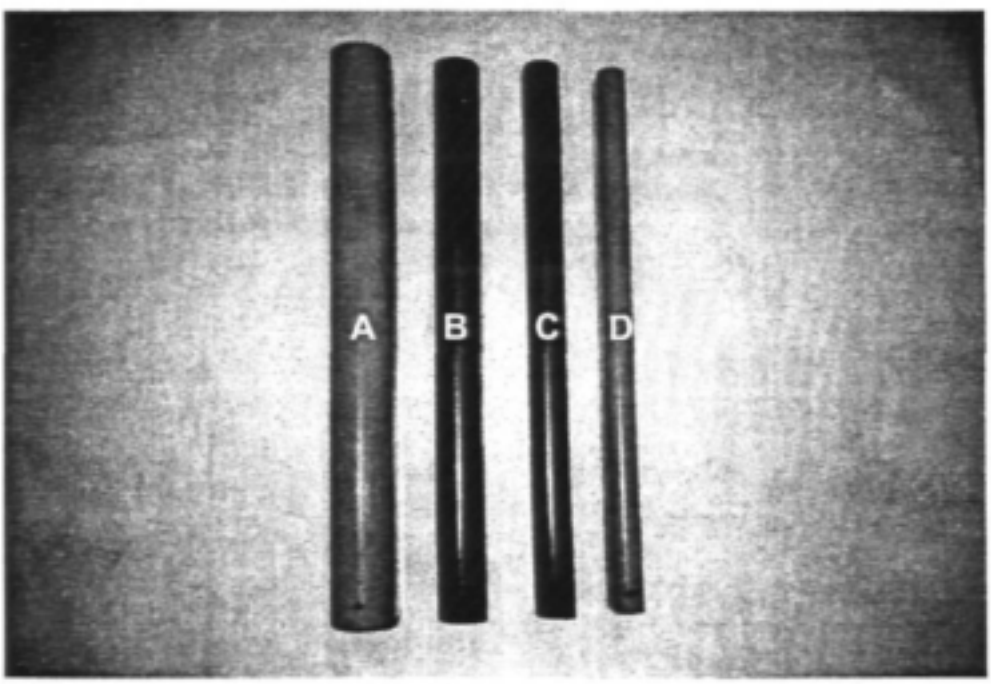

***Photo 4.8**: Four different pier widths of the model piers: A=63 mm (B/b_p=9.6), B=50 mm (B/b_p=12.2), C=40 mm (B/b_p=15.2), D=32 mm (B/b_p=19.0)*

For each of the piers with different B/b_p ratios the L/b_p ratio was changed. This was done by adding a central section to a model pier in order to increase the length of the pier (L_p). Three different L/b_p ratios were used for each B/b_p ratio resulting in **12** combinations of width and length ratios. Tests on these **12** combinations covered both super and sub-critical downstream flow conditions (note that for all these tests, flows were in line with the piers, i.e. no rotation of the pier relative to the approaching flow). *Photo 4.9* shows one of the piers with its "building blocks" taken apart. By joining these "building blocks" in different combinations it was possible to obtain different L/b_p ratios for the same B/b_p ratio.

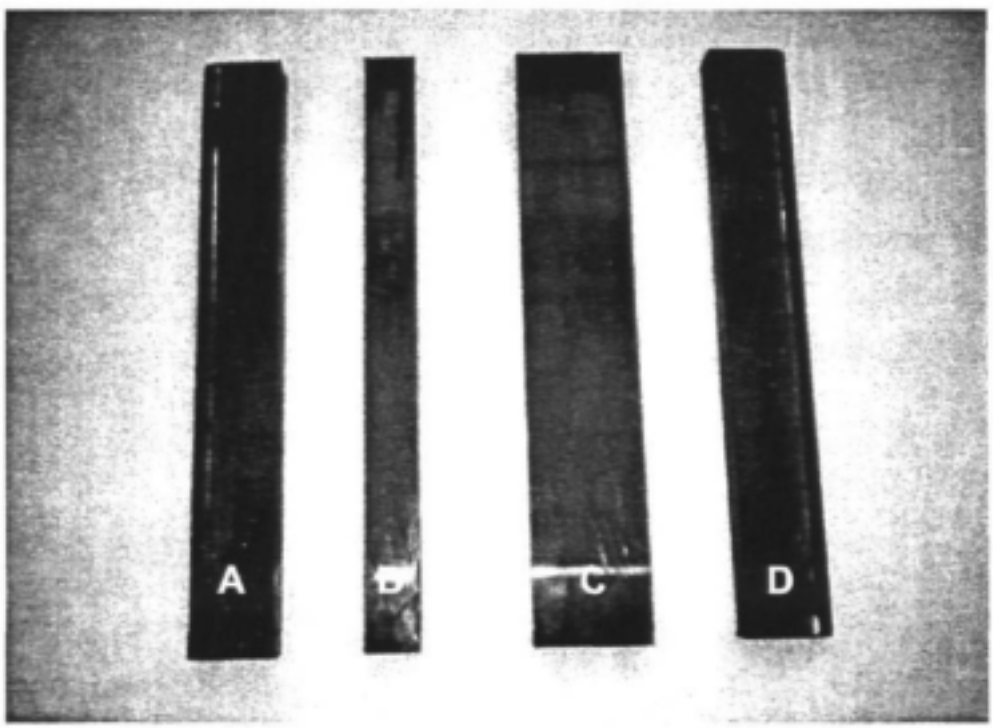

***Photo 4.9**: "Building blocks" of a typical PVC pier model. A=upstream end, B=extension for "MEDIUM" length, C=extension for "LONG" length, D=downstream end)*

❸ Non-parallel flow conditions were also considered and investigated, i.e. conditions where the approaching flow does not enter the constriction between the piers parallel

to the long-axis of the pier, but at a certain angle. As it was not possible to change the approaching flow direction within the laboratory (glass flume) it was necessary to rotate the model pier relative to the flow direction. The degree of rotation was defined as the angle between the direction of approaching flow (**A**) and the long axis (**B**) of the pier. The angle was expressed as theta (θ) as shown in *photo 4.10*. The same pressure measuring lay-out was used as in *figure 4.3*.

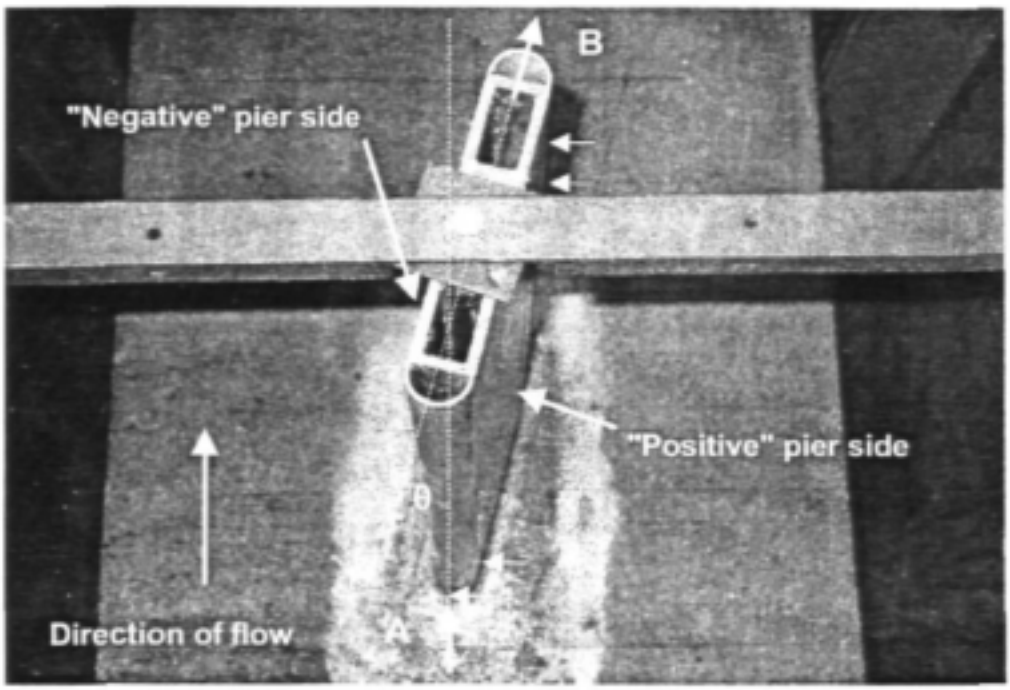

Photo 4.10: *Defining the rotation of the model pier. A=direction of approaching flow, B=long axis direction, θ=relative angle between A and B*

Note that the pier was rotated so that the side on which the pressure holes were made was on the "positive" pier side, i.e. the side that faces the approaching stream and experiences increased pressures. The flow passing on this side displays a more stable flow pattern with associated larger flow depths. The "negative" pier side is also shown in *photo 4.10*. On this lee-side flows are shallower and more turbulent, and unsteady and fluctuating. The small arrows in *photo 4.10* indicate the positions of the pressure measuring holes shown in *photo 4.7*.

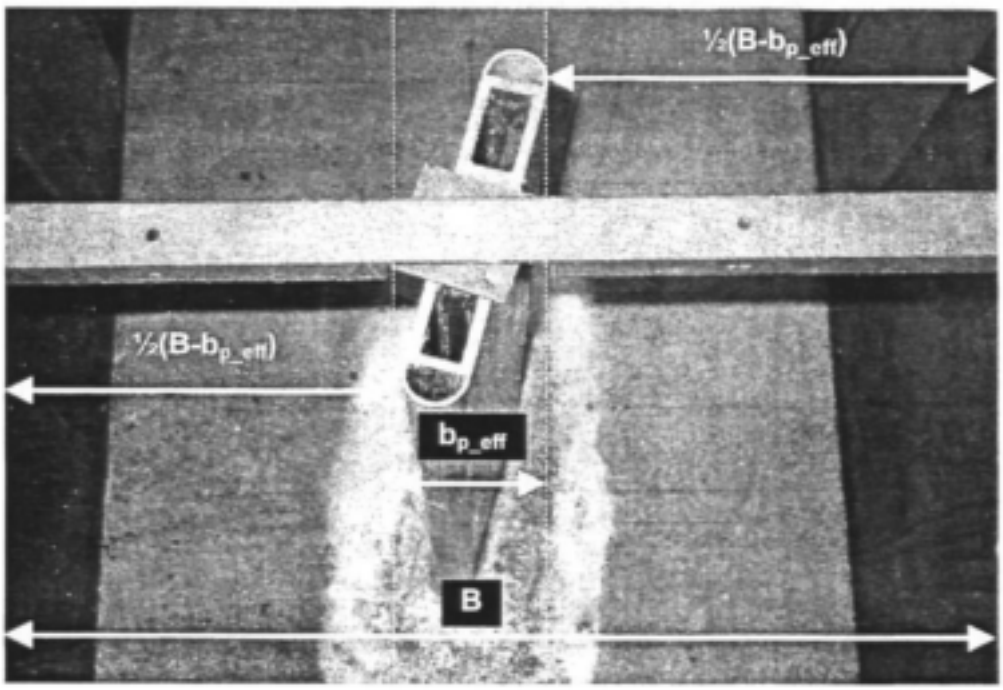

Photo 4.11: *Defining the effective pier width for non-parallel flow conditions, B = total flume width, b_{p_eff} = effective pier width and $(B-b_{p\_eff})$ the effective or net width of passing flow*

4.2.5 Model tests on flow patterns around piers, pictorial record:

4.2.5.1 Parallel flow approaching pier:

SUPERCRITICAL flow conditions downstream of the pier

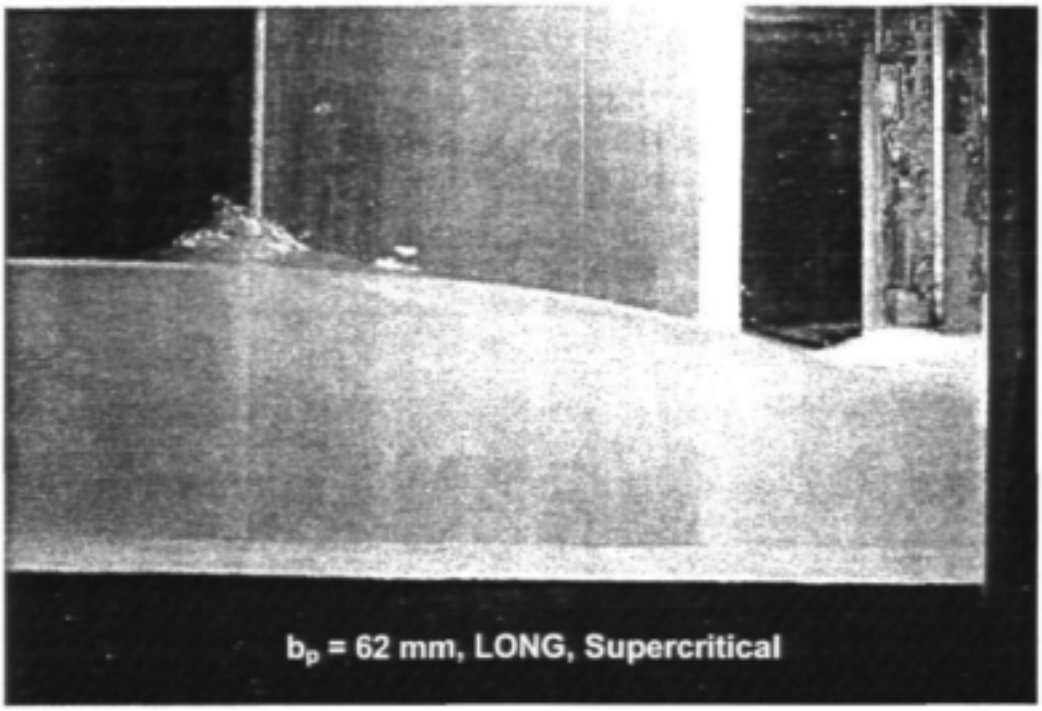

Photo 4.12: *Flow patterns past model pier, parallel approaching flow, B/b_p = 9.7, L/b_p = 6.9 (LONG), Q = ±130 l/s, supercritical flow conditions downstream*

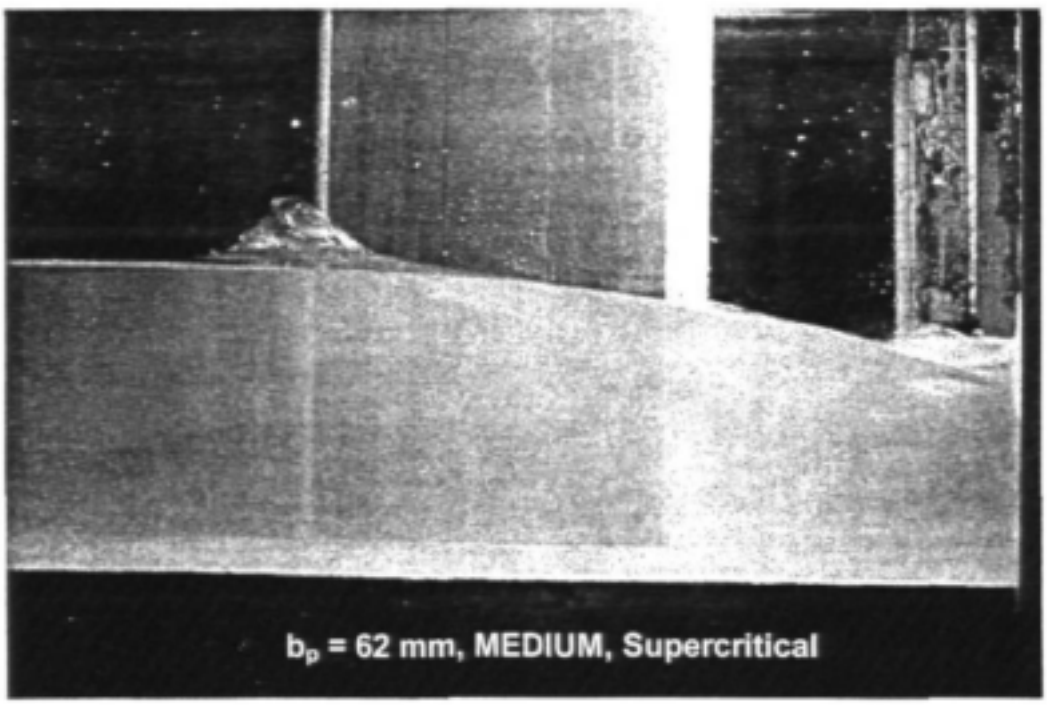

Photo 4.13*: Flow patterns past model pier, parallel approaching flow, B/b_p = 9.7, L/b_p = 5.6 (MEDIUM), Q = ±130 l/s, supercritical flow conditions downstream*

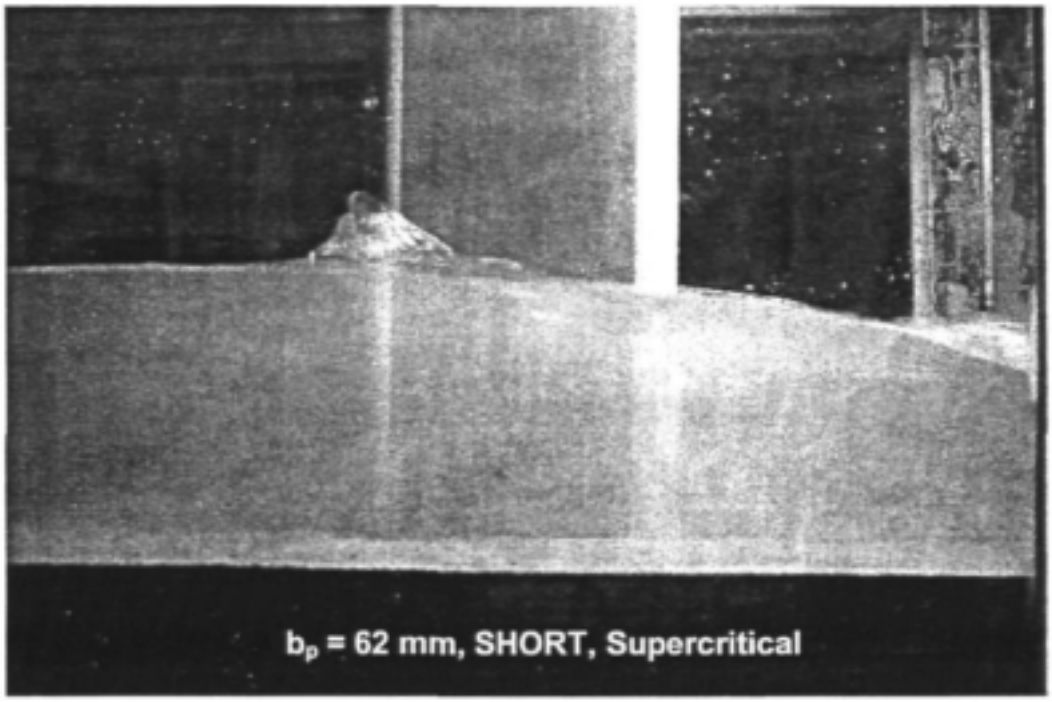

***Photo 4.14**: Flow patterns past model pier, parallel approaching flow, B/b_p = 9.7, L/b_p = 4.2 (SHORT), Q = ±130 l/s, supercritical flow conditions downstream*

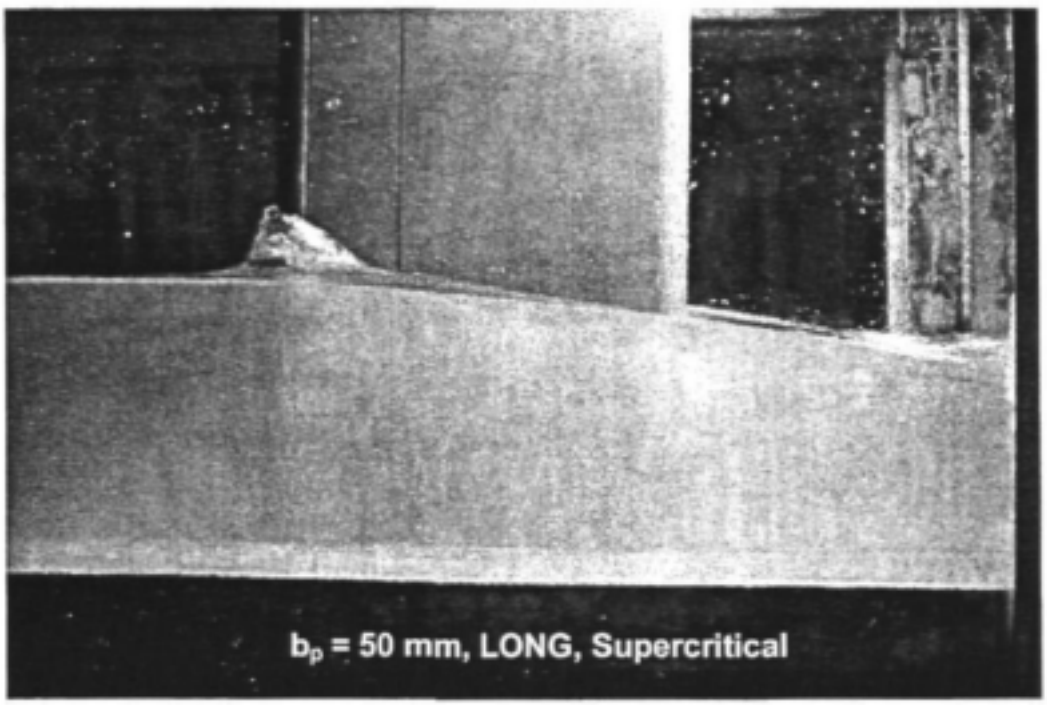

***Photo 4.15**: Flow patterns past model pier, parallel approaching flow, B/b_p = 12.2 , L/b_p = 6.9 (LONG), Q = ±130 l/s, supercritical flow conditions downstream*

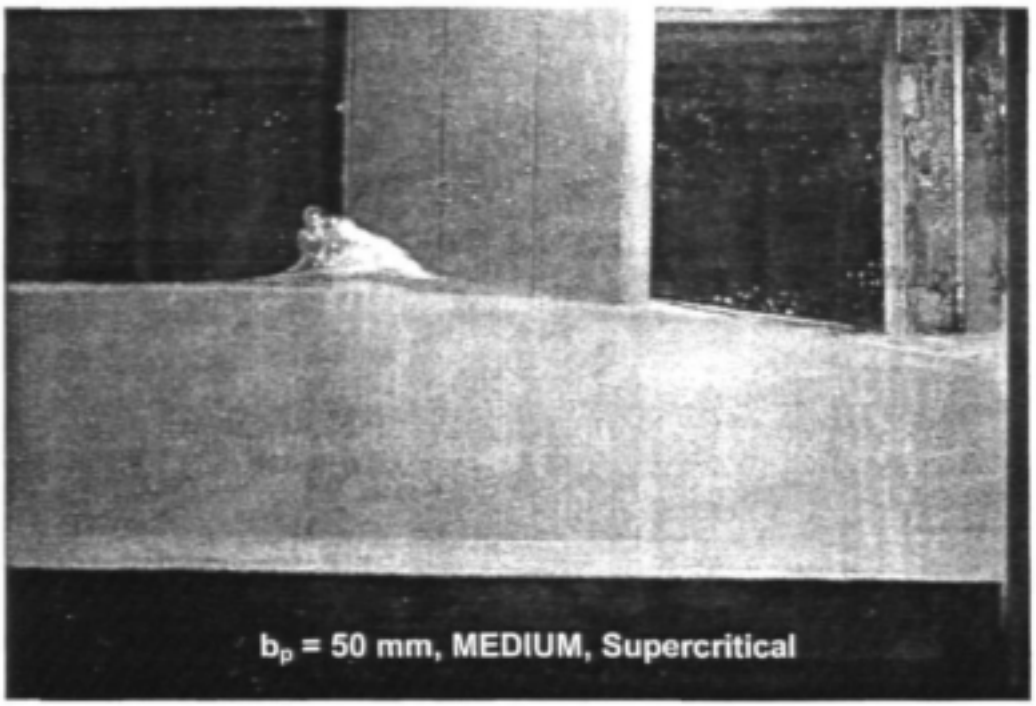

Photo 4.16: *Flow patterns past model pier, parallel approaching flow, B/b_p = 12.2 , L/b_p = 5.6 (MEDIUM), Q = ±130 l/s, supercritical flow conditions downstream*

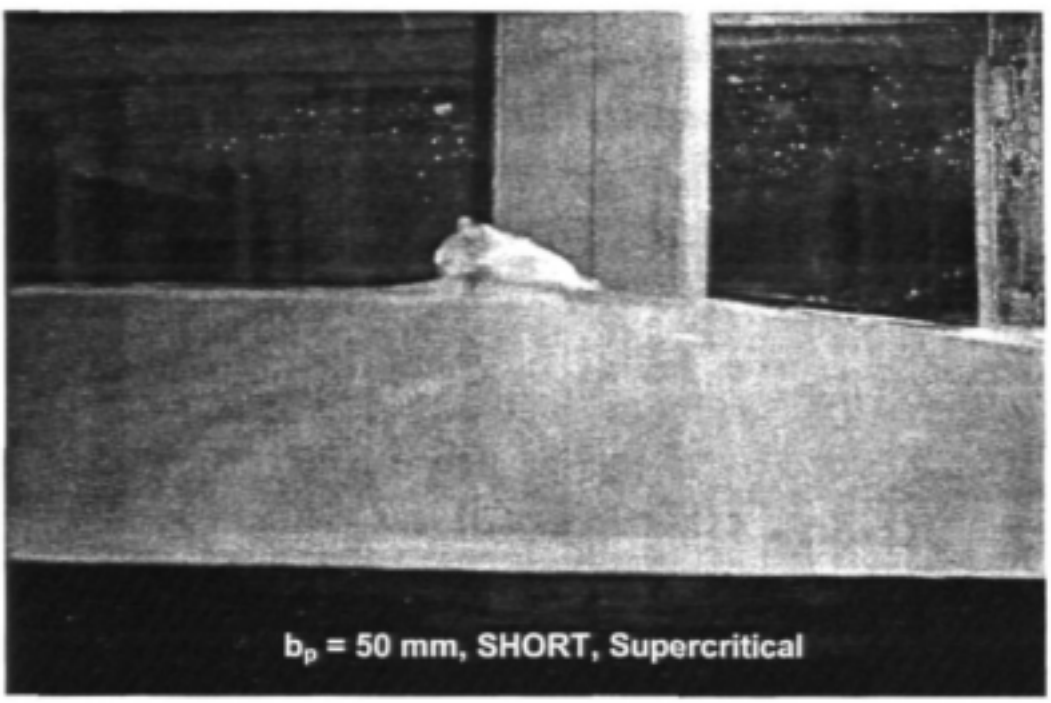

Photo 4.17: *Flow patterns past model pier, parallel approaching flow, B/b_p = 12.2 , L/b_p = 4.2 (SHORT), Q = ±130 l/s, supercritical flow conditions downstream*

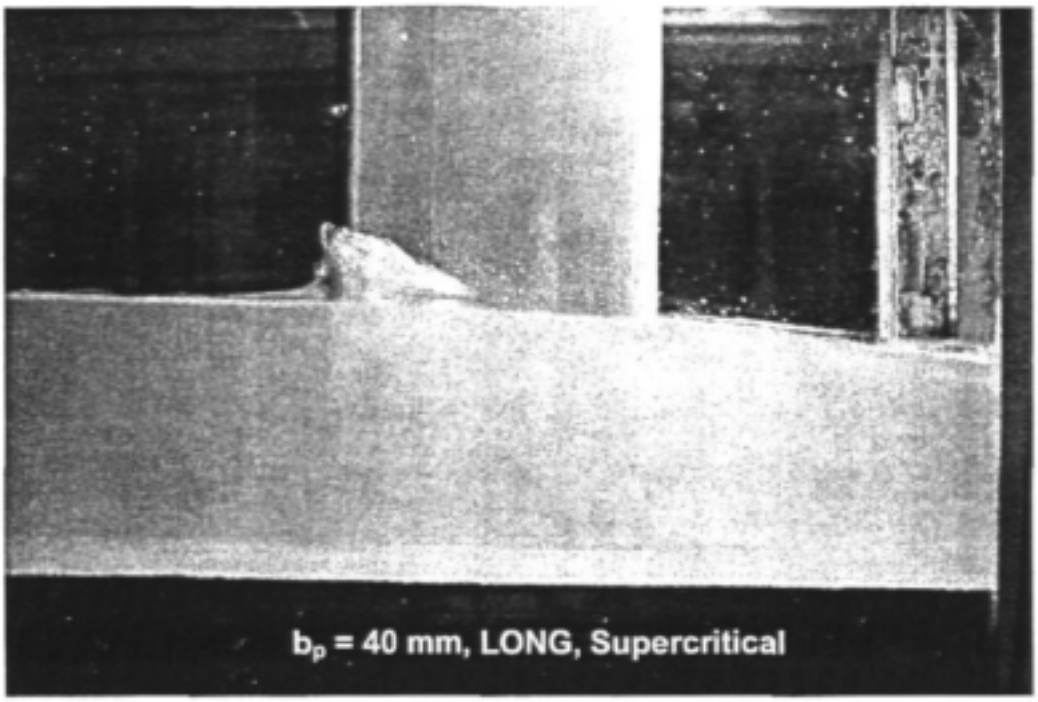

***Photo 4.18**: Flow patterns past model pier, parallel approaching flow, B/b_p = 15.2 , L/b_p = 6.9 (LONG), Q = ±130 l/s, supercritical flow conditions downstream*

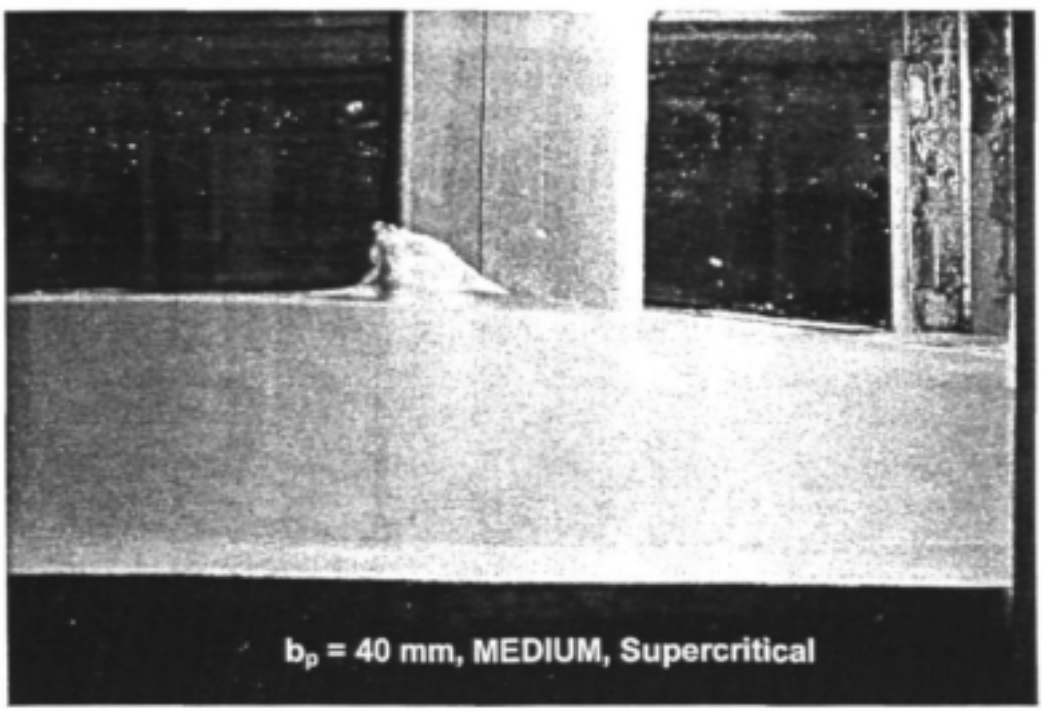

***Photo 4.19:** Flow patterns past model pier, parallel approaching flow, B/b_p = 15.2 , L/b_p = 5.6 (MEDIUM), Q = ±130 l/s, supercritical flow conditions downstream*

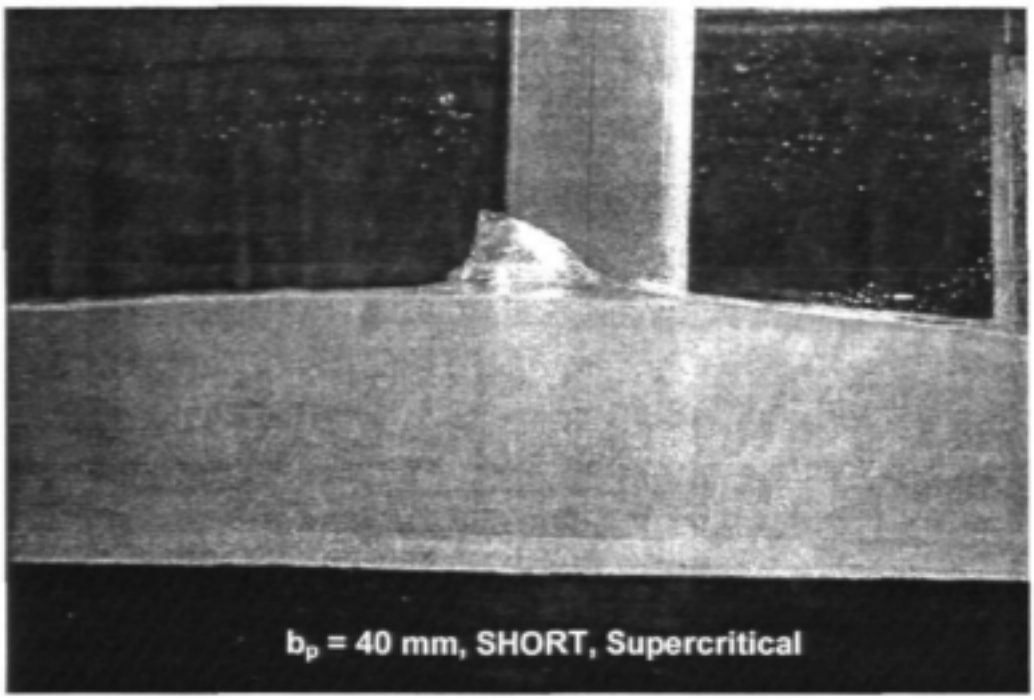

Photo 4.20: *Flow patterns past model pier, parallel approaching flow, B/b_p = 15.2 , L/b_p = 4.2 (SHORT), Q = ±130 l/s, supercritical flow conditions downstream*

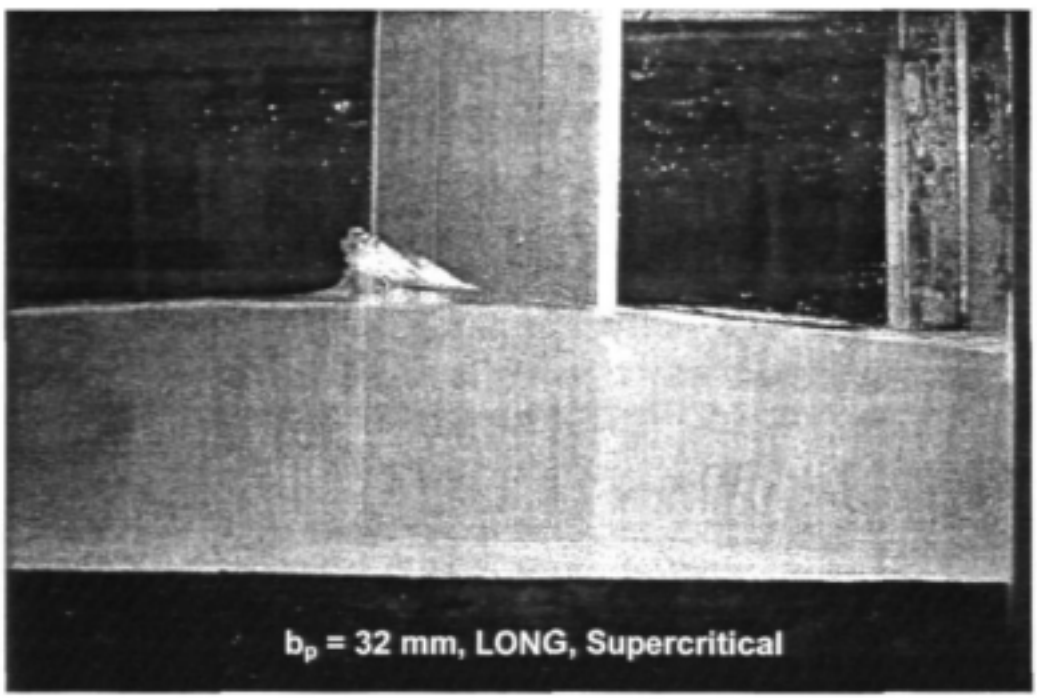

Photo 4.21*: Flow patterns past model pier, parallel approaching flow, B/b_p = 19.0 , L/b_p = 6.9 (LONG), Q = ±130 l/s, supercritical flow conditions downstream*

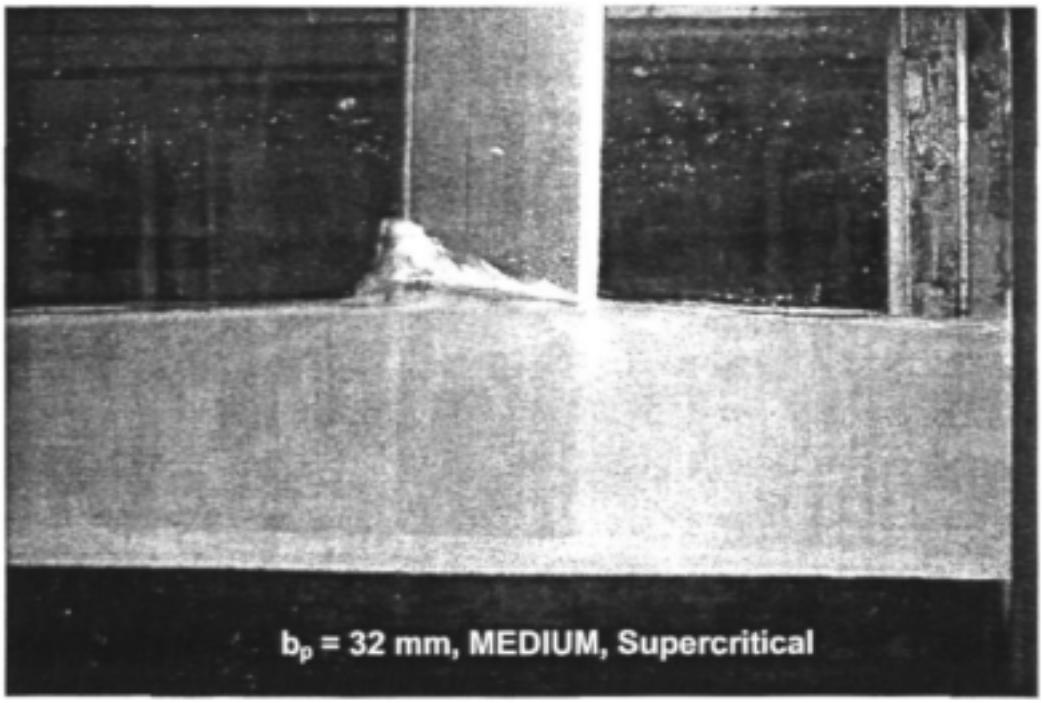

***Photo 4.22**: Flow patterns past model pier, parallel approaching flow, B/b_p = 19.0 , L/b_p = 5.6 (MEDIUM), Q = ±130 l/s, supercritical flow conditions downstream*

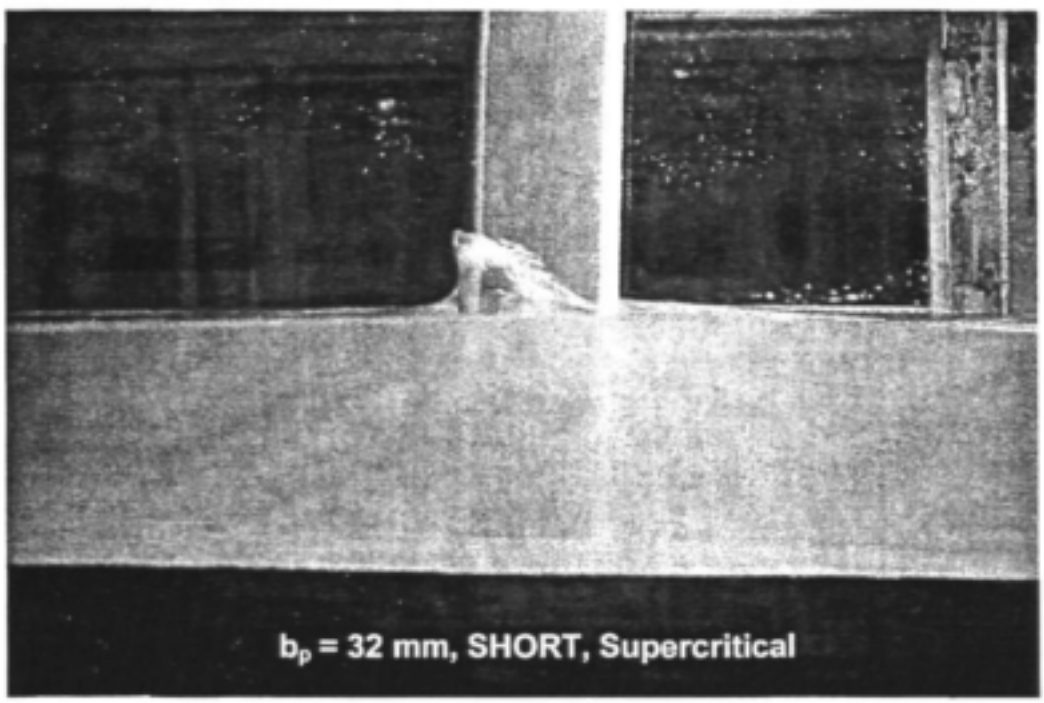

***Photo 4.23:** Flow patterns past model pier, parallel approaching flow, B/b_p = 19.0 , L/b_p = 4.2 (SHORT), Q = ±130 l/s, supercritical flow conditions downstream*

DROWNED flow conditions downstream of the pier

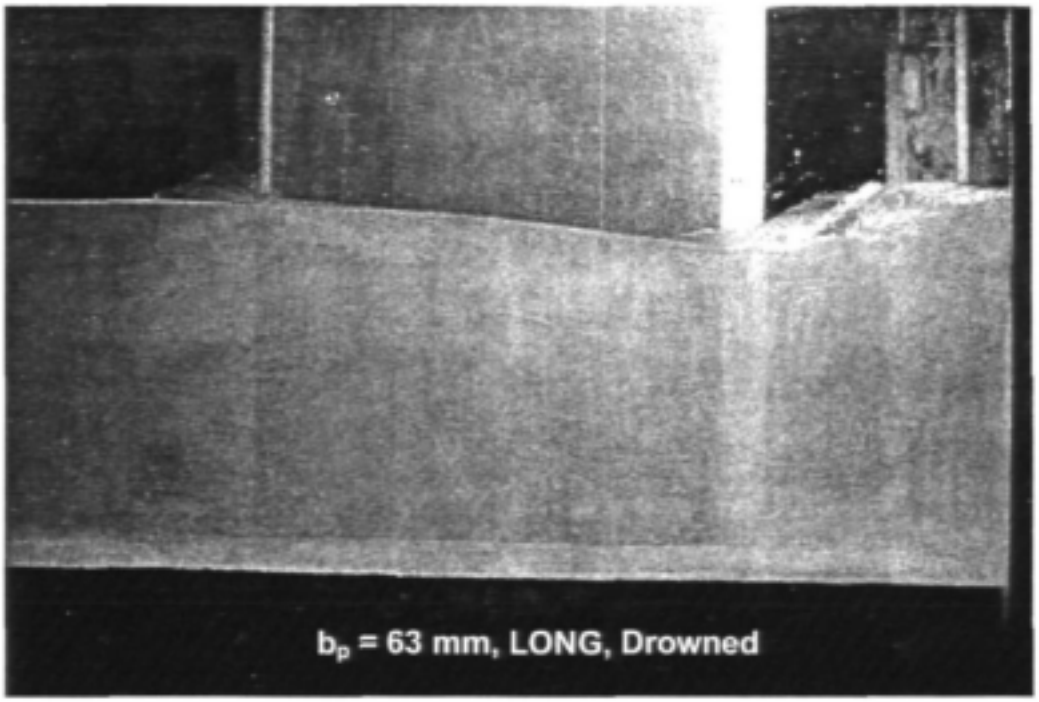

Photo 4.24: *Flow patterns past model pier, parallel approaching flow, B/b_p = 9.7 , L/b_p = 6.9 (LONG), Q = ±130 l/s, drowned flow conditions downstream*

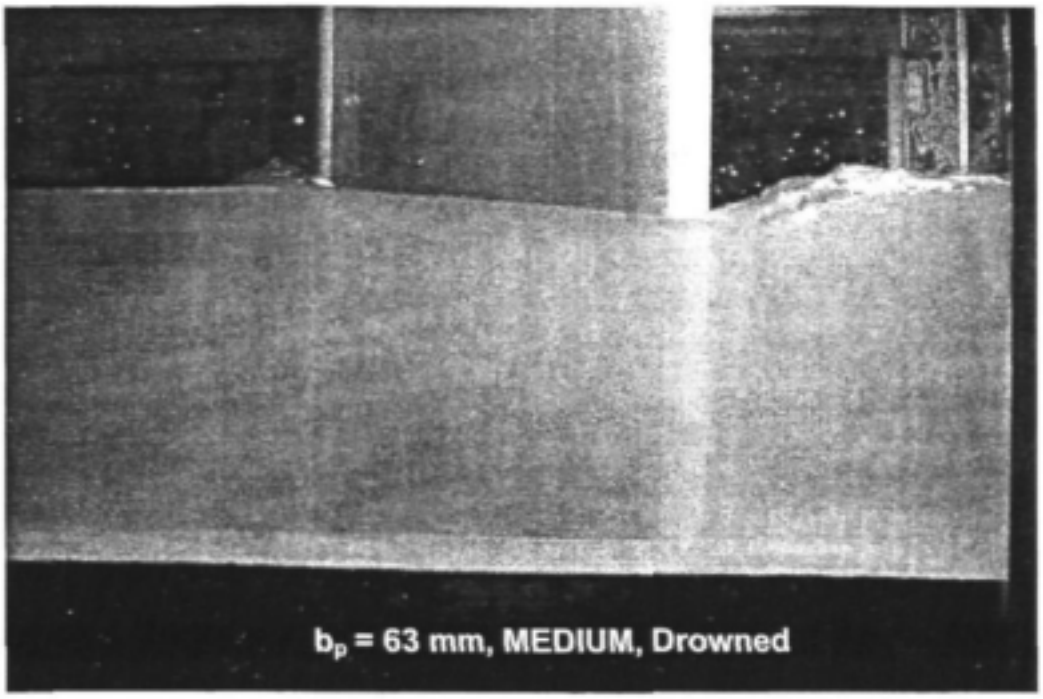

Photo 4.25: *Flow patterns past model pier, parallel approaching flow, B/b_p = 9.7 , L/b_p = 5.6 (MEDIUM), Q = ±130 l/s, drowned flow conditions downstream*

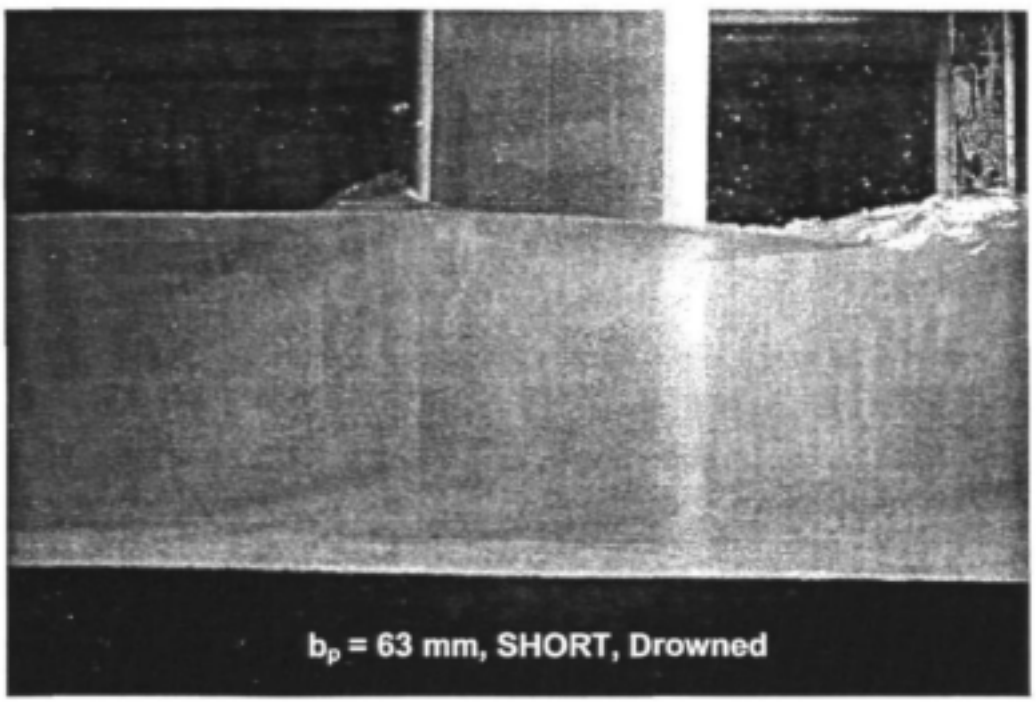

Photo 4.26: *Flow patterns past model pier, parallel approaching flow, B/b_p = 9.7 , L/b_p = 4.2 (SHORT), Q = ±130 l/s, drowned flow conditions downstream*

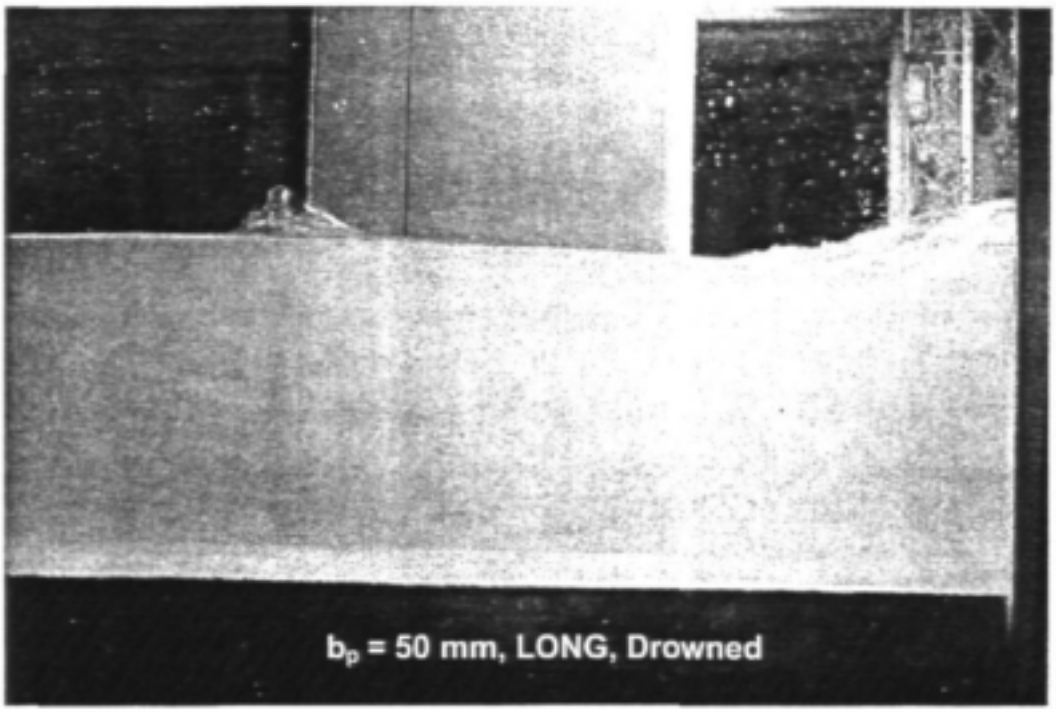

***Photo 4.27**: Flow patterns past model pier, parallel approaching flow, B/b_p = 12.2 , L/b_p = 6.9 (LONG), Q = ±130 l/s, drowned flow conditions downstream*

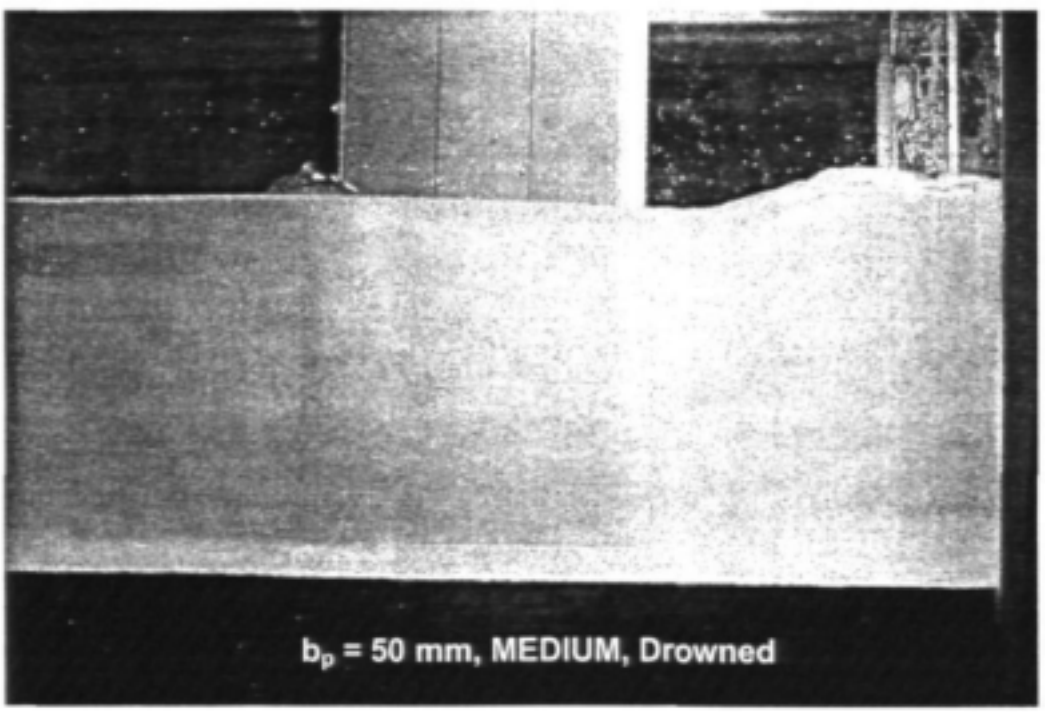

***Photo 4.28:** Flow patterns past model pier, parallel approaching flow, B/b_p = 12.2 , L/b_p = 5.6 (MEDIUM), Q = ±130 l/s, drowned flow conditions downstream*

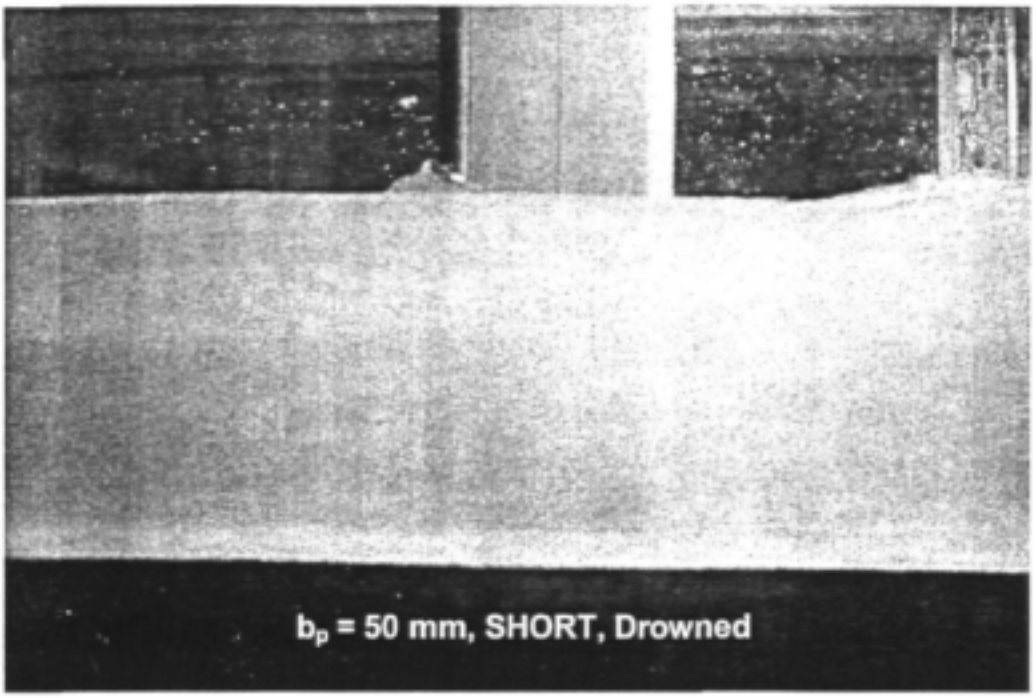

***Photo 4.29**: Flow patterns past model pier, parallel approaching flow, B/b_p = 12.2 , L/b_p = 4.2 (SHORT), Q = ±130 l/s, drowned flow conditions downstream*

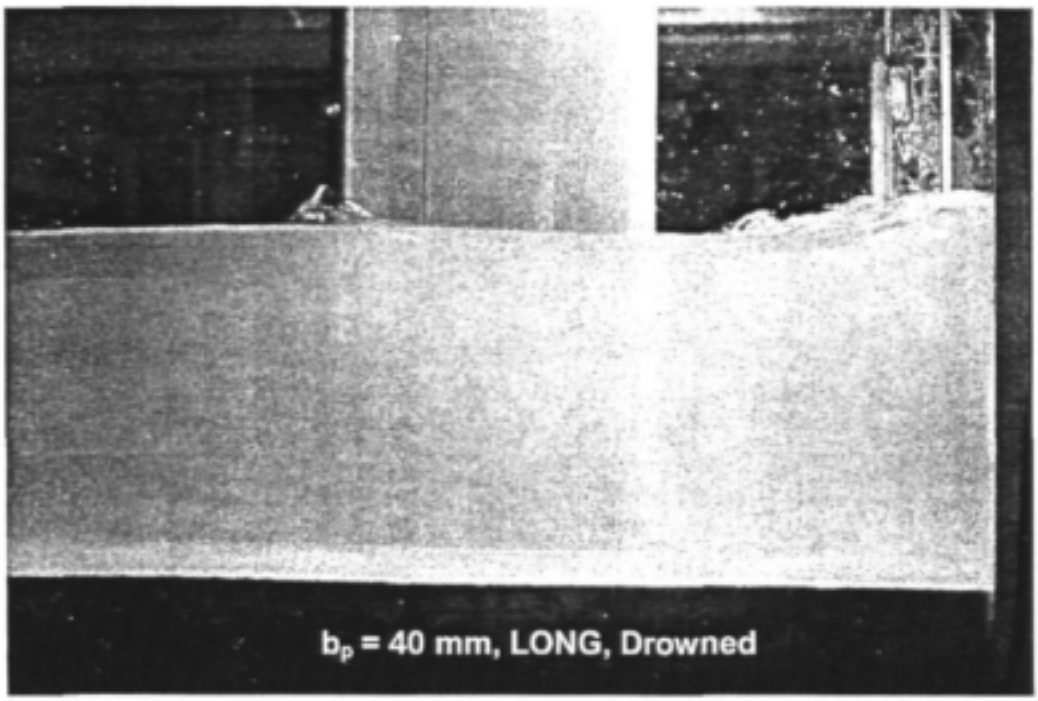

***Photo 4.30:** Flow patterns past model pier, parallel approaching flow, B/b_p = 15.2 , L/b_p = 6.9 (LONG), Q = ±130 l/s, drowned flow conditions downstream*

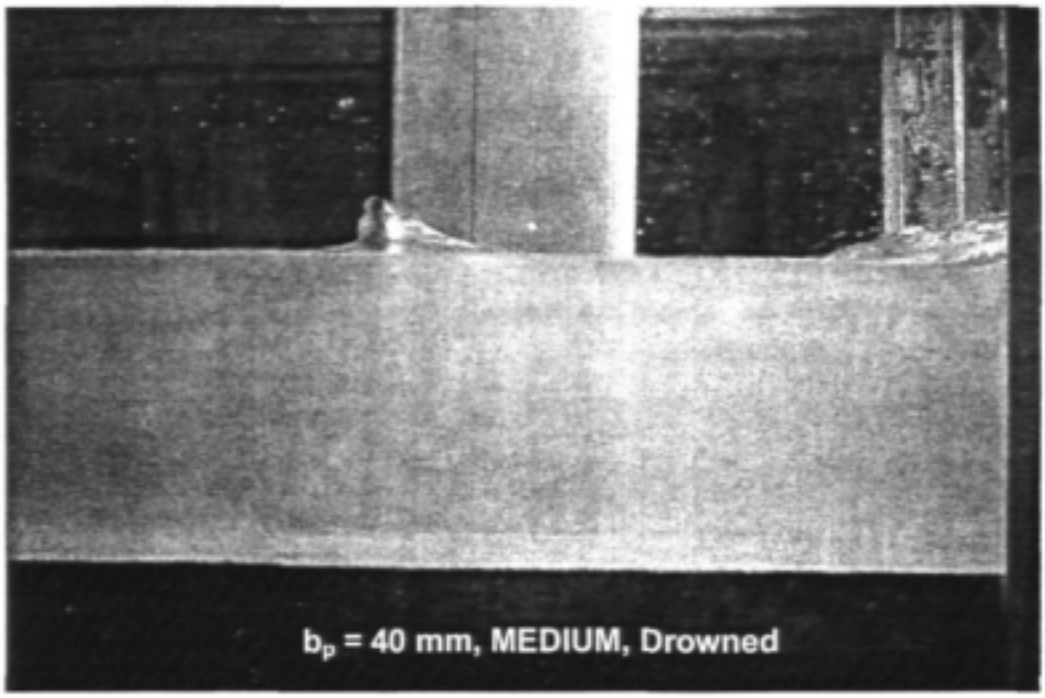

***Photo 4.31**: Flow patterns past model pier, parallel approaching flow, B/b_p = 15.2 , L/b_p = 5.6 (MEDIUM), Q = ±130 l/s, drowned flow conditions downstream*

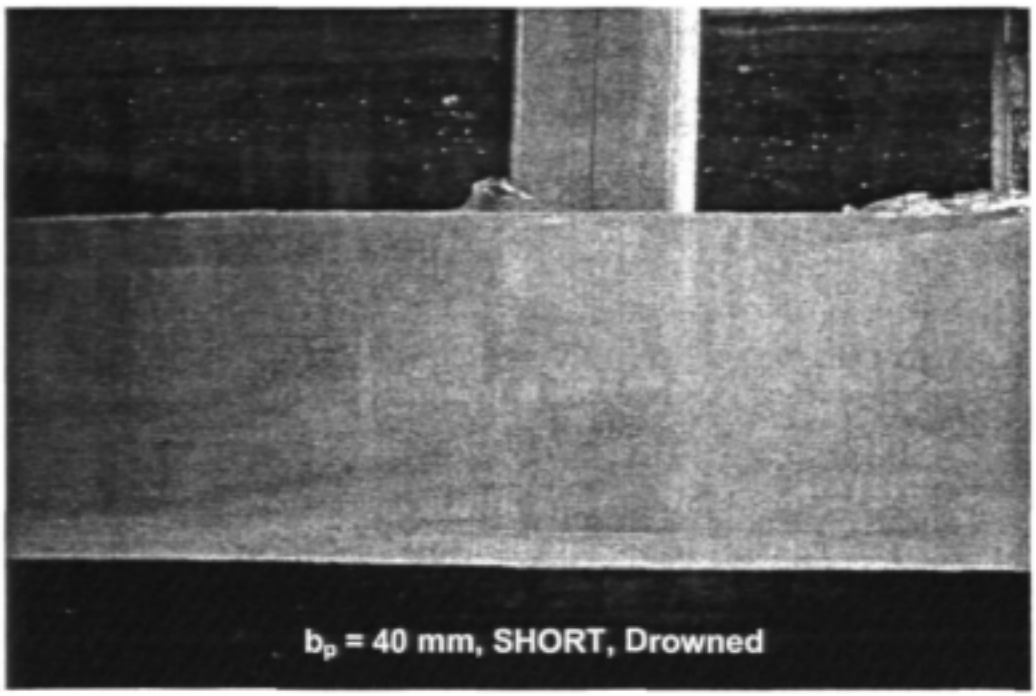

***Photo 4.32**: Flow patterns past model pier, parallel approaching flow, B/b_p = 15.2 , L/b_p = 4.2 (SHORT), Q = ±130 l/s, drowned flow conditions downstream*

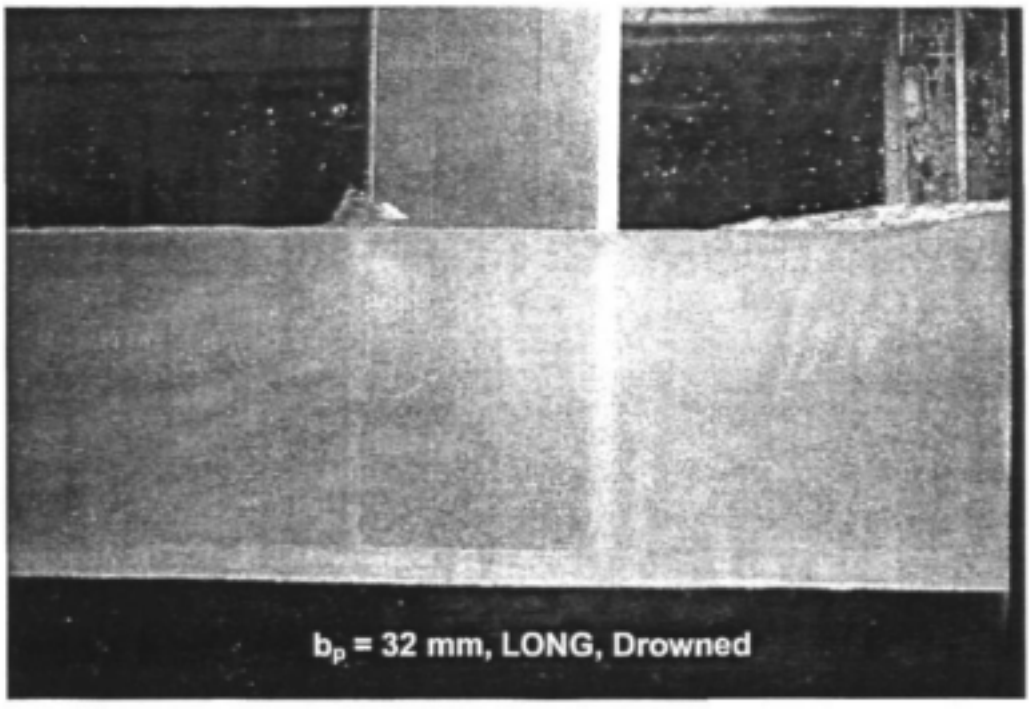

***Photo 4.33**: Flow patterns past model pier, parallel approaching flow, B/b_p = 19.0 , L/b_p = 6.9 (LONG), Q = ±130 l/s, drowned flow conditions downstream*

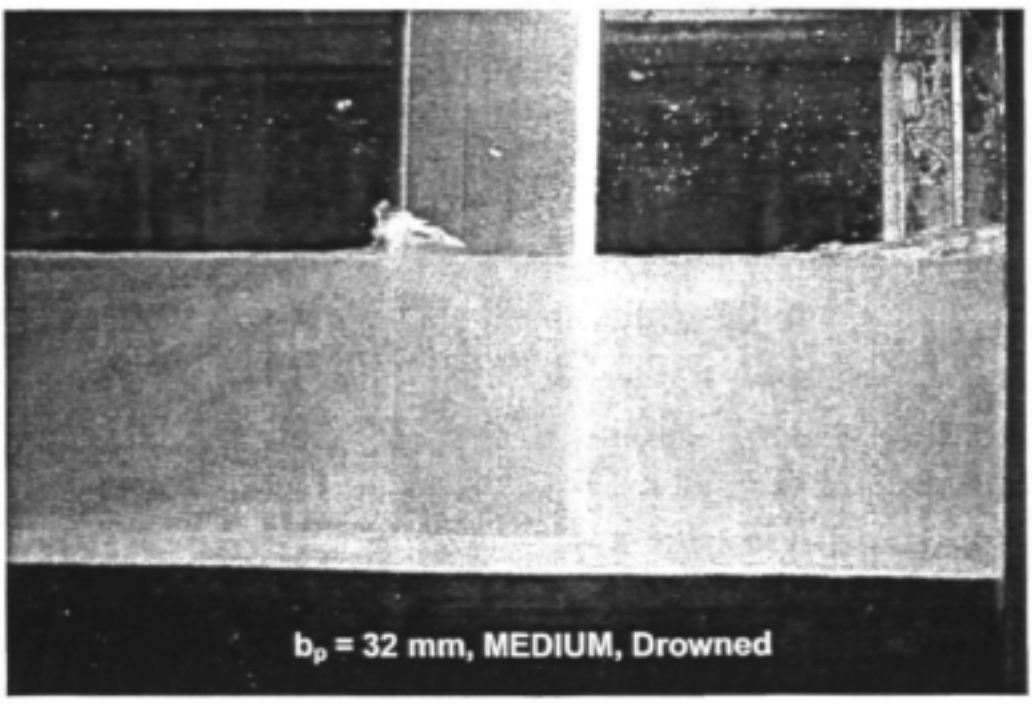

***Photo 4.34**: Flow patterns past model pier, parallel approaching flow, B/b_p = 19.0 , L/b_p = 5.6 (MEDIUM), Q = ±130 l/s, drowned flow conditions downstream*

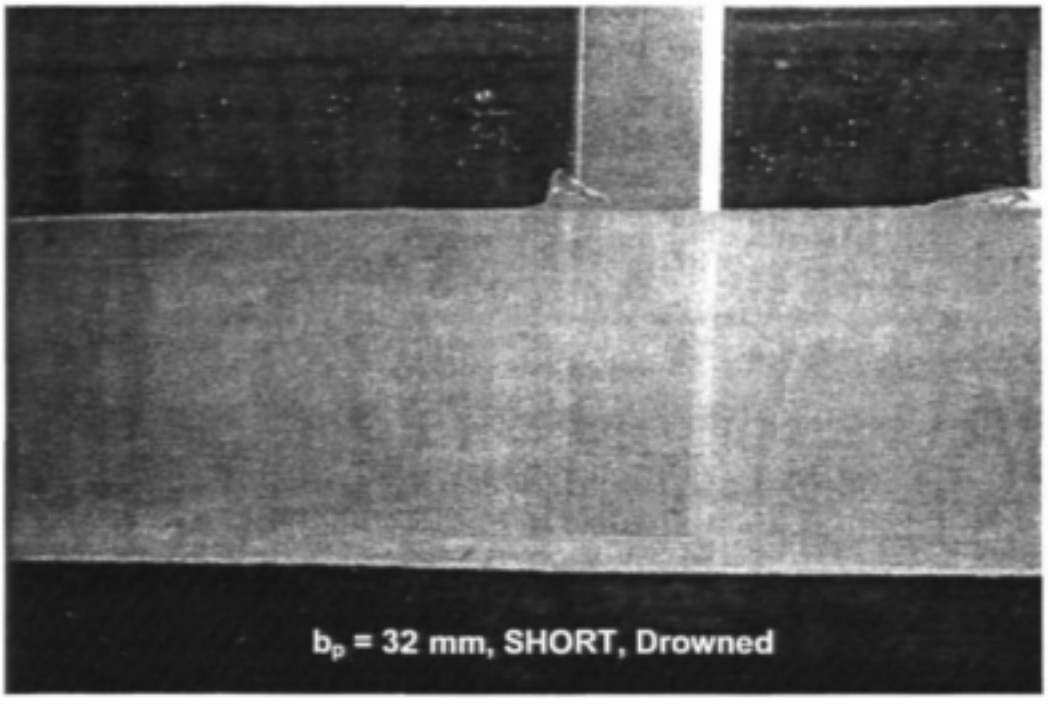

Photo 4.35: *Flow patterns past model pier, parallel approaching flow, B/b_p = 19.0 , L/b_p = 4.2 (SHORT), Q = ±130 l/s, drowned flow conditions downstream*

4.2.5.2 Non-parallel approaching flow:

DROWNED flow conditions downstream of the pier

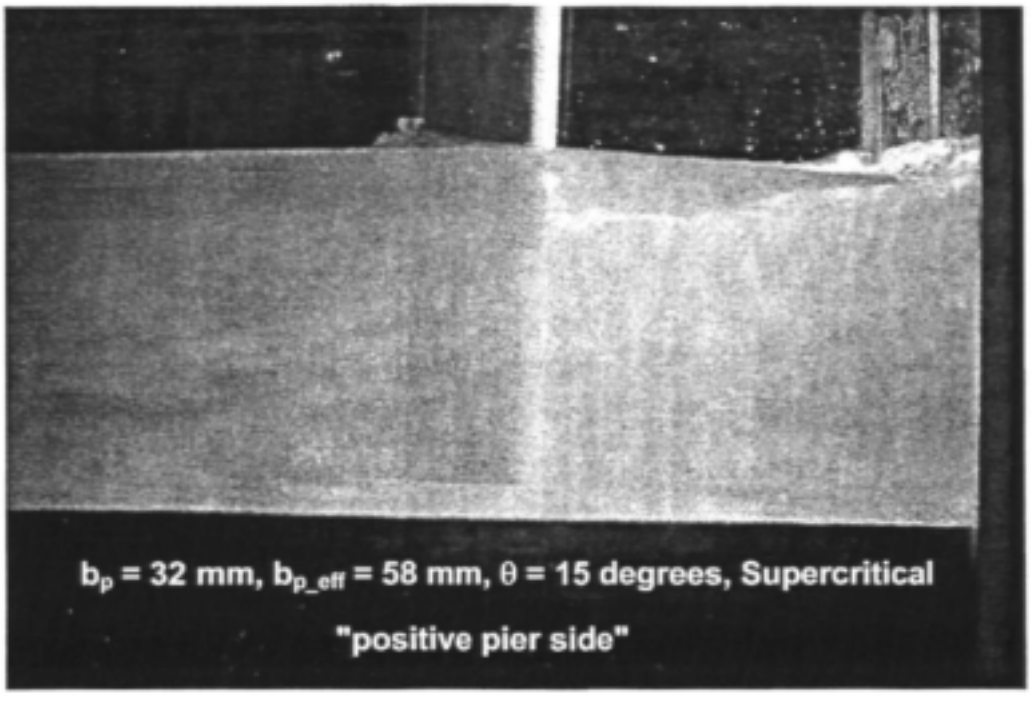

***Photo 4.36**: Flow patterns past model pier, non-parallel approaching flow, B/b_p = 19.0 , L/b_p = 4.2 (SHORT), θ = 15 degrees, "positive pier side" shown, Q = ±130 l/s, supercritical flow conditions downstream*

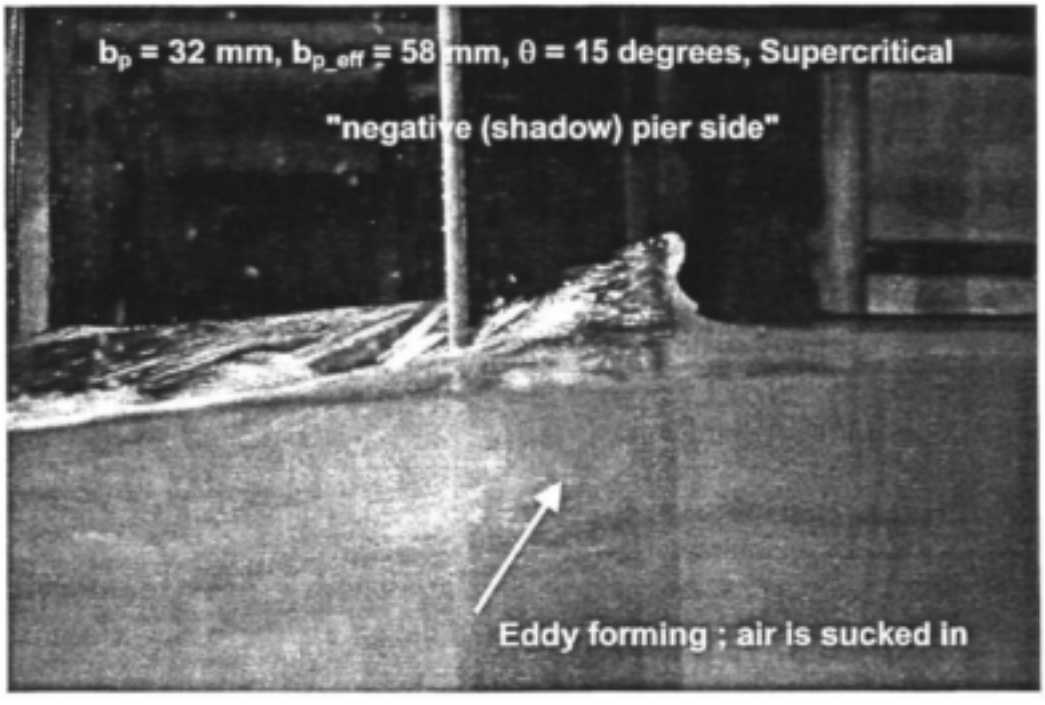

***Photo 4.37**: Flow patterns past model pier, non-parallel approaching flow, B/b_p = 19.0 , L/b_p = 4.2 (SHORT), θ = 15 degrees, "negative (lee) pier side" shown, Q = ±130 l/s, supercritical flow conditions downstream*

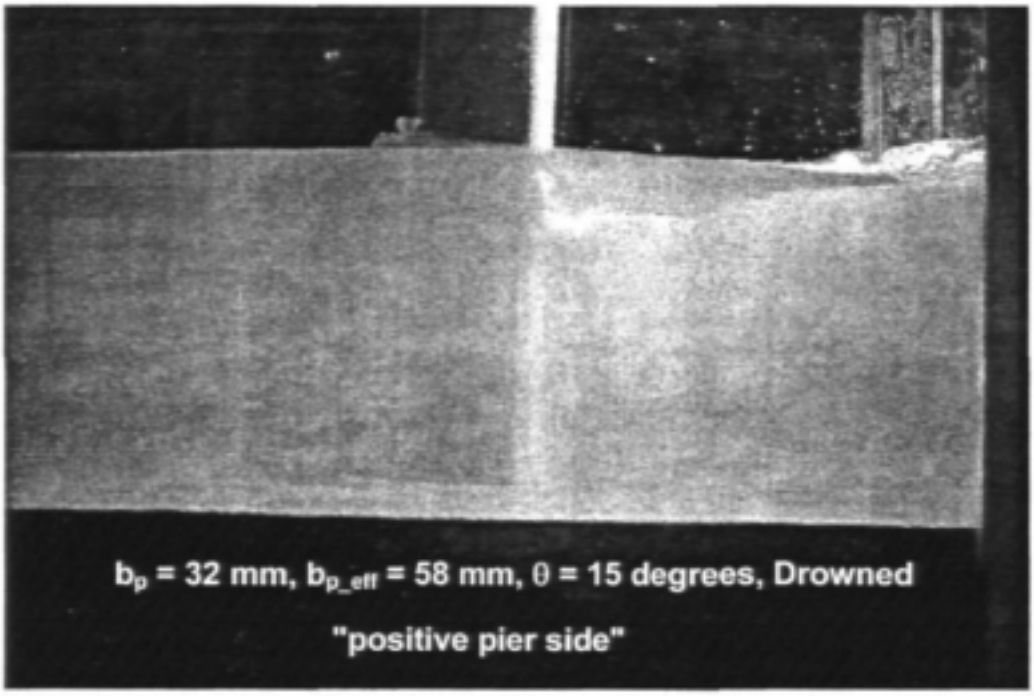

***Photo 4.38**: Flow patterns past model pier, non-parallel approaching flow, B/b_p = 19.0 , L/b_p = 4.2 (SHORT), θ = 15 degrees, "negative (lee) pier side" shown, Q = ±130 l/s, drowned flow conditions downstream*

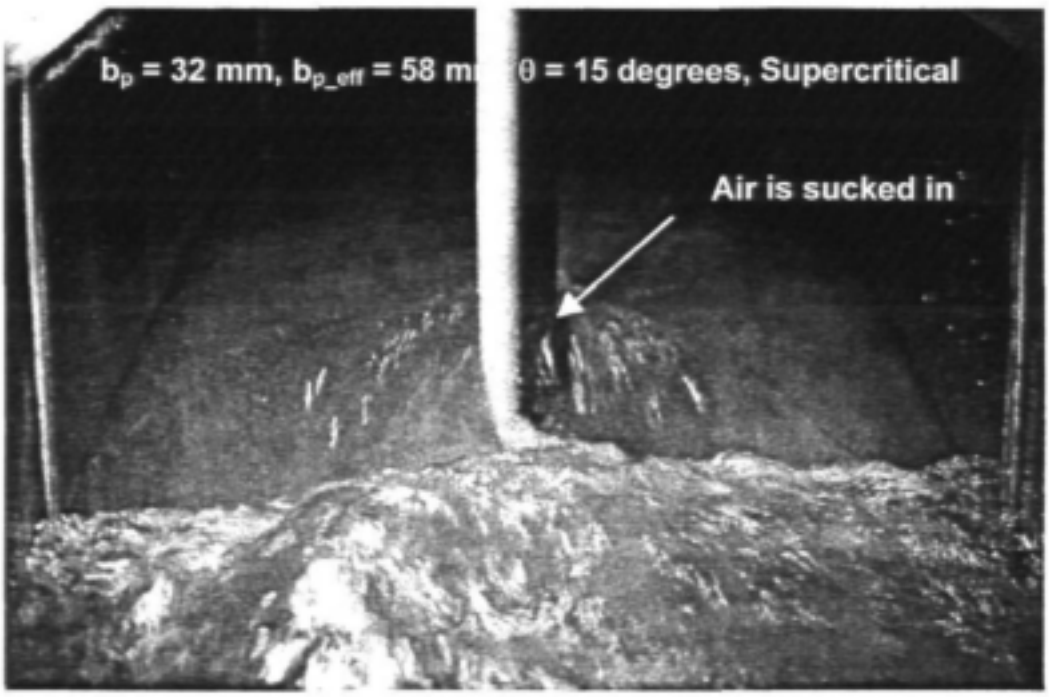

***Photo 4.39**: Flow patterns past model pier, non-parallel approaching flow, B/b_p = 19.0 , L/b_p = 4.2 (SHORT), θ = 15 degrees, "looking upstream" view, Q = ±130 l/s, supercritical flow conditions downstream*

4.2.6 *Defining the energy based discharge equation in terms of the new configuration of pressure measurements:*

The energy equation of Bernoulli was derived from Newton's second law in *section 3.6*:

$$\Rightarrow \quad \frac{\alpha \bar{v}_1^{\,2}}{2g} + y_1 + z_1 = \frac{\alpha \bar{v}_2^{\,2}}{2g} + y_2 + z_2 + \sum h_{L_{1-2}} + h_{f_{1-2}} \qquad \textit{(Equation 4.1)}$$

It is only applicable between two points (**1 and 2**) on a streamline. Consider a stream line taken between **UE** and **DS** (*figure 4.3*). Ignoring frictional losses as the distance is very short, it is therefore justifiable to delete the term $\Sigma h_{f1\text{-}2}$ from *equation 4.1* and thus:

$$\frac{\alpha \bar{v}_{UE}^{\,2}}{2g} + y_{UE} + z_{UE} = \frac{y_{DS}^{\,2}}{2g} + y_{DS} + z_{DS} + h_{L_{UE-DS}} \qquad \textit{(Equation 3.21)}$$

$h_{LUE\text{-}DS}$ represents the transitional losses between positions **UE** and **DS**.

Assuming a horizontal bed, i.e.:

$z_{UE} = z_{DS}$

Substituting $z_{UE}=z_{DS}$, *equation 4.1* simplifies to:

$$\frac{\alpha \bar{v}_{UE}^{\,2}}{2g} + y_{UE} = \frac{\alpha \bar{v}_{DS}^{\,2}}{2g} + y_{DS} + h_{L_{UE-DS}} \qquad \textit{(Equation 4.2)}$$

A stagnation point forms at **UE** where the water is decelerated to zero velocity next to the upstream head of the pier. We can therefore assume:

$$v_{UE} \approx 0$$

$$\Rightarrow \frac{v_{UE}^{\,2}}{2g} \approx 0$$

$$\Rightarrow y_{UE} = y_{DS} + \frac{\alpha \bar{v}_{DS}^{\,2}}{2g} + h_{L_{UE-DS}}$$

$$\Rightarrow v_{DS}^{\,2} = \frac{2g}{\alpha}\left[\left(y_{UE} - y_{DS}\right) - h_{L_{UE-DS}}\right]$$

$$\Rightarrow v_{DS} = \sqrt{\frac{2g}{\alpha}\left[\left(y_{UE} - y_{DS}\right) - h_{L_{UE-DS}}\right]} \qquad \textit{(Equation 4.3)}$$

Applying the continuity equation at **section 3** at **DS** (*figure 4.2*):

$$Q = \bar{v}_3 A_3 = \bar{v}_{DS} A_{DS} = \bar{v}_{DS} y_{DS} B$$

This implies that we assume a uniform flow depth across the width at **section 3** and also a uniform velocity. This is a reasonable assumption as the flow at **section 3** has not yet

experienced any divergence as it is still contained within the space between the two neighbouring piers. Combining the energy and continuity equations and taking $\propto = 1$:

$$v_{DS} = \frac{Q}{B_{DS} y_{DS}} = \sqrt{\frac{2g}{\alpha}\left[\left(y_{UE} - y_{DS}\right) - h_{L_{UE-DS}}\right]}$$

$$\Rightarrow Q = B_{DS} y_{DS} \sqrt{\frac{2g}{\alpha}\left[\left(y_{UE} - y_{DS}\right) - h_{L_{UE-DS}}\right]} = C_d B_{DS} y_{DS} \sqrt{2g\left[\left(y_{UE} - y_{DS}\right)\right]} \qquad \textit{(Equation 4.4)}$$

The **C_d-value** is known as a flow correction factor and compensates for the transitional losses and simplified assumptions made in the energy based model.

It can be shown that the **C_d-value** in *equation 4.4* is a function of the **C_L-value** used in the formula for the calculation of a convergence head loss (as found at a bridge pier). This formula defines the head loss due to the convergence effect in terms of the downstream velocity (within the contraction), viz:

The following definitions hold:

H_L: Transitional head loss [m]

C_L: Transitional loss coefficient [non dim]

v: Average velocity at the downstream end of the converging section [m/s]

$$h_L = C_L \frac{v^2}{2g} \qquad \textit{(Equation 4.5)}$$

Consider the following two figures illustrating the analogy between convergence within a channel contraction and convergence around a pier. This analogy will be used to

illustrate that C_d should be a function of C_L, viz. the degree of contraction through the transition section.

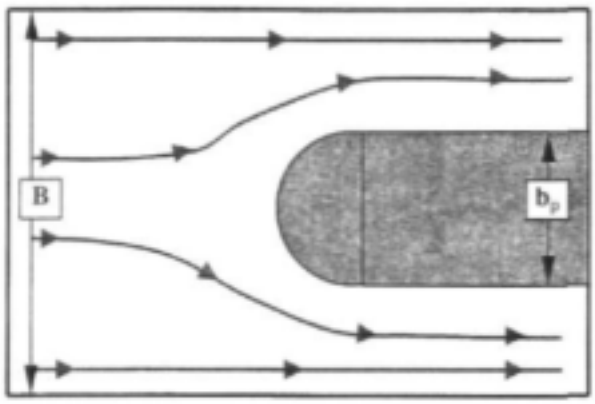

***Figure 4.4**: Typical flow lines around the upstream end of a bridge pier, flow convergence takes place when the width of flow changes from **B** to **(B-b_p)** where **b_p** depicts the pier width*

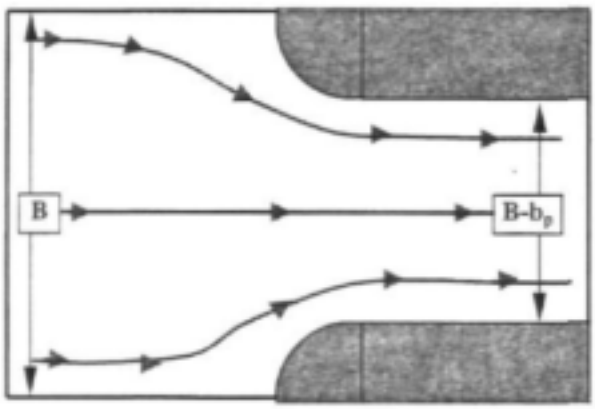

***Figure 4.5:** Typical flow lines past a converging transition channel when the width of flow changes from **B** to **(B-b_p)** where **(B-b_p)** depicts the contracted width (analogous to flow entering between piers*

Now, if *equation 4.5* is substituted for the h_{LUE-DS} term in *equation 4.2*, a discharge equation in terms of C_L (convergence coefficient) can be found:

$$\Rightarrow \quad \frac{\alpha \bar{v}_{UE}^{\,2}}{2g} + y_{UE} = \frac{\alpha \bar{v}_{DS}^{\,2}}{2g} + y_{DS} + C_L\left(\frac{\alpha \bar{v}_{DS}^{\,2}}{2g}\right)$$

$v_{UE} \approx 0$

$$\Rightarrow \quad y_{UE} = \frac{\alpha \bar{v}_{DS}^{\,2}}{2g} + y_{DS} + C_L\left(\frac{\alpha \bar{v}_{DS}^{\,2}}{2g}\right)$$

$$\Rightarrow \quad \frac{\alpha \bar{v}_{DS}^{\,2}}{2g} + C_L\left(\frac{\alpha \bar{v}_{DS}^{\,2}}{2g}\right) = y_{UE} - y_{DS}$$

$$\Rightarrow \quad \frac{\alpha \bar{v}_{DS}^{\,2}}{2g} = \frac{1}{(1+C_L)}(y_{UE} - y_{DS})$$

taking α = 1 and applying the continuity equation, $Q = v_{DE} B_{DE} y_{DE}$

$$\Rightarrow Q = \sqrt{\left(\tfrac{1}{1+C_L}\right)}\, B_{DS}\, y_{DS} \sqrt{2g\left[(y_{UE} - y_{DS})\right]} \qquad \textit{(Equation 4.6)}$$

Comparing *equation 4.6* with *equation 4.4* it is seen that C_d is indeed a function of C_L. This result is to be expected as C_d compensates for transitional losses and C_L is a transitional converging loss coefficient. From this result a rough prediction of the C_d values can be made according to a predicted **C_L-value** for the converging flow past the pier.

4.2.7 ***Calibrating the energy based flow rate equation (equation 4.4) for the different flows considered, paragraph 4.2.4:***

4.2.7.1 Parallel approaching flow direction:

Introduction:

This section deals with the calibration of *equation 4.4* in terms of laboratory data collected during tests on model piers with **4** different $\mathbf{B/b_p}$ ratios. Each model pier was constructed so as to be lengthened by introducing a straight section between the upstream and downstream nose ends. The **4** different $\mathbf{B/b_p}$ ratios that were considered were: $\mathbf{B/b_p = 609/32 = 19.0; 609/40 = 15.2; 609/50 = 12.2}$ and $\mathbf{609/63 = 9.7}$. For each pier **3** different $\mathbf{L/b_p}$ ratios were used, namely: $\mathbf{L/b_p = 4.2, 5.6}$ and **6.9**. These combinations of $\mathbf{B/b_p}$ and $\mathbf{L/b_p}$ values were intended to cover most combinations found in practice.

Calculating C_d-values:

In order to calculate the $\mathbf{C_d}$**-values** in *equation 4.4*, it was necessary to determine the values of $\mathbf{B_C}$, taking $\mathbf{g = 9.81\ m/s^2}$ and measuring the depths $\mathbf{y_A}$ and $\mathbf{y_C}$ for each measured discharge **Q**. Therefore, *equation 4.4* was rewritten with $\mathbf{C_d}$ as subject and $\mathbf{Q, g, B_C, y_A}$ **and** $\mathbf{y_C}$ as known values, being either measured or assuming as being constant during the tests:

$$\Rightarrow C_d = \frac{Q_{measured}}{B_{DS_{constant}}\, y_{DS_{measured}} \sqrt{2g\left[\left(y_{UE_{measured}} - y_{DS_{measured}}\right)\right]}}$$

The following results were obtained for the parallel approaching flows, i.e. flow conditions where the angle between the approaching flow direction and the long axis of the pier was zero. The results are given in table format. Note that *table 4.1* refers to supercritical flow conditions downstream of the pier and *table 4.2* to drowned conditions downstream of the pier.

PARALLEL APPROACHING FLOW NORMAL FLOW CONDITIONS DOWNSTREAM OF PIER			
	$L/b_p = 6.9$ (LONG)	$L/b_p = 5.6$ (MEDIUM)	$L/b_p = 4.2$ (SHORT)
$B/b_p = 19.0$ (32 mm)	$C_d = 1.03\text{-}1.05$ $C_{d\_avg} = 1.04$	$C_d = 1.04\text{-}1.08$ $C_{d\_avg} = 1.07$	$C_d = 0.97\text{-}1.09$ $C_{d\_avg} = 1.06$
$B/b_p = 15.2$ (40 mm)	$C_d = 1.00\text{-}1.05$ $C_{d\_avg} = 1.04$	$C_d = 1.02\text{-}1.04$ $C_{d\_avg} = 1.03$	$C_d = 1.01\text{-}1.06$ $C_{d\_avg} = 1.03$
$B/b_p = 12.2$ (50 mm)	$C_d = 0.96\text{-}1.05$ $C_{d\_avg} = 1.02$	$C_d = 1.01\text{-}1.07$ $C_{d\_avg} = 1.04$	$C_d = 1.00\text{-}1.06$ $C_{d\_avg} = 1.03$
$B/b_p = 9.7$ (63 mm)	$C_d = 0.99\text{-}1.02$ $C_{d\_avg} = 1.01$	$C_d = 0.95\text{-}1.04$ $C_{d\_avg} = 1.01$	$C_d = 0.99\text{-}1.06$ $C_{d\_avg} = 1.01$

Table 4.1: *Calibrated C_d-values, parallel approaching flow, supercritical flow condtions downstream*

PARALLEL APPROACHING FLOW DROWNED FLOW CONDITIONS DOWNSTREAM OF PIER			
	$L/b_p = 6.9$ (LONG)	$L/b_p = 5.6$ (MEDIUM)	$L/b_p = 4.2$ (SHORT)
$B/b_p = 19.0$ (32 mm)	$C_d = 0.95\text{-}1.03$ $C_{d\_avg} = 0.98$	$C_d = 0.95\text{-}1.05$ $C_{d\_avg} = 0.97$	$C_d = 0.92\text{-}1.05$ $C_{d\_avg} = 0.98$
$B/b_p = 15.2$ (40 mm)	$C_d = 0.95\text{-}1.03$ $C_{d\_avg} = 0.99$	$C_d = 0.95\text{-}1.05$ $C_{d\_avg} = 0.99$	$C_d = 0.95\text{-}1.05$ $C_{d\_avg} = 1.00$
$B/b_p = 12.2$ (50 mm)	$C_d = 0.93\text{-}1.01$ $C_{d\_avg} = 0.98$	$C_d = 0.95\text{-}1.01$ $C_{d\_avg} = 0.97$	$C_d = 0.95\text{-}1.01$ $C_{d\_avg} = 0.98$
$B/b_p = 9.7$ (63 mm)	$C_d = 0.93\text{-}1.01$ $C_{d\_avg} = 0.96$	$C_d = 0.92\text{-}1.01$ $C_{d\_avg} = 0.97$	$C_d = 0.95\text{-}1.01$ $C_{d\_avg} = 0.97$

Table 4.2: *Calibrated C_d-values, parallel approaching flow, drowned flow conditions downstream*

Values of $\mathbf{C_L}$ (*equation 4.6*) corresponding to the above mentioned **C_d-values** varied from **0.00** to **0.09** for the sub-critical (drowned) downstream flow condition (*table 4.2*) implying very small transitional losses between points **UE** and **DS** along the pier.

Refer to Appendix B for the laboratory data and results.

4.2.7.2 Non-parallel approaching flow direction:

Introduction:

Calibrating the discharge equation for the non-parallel flow test results was somewhat different to that for parallel flows. The tests conducted on parallel flows covered 3 different $\mathbf{L/b_p}$ ratios for the pier model and for each of these 3, different rotation angles were used. It was possible to obtain a range of $\mathbf{b_{p\_eff}}$ (the effective pier width) values which are commonly found in practice. The **32 mm** pier was used for the tests on non-parallel flow conditions. The **3** different $\mathbf{L/b_p}$ values were: $\mathbf{L/b_p = 4.2, 5.6}$ and **6.9**. The **3** rotation angles used were: θ **= 5°, 10°** and **15°**. Combining these different values, **9** different tests were performed. These **9** different tests were performed for both supercritical and drowned conditions downstream of the pier.

Calculating the C_d-values*:*

In order to calculate the $\mathbf{C_d}$**-values** in *equation 4.4*, it was necessary to calculate the effective flow area first. The effective flow width $\mathbf{B_{eff}}$ was taken as the projected width between two neighbouring rotated isolated piers. $\mathbf{B_{eff}}$ was calculated as follows (refer to *photo 4.11*):

$$B_{eff} = B - b_{p\_eff} = B - \left(L_p \sin(\theta) + b_p(1 - \sin(\theta))\right) \qquad \textit{(Equation 4.7)}$$

Note that the value of $\mathbf{B_{eff}}$ is a function of the pier length ($\mathbf{L_p}$) and the rotation angle (θ) as well as the pier width ($\mathbf{b_p}$). As $\mathbf{b_p}$ was a constant during the tests and $\mathbf{L_p}$ and θ each had **3** different values, there were **3*3=9** different $\mathbf{B_{eff}}$ values used during the tests.

The gravitational acceleration value was taken as $g = 9.81\ m/s^2$ and the depths y_A and y_C were measured for each measured flow rate Q. *Equation 4.4* was rewritten with C_d as subject and Q, g, B_{eff}, y_{UE} and y_{DS} as known values, being either measured or taken as constants during the tests:

$$\Rightarrow C_d = \frac{Q_{measured}}{B_{eff_{constant}} y_{DS_{measured}} \sqrt{2g\left[\left(y_{UE_{measured}} - y_{DS_{measured}}\right)\right]}}$$

The following results were obtained for the non-parallel approaching flows, i.e. flow conditions where there was an angle between the approaching flow direction and the long axis of the pier. The results are given in table format, (note that *table 4.3* refers to supercritical flow conditions downstream of the pier and *table 4.4* to drowned conditions downstream of the pier.

NON-PARALLEL APPROACHING FLOW *NORMAL FLOW CONDITIONS* DOWNSTREAM OF PIER			
	$L/b_p = 6.9$ (LONG)	$L/b_p = 5.6$ (MEDIUM)	$L/b_p = 4.2$ (SHORT)
($\theta = 5$ degrees)	$B/b_{p\_eff} = 12.4$ $C_d = 1.01\text{-}1.14$ $C_{d\_avg} = 1.08$	$B/b_{p\_eff} = 13.5$ $C_d = 0.93\text{-}1.11$ $C_{d\_avg} = 1.05$	$B/b_{p\_eff} = 15.2$ $C_d = 0.91\text{-}1.14$ $C_{d\_avg} = 1.06$
($\theta = 10$ degrees)	$B/b_{p\_eff} = 9.4$ $C_d = 1.10\text{-}1.43$ $C_{d\_avg} = 1.29$	$B/b_{p\_eff} = 10.7$ $C_d = 0.90\text{-}1.31$ $C_{d\_avg} = 1.13$	$B/b_{p\_eff} = 12.4$ $C_d = 0.87\text{-}1.21$ $C_{d\_avg} = 1.11$
($\theta = 15$ degrees)	$B/b_{p\_eff} = 7.5$ $C_d = 1.12\text{-}1.24$ $C_{d\_avg} = 1.17$	$B/b_{p\_eff} = 8.7$ $C_d = 1.17\text{-}1.38$ $C_{d\_avg} = 1.27$	$B/b_{p\_eff} = 10.5$ $C_d = 1.12\text{-}1.65$ $C_{d\_avg} = 1.41$

Table 4.3: *Calibrated C_d-values, non-parallel approaching flow, supercritical flow conditions downstream*

NON-PARALLEL APPROACHING FLOW			
DROWNED FLOW CONDITIONS DOWNSTREAM OF PIER			
	L/b_p = 6.9 (LONG)	L/b_p = 5.6 (MEDIUM)	L/b_p = 4.2 (SHORT)
(θ = 5 degrees)	B/b_{p_eff} = 12.4 C_d = 0.92-1.09 C_{d_avg} = 1.12	B/b_{p_eff} = 13.5 C_d = 1.03-1.15 C_{d_avg} = 1.10	B/b_{p_eff} = 15.2 C_d = 1.06-1.16 C_{d_avg} = 1.12
(θ = 10 degrees)	B/b_{p_eff} = 9.4 C_d = 1.25-1.42 C_{d_avg} = 1.34	B/b_{p_eff} = 10.7 C_d = 1.20-1.35 C_{d_avg} = 1.29	B/b_{p_eff} = 12.4 C_d = 1.15-1.30 C_{d_avg} = 1.23
(θ = 15 degrees)	B/b_{p_eff} = 7.5 C_d = 1.11-1.20 C_{d_avg} = 1.17	B/b_{p_eff} = 8.7 C_d = 1.22-1.32 C_{d_avg} = 1.28	B/b_{p_eff} = 10.5 C_d = 1.40-1.56 C_{d_avg} = 1.45

***Table 4.4**: Calibrated C_d-values, non-parallel approaching flow, drowned flow conditions downstream*

Refer to Appendix B for detail on the laboratory data and results.

4.2 *RESULTS IN GRAPH FORM, DISCUSSION*

It was shown in *section 3.9* (*using the ENERGY approach*) that the energy equation (*equation 4.4*) can be written in terms of dimensionless coefficients, namely in terms of the **Froude** number at the downstream section of the pier (**section 3**, *figure 4.2*) and also the ratio of upstream stagnation head (y_{UE}) to downstream flow depth or head (y_{DS}, also **section 3**), viz. in terms of F_{rDS} and y_{UE}/y_{DS}, therefore:

The following definitions hold:

Q: Flow rate [m^3/s]

C_d: Discharge coefficient compensating for transitional losses [non dim]

B: Representative width of oncoming flow for each bridge pier [m]

y: Flow depth [m]

α: Coriolis coefficient compensating for assumption of average velocity [non dim]

v: Velocity of flow [m/s]

g: Unit gravitational force [m/s^2]

H: Energy head at the upstream end of the pier [m]

F_{ri}: Froude number at section i [non dim]

k: Constant [non dim]

$$Q = C_d B_{DS} y_{DS} \sqrt{2g[(y_{UE} - y_{DS})]}$$

$$\Rightarrow \quad C_d = \frac{kF_{r_{DS}}}{\sqrt{\left(\frac{y_{UE}}{y_{DS}} - 1\right)}}$$

The rewritten discharge equation (above, but see also *equation 3.74*) is now used to construct graphs in terms of C_d, F_{rDS} and y_{UE}/y_{DS} for each of the flow conditions mentioned earlier on, viz. for the parallel approaching flows (supercritical and drowned) and non-parallel flows (supercritical and drowned). Note that the terms F_{r4}, H and y_4 (*equation 3.74*) become Fr_{DS}, y_{UE} and y_{DS} respectively. These graphs can then be used to find a **C_d-value** in terms of measured values of y_{UE} and y_{DS} and calculated values of y_{UE}/y_{DS} and F_{rDS}. The **C_d-value** is then used to calculate the flow rate in terms of the measured pressures alongside the pier (y_{UE} and y_{DS}).

4.3.1 Parallel approaching flow direction:

The following **14** graphs show the calibrated **C_d-values** according to the laboratory data mentioned earlier. The graphs are in terms of dimensionless parameters which were shown to be significant variables in the revised energy based discharge equation (*equation 4.4*). These variables are: **C_d**, **y_{UE}/y_{DS}** and **F_{rDS}** where **C_d** denotes the discharge coefficient compensating for transitional losses, **y_{UE}/y_{DS}** the pressure head ratio of upstream dynamic pressure head to downstream depth measured alongside the pier and **F_{rDS}** the **Froude** number at **section DS**.

i) The general tendency of constant **C_d-value** lines following a convex curve sloping upwards from left to right was evident for all **12** model pier combinations that were tested. It is for this reason that all values were plotted on one diagram (*figure 4.19*) in order to show the limited distribution of **C_d-values** in terms of the pressure ratio (**y_{UE}/y_{DS}**) and **Froude** number (**Fr_{DS}**) as described earlier. It is evident from *figure 4.19* that the data points fall in a narrow band following the general tendency found on each of the individual graphs (*figure 4.6 to figure 4.17*). Calibration curves were therefore constructed according to the combined data points. It was possible to draw constant **C_d-lines** representing all combinations of **B/b_p** and **L/b_p** ratios considered. *Figure 4.19* shows the calibration curves with **C_d-values** varying from **0.93** to **1.04** for sub-critical conditions at **DS** and from **0.95** to **1.09** for supercritical conditions also at **DS**.

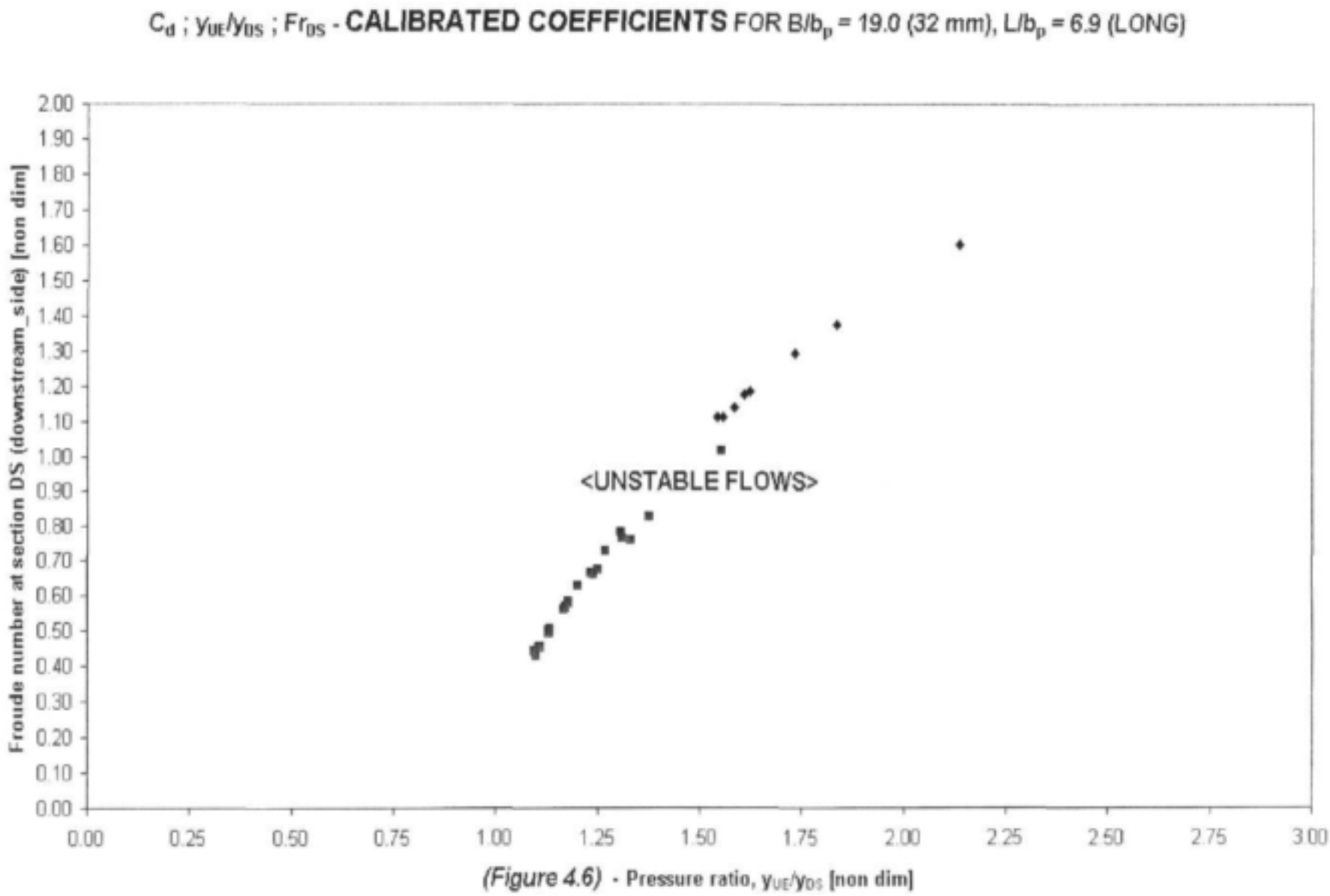

(Figure 4.6) - Pressure ratio, y_{UE}/y_{DS} [non dim]

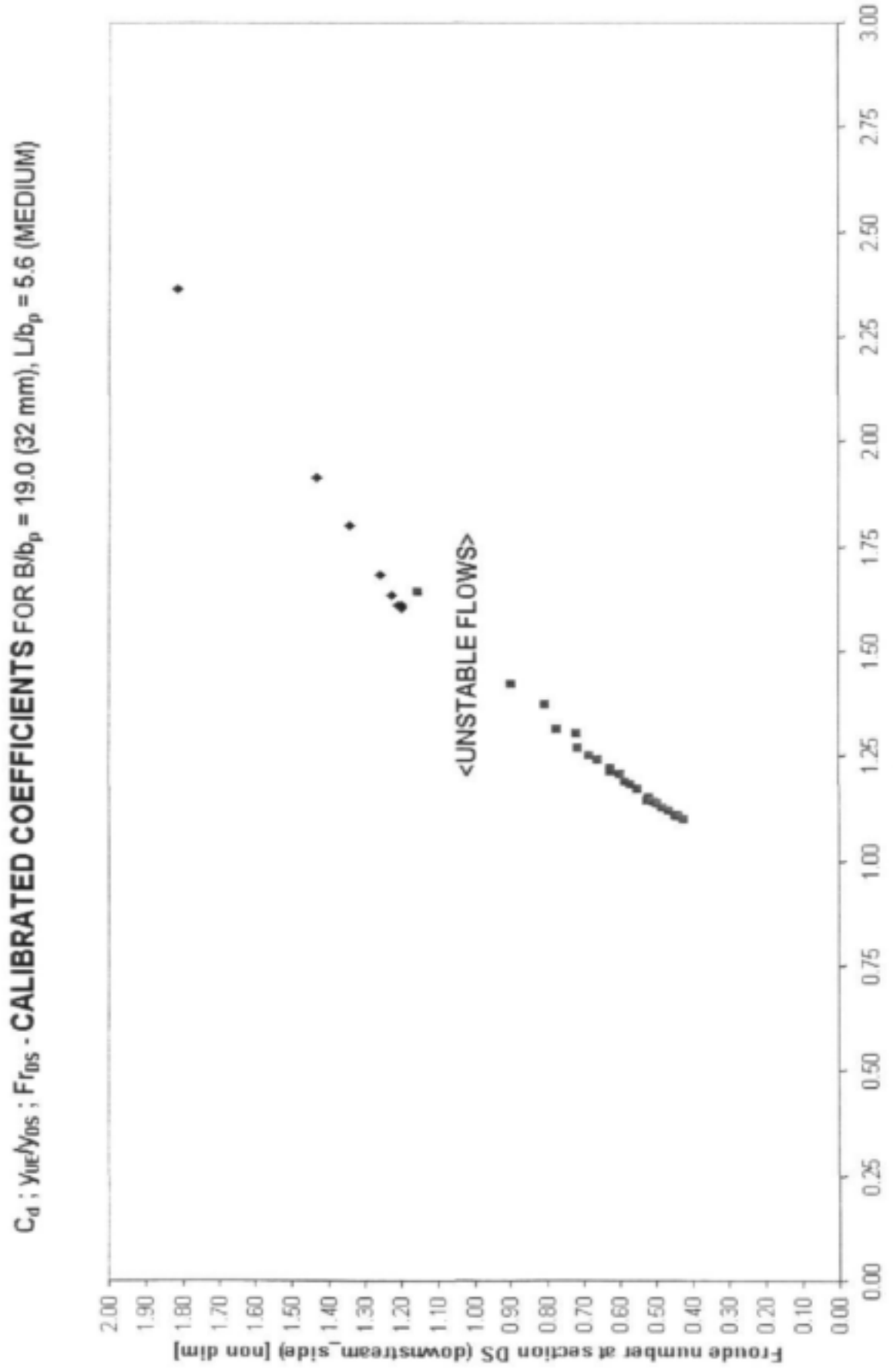

(Figure 4.7) - Pressure ratio, y_{UE}/y_{DS} [non dim]

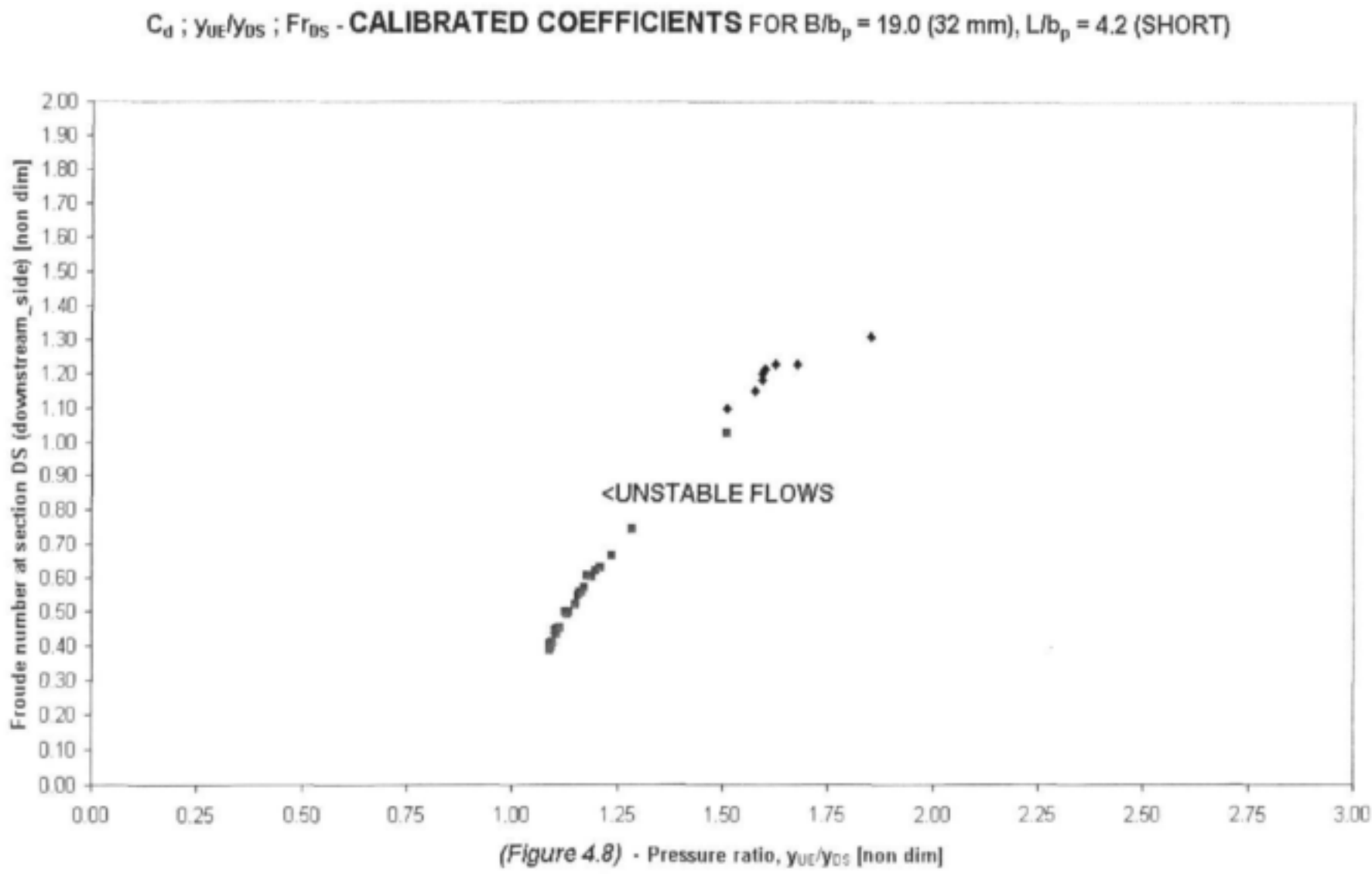
C_d ; y_{UE}/y_{DS} ; Fr_{DS} - CALIBRATED COEFFICIENTS FOR B/b_p = 19.0 (32 mm), L/b_p = 4.2 (SHORT)
Froude number at section DS (downstream_side) [non dim]
2.00
1.90
1.80
1.70
1.60
1.50
1.40
1.30
1.20
1.10
1.00
0.90
0.80
0.70
0.60
0.50
0.40
0.30
0.20
0.10
0.00
<UNSTABLE FLOWS
0.00
0.25
0.50
0.75
1.00
1.25
1.50
1.75
2.00
2.25
2.50
2.75
3.00
Pressure ratio, y_{UE}/y_{DS} [non dim]

(Figure 4.8)

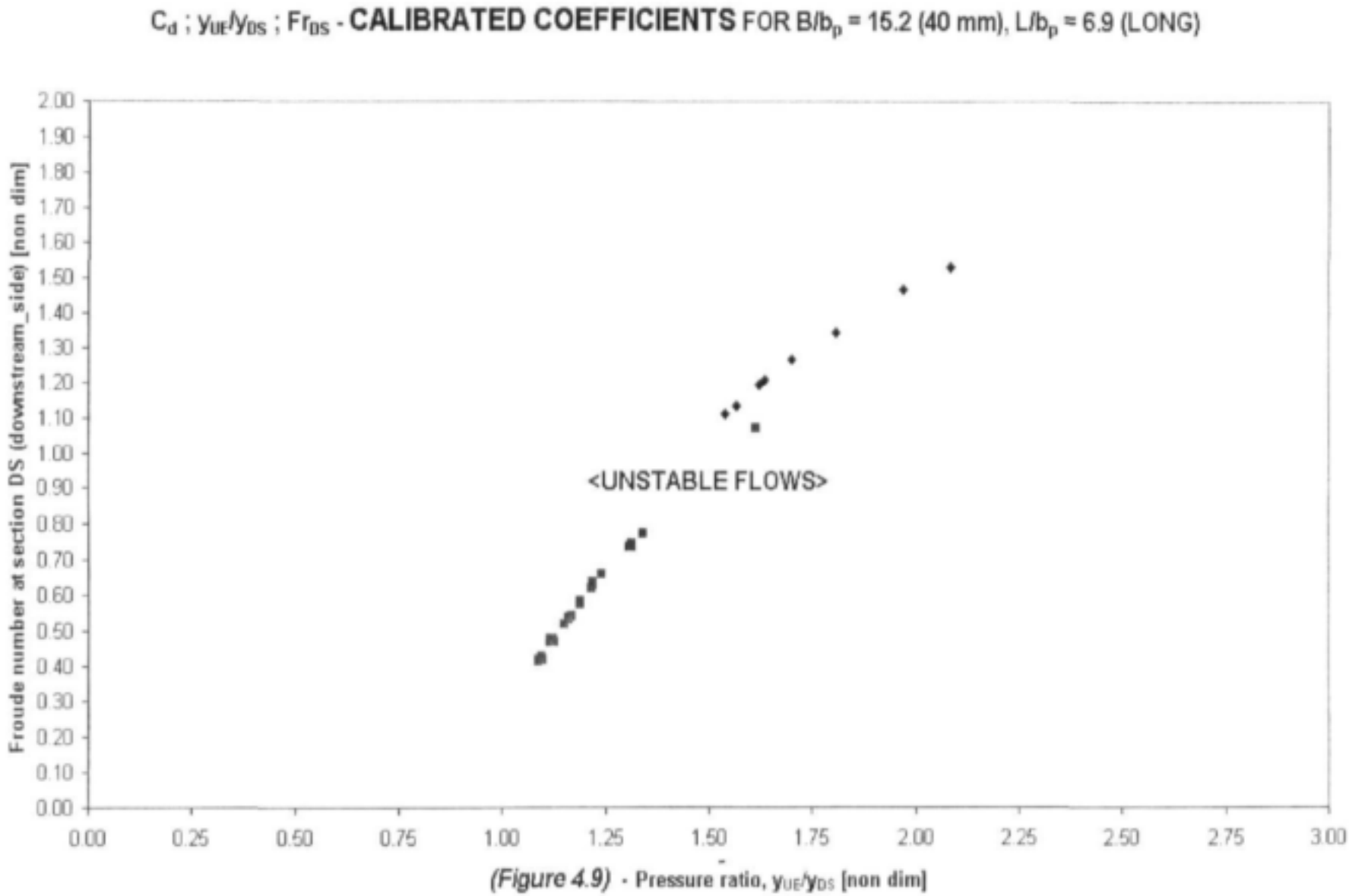
C_d ; y_{UE}/y_{DS} ; Fr_{DS} - CALIBRATED COEFFICIENTS FOR B/b_p = 15.2 (40 mm), L/b_p = 6.9 (LONG)
Froude number at section DS (downstream_side) [non dim]
2.00
1.90
1.80
1.70
1.60
1.50
1.40
1.30
1.20
1.10
1.00
0.90
0.80
0.70
0.60
0.50
0.40
0.30
0.20
0.10
0.00
<UNSTABLE FLOWS>
0.00
0.25
0.50
0.75
1.00
1.25
1.50
1.75
2.00
2.25
2.50
2.75
3.00
Pressure ratio, y_{UE}/y_{DS} [non dim]

(Figure 4.9)

C_d ; y_{UE}/y_{DS} ; Fr_{DS} - **CALIBRATED COEFFICIENTS** FOR B/b_p = 15.2 (40 mm), L/b_p = 5.6 (MEDIUM)

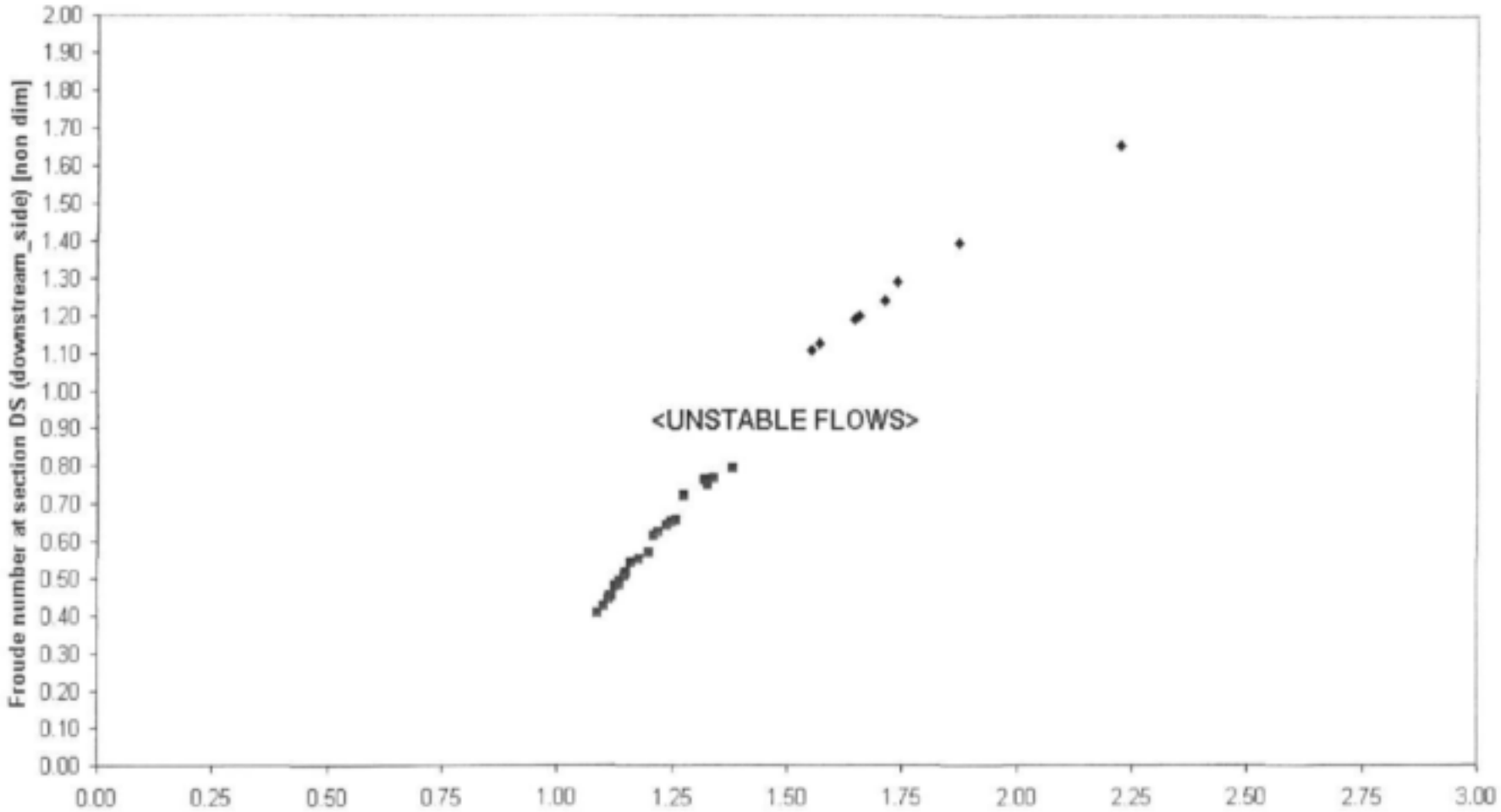

(Figure 4.10) - **Pressure ratio, y_{UE}/y_{DS} [non dim]**

C_d ; y_{UE}/y_{DS} ; Fr_{DS} - **CALIBRATED COEFFICIENTS** FOR B/b_p = 15.2 (40 mm), L/b_p = 4.2 (SHORT)

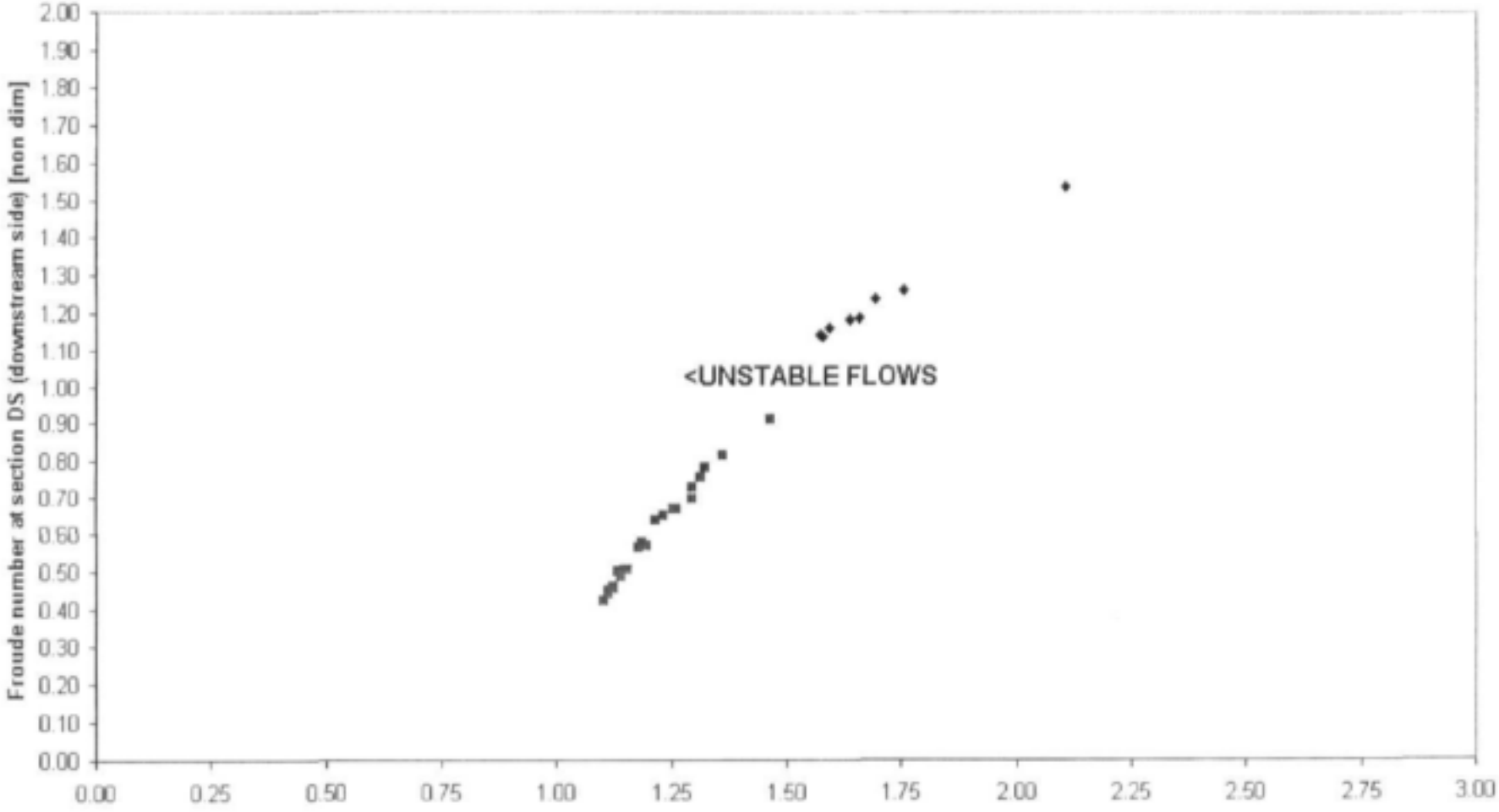

(Figure 4.11) - **Pressure ratio, y_{UE}/y_{DS} [non dim]**

C_d ; y_{UE}/y_{DS} ; Fr_{DS} - **CALIBRATED COEFFICIENTS** FOR B/b_p = 12.4 (49 mm), L/b_p = 6.9 (LONG)

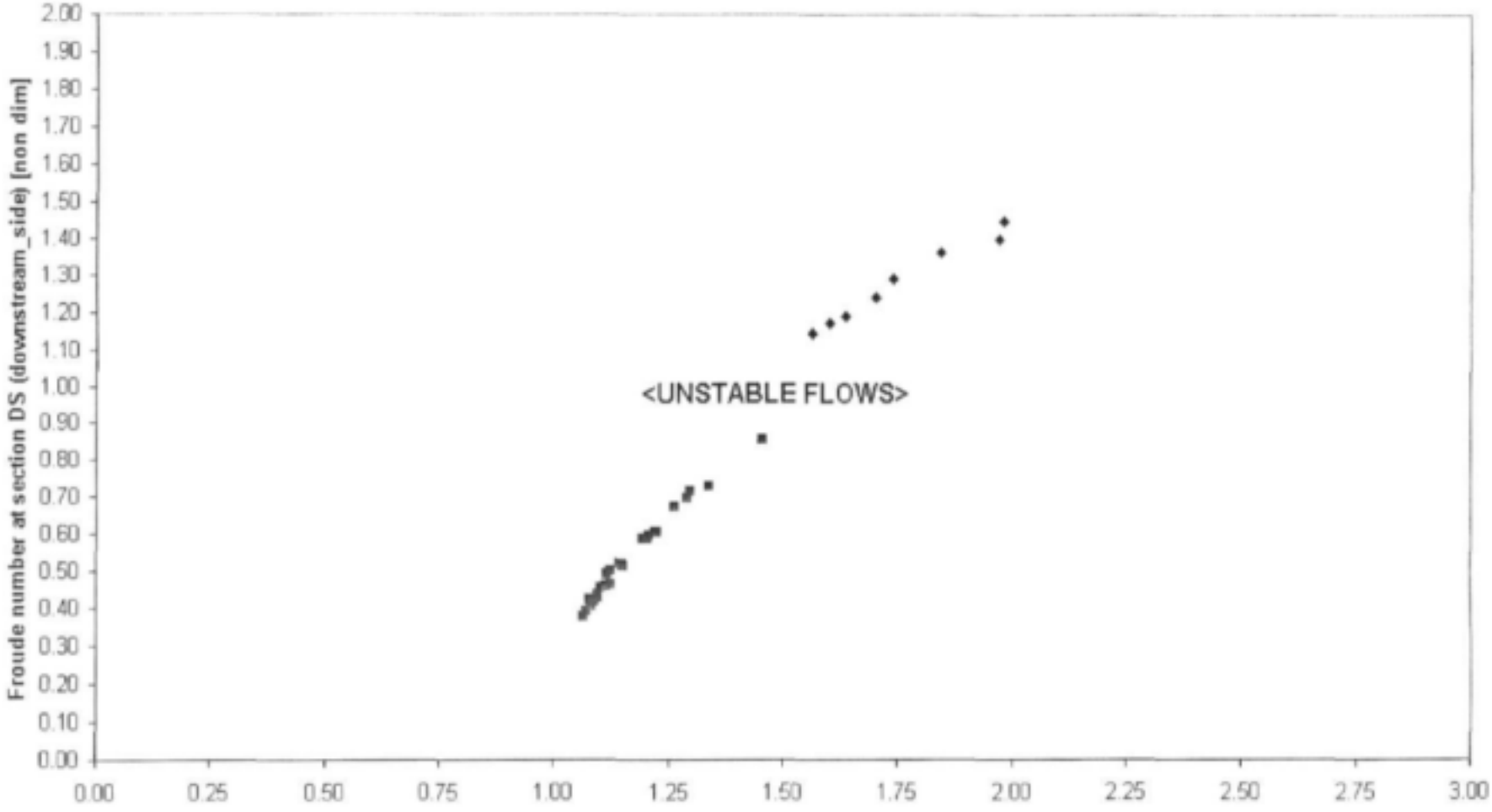

(Figure 4.12) - **Pressure ratio, y_{UE}/y_{DS} [non dim]**

C_d ; y_{UE}/y_{DS} ; Fr_{DS} - **CALIBRATED COEFFICIENTS** FOR B/b_p = 12.4 (49 mm), L/b_p = 5.6 (MEDIUM)

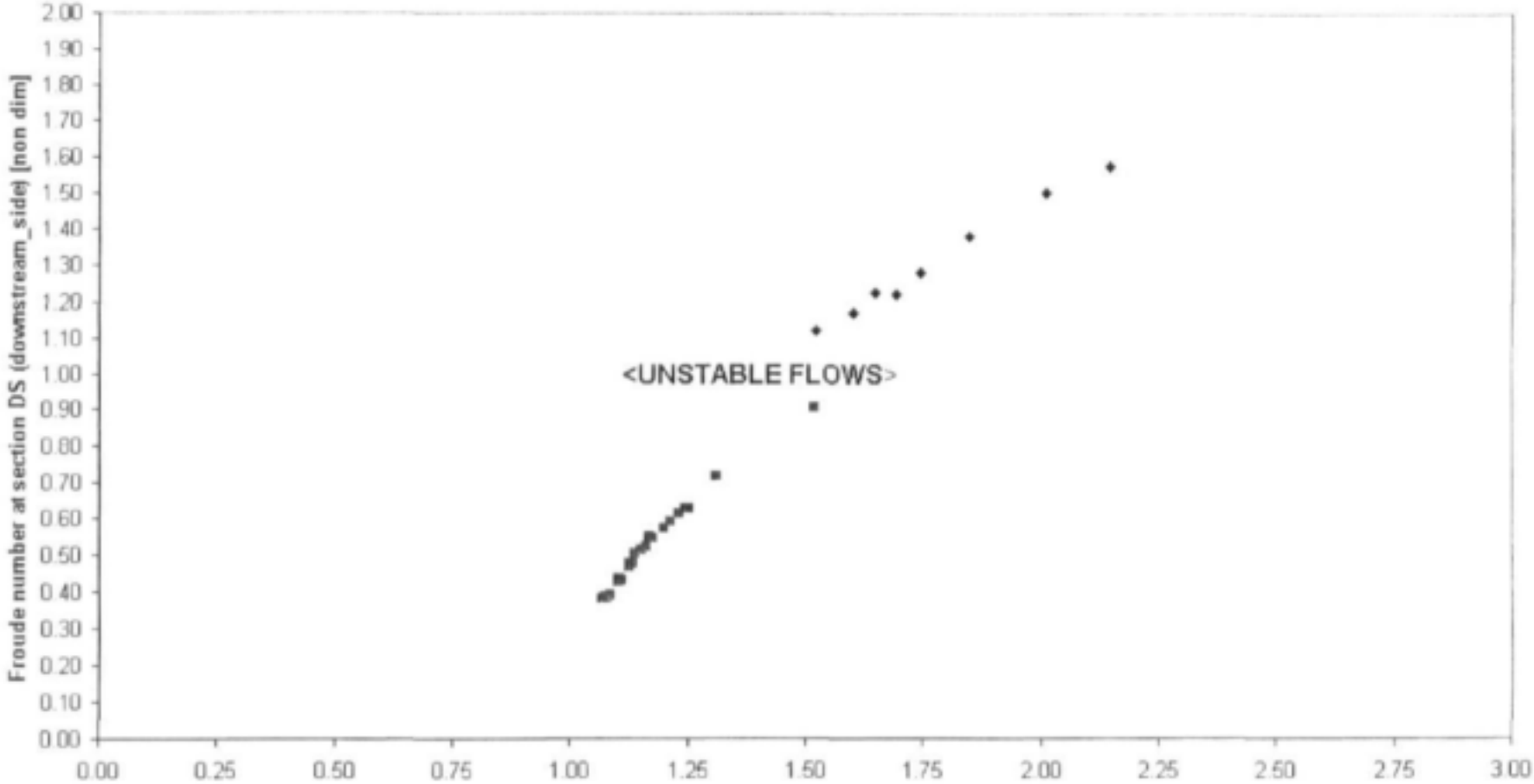

(Figure 4.13) - **Pressure ratio, y_{UE}/y_{DS} [non dim]**

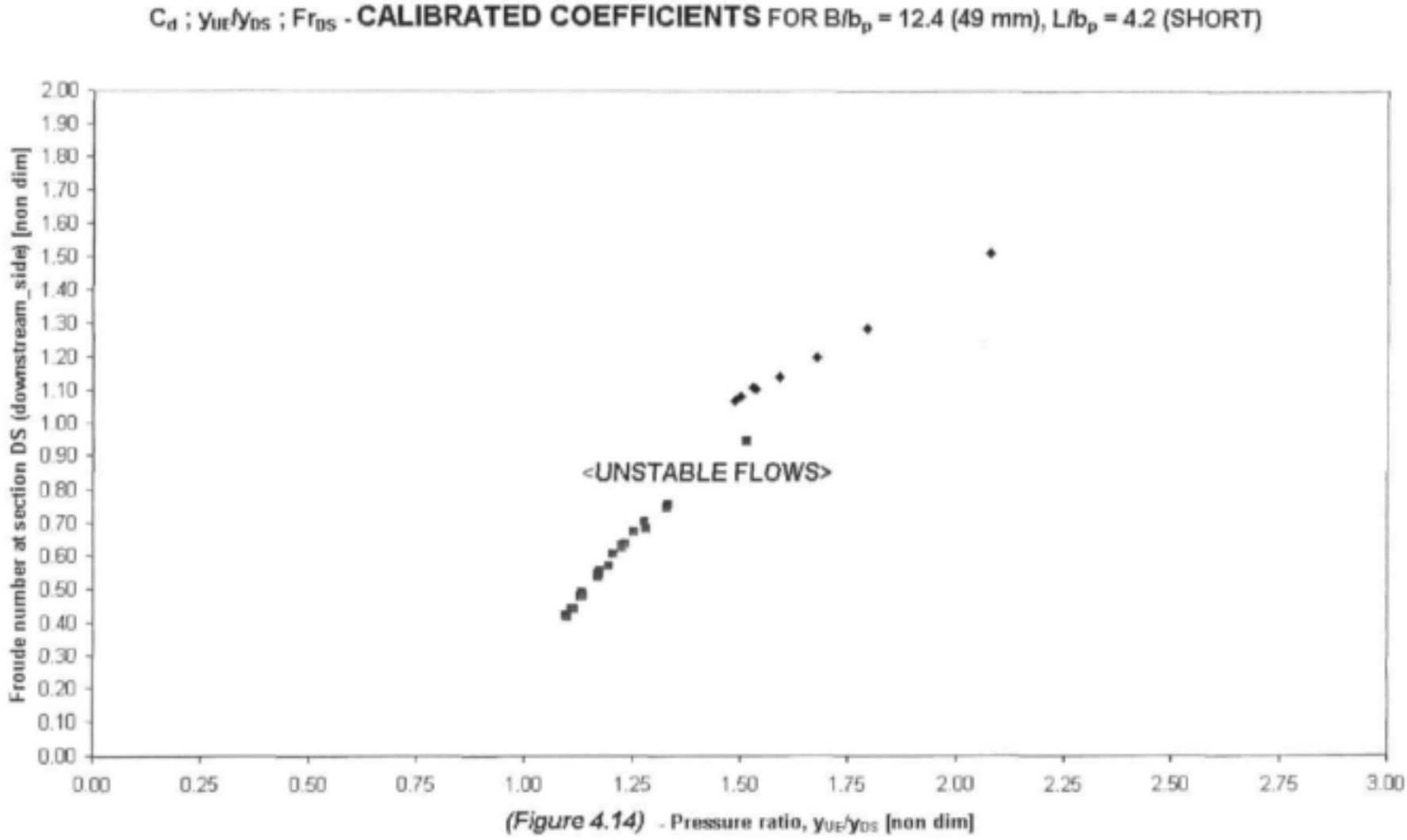

(Figure 4.14) - Pressure ratio, y_{UE}/y_{DS} [non dim]

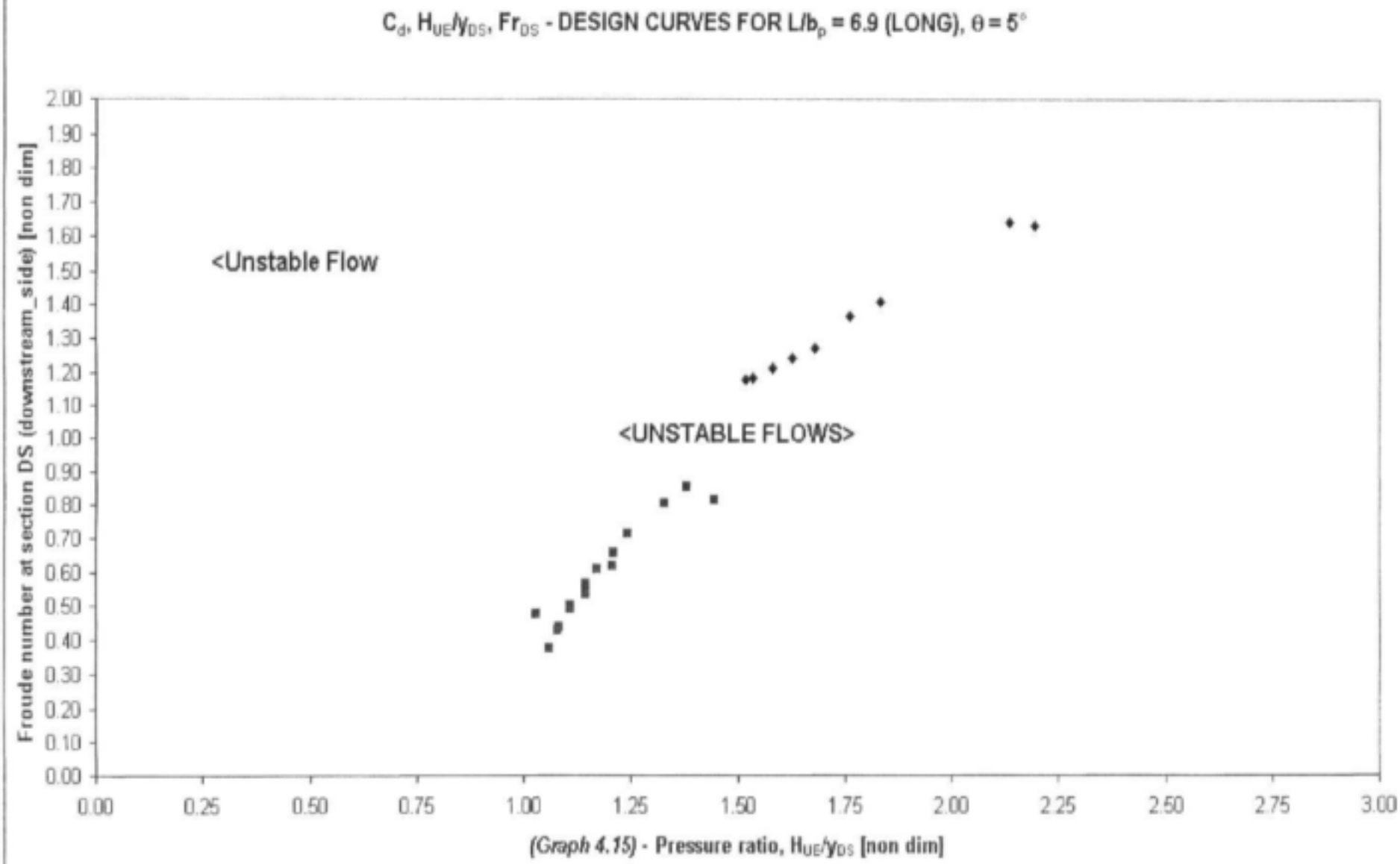

(Graph 4.15) - Pressure ratio, H_{UE}/y_{DS} [non dim]

C_d ; y_{UE}/y_{DS} ; Fr_{DS} - **CALIBRATED COEFFICIENTS** FOR B/b_p = 9.7 (62.5 mm), L/b_p = 5.6 (MEDIUM)

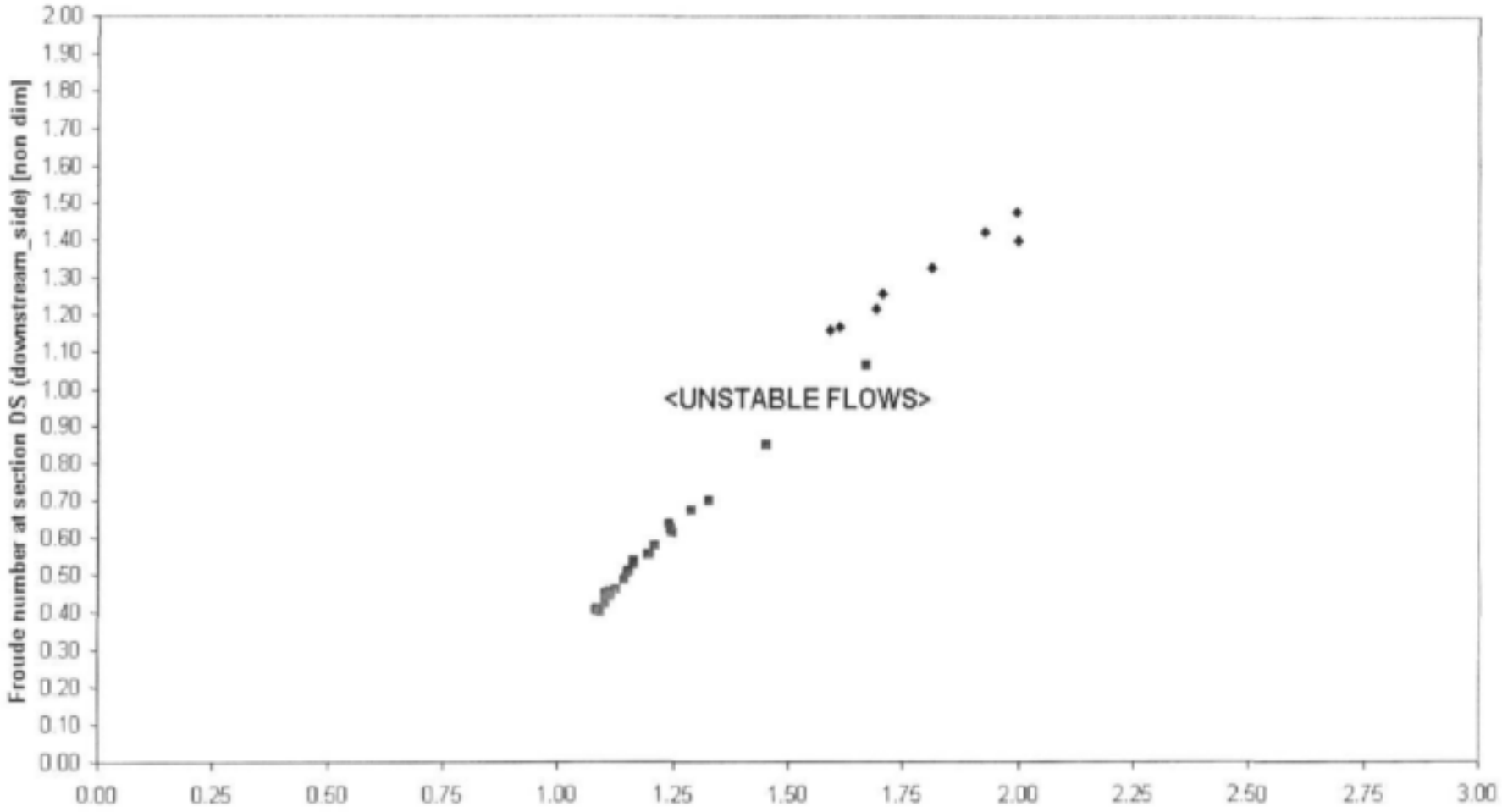

(Figure 4.16) - Pressure ratio, y_{UE}/y_{DS} [non dim]

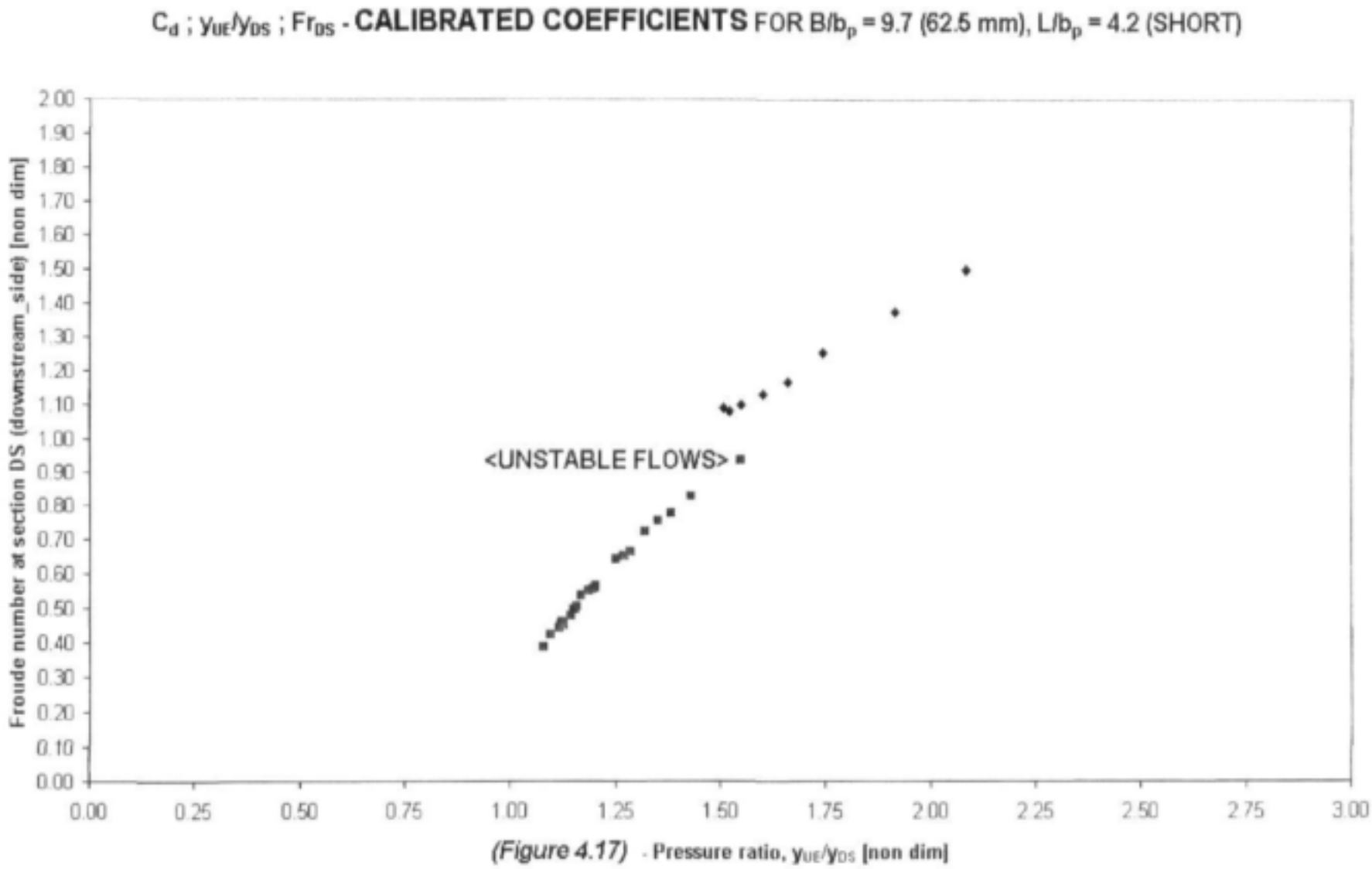
C_d ; y_{UE}/y_{DS} ; Fr_{DS} - CALIBRATED COEFFICIENTS FOR B/b_p = 9.7 (62.5 mm), L/b_p = 4.2 (SHORT)
Froude number at section DS (downstream_side) [non dim]
2.00
1.90
1.80
1.70
1.60
1.50
1.40
1.30
1.20
1.10
1.00
0.90
0.80
0.70
0.60
0.50
0.40
0.30
0.20
0.10
0.00
<UNSTABLE FLOWS>
0.00
0.25
0.50
0.75
1.00
1.25
1.50
1.75
2.00
2.25
2.50
2.75
3.00
Pressure ratio, y_{UE}/y_{DS} [non dim]

(Figure 4.17)

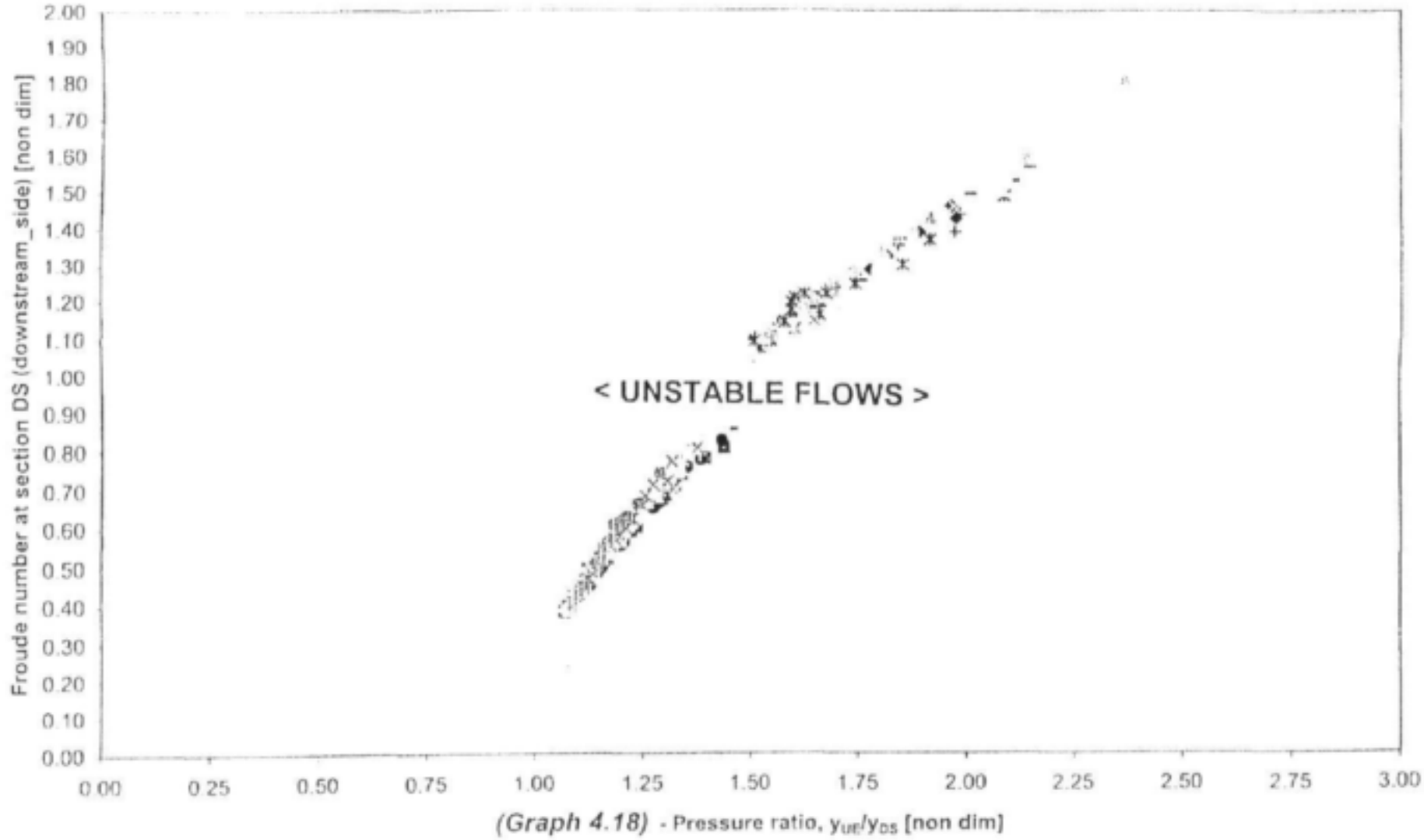
C_d ; y_{UE}/y_{DS} ; Fr_{DS} - CALIBRATION CURVES , ALL B/b_p and L/b_p combinations
Froude number at section DS (downstream_side) [non dim]
2.00
1.90
1.80
1.70
1.60
1.50
1.40
1.30
1.20
1.10
1.00
0.90
0.80
0.70
0.60
0.50
0.40
0.30
0.20
0.10
0.00
< UNSTABLE FLOWS >
0.00
0.25
0.50
0.75
1.00
1.25
1.50
1.75
2.00
2.25
2.50
2.75
3.00
(Graph 4.18) - Pressure ratio, y_{UE}/y_{DS} [non dim]

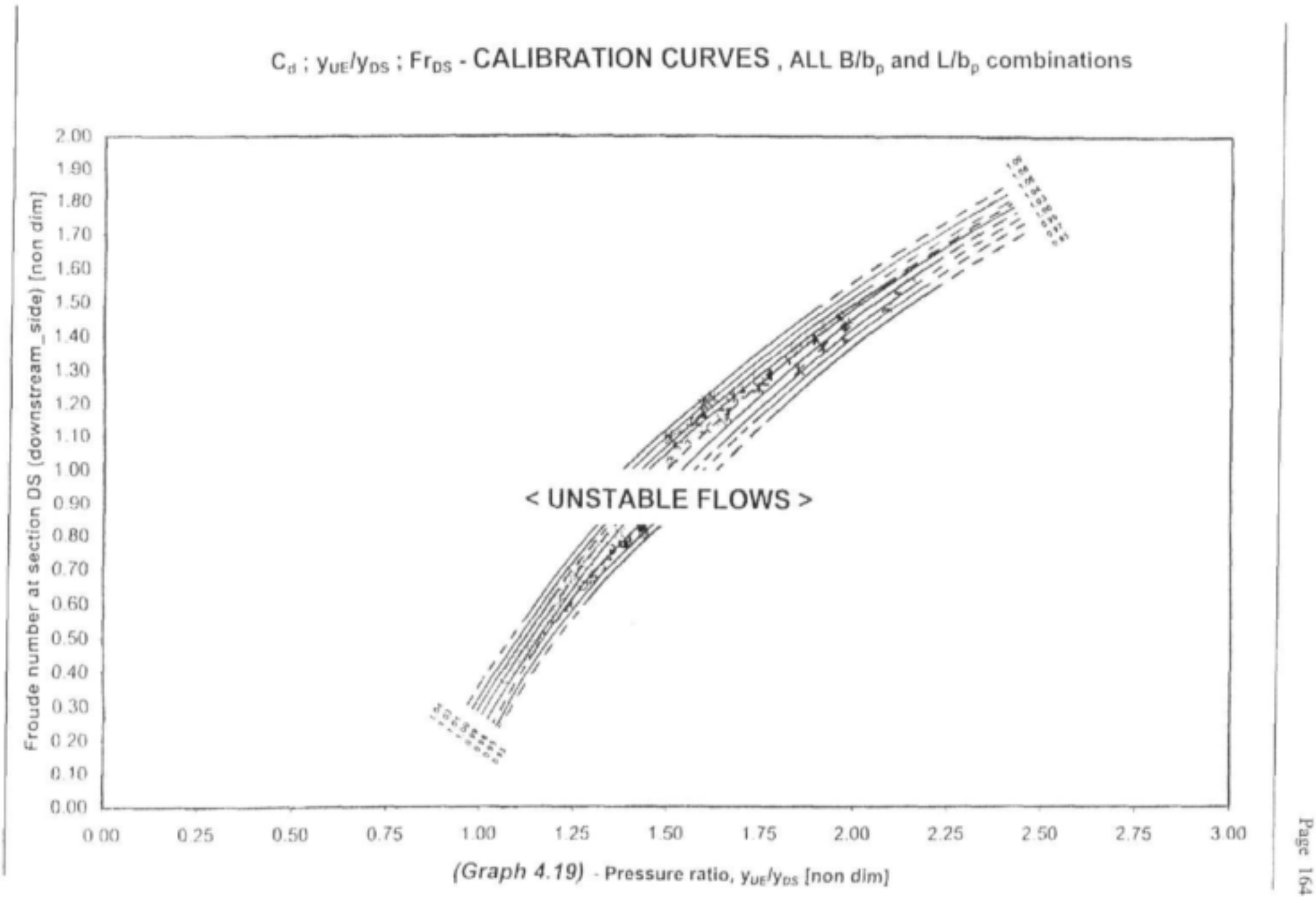
C_d ; y_{UE}/y_{DS} ; Fr_{DS} - CALIBRATION CURVES , ALL B/b_p and L/b_p combinations
Froude number at section DS (downstream_side) [non dim]
2.00
1.90
1.80
1.70
1.60
1.50
1.40
1.30
1.20
1.10
1.00
0.90
0.80
0.70
0.60
0.50
0.40
0.30
0.20
0.10
0.00
0.00
0.25
0.50
0.75
1.00
1.25
1.50
1.75
2.00
2.25
2.50
2.75
3.00
< UNSTABLE FLOWS >
Pressure ratio, y_{UE}/y_{DS} [non dim]

(Graph 4.19)

ii) Note that the dotted lines depict extrapolated parts of curves following the generalised trend whilst the solid lines pass through measured data (from laboratory tests). These generalised curves are recommended for practical use, applicable to all combinations with **B/b_p**-values ranging from **9.7** to **19.0** and **L/b_p**–values ranging from **4.2** to **6.9**.

iii) Note that the calibration represents constant **C_d-value** or discharge coefficient lines as functions of the **Froude** number at section **DS**, i.e. **Fr_{DS}** = **Froude** number at the downstream_side position as well as the pressure ratio **y_{UE}/y_{DS}**, i.e. the ratio: dynamic pressure measured at **UE** (upstream end of pier) to the hydrostatic pressure measured at **DS** (downstream and side of pier). The **y_{UE}/y_{DS}** ratio varies from ± **1.0** to almost **2.5.** This ratio gives an indication of the energy slope over the pier length and the relative velocity found at **DS**. Constant **C_d-value** lines vary for each combination of (**B/b_p; L/b_p**) values according to *table 4.1* and *table 4.2*.

Conclusions and Recommendations:

i) Changing the length of a pier for a constant **B/b_p**-value does not have a significant effect on the shape and position of the constant **C_d**-lines, therefore, length is not a primary variable influencing the transitional losses past a pier.

ii) Changing the width of a pier for a constant **L/b_p**-value does not have a significant influence on the shape and position of the constant **C_d**-lines, therefore, width is not a primary variable influencing the transitional losses past a pier either.

iii) Remarks **(i)** and **(ii)** above can be explained in terms of the geometry of flow lines. Considering *photo's 4.12* to *4.14*, *4.15* to *4.17*, *4.18* to *4.20* and *4.21* to *4.23* it is clear that the general geometry of the flow profile past the pier does not differ much as the width ratio changes, implying therefore that **C_d-values** are not influenced significantly by the length or width ratio of the pier.

iv) The variability in **C_d-values** for drowned conditions proved to be much less than for the control forming condition (**$Fr_{DS} > 1$** or supercritical). This was to be expected due to the fact that the coefficient varies proportionally to the degree of turbulence of the flow. The more turbulent the more fluctuating the flow, leading to greater variation in coefficient values. This was found to be true for all combinations of (**B/b_p**; **L/b_p**) values tested (*graph 4.6* to *graph 4.17*) and is also evident from *graph 4.18* showing the combined data points.

v) **C_d-curves** have not been drawn in for **Froude numbers** ranging between **0.90** and **1.10**. This is due to the instability of flow for these velocity/depth combinations. Such instability is generally found with **Froude numbers** close to **1**.

vi) Using the calibrated curves in order to calculate the flow rate for a pier with a specific width-ratio and a length-ratio, it is necessary to do an iterative calculation. This can be explained in the following four steps:

Firstly, measure the pressures **H** and **y_{DS}** respectively
Secondly, estimate a flow rate and calculate an estimated **Froude**-number at **DS** according to the measured value of **y_{DS}**.
Thirdly, read off the appropriate **C_d-value** from the curves for the **y_{UE}/y_{DS}** and **Fr_{DS}** values obtained above
Fourthly, use this **C_d-value** in order to calculate a flow rate from *equation 4.4* and check whether the calculated flow rate corresponds to the estimated value. If so, the flow rate was estimated correctly, if not, start with the newly calculated flow rate and repeat the process.

4.3.2 *Non-parallel approaching flow:*

The following **9** graphs (*figure 4.20* to *figure 4.28*) show the calibrated **C_d-values** according to laboratory tests conducted on **9** different model piers as described in *section 4.2.3* and *section 4.2.4*. The results of the **5 degree** rotation tests corresponded well with those for zero rotation (parallel flow) which suggests that small rotations (up to **5 degrees**) do not have a significant influence on the flow patterns and therefore **C_d-values**. A large variation in **C_d-values** was found for the other non-parallel flow tests as can be seen in *table 4.3* and *table 4.4*. It is for this reason that separate curves were constructed for each of the **9** different combinations of **B/b_{p_eff}**.

The graphs are all plotted using the same dimensionless parameters which were shown to be important variables in the energy based discharge equation (*equation 4.4*). These variables are: **C_d**, **y_{UE}/y_{DS}** and **F_{rDS}** where **C_d** denotes the discharge coefficient compensating for transitional losses, **y_{UE}/y_{DS}** the pressure ratio of upstream dynamic pressure head to downstream depth measured on the pier side and **F_{rDS}** the **Froude** number at **section C or DS (downstream_side)**. In some cases the variable **H** has been replaced by **y_{US}** referring to the dynamic pressure at section **B** or **US (upstream_side)**, the reason for this will be discussed now.

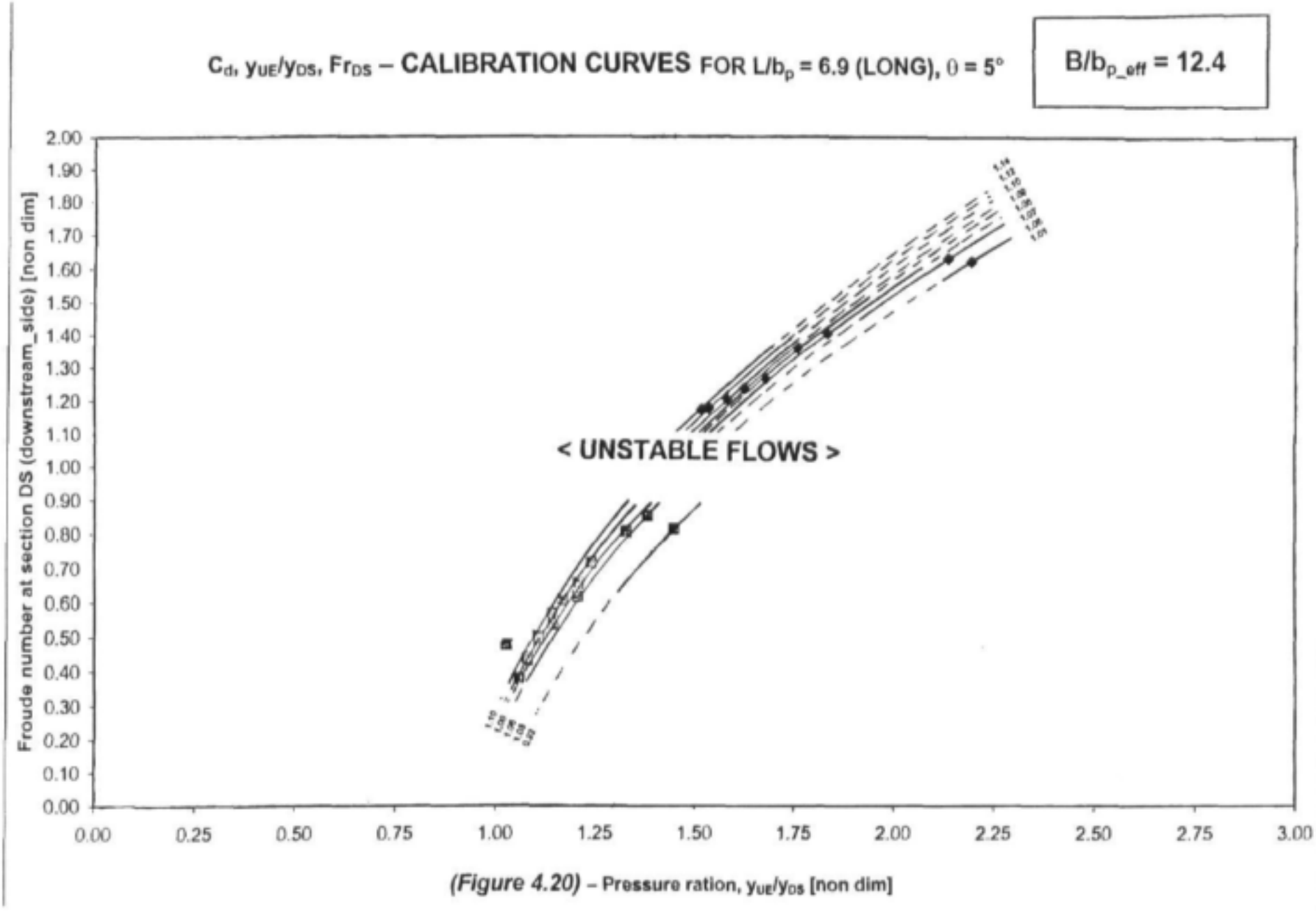

(Figure 4.20) – Pressure ration, y_{UE}/y_{DS} [non dim]

C_d, y_{US}/y_{DS}, Fr_{DS} – **CALIBRATION CURVES** FOR $L/b_p = 6.9$ (LONG), $\theta = 10°$

$B/b_{p\_eff} = 9.4$

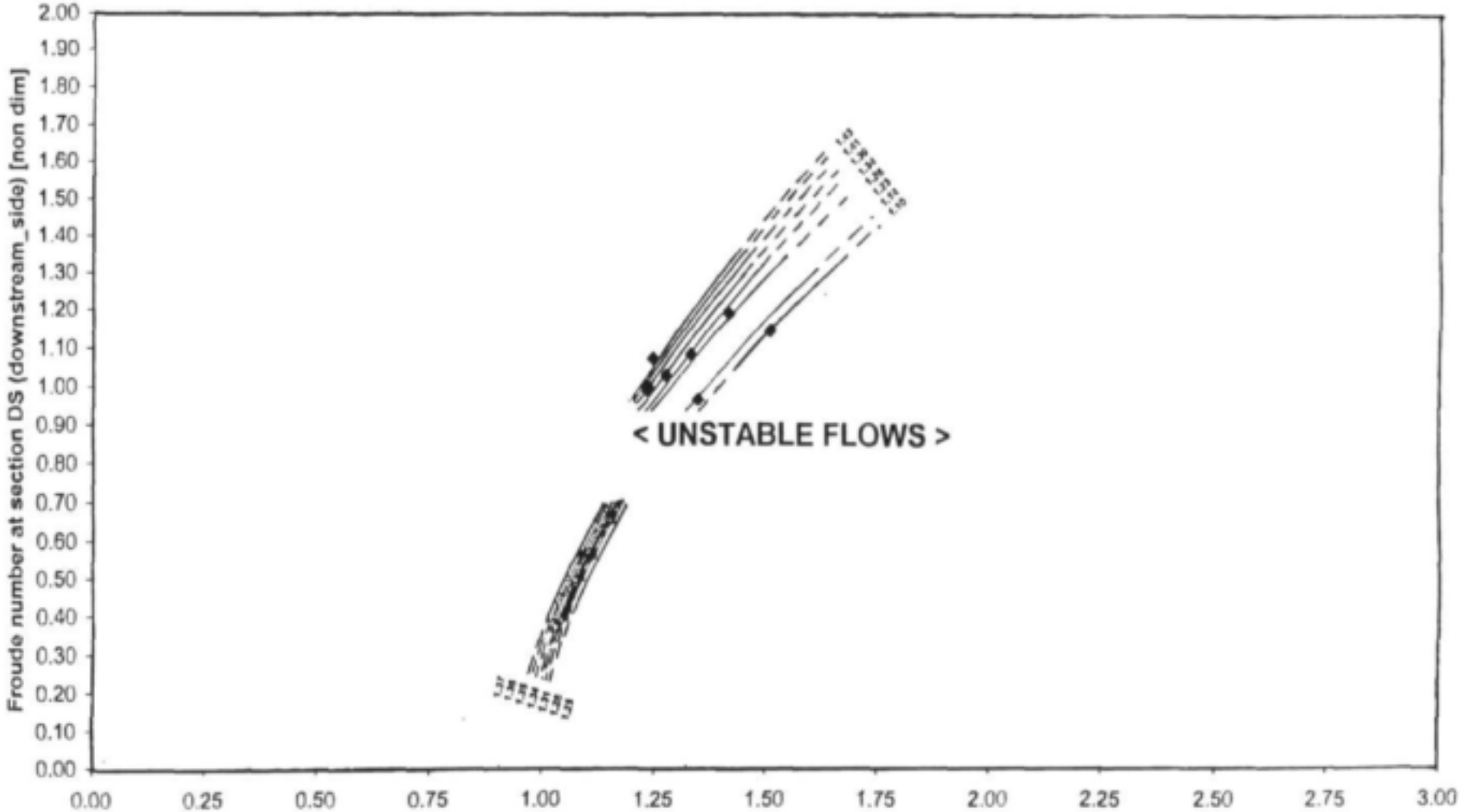

(Figure 4.21) – Pressure ration, y_{US}/y_{DS} [non dim]

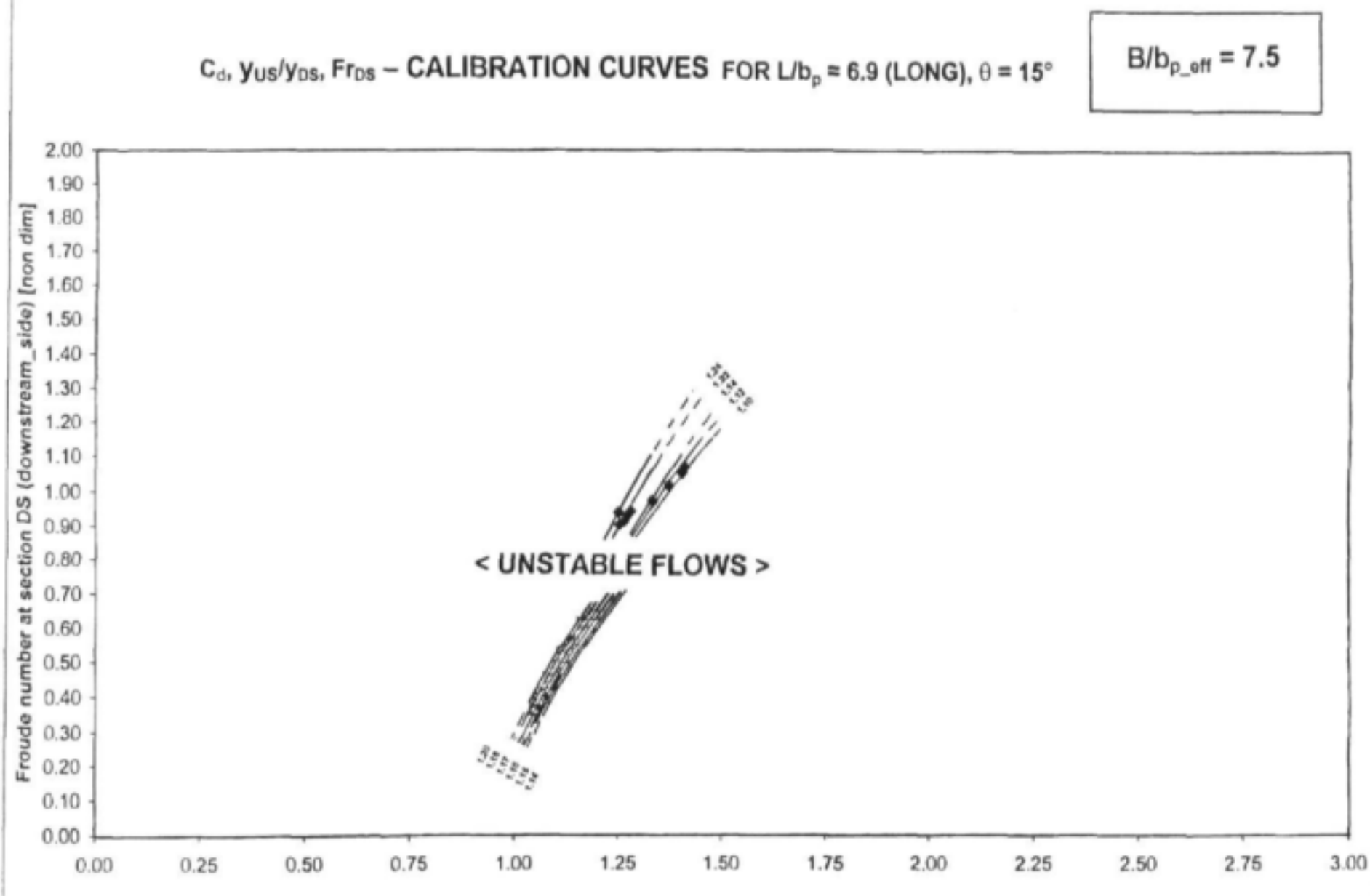

(Figure 4.22) – Pressure ration, y_{US}/y_{DS} [non dim]

C_d, y_{UE}/y_{DS}, Fr_{DS} – **CALIBRATION CURVES** FOR L/b_p = 5.6 (MEDIUM), θ = 5°

B/b_{p_eff} = 13.5

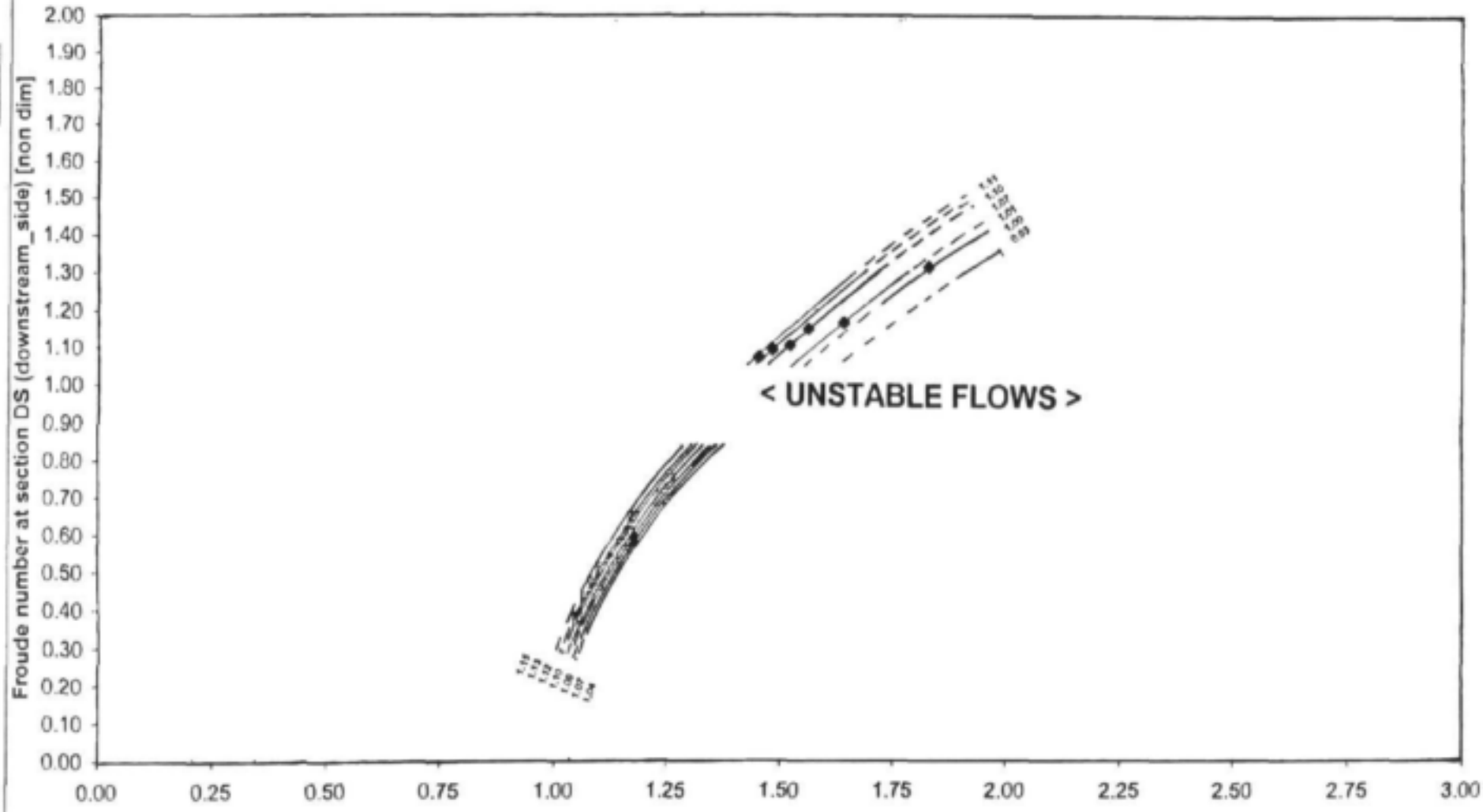

(Figure 4.23) – Pressure ration, y_{UE}/y_{DS} [non dim]

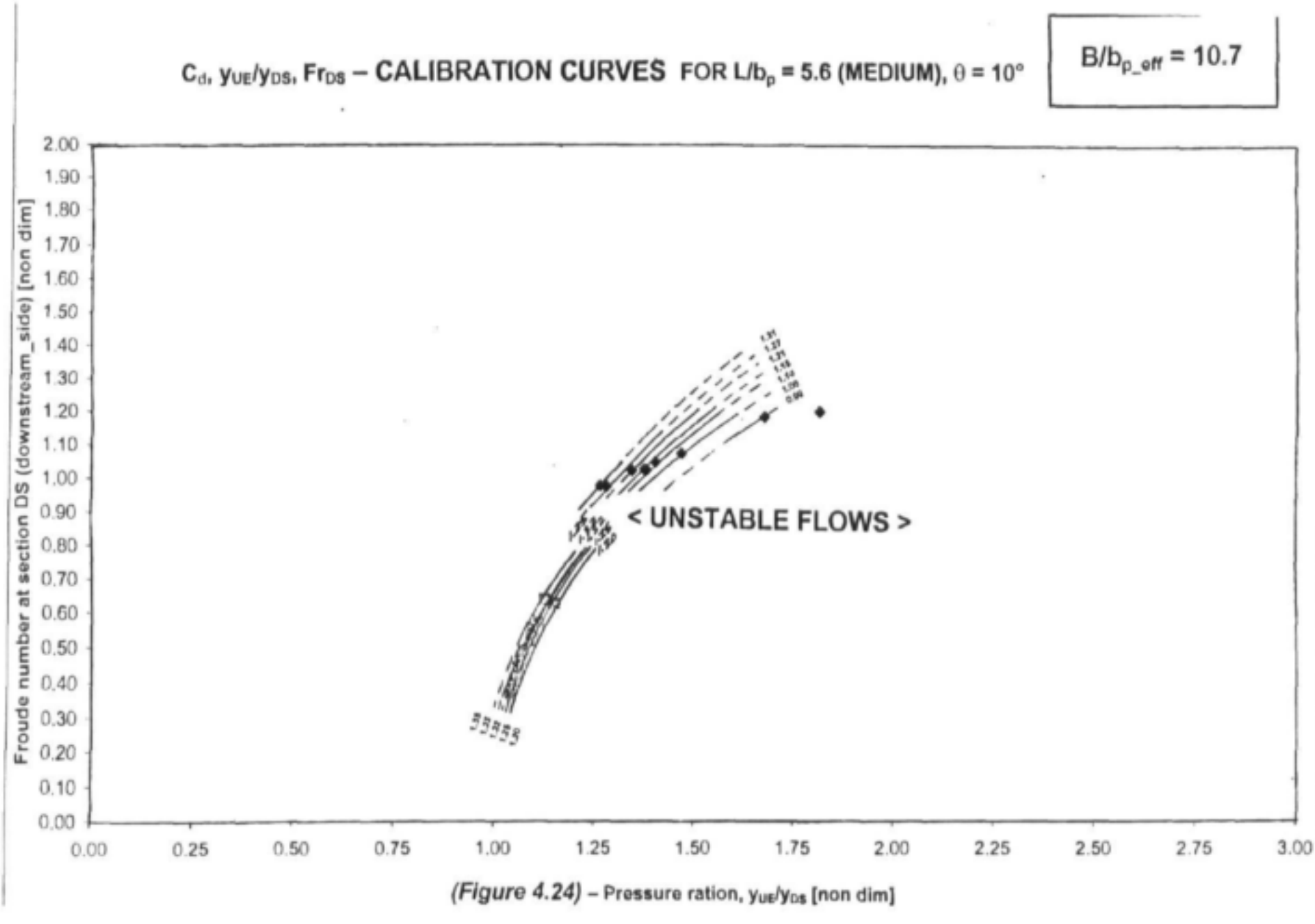

(Figure 4.24) – Pressure ration, y_{UE}/y_{DS} [non dim]

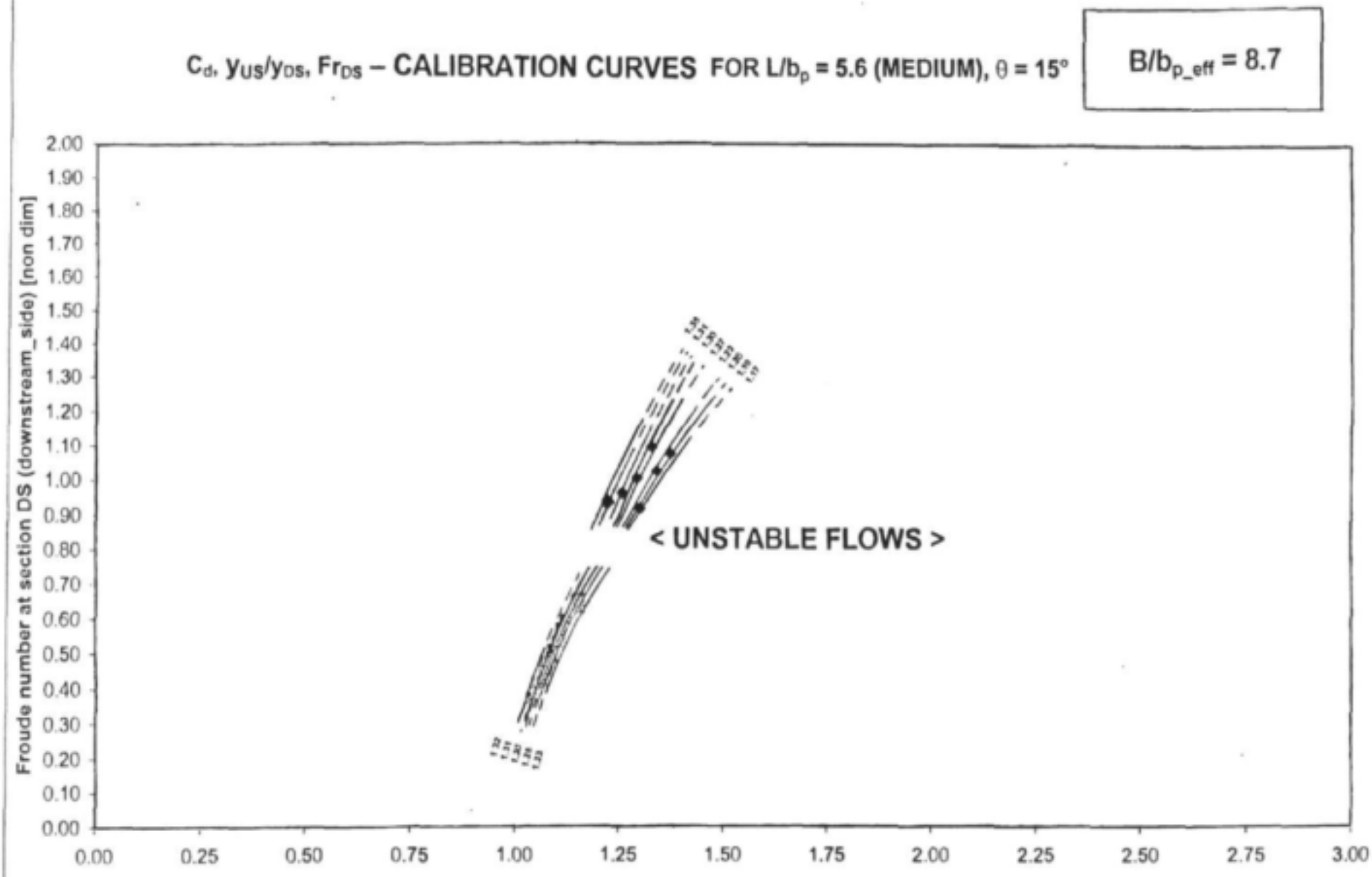

(Figure 4.25) – Pressure ration, y_{US}/y_{DS} [non dim]

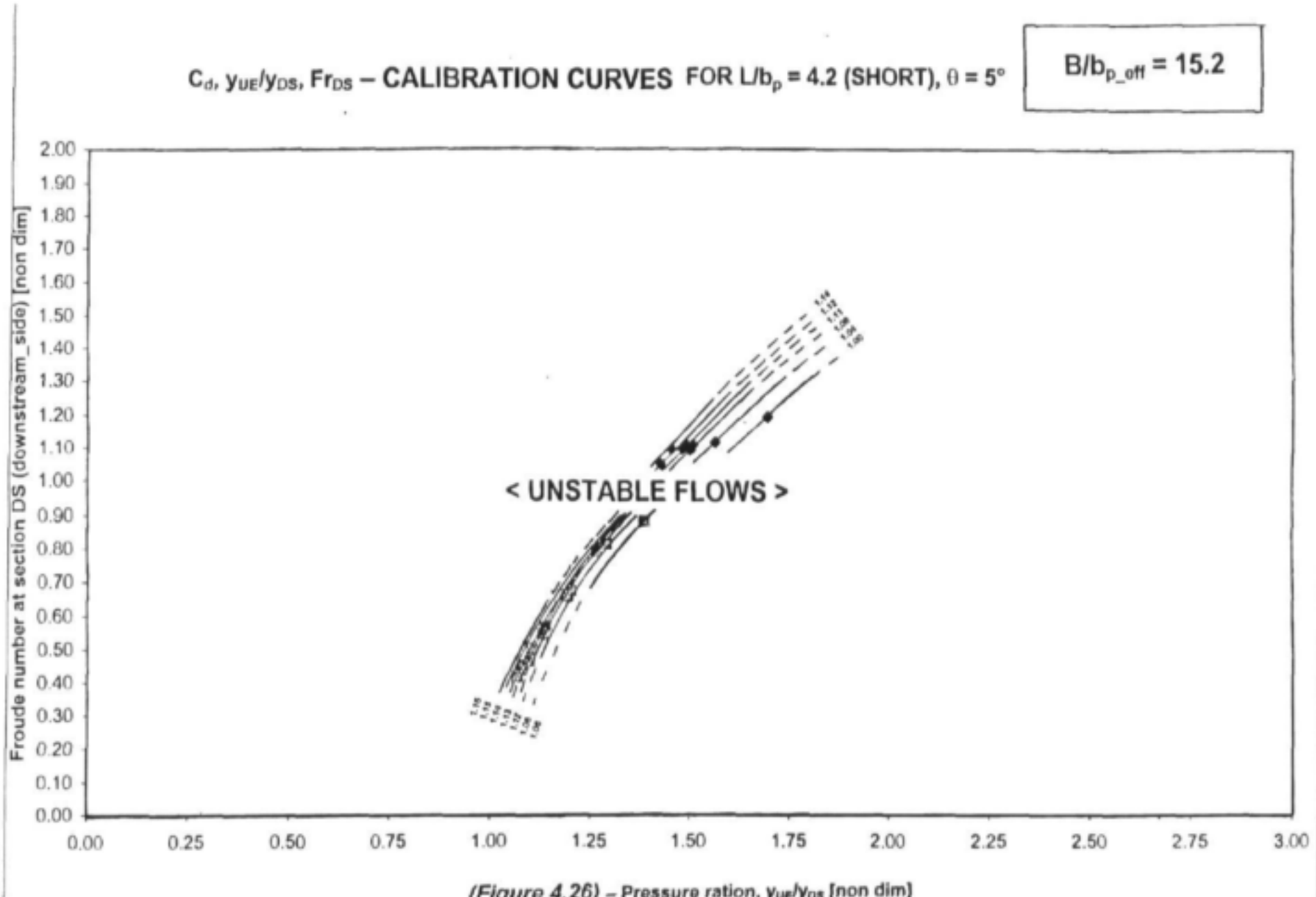

(Figure 4.26) – Pressure ration, y_{UE}/y_{DS} [non dim]

C_d, y_{UE}/y_{DS}, Fr_{DS} – CALIBRATION CURVES FOR L/b_p = 4.2 (SHORT), θ = 10°

B/b_{p_eff} = 12.4

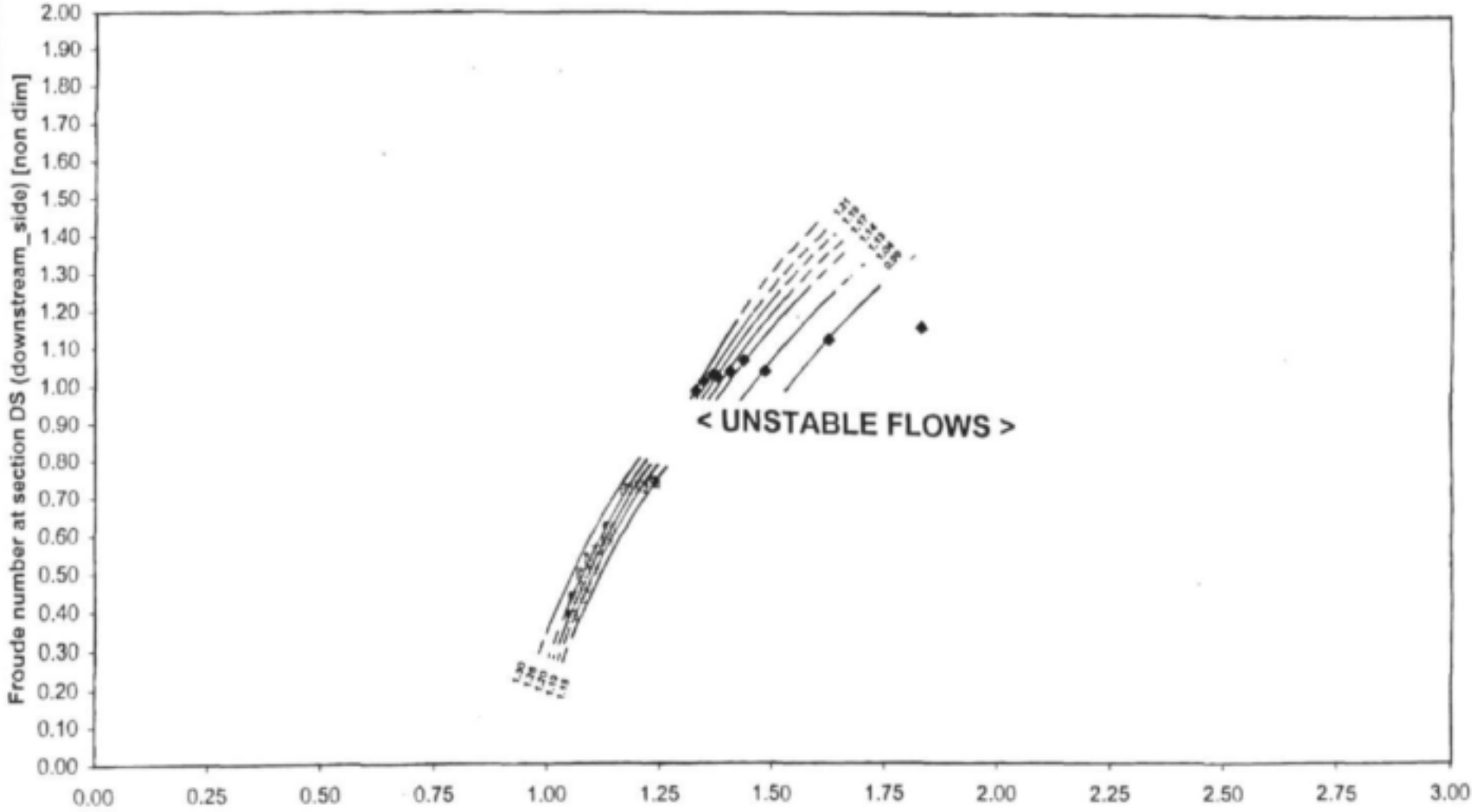

(Figure 4.27) – Pressure ration, y_{UE}/y_{DS} [non dim]

C_d, y_{US}/y_{DS}, Fr_{DS} – CALIBRATION CURVES FOR L/b_p = 4.2 (SHORT), θ = 15°

B/b_{p_eff} = 10.5

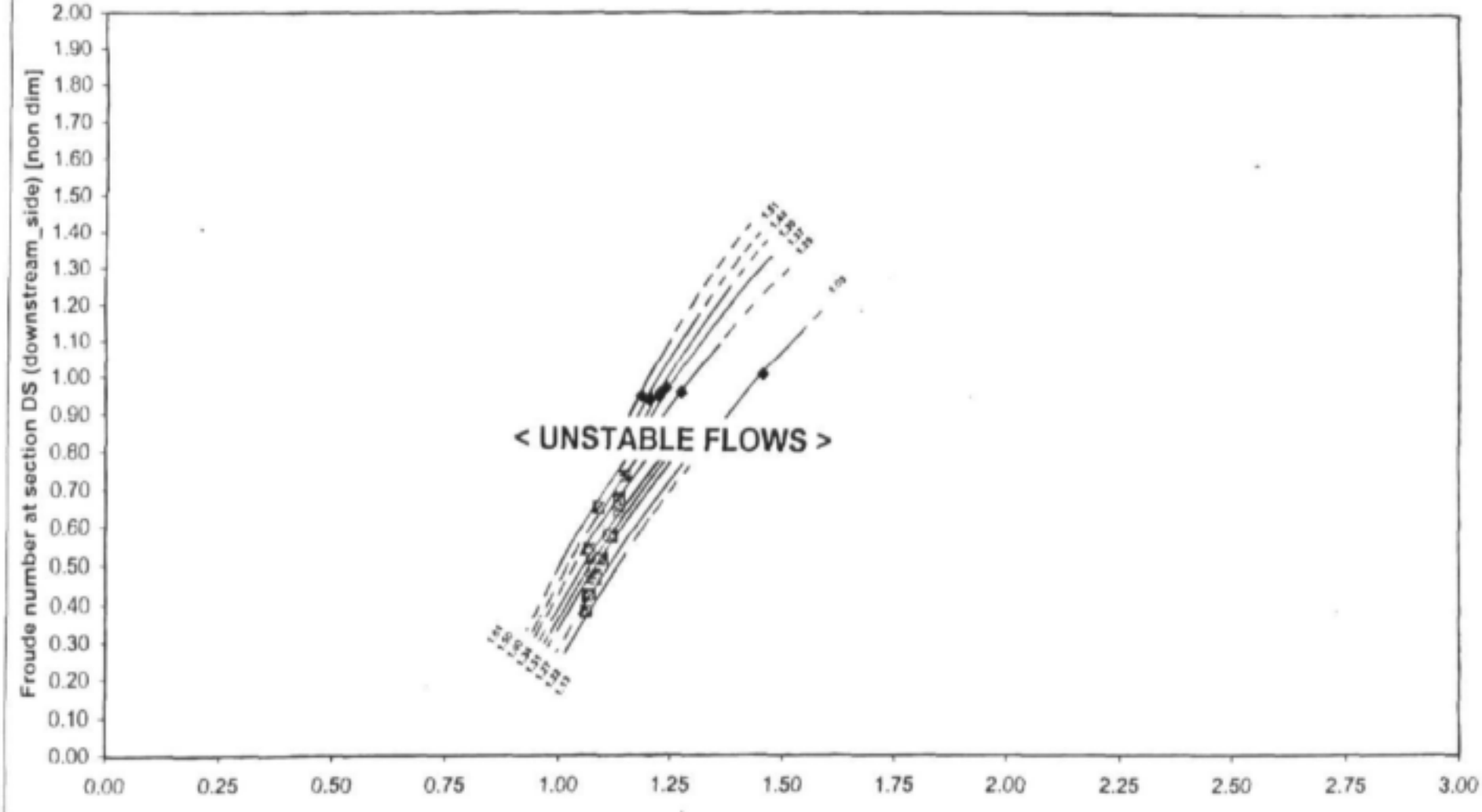

(Figure 4.28) – Pressure ration, y_{US}/y_{DS} [non dim]

From the laboratory data it was evident that rotation of the pier relative to the approaching flow direction results in a change in pressure distribution. The following photograph shows the pressure distribution along the pier (**UE, US, DS** and **DE**) for a typical flow condition with **NO** pier rotation as recorded with manometer stand pipes:

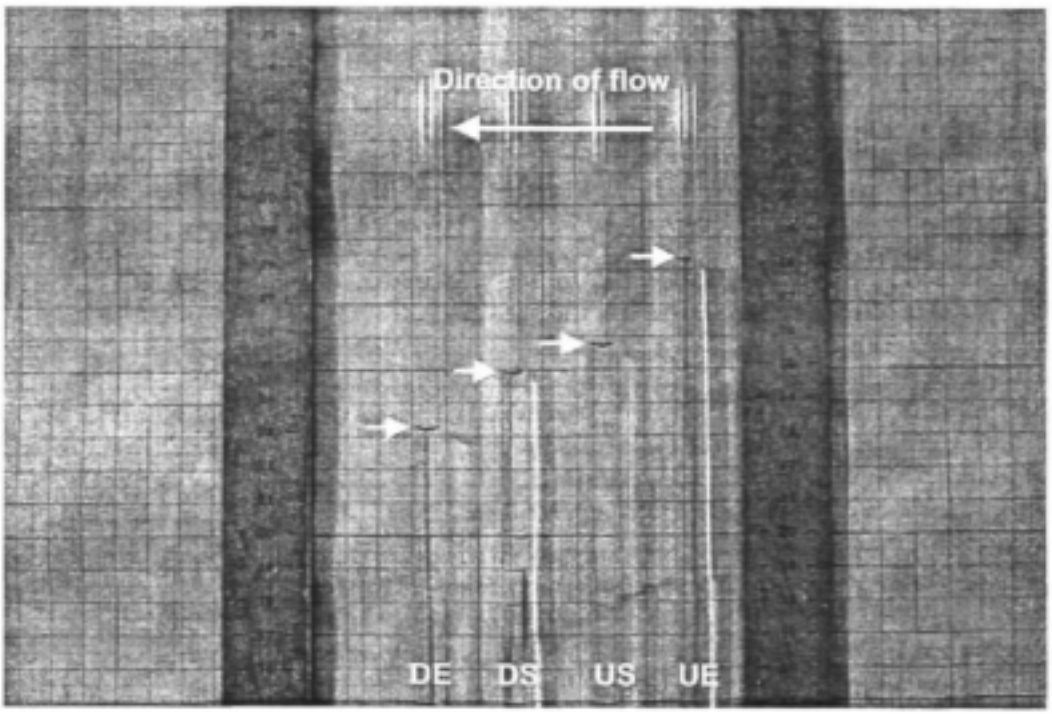

Photo 4.40: *Manometer stand pipe readings for supercritical flow conditions and zero pier rotation*

Note that the highest pressure is being measured as the dynamic pressure at **UE**, the upstream end of the pier. All other pressures show a declining tendency in the downstream direction.

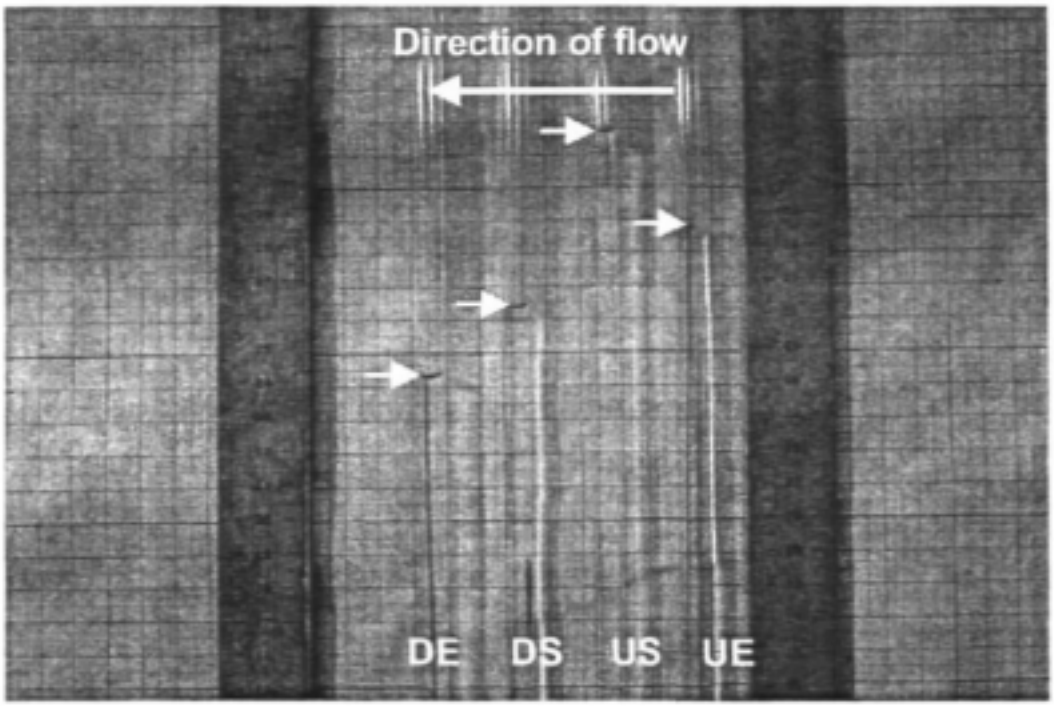

***Photo 4.41**: Manometer stand pipe readings for supercritical flow conditions and non-zero pier rotation*

NON-PARALLEL FLOW APPROACHING	$L/b_p = 6.9$ (LONG)	$L/b_p = 5.6$ (MEDIUM)	$L/b_p = 4.2$ (SHORT)
($\theta = 5$ degrees)			
($\theta = 10$ degrees)	X		
($\theta = 15$ degrees)	X	X	X

***Table 4.5:** Non-parallel flow conditions where pressure US exceeds pressure UE (marked with crosses)*

Photo 4.41 depicts the typical pressure distribution that was found for the combinations marked with a cross in *table 4.5*. Note that the pressure distribution indicates a larger pressure (dynamic) reading at the upstream side point (**US**) than at the upstream end point (**UE**). This is probably due to the fact that air is sucked in as shown in *photo 4.37*. Air is sucked in because the flow lines tend to maintain their direction when passing the

upstream end of the pier and not bend entirely around the pier head. Consequently air is sucked in resulting in a lower pressure head being measured. The eddy that forms whilst air is being sucked in can clearly be seen on *photo 4.36*. This phenomenon of air being sucked in was found for all three cases where the rotation angle was **15 degrees**. In addition, this phenomenon was also found for the combination of $\mathbf{L/b_p = 6.9}$ and θ **= 10 degrees**. This can be ascribed to the fact that although the rotation is not as severe in this case, the fact that the pier is very long combined with a substantial rotation of **10 degrees**, the flow lines again had difficulty bending around the head and air was sucked in. A second reason for the higher pressure head at **US** than at **UE** is the fact that due to the rotation of the pier, the pressure being measured at **US** includes a component perpendicular to the pier long axis, therefore also experiencing a dynamic pressure component (hydrostatic head plus part velocity head).

The calibration of $\mathbf{C_d}$**-values** for the **4** combinations mentioned above (marked with crosses) therefore entailed the use of $\mathbf{y_{US}}$ in stead of $\mathbf{y_{UE}}$ and the calibration curves for these cases were also drawn accordingly. Therefore, note that the calibration curves for the combinations marked with crosses in *table 4.5* should be used in accordance with measured values of $\mathbf{y_{US}}$ and not $\mathbf{y_{UE}}$.

Conclusions and Recommendations:

i) Rotation of the pier through angles up to **5 degrees** does not affect the calibration of the $\mathbf{C_d}$**-values** curves significantly.

ii) It is evident from the calibration curves that as the **rotational angle** θ becomes smaller, the $\mathbf{C_d}$**-value** lines approach those found for zero rotation as is to be expected.

iii) For a rotational angle θ of **15 degrees**, it is found that the pressure head at section **UE** (upstream end) is smaller than that at section **US** (upstream side). This can be ascribed to the fact that air is sucked in when the flow can not sufficiently bend around the upstream head of the pier as it passes the upstream head. This condition is found for the **15 degrees** rotational condition as well as the **10 degrees** rotation combined with the greatest pier length-to-width ratio tested. For the **10 degrees** condition, the phenomenon of air being sucked in can be ascribed to the long pier length having the same effect, i.e. the inability of flow to bend around the upstream head on the "negative pier side" (*photo 4.36*).

iv) **C_d-curves** are not drawn in for **Froude numbers** ranging between **0.90** and **1.10**. This is due to the instability of flow conditions for these velocity/depth combinations associated with **Froude** numbers close to **1**.

v) When using the calibration curves in order to calculate the flow rate associated with a pier with a specific length-ratio as well as rotation, it is necessary to do an iterative calculation. This can be done in the following four steps:

Firstly, measure the pressures y_{UE} (or y_{US} for all **15 degree** pier rotations as well as **10 degree** rotations combined with $L/b_p = 6.9$).
Secondly, estimate a flow rate and calculate the corresponding **Froude**-number at **DS** according to the measured value of y_{DS}. The **Froude**-number should be calculated for the effective flow width as shown in *photo 4.11* (*equation 4.7*).
Thirdly, Read the appropriate **C_d-value** off the curves for measured and calculated values: y_{UE}/y_{DS} and Fr_{DS}.
Fourthly, use this **C_d-value** in order to calculate a flow rate from *equation 4.4* and check whether the calculated flow rate corresponds to that estimated. If so, the flow rate was estimated correctly. If not, start with the previous calculated flow rate and repeat the process. Note that the effective flow width should be used in *equation 4.4*.

5. *OVERALL CONCLUSIONS AND RECOMMENDATIONS:*

i) It has been found possible to develop formulae which can be used to calculate river discharges from pressures measured alongside bridge piers. These formulae cater for both supercritical and sub-critical downstream conditions.

ii) The reliability of these formulae under laboratory conditions is underscored by the limited and systematic variations in the calibration coefficients.

iii) By changing the system of pressure measurement used by *Retief* (*chapter 3*) it was possible to increase the prediction accuracy (decreased **C_d-value** variation) of discharge formulae mentioned above. The new system of pressure measurement is discussed in *chapter 4*.

iv) Calibration curves were constructed in terms of measurable dimensionless flow parameters in the vicinity of bridge piers making it possible to extrapolate these calibration results to prototype structures.

v) It is recommended that piers identified for measuring purposes should ideally be parallel to the flow direction with a maximum rotation of **5** degrees to ensure accurate results. Where pier rotations exceed **10** degrees, special attention should be given to where the upstream pressure is measured.

vi) Bridge piers as flow measuring structures have the following advantages complying with the pre-determined criteria:

- providing an economical solution by using existing structures (bridges)
- minimum maintenance is required
- the pressure sensors can be sunk into piers and can resist the forces of nature as long as the pier does not fail

vii) Application of the methodology at the prototype level needs further investigation.

6. REFERENCES:

***Basson G.R.*, 1990:** "Opdamming by brûe en hidrouliese kragte op strukture."; M-thesis, University of Stellenbosch.

***Du Plessis D.B.*, 1989:** "Documentation of the February-March 1988 floods in the Orange River basin."

***DWAF*, 1986:** "Management of the water resources of the Republic of South Afrca." Pretoria: Department of Water Affairs and Forestry.

***Featherstone R.E., Nalluri C.*, 1995:** "Civil Engineering Hydraulics"; Blackwell Science.

***Finney R.L., Thomas G.B.*, 1994:** "Calculus"; Addison-Wesley publishing company.

***Herschy R.W.*, 1978:** "Hydrometry: Principles and practices." John Wiley & Sons, Chichester.

***Hibbeler R.C.*, 1992:** "Engineering Mechanics (Dynamics)"; McMillan Publishing Company, New York

***Lotriet H.H., Rooseboom A.*, 1995:** "River Discharge Measurement in South African rivers: The development of Improved Measuring Techniques"; WRC Report No 442/2/95

***Liu, H.K.; Bradley, J.N.; Plate, E.J.*, 1957**: "Backwater effects of piers and abutments" Report CER 57HKL10, Civil Engineering Section, Colorado State University

***Massey B.S.*, 1989:** "Mechanics of Fluids"; Chapman & Hall.

***Retief M.J.*, 1998:** "Meting van Hoë Vloeitempo's in riviere", Skripsie Nr. W12/98, University of Stellenbosch.

***Rooseboom A.*, 1985:** "HYDRO '85 Course notes". Pretoria. University of Pretoria.

***Rooseboom A. et al.*, 1986:** "Handleiding vir paddreinering"; Departement van Vervoer

***Rooseboom A.*, 1990:** "Hydraulics 344 class notes on model analysis." Stellenbosch. University of Stellenbosch

***Rooseboom A.*, 1992:** "Sediment Transport in Rivers and Reservoirs – a Southern African Perspective"; WRC Report No 297/1/92

***Rooseboom A., Le Grange A.*, 2000:** "The Hydraulic Resistance of sand streambeds under steady flow conditions"; Journal of Hydraulic Research, Vol 38, 2000, No 1.

***Rossouw J., Loubser C., Rooseboom A., Bester A.*, 1998:** "A New Structure for Discharge Measurement in Sediment-laden Rivers". WRC Report No TT 103/98.

***Serway R.A.*, 1982**: "Physics for Scientists and Engineers", Saunders College Publishing, London Sydney Tokyo.

***The Institution of Civil Engineers, London*, 1966:** "River Flood Hydrology"

United States, Department of Transportation: Federal Highway Administration, 1973: "Hydraulics of Bridge Waterways".

***Ven te Chow*, 1959:** "Open-channel Hydraulics"; McGraw-Hill Book Company Inc.

***Webber N.B.*, 1971:** "Fluid Mechanics for Civil Engineers", S.I. Edition, Chapman and Hall, London; New York

***White F.M.*, 1986:** "Fluid Mechanics", Second Edition, McGraw-Hill Book Company

APPENDIX A

ENERGY, MOMENTUM AND POWER APPROACHES,
LABORATORY RESULTS AND CALIBRATED
COEFFICIENTS - *Retief's* (1998) DATA

ENERGY APPROACH, RESULTS (LABORATORY):

Calculation of C_d-values for flow rate equations which have been derived:

EQUATION (Flow line FG):

$$Q_w = C_d B_F y_F \sqrt{\frac{2g(y_G - y_F)}{\alpha}}$$

90 mm Pier:

Pier characteristics: **B = 0.609 m** **b_p = 0.09 m** $\frac{B}{b_p} = 6.77$ $\frac{L}{b_p} = 5.56$

Q_w [l/s]	y_F [m]	y_G [m]	B_F [m]	Q_t [l/s]	C_d [ ]
0.03073	0.1010	0.1130	0.609	0.0298	1.03
0.06257	0.1620	0.1820	0.609	0.0618	1.01
0.09091	0.2085	0.2280	0.609	0.0785	1.16
0.11960	0.2500	0.2740	0.609	0.1045	1.15
0.15060	0.2850	0.3200	0.609	0.1438	1.05
0.16591	0.3020	0.3400	0.609	0.1588	1.04
0.18027	0.3190	0.3600	0.609	0.1742	1.03
Measured data			Geometry	Calculated	

45 mm Pier:

Pier characteristics: **B = 0.609 m** **b_p = 0.045 m** $\frac{B}{b_p} = 13.53$ $\frac{L}{b_p} = 5.56$

Q_w [l/s]	y_F [m]	y_G [m]	B_F [m]	Q_t [l/s]	C_d [ ]
0.03032	0.0830	0.1020	0.609	0.0238	1.27
0.06247	0.1440	0.1720	0.609	0.0650	0.96
0.09022	0.1800	0.2050	0.609	0.0768	1.18
0.12084	0.2150	0.2460	0.609	0.1021	1.18
0.14956	0.2400	0.2810	0.609	0.1311	1.14
0.16459	0.2530	0.3050	0.609	0.1556	1.06
0.18010	0.2710	0.3200	0.609	0.1618	1.11
Measured data			Geometry	Calculated	

30 mm Pier:

Pier characteristics: **B = 0.609 m** **b_p = 0.03 m** $\frac{B}{b_p} = 20.30$ $\frac{L}{b_p} = 5.56$

Q_w [l/s]	y_F [m]	y_G [m]	B_F [m]	Q_t [l/s]	C_d [ ]
0.03153	0.0920	0.1060	0.609	0.0294	1.07
0.06187	0.1340	0.1650	0.609	0.0636	0.97
0.09293	0.1750	0.2050	0.609	0.0818	1.14
0.11929	0.2040	0.2400	0.609	0.1044	1.14
0.14956	0.2270	0.2750	0.609	0.1342	1.11
0.16572	0.2450	0.2950	0.609	0.1478	1.12
0.18044	0.2590	0.3160	0.609	0.1668	1.08
Measured data			Geometry	Calculated	

EQUATION (Flow line GI):

$$Q_w = C_d B_I y_I \sqrt{\frac{2g(y_G - y_I)}{\alpha}}$$

90 mm Pier:

Pier characteristics: **B = 0.609 m** **b_p = 0.09 m** $\frac{B}{b_p} = 6.77$ $\frac{L}{b_p} = 5.56$

Q_w [l/s]	y_I [m]	y_G [m]	B_I [m]	Q_t [l/s]	$F_{<GI}$ [ ]	C_d [ ]
0.03073	0.0260	0.1130	0.609	0.0202	3.84	1.52
0.06257	0.0750	0.1820	0.609	0.0646	1.60	0.97
0.09091	0.1040	0.2280	0.609	0.0964	1.42	0.94

0.11980	0.1320	0.2740	0.609	0.1309	1.31	0.91
0.15080	0.1590	0.3200	0.609	0.1680	1.25	0.90
0.16591	0.1710	0.3400	0.609	0.1851	1.23	0.90
0.18027	0.1840	0.3600	0.609	0.2032	1.20	0.89
Measured data			Geometry		Calculated	

45 mm Pier:

Pier characteristics: **B = 0.609 m** **b_p = 0.045 m** $\frac{B}{b_p} = 13.53$ $\frac{L}{b_p} = 5.56$

Q_w [l/s]	y_1 [m]	y_c [m]	B_1 [m]	Q_1 [l/s]	$F_{r@1}$ [ ]	C_d [ ]
0.03032	0.0480	0.1020	0.609	0.0294	1.51	1.03
0.06247	0.0840	0.1720	0.609	0.0656	1.35	0.95
0.09022	0.1150	0.2050	0.609	0.0908	1.21	0.99
0.12084	0.1470	0.2460	0.609	0.1218	1.12	0.99
0.14956	0.1780	0.2610	0.609	0.1504	1.04	0.99
0.16459	0.1890	0.3050	0.609	0.1695	1.05	0.97
0.18010	0.2030	0.3200	0.609	0.1828	1.03	0.99
Measured data			Geometry		Calculated	

30 mm Pier:

Pier characteristics: **B = 0.609 m** **b_p = 0.03 m** $\frac{B}{b_p} = 20.30$ $\frac{L}{b_p} = 5.56$

Q_w [l/s]	y_1 [m]	y_c [m]	B_1 [m]	Q_1 [l/s]	$F_{r@1}$ [ ]	C_d [ ]
0.03153	0.0520	0.1060	0.609	0.0318	1.39	0.99
0.06187	0.0900	0.1650	0.609	0.0649	1.20	0.95
0.09293	0.1260	0.2050	0.609	0.0932	1.09	1.00
0.11929	0.1540	0.2400	0.609	0.1189	1.03	1.00
0.14956	0.1770	0.2750	0.609	0.1459	1.05	1.03
0.16572	0.1920	0.2950	0.609	0.1622	1.03	1.02
0.18044	0.2010	0.3160	0.609	0.1794	1.05	1.01
Measured data			Geometry		Calculated	

30 mm Pier (with debris):

Pier characteristics: **B = 0.609 m** **b_p = 0.03 m** $\frac{B}{b_p} = 20.30$ $\frac{L}{b_p} = 5.56$

Q_w [l/s]	y_1 [m]	y_c [m]	B_1 [m]	Q_1 [l/s]	$F_{r@1}$ [ ]	C_d [ ]
0.03212	0.0485	0.1070	0.609	0.0309	1.58	1.04
0.06217	0.0860	0.1640	0.609	0.0632	1.29	0.98
0.09350	0.1290	0.2110	0.609	0.0972	1.06	0.96
0.11903	0.1600	0.2450	0.609	0.1228	0.98	0.97
0.14980	0.1890	0.2830	0.609	0.1525	0.96	0.98
0.16497	0.2020	0.3060	0.609	0.1715	0.95	0.96
0.18080	0.2130	0.3270	0.609	0.1893	0.96	0.95
Measured data			Geometry		Calculated	

30 mm Pier (drowned conditions):

Pier characteristics: **B = 0.609 m** **b_p = 0.03 m** $\frac{B}{b_p} = 20.30$ $\frac{L}{b_p} = 5.56$

Q_w [l/s]	y_1 [m]	y_c [m]	B_1 [m]	Q_1 [l/s]	$F_{r@1}$ [ ]	C_d [ ]
0.06106	0.0920	0.1640	0.609	0.0650	1.15	0.94
0.06106	0.1350	0.1790	0.609	0.0745	0.65	0.82
0.06106	0.1640	0.1940	0.609	0.0748	0.48	0.82
0.11955	0.1560	0.2410	0.609	0.1197	1.02	1.00
0.11955	0.2080	0.2590	0.609	0.1237	0.66	0.97
0.11955	0.2670	0.3030	0.609	0.1334	0.45	0.90
0.17941	0.2120	0.3150	0.609	0.1791	0.96	1.00
0.17941	0.2960	0.3600	0.609	0.1971	0.58	0.91
0.17941	0.3520	0.3980	0.609	0.1987	0.45	0.90
Measured data			Geometry		Calculated	

MOMENTUM APPROACH, RESULTS (LABORATORY):

Calculation of C_d-values for flow rate equations which have been derived:

EQUATION (Section 1-3 combination):

$$Q_w = C_d \sqrt{\frac{g\left(y_1^2 B_1 - y_3^2 B_3\right)}{2\left(\frac{1}{y_1 B_1} - \frac{1}{y_3 B_3} + \frac{C_d^* \cdot A^*}{2 y_1^2 B_1^2}\right)}}$$

90 mm Pier:

Pier characteristics: B = 0.609 m b_p = 0.09 m $\frac{B}{b_p} = 6.77$ $\frac{L}{b_p} = 5.56$

Q_w [l/s]	y_1 [m]	y_2 [m]	y_3 [m]	B_1 [m]	B_3 [m]	C_d^* [m]	A^* [m²]	Q_t [l/s]	C_d [ ]
0.03073	0.1010	0.1130	0.0660	0.609	0.519	0.7	0.0102	0.0374	0.82
0.06257	0.1620	0.1820	0.1080	0.609	0.519	0.7	0.0164	0.0766	0.82
0.09091	0.2085	0.2280	0.1470	0.609	0.519	0.7	0.0205	0.1148	0.79
0.11980	0.2500	0.2740	0.1840	0.609	0.519	0.7	0.0247	0.1533	0.78
0.15050	0.2850	0.3200	0.2170	0.609	0.519	0.7	0.0288	0.1886	0.80
0.16591	0.3020	0.3400	0.2320	0.609	0.519	0.7	0.0306	0.2062	0.80
0.18027	0.3190	0.3600	0.2470	0.609	0.519	0.7	0.0324	0.2243	0.80
Measured data				Geometry		Constant		Calculated	

0.80

45 mm Pier:

Pier characteristics: B = 0.609 m b_p = 0.045 m $\frac{B}{b_p} = 13.53$ $\frac{L}{b_p} = 5.56$

Q_w [l/s]	y_1 [m]	y_2 [m]	y_3 [m]	B_1 [m]	B_3 [m]	C_d^* [m]	A^* [m²]	Q_t [l/s]	C_d [ ]
0.03032	0.0930	0.1020	0.0660	0.609	0.564	0.7	0.0046	0.0377	0.80
0.06247	0.1440	0.1720	0.1170	0.609	0.564	0.7	0.0077	0.0766	0.82
0.09022	0.1800	0.2050	0.1510	0.609	0.564	0.7	0.0092	0.1080	0.84
0.12084	0.2150	0.2460	0.1830	0.609	0.564	0.7	0.0111	0.1412	0.86
0.14956	0.2400	0.2810	0.2380	0.609	0.564	0.7	0.0126	0.1373	1.09
0.16459	0.2530	0.3060	0.2220	0.609	0.564	0.7	0.0137	0.1797	0.92
0.18010	0.2710	0.3200	0.2370	0.609	0.564	0.7	0.0144	0.1995	0.90
Measured data				Geometry		Constant		Calculated	

30 mm Pier:

Pier characteristics: B = 0.609 m b_p = 0.03 m $\frac{B}{b_p} = 20.30$ $\frac{L}{b_p} = 5.56$

Q_w [l/s]	y_1 [m]	y_2 [m]	y_3 [m]	B_1 [m]	B_3 [m]	C_d^* [m]	A^* [m²]	Q_t [l/s]	C_d [ ]
0.03153	0.0920	0.1060	0.0710	0.609	0.579	0.7	0.0032	0.0401	0.79
0.06187	0.1340	0.1650	0.1140	0.609	0.579	0.7	0.0050	0.0728	0.85
0.09293	0.1750	0.2050	0.1470	0.609	0.579	0.7	0.0062	0.1085	0.86
0.11929	0.2040	0.2400	0.1730	0.609	0.579	0.7	0.0072	0.1369	0.87
0.14956	0.2270	0.2750	0.1970	0.609	0.579	0.7	0.0083	0.1611	0.93
0.16572	0.2450	0.2950	0.2120	0.609	0.579	0.7	0.0089	0.1806	0.92
0.18044	0.2590	0.3150	0.2250	0.609	0.579	0.7	0.0095	0.1953	0.92
Measured data				Geometry		Constant		Calculated	

EQUATION (Section 1-4 combination):

$$Q_w = C_d \sqrt{\frac{g\left(y_1^2 B_1 - y_4^2 B_4\right)}{2\left(\frac{1}{y_1 B_1} - \frac{1}{y_4 B_4} + \frac{C_d^* \cdot A^*}{2 y_1^2 B_1^2}\right)}}$$

90 mm Pier:

Pier characteristics: B = 0.609 m b_p = 0.09 m $\frac{B}{b_p} = 6.77$ $\frac{L}{b_p} = 5.56$

Q_w [l/s]	y_1 [m]	y_2 [m]	y_3 [m]	y_4 [m]	B_1 [m]	B_4 [m]	C_d^* [m]	A^* [m²]	Q_t [l/s]	C_d [ ]	y_1/y_4	Fr_4	H^1/y_4
0.03073	0.1010	0.1130	0.0660	0.0260	0.609	0.609	0.7	0.0102	0.0244	1.26	3.88	3.84	3.88
0.06257	0.1620	0.1820	0.1080	0.0750	0.609	0.609	0.7	0.0164	0.0706	0.89	2.16	1.60	2.16
0.09091	0.2085	0.2280	0.1470	0.1040	0.609	0.609	0.7	0.0205	0.1080	0.84	2.00	1.42	2.00
0.11980	0.2500	0.2740	0.1840	0.1320	0.609	0.609	0.7	0.0247	0.1468	0.82	1.89	1.31	1.89

0.15060	0.2850	0.3200	0.2170	0.1590	0.609	0.609	0.7	0.0288	0.1847	0.82	1.79	1.25	1.79
0.16591	0.3020	0.3400	0.2320	0.1710	0.609	0.609	0.7	0.0306	0.2032	0.82	1.77	1.23	1.77
0.18027	0.3190	0.3600	0.2470	0.1840	0.609	0.609	0.7	0.0324	0.2230	0.81	1.73	1.20	1.73
	Measured data				Geometry		Constant		Calculated				
										0.89			

45 mm Pier:

Pier characteristics: **B = 0.609 m** **b_p = 0.045 m** $\frac{B}{b_p} = 13.53$ $\frac{L}{b_p} = 5.56$

Q_w [l/s]	y_1 [m]	y_2 [m]	y_3 [m]	y_4 [m]	B_1 [m]	B_4 [m]	C_d^* [m]	A^* [m^2]	Q_t [l/s]	C_d [ ]	y_1/y_4	Fr_4	H/y_4
0.03032	0.0930	0.1020	0.0660	0.0480	0.609	0.609	0.7	0.0046	0.0333	0.91	1.94	1.51	1.94
0.06247	0.1440	0.1720	0.1170	0.0840	0.609	0.609	0.7	0.0077	0.0693	0.90	1.71	1.35	1.71
0.09022	0.1800	0.2050	0.1510	0.1150	0.609	0.609	0.7	0.0092	0.1026	0.88	1.57	1.21	1.57
0.12084	0.2150	0.2460	0.1630	0.1470	0.609	0.609	0.7	0.0111	0.1399	0.86	1.46	1.12	1.46
0.14956	0.2400	0.2810	0.2380	0.1780	0.609	0.609	0.7	0.0126	0.1729	0.87	1.35	1.04	1.35
0.15459	0.2530	0.3050	0.2220	0.1890	0.609	0.609	0.7	0.0137	0.1876	0.88	1.34	1.05	1.34
0.18010	0.2710	0.3200	0.2370	0.2030	0.609	0.609	0.7	0.0144	0.2085	0.86	1.33	1.03	1.33
	Measured data				Geometry		Constant		Calculated				

30 mm Pier:

Pier characteristics: **B = 0.609 m** **b_p = 0.03 m** $\frac{B}{b_p} = 20.30$ $\frac{L}{b_p} = 5.56$

Q_w [l/s]	y_1 [m]	y_2 [m]	y_3 [m]	y_4 [m]	B_1 [m]	B_4 [m]	C_d^* [m]	A^* [m^2]	Q_t [l/s]	C_d [ ]	y_1/y_4	Fr_4	H/y_4
0.03153	0.0920	0.1060	0.0710	0.0520	0.609	0.609	0.7	0.0032	0.0350	0.90	1.77	1.39	1.77
0.06187	0.1340	0.1550	0.1140	0.0900	0.609	0.609	0.7	0.0050	0.0686	0.90	1.49	1.20	1.49
0.09293	0.1750	0.2050	0.1470	0.1260	0.609	0.609	0.7	0.0062	0.1071	0.87	1.39	1.09	1.39
0.11929	0.2040	0.2400	0.1730	0.1540	0.609	0.609	0.7	0.0072	0.1388	0.86	1.32	1.03	1.32
0.14956	0.2270	0.2750	0.1970	0.1770	0.609	0.609	0.7	0.0083	0.1658	0.90	1.28	1.05	1.28
0.16572	0.2450	0.2950	0.2120	0.1920	0.609	0.609	0.7	0.0089	0.1865	0.89	1.28	1.03	1.28
0.18044	0.2590	0.3160	0.2260	0.2010	0.609	0.609	0.7	0.0095	0.2015	0.90	1.29	1.05	1.29
	Measured data				Geometry		Constant		Calculated				

30 mm Pier (with debris):

Pier characteristics: **B = 0.609 m** **b_p = 0.03 m** $\frac{B}{b_p} = 20.30$ $\frac{L}{b_p} = 5.56$

Q_w [l/s]	y_1 [m]	y_2 [m]	y_3 [m]	y_4 [m]	B_1 [m]	B_4 [m]	C_d^* [m]	A^* [m^2]	Q_t [l/s]	C_d [ ]	y_1/y_4	Fr_4	H/y_4
0.03212	0.0905	0.1070	0.0690	0.0485	0.609	0.609	0.7	0.0032	0.0329	0.98	1.87	1.58	1.87
0.06217	0.1380	0.1640	0.1115	0.0860	0.609	0.609	0.7	0.0049	0.0684	0.91	1.60	1.29	1.60
0.09350	0.1830	0.2110	0.1530	0.1290	0.609	0.609	0.7	0.0063	0.1131	0.83	1.42	1.06	1.42
0.11903	0.2150	0.2450	0.1820	0.1600	0.609	0.609	0.7	0.0074	0.1490	0.80	1.34	0.98	1.34
0.14980	0.2490	0.2830	0.2120	0.1890	0.609	0.609	0.7	0.0085	0.1879	0.80	1.32	0.96	1.32
0.16497	0.2630	0.3060	0.2250	0.2020	0.609	0.609	0.7	0.0092	0.2053	0.80	1.30	0.95	1.30
0.18080	0.2765	0.3270	0.2360	0.2130	0.609	0.609	0.7	0.0096	0.2216	0.82	1.30	0.96	1.30
	Measured data				Geometry		Constant		Calculated				

30 mm Pier (drowned conditions):

Pier characteristics: **B = 0.609 m** **b_p = 0.03 m** $\frac{B}{b_p} = 20.30$ $\frac{L}{b_p} = 5.56$

Q_w [l/s]	y_1 [m]	y_2 [m]	y_3 [m]	y_4 [m]	B_1 [m]	B_4 [m]	C_d^* [m]	A^* [m^2]	Q_t [l/s]	C_d [ ]	y_1/y_4	Fr_4	H/y_4
0.06106	0.1390	0.1640	0.1160	0.0920	0.609	0.609	0.7	0.0049	0.0705	0.87	1.48	1.147	1.48
0.06106	0.1580	0.1790	0.1430	0.1350	0.609	0.609	0.7	0.0054	0.1010	0.60	1.17	0.645	1.17
0.06106	0.1760	0.1940	0.1675	0.1640	0.609	0.609	0.7	0.0058	0.1190	0.51	1.07	0.482	1.07
0.11955	0.2050	0.2410	0.1760	0.1560	0.609	0.609	0.7	0.0072	0.1405	0.85	1.31	1.017	1.31
0.11955	0.2380	0.2590	0.2190	0.2080	0.609	0.609	0.7	0.0078	0.1685	0.63	1.14	0.661	1.14
0.11955	0.2840	0.3030	0.2760	0.2670	0.609	0.609	0.7	0.0091	0.2428	0.49	1.06	0.454	1.06
0.17941	0.2650	0.3150	0.2350	0.2120	0.609	0.609	0.7	0.0095	0.2123	0.85	1.25	0.964	1.25
0.17941	0.3230	0.3600	0.3090	0.2960	0.609	0.609	0.7	0.0108	0.2982	0.60	1.09	0.584	1.09
0.17941	0.3710	0.3980	0.3610	0.3520	0.609	0.609	0.7	0.0119	0.3577	0.50	1.05	0.450	1.05
	Measured data				Geometry		Constant		Calculated				

POWER APPROACH, RESULTS (LABORATORY):

Calculation of κ- en C_d-values for flow rate equations which have been derived

κ-EQUATION (Section 1-3 combination, control volume 1):

$$Q = \sqrt{\frac{g\left[\left(y_1 - y_3\right) + \frac{\kappa}{2 y_3 B}\left(y_1^{\,2} B_1 - y_3^{\,2} B_3\right)\right]}{\frac{\kappa}{y_1 B_1}\left(\frac{1}{y_3 B_3} - \frac{1}{y_1 B_1}\right) + \frac{1}{2}\left(\frac{1}{y_3^{\,2} B_3^{\,2}} - \frac{1}{y_1^{\,2} B_1^{\,2}}\right)}}$$

Note that if we make κ (kappa) the subject of the equation we have:

$$\kappa = \frac{g\left(y_1 - y_3\right) + \frac{1}{2} Q^2\left(\frac{1}{y_1^{\,2} B_1^{\,2}} - \frac{1}{y_3^{\,2} B_3^{\,2}}\right)}{\left[\frac{1}{2} g\left(y_3^{\,2} B_3 - y_1^{\,2} B_1\right) + Q^2\left(\frac{1}{y_3 B_3} - \frac{1}{y_1 B_1}\right)\right]\left(\frac{1}{y_1 B_1}\right)}$$

90 mm Pier:

Pier characteristics: **B = 0.609 m** **b_p = 0.09 m**

$\frac{B}{b_p} = 6.77$ $\frac{L}{b_p} = 5.56$

Q_w [l/s]	y_1 [m]	y_3 [m]	B_1 [m]	B_3 [m]	Q_t (κ = 1) [l/s]	κ [-]
0.03073	0.1010	0.0660	0.609	0.519	0.0361	0.56
0.06257	0.1620	0.1080	0.609	0.519	0.0742	0.57
0.09091	0.2085	0.1470	0.609	0.519	0.1114	0.60
0.11980	0.2500	0.1840	0.609	0.519	0.1490	0.58
0.15060	0.2850	0.2170	0.609	0.519	0.1836	0.50
0.16591	0.3020	0.2320	0.609	0.519	0.2008	0.47
0.18027	0.3190	0.2470	0.609	0.519	0.2185	0.46
Measured data			Geometry		Calculated	

45 mm Pier:

Pier characteristics: **B = 0.609 m** **b_p = 0.045 m**

$\frac{B}{b_p} = 13.53$ $\frac{L}{b_p} = 5.56$

Q_w [l/s]	y_1 [m]	y_3 [m]	B_1 [m]	B_3 [m]	Q_t (κ = 1) [l/s]	κ [-]
0.03032	0.0930	0.0660	0.609	0.564	0.0372	0.81
0.06247	0.1440	0.1170	0.609	0.564	0.0763	0.66
0.09022	0.1800	0.1510	0.609	0.564	0.1075	0.55
0.12084	0.2150	0.1830	0.609	0.564	0.1406	0.46
0.14956	0.2400	0.2380	0.609	0.564	0.1211	-6.44
0.16459	0.2530	0.2220	0.609	0.564	0.1793	0.11
0.18010	0.2710	0.2370	0.609	0.564	0.1988	0.20
Measured data			Geometry		Calculated	

30 mm Pier:

Pier characteristics: **B = 0.609 m** **b_p = 0.03 m**

$\frac{B}{b_p} = 20.30$ $\frac{L}{b_p} = 5.56$

Q_w [l/s]	y_1 [m]	y_3 [m]	B_1 [m]	B_3 [m]	Q_t (κ = 1) [l/s]	κ [-]
0.03153	0.0920	0.0710	0.609	0.579	0.0399	0.87
0.06187	0.1340	0.1140	0.609	0.579	0.0731	0.64
0.09293	0.1750	0.1470	0.609	0.579	0.1087	0.65
0.11929	0.2040	0.1730	0.609	0.579	0.1371	0.59
0.14956	0.2270	0.1970	0.609	0.579	0.1617	0.29
0.16572	0.2450	0.2120	0.609	0.579	0.1812	0.36
0.18044	0.2590	0.2260	0.609	0.579	0.1971	0.33
Measured data			Geometry		Calculated	

κ-EQUATION (Section 1-4 combination, control volume 2):

$$Q = \sqrt{\frac{g\left[\left(y_1 - y_4\right) + \frac{\kappa}{2 y_4 B}\left(y_1^{\,2} B_1 - y_4^{\,2} B_4\right)\right]}{\frac{\kappa}{y_1 B_1}\left(\frac{1}{y_4 B_4} - \frac{1}{y_1 B_1}\right) + \frac{1}{2}\left(\frac{1}{y_4^{\,2} B_4^{\,2}} - \frac{1}{y_1^{\,2} B_1^{\,2}}\right)}}$$

Note that if we make κ (kappa) the subject of the equation we have:

$$\kappa = \frac{g\left(y_1 - y_4\right) + \frac{1}{2} Q^2\left(\frac{1}{y_1^{\,2} B_1^{\,2}} - \frac{1}{y_4^{\,2} B_4^{\,2}}\right)}{\left[\frac{1}{2} g\left(y_4^{\,2} B_4 - y_1^{\,2} B_1\right) + Q^2\left(\frac{1}{y_4 B_4} - \frac{1}{y_1 B_1}\right)\right]\left(\frac{1}{y_1 B_1}\right)}$$

$$\kappa = \frac{g\left(y_1 - y_4\right) + \frac{1}{2}Q^2\left(\frac{1}{y_1^2 B_1^2} - \frac{1}{y_4^2 B_4^2}\right)}{\left[\frac{1}{2}g\left(y_4^2 B_4 - y_1^2 B_1\right) + Q^2\left(\frac{1}{y_4 B_4} - \frac{1}{y_1 B_1}\right)\right]\left(\frac{1}{y_1 B_1}\right)}$$

90 mm Pier:

Pier characteristics: **B = 0.609 m** **b_p = 0.09 m**

$\frac{B}{b_p} = 6.77$ $\frac{L}{b_p} = 5.56$

Q_w [l/s]	y_1 [m]	y_4 [m]	B_1 [m]	B_4 [m]	Q_t (κ = 1) [l/s]	κ []
0.03073	0.1010	0.0260	0.609	0.609	0.0214	3.97
0.06257	0.1620	0.0750	0.609	0.609	0.0693	0.74
0.09091	0.2085	0.1040	0.609	0.609	0.1072	0.99
0.11980	0.2500	0.1320	0.609	0.609	0.1471	1.08
0.15060	0.2850	0.1590	0.609	0.609	0.1868	1.10
0.16591	0.3020	0.1710	0.609	0.609	0.2061	1.10
0.18027	0.3190	0.1840	0.609	0.609	0.2269	1.12
Measured data			Geometry		Calculated	

45 mm Pier:

Pier characteristics: **B = 0.609 m** **b_p = 0.045 m**

$\frac{B}{b_p} = 13.53$ $\frac{L}{b_p} = 5.56$

Q_w [l/s]	y_1 [m]	y_4 [m]	B_1 [m]	B_4 [m]	Q_t (κ = 1) [l/s]	κ []
0.03032	0.0930	0.0480	0.609	0.609	0.0328	0.71
0.06247	0.1440	0.0840	0.609	0.609	0.0694	0.93
0.09022	0.1800	0.1150	0.609	0.609	0.1040	1.05
0.12084	0.2150	0.1470	0.609	0.609	0.1429	1.09
0.14956	0.2400	0.1780	0.609	0.609	0.1792	1.09
0.16459	0.2530	0.1890	0.609	0.609	0.1950	1.09
0.18010	0.2710	0.2030	0.609	0.609	0.2166	1.09
Measured data			Geometry		Calculated	

30 mm Pier:

Pier characteristics: **B = 0.609 m** **b_p = 0.03 m**

$\frac{B}{b_p} = 20.30$ $\frac{L}{b_p} = 5.56$

Q_w [l/s]	y_1 [m]	y_4 [m]	B_1 [m]	B_4 [m]	Q_t (κ = 1) [l/s]	κ []
0.03153	0.0920	0.0520	0.609	0.609	0.0346	0.87
0.06187	0.1340	0.0900	0.609	0.609	0.0693	1.03
0.09293	0.1750	0.1260	0.609	0.609	0.1091	1.08
0.11929	0.2040	0.1540	0.609	0.609	0.1423	1.09
0.14956	0.2270	0.1770	0.609	0.609	0.1711	1.07
0.16572	0.2450	0.1920	0.609	0.609	0.1926	1.07
0.18044	0.2590	0.2010	0.609	0.609	0.2078	1.07
Measured data			Geometry		Calculated	

C_d-EQUATION (Section 1-3 combination, control volume 1):

$$Q = C_d\sqrt{\frac{g\left[\left(y_1 - y_3\right) + \frac{1}{2}\left(y_1 - \frac{y_3^2 B_3}{y_1 B_1}\right)\right]}{\left(\frac{1}{y_3 B_3} - \frac{1}{y_1 B_1}\right)\left[\frac{1}{y_1 B_1} + \frac{1}{2}\left(\frac{1}{y_3 B_3} + \frac{1}{y_1 B_1}\right)\right]}}$$

Note that if B_1 is not equal to B_3 then no further simplification of the above equation is possible.

90 mm Pier:

Pier characteristics: **B = 0.609 m** **b_p = 0.09 m**

$\frac{B}{b_p} = 6.77$ $\frac{L}{b_p} = 5.56$

Q_w [l/s]	y_1 [m]	y_3 [m]	B_1 [m]	B_3 [m]	Q_t [l/s]	C_d []
0.03073	0.1010	0.0990	0.609	0.519	0.0361	0.85
0.06257	0.1620	0.1080	0.609	0.519	0.0742	0.84
0.09091	0.2085	0.1470	0.609	0.519	0.1114	0.82
0.11980	0.2500	0.1840	0.609	0.519	0.1490	0.80
0.15060	0.2850	0.2170	0.609	0.519	0.1836	0.82
0.16591	0.3020	0.2320	0.609	0.519	0.2008	0.83

0.18027	0.3190	0.2470	0.609	0.519	0.2185	0.83
Measured data			Geometry		Calculated	

45 mm Pier:

Pier characteristics: **B = 0.609 m** **b_p = 0.045 m** $\frac{B}{b_p} = 13.53$ $\frac{L}{b_p} = 5.56$

Q_w [l/s]	y_1 [m]	y_3 [m]	B_1 [m]	B_3 [m]	Q_t [l/s]	C_d [ ]
0.03032	0.0930	0.0660	0.609	0.564	0.0372	0.82
0.06247	0.1440	0.1170	0.609	0.564	0.0763	0.82
0.09022	0.1800	0.1510	0.609	0.564	0.1075	0.84
0.12084	0.2150	0.1830	0.609	0.564	0.1406	0.86
0.14956	0.2400	0.2380	0.609	0.564	0.1211	1.24
0.16459	0.2530	0.2220	0.609	0.564	0.1793	0.92
0.18010	0.2710	0.2370	0.609	0.564	0.1988	0.91
Measured data			Geometry		Calculated	

30 mm Pier:

Pier characteristics: **B = 0.609 m** **b_p = 0.03 m** $\frac{B}{b_p} = 20.30$ $\frac{L}{b_p} = 5.56$

Q_w [l/s]	y_1 [m]	y_3 [m]	B_1 [m]	B_3 [m]	Q_t [l/s]	C_d [ ]
0.03153	0.0920	0.0710	0.609	0.579	0.0399	0.79
0.06187	0.1340	0.1140	0.609	0.579	0.0731	0.85
0.09293	0.1750	0.1470	0.609	0.579	0.1087	0.86
0.11929	0.2040	0.1730	0.609	0.579	0.1371	0.87
0.14956	0.2270	0.1970	0.609	0.579	0.1617	0.93
0.16572	0.2450	0.2120	0.609	0.579	0.1812	0.91
0.18044	0.2590	0.2260	0.609	0.579	0.1971	0.92
Measured data			Geometry		Calculated	

C_d-EQUATION (Section 1-4 combination, control volume 2):

$$Q_w = C_d \sqrt{\frac{g\left[\left(y_4 - y_1\right) - \frac{1}{2}\left(\frac{y_4^2 B_4}{y_1 B_1} - y_1\right)\right]}{\left(\frac{1}{y_4 B_4} - \frac{1}{y_1 B_1}\right)\left[\frac{1}{y_1 B_1} - \frac{1}{2}\left(\frac{1}{y_4 B_4} + \frac{1}{y_1 B_1}\right)\right]}}$$

Note that $B_1 = B_4 = B$ and therefor the equation above will simplify as follows:

$$Q = C_d \sqrt{B^2 g y_1 y_4^{\,2} \frac{(3y_1 - y_4)}{(y_1 - 3y_4)}} \Rightarrow Q = C_d B y_4 \sqrt{g y_1} \sqrt{\frac{(3y_1 - y_4)}{(y_1 - 3y_4)}}$$

90 mm Pier:

Pier characteristics: **B = 0.609 m** **b_p = 0.09 m** $\frac{B}{b_p} = 6.77$ $\frac{L}{b_p} = 5.56$

Q_w [l/s]	y_1 [m]	y_4 [m]	B_1 [m]	B_4 [m]	Q_t [l/s]	C_d [ ]	v_4	y_1/y_4	Fr_4
0.03073	0.1010	0.0260	0.609	0.609	0.0214	1.44	1.94	3.88	3.84
0.06257	0.1620	0.0750	0.609	0.609	0.0693	0.90	1.37	2.16	1.60
0.09091	0.2065	0.1040	0.609	0.609	0.1072	0.85	1.44	2.00	1.42
0.11980	0.2500	0.1320	0.609	0.609	0.1471	0.81	1.49	1.89	1.31
0.15060	0.2850	0.1590	0.609	0.609	0.1868	0.81	1.56	1.79	1.25
0.16591	0.3020	0.1710	0.609	0.609	0.2061	0.81	1.59	1.77	1.23
0.18027	0.3190	0.1840	0.609	0.609	0.2269	0.79	1.61	1.73	1.20
Measured data			Geometry		Calculated				

45 mm Pier:

Pier characteristics: **B = 0.609 m** **b_p = 0.045 m** $\frac{B}{b_p} = 13.53$ $\frac{L}{b_p} = 5.56$

Q_w [l/s]	y_1 [m]	y_4 [m]	B_1 [m]	B_4 [m]	Q_t [l/s]	C_d [ ]	v_4	y_1/y_4	Fr_4
0.03032	0.0930	0.0480	0.609	0.609	0.0328	0.92	1.04	1.94	1.51
0.06247	0.1440	0.0840	0.609	0.609	0.0694	0.90	1.22	1.71	1.35
0.09022	0.1800	0.1150	0.609	0.609	0.1040	0.87	1.29	1.57	1.21
0.12084	0.2150	0.1470	0.609	0.609	0.1429	0.85	1.35	1.46	1.12
0.14956	0.2400	0.1780	0.609	0.609	0.1792	0.83	1.38	1.35	1.04

0.16459	0.2530	0.1890	0.609	0.609	0.1950	0.84	1.43	1.34	1.05
0.18010	0.2710	0.2030	0.609	0.609	0.2166	0.83	1.48	1.33	1.03
Measured data			Geometry		Calculated				

30 mm Pier:

Pier characteristics: **B = 0.609 m** **b_p = 0.03 m**

$$\frac{B}{b_p} = 20.30 \qquad \frac{L}{b_p} = 5.56$$

Q_w [l/s]	y_1 [m]	y_4 [m]	B_1 [m]	B_4 [m]	Q_t [l/s]	C_d [ ]	v_4	y_1/y_4	Fr_4
0.03153	0.0920	0.0520	0.609	0.609	0.0345	0.91	1.00	1.77	1.39
0.06187	0.1340	0.0900	0.609	0.609	0.0693	0.89	1.13	1.49	1.20
0.09293	0.1750	0.1260	0.609	0.609	0.1091	0.85	1.21	1.39	1.09
0.11929	0.2040	0.1540	0.609	0.609	0.1423	0.84	1.27	1.32	1.03
0.14956	0.2270	0.1770	0.609	0.609	0.1711	0.87	1.39	1.28	1.05
0.16572	0.2450	0.1920	0.609	0.609	0.1926	0.86	1.42	1.28	1.03
0.18044	0.2590	0.2010	0.609	0.609	0.2078	0.87	1.47	1.29	1.05
Measured data			Geometry		Calculated				

30 mm Pier (with debris):

Pier characteristics: **B = 0.609 m** **b_p = 0.03 m**

$$\frac{B}{b_p} = 20.30 \qquad \frac{L}{b_p} = 5.56$$

Q_w [l/s]	y_1 [m]	y_4 [m]	B_1 [m]	B_4 [m]	Q_t [l/s]	C_d [ ]	v_4	y_1/y_4	Fr_4
0.03212	0.0905	0.0485	0.609	0.609	0.0324	0.99	1.09	1.87	1.58
0.06217	0.1380	0.0860	0.609	0.609	0.0685	0.91	1.19	1.60	1.29
0.09350	0.1830	0.1290	0.609	0.609	0.1148	0.81	1.19	1.42	1.06
0.11903	0.2150	0.1600	0.609	0.609	0.1523	0.78	1.22	1.34	0.98
0.14980	0.2490	0.1890	0.609	0.609	0.1927	0.78	1.30	1.32	0.96
0.16497	0.2630	0.2020	0.609	0.609	0.2110	0.78	1.34	1.30	0.95
0.18080	0.2765	0.2130	0.609	0.609	0.2280	0.79	1.39	1.30	0.96
Measured data			Geometry		Calculated				

30 mm Pier (drowned conditions):

Pier characteristics: **B = 0.609 m** **b_p = 0.03 m**

$$\frac{B}{b_p} = 20.30 \qquad \frac{L}{b_p} = 5.56$$

Q_w [l/s]	y_1 [m]	y_4 [m]	B_1 [m]	B_4 [m]	Q_t [l/s]	C_d [ ]	v_4	y_1/y_4	Fr_4
0.06106	0.1360	0.0920	0.609	0.609	0.0713	0.86	1.09	1.48	1.15
0.06106	0.1580	0.1350	0.609	0.609	0.1065	0.57	0.74	1.17	0.65
0.06106	0.1760	0.1640	0.609	0.609	0.1336	0.46	0.61	1.07	0.48
0.11955	0.2050	0.1560	0.609	0.609	0.1442	0.83	1.29	1.31	1.02
0.11955	0.2380	0.2080	0.609	0.609	0.2002	0.60	0.94	1.14	0.66
0.11955	0.2840	0.2670	0.609	0.609	0.2756	0.43	0.74	1.06	0.45
0.17941	0.2650	0.2120	0.609	0.609	0.2201	0.82	1.39	1.25	0.96
0.17941	0.3230	0.2960	0.609	0.609	0.3280	0.55	1.00	1.09	0.58
0.17941	0.3710	0.3520	0.609	0.609	0.4144	0.43	0.84	1.05	0.45
Measured data			Geometry		Calculated				

APPENDIX B

ENERGY APPROACH, LABORATORY DATA AND CALIBRATED COEFFICIENTS - ADDITIONAL LABORATORY TESTS

MODEL PIER, bp = 32 mm_SHORT_NORMAL Q's

OK

DATA: *Saturday, 5 August 2000*

Q	h_{tran_1}	h_{tran_2}	0 m	1 m	2 m	3 m	4 m	UE upstream end	US upstream side	DS downstream side	DE downstream end	6 m	7 m
bed levels			12.5	10.5	15.0	13.8	15.5					147.5	147.0
10	11.5	11.0	NOT MEASURABLE			58.6	56.9	56.0	35.0	22.5	16.0	197.5	193.3
30	73.0	73.0				92.4	90.0	101.0	62.5	51.3	42.3	224.8	240.5
50	204.0	205.0				119.4	114.4	134.5	82.5	77.0	71.8	274.4	260.6
70	400.0	400.0				145.9	142.0	164.3	103.5	99.8	97.5	299.2	275.0
90	665.0	675.0				171.7	163.0	196.5	122.0	121.3	124.0	312.9	306.3
110	970.0	975.0				191.6	181.0	219.3	139.8	142.0	144.5	343.3	327.2
130	1385.0	1385.0				217.6	210.8	246.8	144.3	148.8	152.8	313.1	333.5
150	1850.0	1830.0				233.1	225.3	269.1	160.0	164.8	169.8	338.6	353.2
170	2330.0	2320.0				249.6	244.3	291.9	173.8	179.8	184.5	363.1	366.4

Geometric properties:

D =	31.5 mm
L_p =	132 mm
z_a =	0.7 mm
z_b =	1.4 mm
z_c =	3.3 mm
z_d =	4.0 mm

CALCULATIONS

FLOW DEPTHS

h_{tran_avg}	Q_{calc}	Q [l/s]	Distance measured downstream within the flume: 0 m y_0	1 m y_1	2 m y_2	3 m y_3	4 m y_4	UE upstream end y_{ue}	US upstream side y_{us}	DS downstream side y_{ds}	DE downstream end y_{de}	6 m y_6	7 m y_7	B	B-b_p	v_c = $\sqrt{2g(y_{ue}-y_{cal})^{2.5}}$	Q_{theory}	C_d = Q_{calc}/Q_{theory}	Fr_4m	Fr_DS	Fr_DE
11.3	0.011824	11.8				45.3	41.4	58.0	36.4	25.8	20.0	50.0	46.3	0.609	0.576	0.83	0.012311	0.96	0.74	1.58	2.19
73.0	0.030120	30.1				78.9	74.5	101.0	63.9	54.6	46.3	77.3	93.5	0.609	0.576	0.98	0.030904	0.97	0.78	1.31	1.59
204.5	0.050413	50.4				105.9	98.9	134.5	83.9	80.3	75.8	126.9	113.6	0.609	0.576	1.06	0.048954	1.03	0.85	1.22	1.27
400.0	0.070506	70.5				132.4	126.5	164.3	104.9	103.1	101.5	151.7	126.6	0.609	0.576	1.12	0.066582	1.06	0.82	1.18	1.14
670.0	0.091246	91.2				158.2	147.5	196.5	123.4	124.6	128.0	165.4	156.3	0.609	0.576	1.21	0.086990	1.05	0.84	1.15	1.04
972.5	0.109635	109.9				178.1	165.5	219.3	141.2	145.3	148.5	195.8	180.2	0.609	0.576	1.23	0.102835	1.07	0.86	1.10	1.01
1385.0	0.131195	131.2				204.1	195.3	246.8	145.7	152.1	156.8	165.6	186.5	0.609	0.576	1.38	0.121323	1.08	0.83	1.22	1.11
1840.0	0.151217	151.2				219.6	209.8	269.1	161.4	168.1	173.8	191.3	206.2	0.609	0.576	1.43	0.138396	1.09	0.82	1.21	1.09
2325.0	0.169983	170.0				236.1	228.8	291.9	175.2	183.1	188.5	215.6	219.4	0.609	0.576	1.48	0.156319	1.09	0.81	1.20	1.09
																		1.06			

MODEL PIER, bp = 32 mm_SHORT_DROWNED Q's

DATA: *Saturday, 5 August 2000; Sunday, 6 August 2000*

h_{tran_1}	h_{tran_2}	4 m	UE upstream end	US upstream side	DS downstream side	DE downstream end	6 m	7 m
		15.5					147.5	147.0
675.0	660.0	166.3	195.4	127.5	126.0	126.5	322.5	314.3
675.0	660.0	186.5	206.3	155.0	157.0	154.0	335.0	335.2
675.0	660.0	207.8	219.3	180.0	181.0	178.5	356.2	353.2
675.0	660.0	225.4	235.4	200.8	201.0	201.3	369.7	372.9
675.0	660.0	244.1	249.6	221.0	222.8	221.0	392.2	388.5

h_{tran_1}	h_{tran_2}	4 m	UE upstream end	US upstream side	DS downstream side	DE downstream end	6 m	7 m
		15.5					147.5	147.0
965.0	975.0	222.1	242.0	191.3	192.5	190.8	370.3	368.4
965.0	975.0	239.5	254.6	213.0	214.3	212.3	391.0	382.2
965.0	975.0	256.8	269.5	232.3	234.5	232.8	403.1	404.2
965.0	975.0	276.8	287.5	255.0	256.8	255.5	425.5	425.7
965.0	975.0	297.3	306.0	274.3	277.5	276.0	445.1	443.8

h_{tran_1}	h_{tran_2}	4 m	UE upstream end	US upstream side	DS downstream side	DE downstream end	6 m	7 m

		15.5					147.5	147.0
1370.0	1375.0	254.9	276.3	223.3	224.8	222.3	397.1	394.2
1370.0	1375.0	270.7	288.3	243.0	244.0	242.0	423.9	420.5
1370.0	1375.0	290.2	303.1	263.5	264.8	263.5	455.9	453.6
1370.0	1375.0	308.2	318.6	283.0	285.8	285.0	483.1	483.8
1370.0	1375.0	326.2	338.6	305.0	306.8	306.0	475.4	476.8

h_{man_1}	h_{man_2}	4 m	UE upstream end	US upstream side	DS downstream side	DE downstream end	6 m	7 m
		15.5					147.5	147.0
1810.0	1830.0	282.1	302.9	248.8	249.5	249.3	420.0	420.0
1810.0	1830.0	296.2	315.8	266.0	268.5	268.8	446.7	44.5
1810.0	1830.0	316.6	331.3	287.8	290.0	289.8	469.8	469.5
1810.0	1830.0	335.8	348.3	310.5	311.5	310.0	493.5	493.6
1810.0	1830.0	353.8	365.4	330.0	332.0	331.0	497.0	499.1

h_{man_1}	h_{man_2}	4 m	UE upstream end	US upstream side	DS downstream side	DE downstream end	6 m	7 m
		15.5					147.5	147.0
2320.0	2320.0	306.0	328.4	274.5	275.0	273.5	441.3	456.6
2320.0	2320.0	322.5	344.5	291.8	294.5	291.8	469.2	459.8
2320.0	2320.0	342.4	358.9	317.5	314.8	313.8	496.2	494.0
2320.0	2320.0	361.5	379.0	335.3	336.8	336.0	508.1	503.6
2320.0	2320.0	380.8	394.9	355.0	357.5	355.8	525.0	529.0

CALCULATIONS:

FLOW DEPTHS

h_{man_avg}	Q_{calc}	Q [l/s]	4 m y_4	UE upstream end y_{UE}	US upstream side y_{US}	DS downstream side y_{DS}	DE downstream end y_{DE}	6 m y_6	7 m y_7	B	B-b_y	v_c = $2g(y_{UE}-y_{DS})^{2/3}$	Q_{theor2}		$Fr_{...4m}$	$Fr_{...DS}$	$Fr_{...6m}$
667.5	0.091079	91.1	150.8	160.4	128.9	129.3	130.5	175.0	167.3	0.609	0.578	1.16	0.086676	1.05	0.82	1.03	0.65
667.5	0.091079	91.1	171.0	206.3	156.4	160.3	158.0	187.5	188.2	0.609	0.578	0.98	0.090359	1.01	0.68	0.74	0.59
667.5	0.091079	91.1	192.1	219.3	181.4	184.3	182.5	207.7	206.2	0.609	0.578	0.86	0.091355	1.00	0.57	0.60	0.50
667.5	0.091079	91.1	209.9	235.4	202.2	204.3	205.3	222.2	225.8	0.609	0.578	0.81	0.090901	0.95	0.50	0.52	0.46
667.5	0.091079	91.1	228.6	249.6	222.4	226.1	225.0	244.7	241.5	0.609	0.578	0.72	0.093551	0.97	0.44	0.44	0.39

h_{man_avg}	Q_{calc}	Q [l/s]	4 m y_4	UE upstream end y_{UE}	US upstream side y_{US}	DS downstream side y_{DS}	DE downstream end y_{DE}	6 m y_6	7 m y_7	B	B-b_y	v_c = $2g(y_{UE}-y_{DS})^{2/3}$	Q_{theor2}		$Fr_{...4m}$	$Fr_{...DS}$	$Fr_{...6m}$
970.0	0.109794	109.8	206.6	242.0	192.7	195.0	194.8	222.8	221.4	0.609	0.578	0.98	0.110043	0.99	0.61	0.66	0.55
970.0	0.109794	109.8	224.0	254.6	214.4	217.6	216.3	243.5	235.2	0.609	0.578	0.88	0.110846	0.99	0.54	0.57	0.48
970.0	0.109794	109.8	243.3	269.5	233.7	237.8	236.8	255.6	257.2	0.609	0.578	0.82	0.112658	0.97	0.48	0.50	0.45
970.0	0.109794	109.8	263.3	287.5	256.4	260.1	259.5	278.0	278.7	0.609	0.578	0.77	0.115314	0.95	0.43	0.43	0.39
970.0	0.109794	109.8	281.8	306.0	275.7	280.8	280.0	297.6	296.8	0.609	0.578	0.74	0.119763	0.92	0.38	0.39	0.35

h_{man_avg}	Q_{calc}	Q [l/s]	4 m y_4	UE upstream end y_{UE}	US upstream side y_{US}	DS downstream side y_{DS}	DE downstream end y_{DE}	6 m y_6	7 m y_7	B	B-b_y	v_c = $2g(y_{UE}-y_{DS})^{2/3}$	Q_{theor2}		$Fr_{...4m}$	$Fr_{...DS}$	$Fr_{...6m}$
1372.5	0.130602	130.6	239.4	276.3	224.7	228.1	226.3	249.6	247.2	0.609	0.578	1.00	0.131481	0.99	0.58	0.63	0.55
1372.5	0.130602	130.6	255.2	288.3	244.4	247.3	246.0	276.4	273.5	0.609	0.578	0.92	0.132014	0.99	0.53	0.56	0.47
1372.5	0.130602	130.6	274.7	303.1	264.9	268.1	267.5	286.4	286.6	0.609	0.578	0.86	0.133090	0.98	0.48	0.49	0.44
1372.5	0.130602	130.6	292.7	318.6	284.4	289.1	289.0	305.6	306.8	0.609	0.578	0.79	0.132629	0.98	0.43	0.44	0.41
1372.5	0.130602	130.6	312.7	338.6	306.4	310.1	310.0	327.9	329.8	0.609	0.578	0.75	0.140035	0.93	0.39	0.40	0.36

			UE upstream	US upstream	DS downstream	DE downstream

h_{weir_avg}	Q_{calc}	Q [l/s]	4 m y_4	end y_{ue}	side y_{us}	side y_{ds}	end y_{de}	6 m y_6	7 m y_7	B	$B-b_p$	$v_0 = \sqrt{2g(y_{us}-y_{ds})}$	Q_{theory}	$C_d = Q_{calc}/Q_{theory}$	Fr_{4m}	Fr_{ds}	Fr_{6m}
1820.0	0.150393	150.4	295.8	302.9	250.2	252.8	253.3	272.5	273.0	0.609	0.578	1.02	0.148416	1.01	0.57	0.62	0.55
1820.0	0.150393	150.4	280.7	315.8	267.4	271.8	272.8	299.2	-102.1	0.609	0.578	0.96	0.150097	1.00	0.53	0.58	0.48
1820.0	0.150393	150.4	301.1	331.3	289.2	293.3	293.8	319.1	312.5	0.609	0.578	0.89	0.151081	1.00	0.48	0.50	0.44
1820.0	0.150393	150.4	320.1	348.3	311.9	314.8	314.0	333.0	336.6	0.609	0.578	0.84	0.152893	0.98	0.44	0.45	0.41
1820.0	0.150393	150.4	338.3	365.4	331.4	335.3	335.0	349.5	352.1	0.609	0.578	0.80	0.155046	0.97	0.40	0.41	0.38

h_{weir_avg}	Q_{calc}	Q [l/s]	4 m y_4	UE upstream end y_{ue}	US upstream side y_{us}	DS downstream side y_{ds}	DE downstream end y_{de}	6 m y_6	7 m y_7	B	$B-b_p$	$v_0 = \sqrt{2g(y_{us}-y_{ds})}$	Q_{theory}	$C_d = Q_{calc}/Q_{theory}$	Fr_{4m}	Fr_{ds}	Fr_{6m}
2320.0	0.169800	169.8	290.5	328.4	275.9	278.3	277.5	293.8	309.6	0.609	0.578	1.02	0.163387	1.04	0.57	0.61	0.56
2320.0	0.169800	169.8	307.0	344.5	293.2	297.8	295.8	321.7	312.8	0.609	0.578	0.98	0.169141	1.00	0.52	0.55	0.49
2320.0	0.169800	169.8	326.9	358.9	314.9	318.1	317.8	348.7	347.0	0.609	0.578	0.92	0.169538	1.00	0.48	0.50	0.43
2320.0	0.169800	169.8	346.0	379.0	336.7	340.1	340.0	360.6	356.6	0.609	0.578	0.90	0.177309	0.96	0.44	0.45	0.41
2320.0	0.169800	169.8	365.3	394.9	356.4	360.8	359.8	377.5	382.0	0.609	0.578	0.85	0.176747	0.96	0.40	0.41	0.38
														0.98			

MODEL PIER, bp = 32 mm_MEDIUM_NORMAL Q's

OK

DATA: *Friday, 4 August 2000*

Q	$h_{main,1}$	$h_{main,2}$	0 m	1 m	2 m	3 m	4 m	UE upstream end	US upstream side	DS downstream side	DE downstream end	6 m	7 m
bed level's			12.5	10.5	15.0	13.5	15.5					*147.5*	*147.0*
10	9.7	9.5	NOT MEASURABLE			57.1	56.3	56.0	34.5	22.0	17.3	190.2	192.6
30	73.5	72.5				95.1	93.5	103.5	65.0	41.3	40.0	198.8	228.3
50	204.5	202.0				122.8	119.5	135.0	89.5	69.5	67.3	230.1	260.5
70	390.0	386.5				147.6	145.5	169.0	106.5	91.3	91.3	301.4	289.5
90	650.0	660.0				170.8	166.4	195.6	126.0	113.8	114.8	301.1	307.8
110	970.0	975.0				192.9	184.2	221.0	142.8	132.5	135.3	276.5	306.0
130	1370.0	1380.0				217.7	210.2	247.5	150.8	151.3	159.3	306.3	329.7
150	1810.0	1800.0				234.7	227.0	270.0	163.5	165.0	172.8	331.0	347.2
170	2350.0	2340.0				251.0	245.7	295.0	178.3	181.3	190.5	354.6	367.5

Geometric properties:

D =	31.5 mm
L_p =	178 mm
z_A =	0 mm
z_B =	0.4 mm
z_C =	2.5 mm
z_D =	3.0 mm

CALCULATIONS:

FLOW DEPTHS

Distance measured downstream within the flume

$h_{main,avg}$	Q_{calc}	Q [l/s]	0 m y_0	1 m y_1	2 m y_2	3 m y_3	4 m y_4	UE upstream end y_{UE}	US upstream side y_{US}	DS downstream side y_{DS}	DE downstream end y_{DE}	6 m y_6	7 m y_7	B	B-b_p	v_C = $2g(y_{UE}-y_{DS})^{0.5}$	Q_{theory}	C_d = Q_{calc}/Q_{theory}	Fr_4m	Fr_DS	Fr_DE
9.6	0.010323	10.9				43.6	43.8	56.0	34.9	24.5	20.2	42.7	45.6	0.609	0.578	0.82	0.011579	0.94	0.70	1.57	1.99
73.0	0.030120	30.1				81.6	78.0	103.5	65.4	43.8	43.0	51.3	81.3	0.609	0.578	1.11	0.027954	1.08	0.73	1.82	1.77
203.3	0.050258	50.3				109.3	104.0	138.0	89.9	72.0	70.2	82.6	113.5	0.609	0.578	1.16	0.048237	1.04	0.79	1.44	1.42
393.3	0.069908	69.9				134.1	133.3	169.0	106.9	93.8	94.2	153.9	122.5	0.609	0.578	1.24	0.066904	1.04	0.78	1.35	1.27
655.0	0.090222	90.2				157.3	153.9	195.5	126.4	116.3	117.7	153.6	160.8	0.609	0.578	1.27	0.085112	1.06	0.81	1.26	1.17
972.5	0.109935	109.9				179.4	168.7	221.0	143.2	135.0	138.2	129.0	159.0	0.609	0.578	1.32	0.102779	1.07	0.83	1.22	1.12
1375.0	0.130721	130.7				204.2	194.7	247.5	151.2	153.8	162.2	158.8	192.7	0.609	0.578	1.37	0.122055	1.07	0.80	1.20	1.05
1805.0	0.149772	149.8				221.2	211.5	270.0	163.9	167.5	175.7	183.5	200.2	0.609	0.578	1.44	0.138880	1.08	0.81	1.21	1.07
2345.0	0.170712	170.7				237.5	230.2	295.0	178.7	183.8	193.5	207.1	220.5	0.609	0.578	1.49	0.158570	1.08	0.81	1.20	1.05
																		1.07			

MODEL PIER, bp = 32 mm_MEDIUM_DROWNED Q's

DATA: *Friday, 4 August 2000*

$h_{main,1}$	$h_{main,2}$	4 m	UE upstream end	US upstream side	DS downstream side	DE downstream end	6 m	7 m
		15.5					*147.5*	*147.0*
645.0	640.0	168.1	194.7	129.0	115.8	117.8	323.8	302.5
645.0	640.0	185.4	205.9	151.8	147.3	147.5	335.3	335.5
645.0	640.0	205.6	218.0	177.5	175.5	174.8	351.6	356.2
645.0	640.0	222.4	231.8	197.3	198.0	197.3	367.5	372.3
645.0	640.0	241.1	247.4	218.5	220.0	218.3	390.1	388.5

$h_{main,1}$	$h_{main,2}$	4 m	UE upstream end	US upstream side	DS downstream side	DE downstream end	6 m	7 m
		15.5					*147.5*	*147.0*
975.0	975.0	203.4	228.6	165.0	158.0	158.8	333.8	359.8
975.0	975.0	220.5	242.3	187.5	183.0	185.0	370.3	372.8
975.0	975.0	239.7	254.3	210.3	207.8	209.3	387.8	381.7
975.0	975.0	261.0	269.5	233.3	232.8	233.3	401.0	403.2
975.0	975.0	278.7	286.0	254.0	255.0	254.8	430.1	425.5

$h_{main,1}$	$h_{main,2}$	4 m	UE upstream end	US upstream side	DS downstream side	DE downstream end	6 m	7 m

		15.5					147.5	147.0
1380.0	1375.0	234.1	262.0	199.0	196.5	196.0	372.1	390.5
1380.0	1375.0	254.3	275.4	218.0	218.5	218.5	404.0	397.0
1380.0	1375.0	273.1	290.1	242.8	242.0	242.0	424.5	418.3
1380.0	1375.0	292.1	304.3	264.5	264.3	264.3	436.5	439.8
1380.0	1375.0	310.9	321.3	286.8	286.3	287.3	455.2	455.2

h_{max_1}	h_{max_2}	4 m	UE upstream end	US upstream side	DS downstream side	DE downstream end	6 m	7 m
		15.5					147.5	147.0
1810.0	1800.0	264.5	291.9	229.3	227.0	228.0	400.3	422.9
1810.0	1800.0	284.1	306.1	249.5	249.0	250.0	428.0	417.8
1810.0	1800.0	302.5	320.1	270.5	270.0	269.8	456.4	453.2
1810.0	1800.0	321.9	335.9	293.5	294.5	294.3	466.9	464.6
1810.0	1800.0	340.8	353.0	314.3	315.5	315.5	482.2	489.3

h_{max_1}	h_{max_3}	4 m	UE upstream end	US upstream side	DS downstream side	DE downstream end	6 m	7 m
		15.5					147.5	147.0
2310.0	2310.0	293.0	321.4	256.0	253.8	255.5	427.0	451.5
2310.0	2310.0	315.1	338.9	283.0	282.0	281.8	458.0	448.2
2310.0	2310.0	336.9	352.5	305.5	304.5	304.5	490.6	486.5
2310.0	2310.0	357.5	372.3	326.5	326.5	326.5	504.5	448.9
2310.0	2310.0	326.0	368.6	350.3	350.0	351.3	518.2	526.5

CALCULATIONS

FLOW DEPTHS

h_{max_avg}	Q_{calc}	Q [l/s]	4 m y_4	UE upstream end y_{UE}	US upstream side y_{US}	DS downstream side y_{DS}	DE downstream end y_{DE}	6 m y_6	7 m y_7	B	B-b_p	v_c * $2g(y_{UE}-y_{DE})^{0.5}$	Q_{theory}	[illegible]	Fr_{4m}	Fr_{DS}	Fr_{6m}
642.5	0.089357	89.4	152.6	194.7	129.4	118.3	120.7	176.3	155.5	0.609	0.578	1.24	0.089328	1.05	0.76	1.15	0.63
642.5	0.089357	89.4	165.9	205.9	152.2	149.8	150.5	187.8	188.5	0.609	0.578	1.07	0.092799	0.96	0.67	0.81	0.58
642.5	0.089357	89.4	190.1	218.0	177.9	178.0	177.7	204.1	209.2	0.609	0.578	0.91	0.093894	0.95	0.57	0.62	0.51
642.5	0.089357	89.4	206.9	231.8	197.7	200.5	200.2	220.0	225.3	0.609	0.578	0.81	0.094315	0.95	0.50	0.52	0.45
642.5	0.089357	89.4	225.6	247.4	218.9	222.5	222.2	242.8	241.5	0.609	0.578	0.73	0.094233	0.95	0.44	0.45	0.39

h_{max_avg}	Q_{calc}	Q [l/s]	4 m y_4	UE upstream end y_{UE}	US upstream side y_{US}	DS downstream side y_{DS}	DE downstream end y_{DE}	6 m y_6	7 m y_7	B	B-b_p	v_c * $2g(y_{UE}-y_{DE})^{0.5}$	Q_{theory}	[illegible]	Fr_{4m}	Fr_{DS}	Fr_{6m}
975.0	0.110077	110.1	187.9	228.6	165.4	160.5	161.7	186.3	212.8	0.609	0.578	1.18	0.109122	1.01	0.71	0.90	0.72
975.0	0.110077	110.1	205.0	242.3	187.9	185.5	188.0	222.8	225.8	0.609	0.578	1.08	0.115582	0.95	0.62	0.72	0.55
975.0	0.110077	110.1	224.2	254.3	210.7	210.3	212.2	240.1	234.7	0.609	0.578	0.96	0.116064	0.95	0.54	0.63	0.49
975.0	0.110077	110.1	245.5	269.5	233.7	235.3	236.2	253.5	256.2	0.609	0.578	0.85	0.115385	0.95	0.47	0.51	0.45
975.0	0.110077	110.1	263.2	288.0	254.4	257.5	257.7	282.6	278.5	0.609	0.578	0.78	0.115996	0.95	0.43	0.44	0.38

h_{max_avg}	Q_{calc}	Q [l/s]	4 m y_4	UE upstream end y_{UE}	US upstream side y_{US}	DS downstream side y_{DS}	DE downstream end y_{DE}	6 m y_6	7 m y_7	B	B-b_p	v_c * $2g(y_{UE}-y_{DE})^{0.5}$	Q_{theory}	[illegible]	Fr_{4m}	Fr_{DS}	Fr_{6m}
1377.5	0.133839	133.8	218.6	262.0	198.4	199.0	201.0	224.6	243.5	0.609	0.578	1.13	0.130312	1.00	0.67	0.77	0.64
1377.5	0.133839	133.8	238.8	275.4	218.4	221.0	221.5	256.5	250.0	0.609	0.578	1.06	0.134583	0.97	0.59	0.65	0.53
1377.5	0.133839	133.8	257.6	290.1	243.2	244.5	245.0	277.0	271.3	0.609	0.578	0.97	0.137186	0.95	0.52	0.57	0.47
1377.5	0.133839	133.8	276.6	304.3	264.9	266.8	267.2	289.0	282.8	0.609	0.578	0.89	0.136580	0.96	0.47	0.50	0.44
1377.5	0.133839	133.8	295.4	321.3	287.2	288.8	290.2	307.7	308.2	0.609	0.578	0.83	0.138306	0.95	0.43	0.44	0.40

			UE upstream	US upstream	DS downstream	DE downstream

h_{nor_exp}	Q_{calc}	Q [l/s]	4 m y_4	end y_{UE}	side y_{US}	side y_{DS}	end y_{DE}	6 m y_6	7 m y_7	B	$B-b_y$	$v_c = 2g(y_{UE}-y_{DE})^{0.5}$	Q_{theory}	[illegible]	Fr_{-4m}	Fr_{-DS}	Fr_{-6m}
1805.0	0.149772	149.8	249.0	291.9	229.7	229.5	231.0	252.5	275.9	0.609	0.578	1.13	0.149589	1.00	0.83	0.71	0.62
1805.0	0.149772	149.8	268.6	306.1	249.9	251.5	253.0	260.5	270.8	0.609	0.578	1.06	0.153760	0.97	0.56	0.62	0.53
1805.0	0.149772	149.8	287.0	320.1	270.9	272.5	272.7	308.9	306.2	0.609	0.578	0.99	0.156051	0.96	0.51	0.55	0.46
1805.0	0.149772	149.8	306.4	335.6	293.9	297.0	297.2	322.4	317.6	0.609	0.578	0.90	0.154907	0.97	0.46	0.48	0.43
1805.0	0.149772	149.8	325.3	353.0	314.7	318.0	318.5	334.7	342.3	0.609	0.578	0.86	0.157548	0.95	0.42	0.44	0.41

h_{nor_exp}	Q_{calc}	Q [l/s]	4 m y_4	UE upstream end y_{UE}	US upstream side y_{US}	DS downstream side y_{DS}	DE downstream end y_{DE}	6 m y_6	7 m y_7	B	$B-b_y$	$v_c = 2g(y_{UE}-y_{DE})^{0.5}$	Q_{theory}	[illegible]	Fr_{-4m}	Fr_{-DS}	Fr_{-6m}
2310.0	0.169433	169.4	277.5	321.4	256.4	256.3	258.5	279.5	304.5	0.609	0.578	1.15	0.170523	0.99	0.61	0.68	0.60
2310.0	0.169433	169.4	299.5	338.9	283.4	284.5	284.7	310.5	301.2	0.609	0.578	1.06	0.173626	0.98	0.54	0.59	0.51
2310.0	0.169433	169.4	321.4	352.6	305.9	307.0	307.5	343.1	341.5	0.609	0.578	0.97	0.172259	0.98	0.49	0.52	0.44
2310.0	0.169433	169.4	342.9	372.0	328.9	331.0	331.5	357.0	361.9	0.609	0.578	0.92	0.179920	0.96	0.44	0.47	0.42
2310.0	0.169433	169.4	360.5	388.6	350.7	352.5	354.2	370.7	379.5	0.609	0.578	0.87	0.177180	0.96	0.41	0.42	0.39
														0.97			

MODEL PIER, bp = 32 mm_LONG_NORMAL Q's

OK

DATA *Thursday, 3 August 2000*

Q	h_{man_1}	h_{man_2}	0 m	1 m	2 m	3 m	4 m	UE upstream end	US upstream side	DS downstream side	DE downstream end	6 m	7 m
bed level's			*12.5*	*10.5*	*15.0*	*13.5*	*15.5*					*147.5*	*147.0*
10	10.5	10.0	NOT MEASURABLE			58.5	57.2	57.8	35.0	23.0	13.5	192.8	192.5
30	74.0	76.0				95.9	94.4	102.5	65.5	44.8	42.5	213.6	222.2
50	205.0	200.0				123.5	120.3	136.0	91.5	73.8	65.0	224.5	240.3
70	395.0	396.0				148.4	147.0	167.2	109.3	93.3	86.0	241.1	257.8
90	660.0	665.0				173.0	169.2	197.0	131.3	118.3	112.8	257.3	292.0
110	979.0	950.0				193.9	186.2	222.0	146.0	134.8	129.5	276.7	306.9
130	1350.0	1340.0				218.0	208.8	247.1	166.5	157.0	152.8	300.5	323.5
150	1825.0	1830.0				236.8	229.2	276.5	171.0	171.5	169.8	329.9	349.6
170	2350.0	2360.0				253.5	248.2	301.0	188.3	190.3	189.5	356.5	364.5

Geometric properties:

D =	31.5 mm
L_p =	222 mm
z_A =	0 mm
z_B =	0.4 mm
z_C =	3.3 mm
z_D =	3.7 mm

CALCULATIONS

FLOW DEPTHS

h_{man_avg}	Q_{vol}	Q [l/s]	Distance measured downstream within the flume 0 m y_0	1 m y_1	2 m y_2	3 m y_3	4 m y_4	UE upstream end y_{UE}	US upstream side y_{US}	DS downstream side y_{DS}	DE downstream end y_{DE}	6 m y_6	7 m y_7	B	B-b_p	v_c = $2g(y_{US}-y_{DS})^{**}$	Q_{theory}	Q/Q_{theory}	Fr_4m	Fr_DS	Fr_DE
10.3	0.011286	11.3				45.0	41.7	57.8	35.4	26.3	17.2	45.3	45.5	0.609	0.578	0.83	0.012536	0.90	0.70	1.46	2.62
75.0	0.030530	30.5				82.4	78.9	102.5	65.9	48.0	46.2	66.1	75.2	0.609	0.578	1.06	0.029530	1.03	0.72	1.60	1.61
202.5	0.050188	50.2				110.0	104.8	136.0	91.9	74.0	68.7	77.0	93.3	0.609	0.578	1.13	0.048378	1.04	0.78	1.38	1.46
395.5	0.070108	70.1				134.9	131.5	167.2	109.7	96.5	89.7	93.6	140.8	0.609	0.578	1.20	0.067154	1.04	0.77	1.29	1.37
662.5	0.090737	90.7				159.5	153.7	197.0	131.7	121.5	116.5	109.8	145.0	0.609	0.578	1.24	0.087245	1.04	0.79	1.19	1.29
960.0	0.109227	109.2				180.4	170.7	222.0	148.4	138.0	133.2	129.2	159.9	0.609	0.578	1.31	0.104300	1.05	0.81	1.15	1.15
1345.0	0.129287	129.3				204.5	193.3	247.1	166.9	160.3	156.5	153.6	176.5	0.609	0.578	1.33	0.123091	1.05	0.80	1.11	1.10
1827.5	0.150703	150.7				223.3	213.7	276.5	171.4	174.8	173.5	182.4	202.6	0.609	0.578	1.44	0.144660	1.04	0.83	1.14	1.09
2355.0	0.171076	171.1				240.0	232.7	301.0	188.7	193.5	193.2	209.0	217.5	0.609	0.578	1.47	0.164756	1.04	0.83	1.11	1.06
																		1.04			

MODEL PIER, bp = 32 mm_LONG_DROWNED Q's

DATA *Thursday, 3 August 2000*

h_{man_1}	h_{man_2}	4 m	UE upstream end	US upstream side	DS downstream side	DE downstream end	6 m	7 m
		15.5					*147.5*	*147.0*
665.0	660.0	175.2	201.6	137.5	126.8	120.0	338.7	324.5
665.0	660.0	192.3	210.0	161.0	154.5	151.0	348.6	345.1
665.0	660.0	210.4	221.6	182.8	184.5	180.8	354.8	362.2
665.0	660.0	229.6	237.9	204.3	207.3	205.3	369.4	377.9
665.0	660.0	247.8	253.9	223.8	227.5	225.8	401.3	391.5

h_{man_1}	h_{man_2}	4 m	UE upstream end	US upstream side	DS downstream side	DE downstream end	6 m	7 m
		15.5					*147.5*	*147.0*
985.0	1000.0	207.9	234.0	172.3	167.0	160.8	338.3	357.8
985.0	1000.0	225.5	243.6	193.3	194.0	190.5	377.5	381.0
985.0	1000.0	242.3	257.8	215.5	216.5	212.8	395.5	380.5
985.0	1000.0	261.8	271.2	235.5	236.3	234.3	401.1	410.5
985.0	1000.0	276.2	283.2	252.3	255.3	252.5	419.4	424.8

h_{man_1}	h_{man_2}	4 m	UE upstream end	US upstream side	DS downstream side	DE downstream end	6 m	7 m

		15.5					**147.5**	**147.0**
1360.0	1360.0	226.9	256.7	193.3	193.0	188.0	361.7	393.8
1360.0	1360.0	248.0	271.1	215.0	213.3	212.8	391.1	382.3
1360.0	1360.0	267.5	284.0	237.8	237.5	234.5	422.6	419.2
1360.0	1360.0	284.5	298.3	257.0	260.0	256.5	433.5	425.6
1360.0	1360.0	303.9	313.3	276.5	280.0	277.5	442.3	454.1

h_{riser_1}	h_{riser_2}	4 m	UE upstream end	US upstream side	DS downstream side	DE downstream end	6 m	7 m
		15.5					**147.5**	**147.0**
1830.0	1840.0	251.8	288.6	218.8	217.0	211.0	396.3	401.5
1830.0	1840.0	273.9	301.9	239.0	239.8	238.3	407.5	420.0
1830.0	1840.0	294.5	314.8	265.8	265.5	263.0	443.3	437.2
1830.0	1840.0	313.0	330.3	287.0	288.0	286.0	468.5	461.0
1830.0	1840.0	334.3	346.3	306.3	308.8	307.5	477.1	476.3

h_{riser_1}	h_{riser_2}	4 m	UE upstream end	US upstream side	DS downstream side	DE downstream end	6 m	7 m
		15.5					**147.5**	**147.0**
2330.0	2315.0	278.9	311.7	242.8	242.8	240.5	422.7	426.3
2330.0	2315.0	300.5	326.6	269.5	268.3	264.3	435.3	458.2
2330.0	2315.0	320.3	343.8	289.8	290.8	287.3	463.8	455.3
2330.0	2315.0	340.2	357.6	312.0	313.3	311.8	494.8	494.0
2330.0	2315.0	361.5	377.5	334.3	336.8	335.0	510.8	503.2

CALCULATIONS:

FLOW DEPTHS

h_{riser_avg}	Q_{unit}	Q [l/s]	4 m y_4	UE upstream end y_{UE}	US upstream side y_{US}	DS downstream side y_{DS}	DE downstream end y_{DE}	6 m y_6	7 m y_7	B	B-b_p	v_c = $2g(y_{US}-y_{DS})^{0.5}$	Q_{theory}		Fr_{4m}	Fr_{DS}	Fr_{6m}
662.5	0.090737	90.7	159.7	201.6	137.9	130.0	123.7	181.2	177.5	0.609	0.578	1.21	0.091021	1.00	0.75	1.01	0.73
662.5	0.090737	90.7	176.8	210.0	161.4	157.8	154.7	201.1	198.1	0.609	0.578	1.04	0.095088	0.95	0.64	0.78	0.53
662.5	0.090737	90.7	194.9	221.6	183.2	187.8	184.5	207.3	215.2	0.609	0.578	0.85	0.092525	0.98	0.55	0.58	0.50
662.5	0.090737	90.7	214.1	237.9	204.7	210.5	209.0	221.9	230.9	0.609	0.578	0.78	0.094288	0.96	0.48	0.49	0.48
662.5	0.090737	90.7	232.3	253.0	224.2	230.8	229.5	253.8	244.5	0.609	0.578	0.72	0.095822	0.95	0.43	0.43	0.37

h_{riser_avg}	Q_{unit}	Q [l/s]	4 m y_4	UE upstream end y_{UE}	US upstream side y_{US}	DS downstream side y_{DS}	DE downstream end y_{DE}	6 m y_6	7 m y_7	B	B-b_p	v_c = $2g(y_{US}-y_{DS})^{0.5}$	Q_{theory}		Fr_{4m}	Fr_{DS}	Fr_{6m}
992.5	0.111060	111.1	192.4	234.0	172.7	170.3	164.5	190.8	210.8	0.609	0.578	1.15	0.112752	0.98	0.69	0.83	0.70
992.5	0.111060	111.1	210.0	243.8	193.7	197.3	194.2	230.0	234.0	0.609	0.578	0.99	0.112394	0.99	0.61	0.68	0.53
992.5	0.111060	111.1	225.8	257.8	215.9	219.8	216.5	248.0	233.5	0.609	0.578	0.90	0.114168	0.97	0.54	0.57	0.47
992.5	0.111060	111.1	245.3	271.2	235.9	239.5	238.0	253.6	263.5	0.609	0.578	0.83	0.114551	0.97	0.48	0.50	0.46
992.5	0.111060	111.1	263.7	283.2	252.7	258.5	256.5	271.9	277.8	0.609	0.578	0.74	0.110565	1.00	0.44	0.44	0.41

h_{riser_avg}	Q_{unit}	Q [l/s]	4 m y_4	UE upstream end y_{UE}	US upstream side y_{US}	DS downstream side y_{DS}	DE downstream end y_{DE}	6 m y_6	7 m y_7	B	B-b_p	v_c = $2g(y_{US}-y_{DS})^{0.5}$	Q_{theory}		Fr_{4m}	Fr_{DS}	Fr_{6m}
1360.0	0.130006	130.0	211.4	256.7	193.7	196.3	191.7	214.2	246.5	0.609	0.578	1.12	0.126726	1.03	0.70	0.78	0.69
1360.0	0.130006	130.0	232.5	271.1	215.4	216.5	216.5	243.8	235.3	0.609	0.578	1.07	0.133228	0.98	0.61	0.68	0.57
1360.0	0.130006	130.0	252.0	284.0	238.2	240.8	238.2	275.1	272.2	0.609	0.578	0.96	0.132820	0.98	0.54	0.58	0.47
1360.0	0.130006	130.0	269.9	298.3	257.4	263.3	260.2	286.0	279.6	0.609	0.578	0.87	0.131935	0.99	0.49	0.50	0.45
1360.0	0.130006	130.0	288.4	313.3	276.9	283.3	281.2	294.8	307.1	0.609	0.578	0.81	0.132237	0.98	0.44	0.45	0.43

			UE upstream	US upstream	DS downstream	DE downstream

h_{man_exp}	Q_{calc}	Q [l/s]	4 m y_4	end y_{ue}	side y_{us}	side y_{ds}	end y_{de}	6 m y_6	7 m y_7	B	B-b_p	v_c * $2g(y_{us}-y_{ds})^{2.5}$	Q_{theory}	[illegible]	Fr_{4m}	Fr_{DS}	Fr_{6m}
1835.0	0.151012	151.0	235.3	288.6	219.2	220.3	214.7	248.8	254.5	0.609	0.578	1.19	0.150782	1.00	0.69	0.77	0.54
1835.0	0.151012	151.0	258.4	301.9	239.4	243.0	242.0	260.0	273.0	0.609	0.578	1.10	0.154966	0.97	0.60	0.65	0.53
1835.0	0.151012	151.0	279.0	314.8	266.2	268.8	266.7	295.8	290.2	0.609	0.578	0.98	0.152664	0.99	0.54	0.57	0.49
1835.0	0.151012	151.0	297.5	330.3	287.4	291.3	289.7	321.0	314.0	0.609	0.578	0.91	0.153248	0.99	0.49	0.53	0.44
1835.0	0.151012	151.0	318.8	346.3	306.7	312.0	311.2	329.6	329.3	0.609	0.578	0.86	0.154673	0.98	0.44	0.45	0.42

h_{man_exp}	Q_{calc}	Q [l/s]	4 m y_4	UE upstream end y_{ue}	US upstream side y_{us}	DS downstream side y_{ds}	DE downstream end y_{de}	6 m y_6	7 m y_7	B	B-b_p	v_c * $2g(y_{us}-y_{ds})^{2.5}$	Q_{theory}	[illegible]	Fr_{4m}	Fr_{DS}	Fr_{6m}
2322.5	0.169891	169.9	263.4	311.7	243.2	246.0	244.2	275.2	278.3	0.609	0.578	1.16	0.165262	1.03	0.66	0.73	0.62
2322.5	0.169891	169.9	285.0	326.6	269.9	271.5	268.0	287.8	311.2	0.609	0.578	1.07	0.167785	1.01	0.59	0.63	0.58
2322.5	0.169891	169.9	304.8	343.8	290.2	294.0	291.0	316.3	308.3	0.609	0.578	1.02	0.173158	0.98	0.53	0.56	0.50
2322.5	0.169891	169.9	324.7	357.6	312.4	316.5	315.5	347.3	347.0	0.609	0.578	0.93	0.170520	1.00	0.48	0.50	0.44
2322.5	0.169891	169.9	346.0	377.5	334.7	340.0	338.7	363.3	356.2	0.609	0.578	0.89	0.175587	0.97	0.44	0.45	0.41
														0.98			

MODEL PIER, bp = 40 mm_SHORT_NORMAL Q's

OK

DATA: *Wednesday, 2 August 2000*

Q	h_{man_1}	h_{man_2}	0 m	1 m	2 m	3 m	4 m	UE upstream end	US upstream side	DS downstream side	DE downstream end	6 m	7 m
bed levels			12.5	10.5	15.0	13.5	15.5					147.5	147.0
10	11.5	11.5	NOT MEASURABLE			60.2	59.4	61.5	35.5	21.4	16.0	197.5	193.6
30	77.5	75.9				97.3	95.8	105.5	70.3	47.5	39.0	210.0	223.5
50	206.0	205.0				125.4	123.0	139.8	95.5	77.0	66.8	243.1	251.2
70	396.0	394.0				148.7	147.4	169.5	109.0	97.5	93.0	295.1	269.8
90	635.0	640.0				172.0	170.2	200.5	130.0	118.3	114.8	285.8	311.1
110	970.0	955.0				194.2	186.9	227.5	145.0	136.3	137.0	275.3	306.2
130	1360.0	1375.0				218.8	209.4	253.0	164.3	157.8	161.0	299.2	320.4
150	1830.0	1830.0				137.4	230.2	277.5	171.5	171.8	178.0	328.2	344.5
170	2350.0	2350.0				253.5	247.9	301.0	187.3	186.8	196.5	353.6	362.5

Geometric properties:

D =	39.5 mm
L_p =	168 mm
z_A =	0.0 mm
z_B =	0.5 mm
z_C =	2.6 mm
z_D =	3.2 mm

CALCULATIONS:

FLOW DEPTHS

Distance measured downstream within the flume

h_{man_avg}	Q_{calc}	Q [l/s]	0 m y_0	1 m y_1	2 m y_2	3 m y_3	4 m y_4	UE upstream end y_{UE}	US upstream side y_{US}	DS downstream side y_{DS}	DE downstream end y_{DE}	6 m y_6	7 m y_7	B	B-b_p	$y_C = \frac{2}{3}(y_{UE}+y_{DS})^{2/3}$	Q_{theory}	Q/Q$_{theory}$	Fr_{4m}	Fr_{DS}	Fr_{DE}
11.5	0.011955	12.0				46.7	43.9	61.5	36.4	24.0	21.2	50.0	46.6	0.609	0.569	0.89	0.012113	0.99	0.68	1.80	2.04
76.3	0.030783	30.8				83.8	80.3	105.5	71.1	50.1	42.2	62.5	76.5	0.609	0.569	1.07	0.030411	1.01	0.71	1.54	1.86
205.5	0.050536	50.5				111.9	107.5	139.8	96.4	79.6	69.9	95.6	104.2	0.609	0.569	1.31	0.050256	1.01	0.75	1.26	1.43
395.0	0.070063	70.1				135.2	131.9	169.5	109.9	100.1	96.2	147.6	122.8	0.609	0.569	1.53	0.067697	1.03	0.77	1.24	1.23
637.5	0.089009	89.0				158.5	154.7	200.5	130.9	120.9	117.9	138.3	164.1	0.609	0.569	1.27	0.087354	1.02	0.77	1.19	1.15
962.5	0.109369	109.4				180.7	171.3	227.5	145.9	138.9	140.2	127.8	159.2	0.609	0.569	1.34	0.105713	1.03	0.81	1.19	1.09
1367.5	0.130364	130.4				205.3	193.9	253.0	165.1	160.4	164.2	151.7	173.4	0.609	0.569	1.37	0.124729	1.05	0.80	1.14	1.03
1830.0	0.150806	150.8				123.9	214.7	277.5	172.4	174.4	181.2	180.7	197.5	0.609	0.569	1.44	0.142898	1.06	0.79	1.15	1.03
2350.0	0.170894	170.9				243.0	232.4	301.0	188.1	191.4	199.7	206.1	215.5	0.609	0.569	1.48	0.161579	1.06	0.80	1.15	1.00
																		1.03			

MODEL PIER, bp = 40 mm_SHORT_DROWNED Q's

DATA: *Wednesday, 2 August 2000*

h_{man_1}	h_{man_2}	4 m	UE upstream end	US upstream side	DS downstream side	DE downstream end	6 m	7 m
		15.5					147.5	147.0
660.0	650.0	180.5	203.8	143.8	136.5	136.8	319.0	312.5
660.0	650.0	198.2	215.5	168.8	163.5	162.5	349.3	341.5
660.0	650.0	217.1	224.5	189.5	186.8	185.0	359.5	362.0
660.0	650.0	233.8	240.5	210.0	208.5	208.5	393.6	380.5
660.0	650.0	250.5	254.5	229.0	228.5	228.8	397.1	397.9

h_{man_1}	h_{man_2}	4 m	UE upstream end	US upstream side	DS downstream side	DE downstream end	6 m	7 m
		15.5					147.5	147.0
980.0	965.0	213.1	232.8	174.8	173.0	168.8	348.9	348.6
980.0	965.0	227.5	245.8	195.5	192.3	188.0	377.5	375.5
980.0	965.0	246.5	259.5	216.8	214.3	213.0	393.0	390.5
980.0	965.0	262.3	268.5	234.8	234.0	234.0	405.6	405.2
980.0	965.0	279.5	286.5	255.0	254.5	253.3	425.3	426.3

h_{man_1}	h_{man_2}	4 m	UE upstream end	US upstream side	DS downstream side	DE downstream end	6 m	7 m

		15.5					147.5	147.0
1360.0	1375.0	233.9	261.0	197.3	189.0	190.0	367.8	393.0
1360.0	1375.0	252.2	274.0	216.5	215.5	212.5	397.5	390.5
1360.0	1375.0	270.2	285.3	240.5	238.0	236.0	420.1	415.5
1360.0	1375.0	289.6	302.0	262.8	263.5	260.5	434.5	437.5
1360.0	1375.0	308.9	316.8	283.3	282.0	282.8	451.2	452.6

h_{man_1}	h_{man_2}	4 m	UE upstream end	US upstream side	DS downstream side	DE downstream end	6 m	7 m
		15.5					147.5	147.0
1840.0	1860.0	259.0	292.5	220.8	220.0	221.3	395.6	417.0
1840.0	1860.0	282.3	303.8	246.5	243.5	241.5	419.2	410.2
1840.0	1860.0	300.4	316.5	267.3	264.5	266.0	448.3	444.5
1840.0	1860.0	319.9	335.5	290.0	288.5	289.3	457.0	462.2
1840.0	1860.0	337.4	350.0	310.0	309.0	308.5	481.2	479.5

h_{man_1}	h_{man_2}	4 m	UE upstream end	US upstream side	DS downstream side	DE downstream end	6 m	7 m
		15.5					147.5	147.0
2310.0	2300.0	283.5	318.0	246.6	243.0	244.0	419.6	432.8
2310.0	2300.0	302.5	327.0	266.8	265.0	264.5	439.7	453.6
2310.0	2300.0	324.5	342.5	290.5	288.0	288.5	470.8	482.5
2310.0	2300.0	340.4	361.0	311.5	310.0	311.3	489.9	489.1
2310.0	2300.0	360.0	375.8	333.3	331.5	331.0	506.1	503.2

CALCULATIONS

FLOW DEPTHS

h_{man_avg}	Q_{uds}	Q [l/s]	4 m y_4	UE upstream end y_{UE}	US upstream side y_{US}	DS downstream side y_{DS}	DE downstream end y_{DE}	6 m y_6	7 m y_7	B	B-b_2	v_C = $2g(y_{UE}-y_{DE})^{2.5}$	Q_{theory}		$Fr_{...4m}$	$Fr_{...DS}$	$Fr_{...6m}$
655.0	0.090222	90.2	165.0	203.8	144.6	139.1	139.9	171.5	165.5	0.609	0.569	1.15	0.050918	0.99	0.71	0.91	0.67
655.0	0.090222	90.2	182.7	215.5	169.6	166.1	165.7	201.8	194.5	0.609	0.569	1.01	0.055463	0.95	0.61	0.70	0.52
655.0	0.090222	90.2	201.6	224.5	190.4	189.4	188.2	212.0	215.0	0.609	0.569	0.86	0.052723	0.97	0.52	0.57	0.48
655.0	0.090222	90.2	218.3	240.5	210.9	211.1	211.7	233.1	233.5	0.609	0.569	0.79	0.055176	0.95	0.46	0.49	0.42
655.0	0.090222	90.2	235.0	254.5	229.9	231.1	231.9	249.6	250.9	0.609	0.569	0.71	0.053918	0.96	0.42	0.43	0.38

h_{man_avg}	Q_{uds}	Q [l/s]	4 m y_4	UE upstream end y_{UE}	US upstream side y_{US}	DS downstream side y_{DS}	DE downstream end y_{DE}	6 m y_6	7 m y_7	B	B-b_2	v_C = $2g(y_{UE}-y_{DE})^{2.5}$	Q_{theory}		$Fr_{...4m}$	$Fr_{...DS}$	$Fr_{...6m}$
972.5	0.108635	109.9	197.6	232.8	175.6	175.6	171.9	201.4	201.6	0.609	0.569	1.08	0.108853	1.02	0.66	0.78	0.64
972.5	0.108635	109.9	212.0	245.8	196.4	194.9	191.2	230.9	228.5	0.609	0.569	1.02	0.113590	0.97	0.59	0.67	0.52
972.5	0.108635	109.9	230.0	259.5	217.6	216.9	216.2	242.5	243.5	0.609	0.569	0.94	0.116261	0.95	0.52	0.57	0.48
972.5	0.108635	109.9	246.8	268.5	235.6	236.6	237.2	259.1	258.2	0.609	0.569	0.82	0.110761	0.99	0.47	0.50	0.44
972.5	0.108635	109.9	264.0	289.5	255.9	257.1	256.4	277.8	279.3	0.609	0.569	0.79	0.115915	0.95	0.42	0.44	0.39

h_{man_avg}	Q_{uds}	Q [l/s]	4 m y_4	UE upstream end y_{UE}	US upstream side y_{US}	DS downstream side y_{DS}	DE downstream end y_{DE}	6 m y_6	7 m y_7	B	B-b_2	v_C = $2g(y_{UE}-y_{DE})^{2.5}$	Q_{theory}		$Fr_{...4m}$	$Fr_{...DS}$	$Fr_{...6m}$
1357.5	0.130364	130.4	218.4	261.0	198.1	191.6	193.2	220.3	240.0	0.609	0.547	1.19	0.124567	1.05	0.67	0.81	0.66
1357.5	0.130364	130.4	236.7	274.0	217.4	218.1	215.7	250.0	243.5	0.609	0.547	1.07	0.127812	1.02	0.59	0.67	0.55
1357.5	0.130364	130.4	254.7	285.3	241.4	240.6	239.2	272.5	268.5	0.609	0.547	0.96	0.126757	1.03	0.53	0.58	0.48
1357.5	0.130364	130.4	274.1	302.0	263.6	263.1	263.7	287.0	290.5	0.609	0.547	0.90	0.129862	1.00	0.48	0.51	0.44
1357.5	0.130364	130.4	293.4	316.8	284.1	284.6	285.5	303.7	305.6	0.609	0.547	0.83	0.128544	1.01	0.43	0.45	0.41

			UE upstream	US upstream	DS downstream	DE downstream

h_{mean_exp}	Q_{calc}	Q [l/s]	4 m y_4	end y_{ue}	side y_{us}	side y_{ds}	end y_{de}	6 m y_6	7 m y_7	B	B-b_p	v_c = $2g(y_{us}-y_{ds})^{2/3}$	Q_{theory}		Fr_{4m}	Fr_{us}	Fr_{4m}
1850.0	0.151628	151.6	243.5	292.5	221.6	222.6	224.4	247.5	270.0	0.609	0.547	1.19	0.145222	1.04	0.66	0.76	0.65
1850.0	0.151628	151.6	266.8	303.8	247.4	246.1	244.7	271.7	272.2	0.609	0.547	1.09	0.148362	1.04	0.58	0.65	0.56
1850.0	0.151628	151.6	284.9	316.5	268.1	267.1	269.2	300.8	297.5	0.609	0.547	1.01	0.147576	1.03	0.52	0.58	0.48
1850.0	0.151628	151.6	304.4	335.5	290.9	291.1	292.4	319.5	315.2	0.609	0.547	0.96	0.152908	0.99	0.47	0.51	0.44
1850.0	0.151628	151.6	321.9	350.9	310.9	311.6	311.7	333.7	332.5	0.609	0.547	0.90	0.152872	0.99	0.44	0.46	0.41

h_{mean_exp}	Q_{calc}	Q [l/s]	4 m y_4	UE upstream end y_{ue}	US upstream side y_{us}	DS downstream side y_{ds}	DE downstream end y_{de}	6 m y_6	7 m y_7	B	B-b_p	v_c = $2g(y_{us}-y_{ds})^{2/3}$	Q_{theory}		Fr_{4m}	Fr_{us}	Fr_{4m}
2305.0	0.169253	169.2	268.0	318.0	247.6	245.6	247.2	272.1	285.8	0.609	0.547	1.21	0.162966	1.04	0.64	0.73	0.63
2305.0	0.169253	169.2	287.0	327.0	267.6	268.6	267.7	292.2	306.9	0.609	0.547	1.09	0.160735	1.05	0.58	0.64	0.56
2305.0	0.169250	169.2	309.0	342.5	291.4	293.6	291.7	323.3	315.5	0.609	0.547	1.03	0.164374	1.03	0.52	0.57	0.48
2305.0	0.169253	169.2	324.9	361.0	312.4	312.6	314.4	342.4	342.1	0.609	0.547	1.00	0.171046	0.99	0.48	0.51	0.44
2305.0	0.169250	169.2	344.5	375.8	334.1	334.1	334.2	358.6	356.3	0.609	0.547	0.93	0.170283	0.99	0.44	0.46	0.41
														1.00			

MODEL PIER, bp = 40 mm_MEDIUM_NORMAL Q's OK

DATA Wednesday, 2 August 2000

Q	h_{man_1}	h_{man_2}	0 m	1 m	2 m	3 m	4 m	UE upstream end	US upstream side	DS downstream side	DE downstream end	6 m	7 m	
bed levels			12.5	10.5	15.0	13.5	15.5					147.5	147.0	
10	9.5	9.5	NOT MEASURABLE			58.2	57.0	56.3	31.8	21.4	17.5	188.6	192.5	0.94
30	72.5	72.0				96.9	95.6	104.3	69.8	43.8	39.5	203.9	224.3	1.03
50	204.0	206.0				127.4	126.7	139.5	100.5	71.3	64.5	216.0	253.7	1.03
70	398.0	391.0				151.7	149.1	169.8	116.3	94.5	87.8	234.2	271.2	1.04
90	660.0	665.0				178.6	175.2	203.5	135.8	115.8	110.0	252.3	299.5	1.02
110	970.0	970.0				197.4	191.3	226.8	152.0	135.0	132.5	273.0	313.2	1.03
130	1375.0	1380.0				229.4	211.4	257.0	168.8	153.0	152.3	296.0	324.5	1.03
150	1800.0	1800.0				242.9	236.4	277.5	186.0	175.8	176.0	318.5	341.6	1.04
170	2300.0	2300.0				256.1	249.8	302.0	195.8	189.3	191.8	343.1	360.3	1.04

Geometric properties:

D =	39.5 mm
L_p =	222 mm
A_s =	0.0 mm
A_b =	0.6 mm
A_c =	3.2 mm
z_o =	3.7 mm

CALCULATIONS

FLOW DEPTHS

h_{man_avg}	Q_{ups}	Q [l/s]	0 m	1 m	2 m	3 m	4 m	UE upstream end	US upstream side	DS downstream side	DE downstream end	6 m	7 m	B	$B+\delta_b$	$v_c = \sqrt{2g(y_{us}-y_{ue})^{2.5}}$	Q_{theory}	$C_d = Q/Q_{theory}$	Fr_4m	Fr_DS	Fr_DE
			Distance measured downstream within the flume																		
			y_0	y_1	y_2	y_3	y_4	y_{ue}	y_{us}	y_{ds}	y_{de}	y_6	y_7								
9.5	0.010866	10.9	NOT MEASURABLE			44.7	41.5	56.3	32.3	24.6	21.2	41.3	45.5	0.609	0.569	0.83	0.011563	0.94	0.57	1.58	1.84
72.3	0.029965	30.0	NOT MEASURABLE			83.4	80.3	104.3	70.3	46.9	43.2	56.4	77.3	0.609	0.569	1.09	0.029091	1.03	0.60	1.65	1.75
205.0	0.050474	50.5				113.9	111.2	139.5	101.1	74.4	68.2	68.5	106.7	0.609	0.569	1.16	0.049005	1.03	0.71	1.39	1.48
394.5	0.070019	70.0				138.2	133.6	169.8	116.8	97.7	91.5	86.7	124.2	0.609	0.569	1.22	0.067531	1.04	0.75	1.29	1.33
662.5	0.090737	90.7				153.1	159.7	203.5	136.3	118.9	113.7	104.8	152.5	0.609	0.569	1.31	0.088790	1.02	0.75	1.24	1.24
970.0	0.109794	109.8				183.9	175.8	226.8	152.6	136.2	136.2	125.5	166.2	0.609	0.569	1.36	0.106631	1.03	0.75	1.20	1.14
1377.5	0.130839	130.8				206.9	195.9	257.0	169.3	156.2	156.0	148.5	177.5	0.609	0.569	1.43	0.126639	1.03	0.79	1.19	1.11
1800.0	0.149565	149.6				229.4	220.9	277.5	186.6	175.9	179.7	171.0	194.6	0.609	0.569	1.41	0.143848	1.04	0.76	1.11	1.03
2300.0	0.169066	169.1				242.6	234.3	302.0	196.3	192.4	195.5	195.6	213.3	0.609	0.569	1.49	0.162849	1.04	0.76	1.12	1.03
																		1.03			

MODEL PIER, bp = 40 mm_LONG_DROWNED Q's

DATA Wednesday, 2 August 2000

h_{man_1}	h_{man_2}	4 m	UE upstream end	US upstream side	DS downstream side	DE downstream end	6 m	7 m
		15.5					147.5	147.0
650.0	650.0	190.1	210.5	159.9	149.3	142.8	340.9	339.3
650.0	650.0	209.9	218.0	181.3	175.5	173.0	353.5	358.0
650.0	650.0	225.2	233.5	200.9	200.0	200.9	368.6	370.3
650.0	650.0	239.9	247.0	216.3	218.0	216.8	391.1	384.2
650.0	650.0	256.0	260.5	233.8	235.8	236.5	395.6	400.2

h_{man_1}	h_{man_2}	4 m	UE upstream end	US upstream side	DS downstream side	DE downstream end	6 m	7 m
		15.5					147.5	147.0
965.0	955.0	215.9	238.0	182.3	174.3	170.5	365.5	357.2
965.0	955.0	229.2	248.0	199.0	193.8	190.0	383.5	373.1
965.0	955.0	247.9	260.3	218.8	217.5	216.8	391.5	395.2
965.0	955.0	267.1	274.5	240.0	240.3	240.5	410.2	410.5
965.0	955.0	283.7	289.5	259.0	259.8	259.8	435.2	428.5

h_{man_1}	h_{man_2}	4 m	UE upstream end	US upstream side	DS downstream side	DE downstream end	6 m	7 m

		13.5					147.5	147.0
1360.0	1360.0	241.8	268.6	205.8	199.3	197.5	377.0	382.7
1360.0	1360.0	258.1	278.0	224.8	221.3	219.0	407.7	407.9
1360.0	1360.0	275.5	292.8	247.5	245.5	242.5	426.3	418.5
1360.0	1360.0	292.6	305.3	265.0	265.3	263.3	436.3	440.0
1360.0	1360.0	309.9	319.8	283.8	283.8	283.3	450.7	453.4

h_{man_1}	h_{man_2}	4 m	UE upstream end	US upstream side	DS downstream side	DE downstream end	6 m	7 m
		13.5					147.5	147.0
1810.0	1810.0	259.3	291.0	223.0	217.0	213.5	390.8	410.2
1810.0	1810.0	281.9	304.8	244.5	241.0	238.3	419.7	418.5
1810.0	1810.0	299.5	319.8	266.5	263.8	263.0	450.6	445.3
1810.0	1810.0	317.3	332.5	287.0	286.5	286.5	467.2	458.5
1810.0	1810.0	336.5	349.5	308.0	308.5	308.8	477.1	483.5

h_{man_1}	h_{man_2}	4 m	UE upstream end	US upstream side	DS downstream side	DE downstream end	6 m	7 m
		13.5					147.5	147.0
2310.0	2300.0	285.8	316.3	250.3	245.0	243.3	417.6	439.6
2310.0	2300.0	308.9	332.5	273.3	271.5	270.8	450.0	451.5
2310.0	2300.0	330.2	348.8	295.0	296.8	295.5	480.0	475.0
2310.0	2300.0	349.2	366.4	320.0	319.3	318.5	499.7	493.6
2310.0	2300.0	368.1	381.9	340.0	340.3	339.8	510.2	513.1

CALCULATIONS:

FLOW DEPTHS

h_{man_avg}	Q_{calc}	Q [l/s]	4 m y_4	UE upstream end y_{UE}	US upstream side y_{US}	DS downstream side y_{DS}	DE downstream end y_{DE}	6 m y_6	7 m y_7	B	B-b_p	y_c = $2g(y_{UE}-y_{DE})^{2/3}$	Q_{theory}		$Fr_{...4m}$	$Fr_{...DS}$	$Fr_{...6m}$
650.0	0.089877	89.9	174.6	210.5	159.6	152.4	145.5	193.4	192.3	0.609	0.569	1.10	0.095077	0.95	0.65	0.79	0.55
650.0	0.089877	89.9	194.4	218.0	181.8	178.7	176.7	206.0	211.0	0.609	0.569	0.91	0.092838	0.97	0.55	0.62	0.50
650.0	0.089877	89.9	209.7	233.5	200.6	203.2	203.7	221.1	223.3	0.609	0.569	0.81	0.093726	0.96	0.49	0.51	0.45
650.0	0.089877	89.9	224.4	247.0	215.8	221.2	222.5	243.6	237.2	0.609	0.569	0.75	0.094029	0.95	0.44	0.45	0.39
650.0	0.089877	89.9	240.5	260.5	234.3	238.9	240.2	248.1	253.2	0.609	0.569	0.70	0.094736	0.95	0.40	0.40	0.38

h_{man_avg}	Q_{calc}	Q [l/s]	4 m y_4	UE upstream end y_{UE}	US upstream side y_{US}	DS downstream side y_{DS}	DE downstream end y_{DE}	6 m y_6	7 m y_7	B	B-b_p	y_c = $2g(y_{UE}-y_{DE})^{2/3}$	Q_{theory}		$Fr_{...4m}$	$Fr_{...DS}$	$Fr_{...6m}$
960.0	0.109227	109.2	200.4	238.0	182.8	177.4	174.2	218.0	210.2	0.609	0.569	1.12	0.112907	0.97	0.64	0.77	0.56
960.0	0.109227	109.2	213.7	248.0	199.6	196.9	193.7	236.0	226.1	0.609	0.569	1.03	0.115602	0.94	0.58	0.66	0.50
960.0	0.109227	109.2	232.4	260.3	219.3	220.7	220.5	244.0	248.2	0.609	0.569	0.92	0.114997	0.95	0.51	0.55	0.48
960.0	0.109227	109.2	251.6	274.5	240.6	243.4	244.2	262.7	263.5	0.609	0.569	0.82	0.113543	0.96	0.45	0.48	0.43
960.0	0.109227	109.2	268.2	289.5	259.6	262.9	263.5	287.7	281.5	0.609	0.569	0.76	0.114298	0.96	0.41	0.42	0.37

h_{man_avg}	Q_{calc}	Q [l/s]	4 m y_4	UE upstream end y_{UE}	US upstream side y_{US}	DS downstream side y_{DS}	DE downstream end y_{DE}	6 m y_6	7 m y_7	B	B-b_p	y_c = $2g(y_{UE}-y_{DE})^{2/3}$	Q_{theory}		$Fr_{...4m}$	$Fr_{...DS}$	$Fr_{...6m}$
1360.0	0.130006	130.0	226.3	268.6	206.3	202.4	201.2	229.5	235.7	0.609	0.547	1.17	0.129299	1.01	0.63	0.75	0.62
1360.0	0.130006	130.0	242.6	278.0	225.3	224.4	222.7	260.2	260.9	0.609	0.547	1.06	0.129537	1.00	0.57	0.64	0.51
1360.0	0.130006	130.0	260.0	292.8	248.1	248.7	246.2	278.8	271.5	0.609	0.547	0.96	0.130970	0.99	0.51	0.55	0.46
1360.0	0.130006	130.0	277.1	305.3	265.6	268.4	267.0	288.8	293.0	0.609	0.547	0.89	0.130975	1.00	0.47	0.49	0.44
1360.0	0.130006	130.0	294.4	319.8	284.3	286.9	287.0	303.2	306.4	0.609	0.547	0.84	0.131904	0.99	0.43	0.44	0.41

				UE upstream	US upstream	DS downstream	DE downstream										

h_{max_exp}	Q_{calc}	Q [l/s]	4 m y_4	end y_{ue}	side y_{us}	side y_{ds}	end y_{de}	6 m y_6	7 m y_7	B	$B-b_y$	$v_c = \sqrt{2g(y_{us}-y_{ds})}^{0.5}$	Q_{theory}	[illegible]	Fr_{-ue}	Fr_{-ds}	Fr_{-de}
5850.0	0.149680	150.0	243.8	291.0	223.6	220.2	217.2	243.3	263.2	0.609	0.547	1.20	0.145119	1.03	0.65	0.76	0.66
5850.0	0.149680	150.0	266.4	304.8	245.1	244.2	242.0	272.2	271.5	0.609	0.547	1.12	0.146376	1.00	0.57	0.65	0.55
5850.0	0.149680	150.0	284.0	313.8	267.1	266.9	266.7	303.1	298.3	0.609	0.547	1.05	0.153046	0.98	0.52	0.57	0.47
5850.0	0.149680	150.0	301.6	332.5	287.6	289.7	290.2	319.7	311.5	0.609	0.547	0.95	0.150532	1.00	0.47	0.50	0.43
5850.0	0.149680	150.0	321.0	349.5	308.6	311.7	312.5	329.6	330.5	0.609	0.547	0.90	0.152909	0.98	0.43	0.45	0.42

h_{max_exp}	Q_{calc}	Q [l/s]	4 m y_4	UE upstream end y_{ue}	US upstream side y_{us}	DS downstream side y_{ds}	DE downstream end y_{de}	6 m y_6	7 m y_7	B	$B-b_y$	$v_c = \sqrt{2g(y_{us}-y_{ds})}^{0.5}$	Q_{theory}	[illegible]	Fr_{-ue}	Fr_{-ds}	Fr_{-de}
2305.0	0.169250	169.2	270.3	316.3	250.8	248.2	247.0	270.1	292.6	0.609	0.547	1.18	0.160506	1.05	0.63	0.72	0.63
2305.0	0.169250	169.2	293.4	332.5	273.8	274.7	274.5	302.5	304.5	0.609	0.547	1.09	0.164370	1.03	0.56	0.62	0.53
2305.0	*0.169250*	*169.2*	*314.7*	*348.8*	*298.6*	*299.9*	*299.2*	*332.5*	*328.0*	*0.609*	*0.547*	*1.01*	*0.165712*	*1.02*	*0.50*	*0.54*	*0.46*
2305.0	0.169250	169.2	333.7	366.4	320.6	322.4	322.2	352.2	346.6	0.609	0.547	0.96	0.169587	1.00	0.46	0.48	0.42
2305.0	0.169250	169.2	352.6	381.9	340.6	343.4	343.5	362.7	366.1	0.609	0.547	0.90	0.169765	1.00	0.42	0.44	0.41
														0.99			

MODEL PIER, bp = 40 mm_LONG_NORMAL Q's

OK

DATA: *Monday, 31 July 2000*

Q	h_{man_1}	h_{man_2}	0 m	1 m	2 m	3 m	4 m	UE upstream end	US upstream side	DS downstream side	DE downstream end	6 m	7 m	
bed levels			**12.5**	**10.5**	**15.0**	**13.5**	**15.5**					***147.5***	***147.0***	
10	10.5	10.0	NOT MEASURABLE			60.4	59.4	59.0	63.5	23.5	16.2	199.0	193.2	0.86
30	75.5	75.5				98.4	97.5	104.5	71.0	46.0	41.3	207.6	225.0	1.00
50	203.0	201.0				128.3	128.3	141.0	101.3	67.5	64.8	214.5	251.0	1.02
70	397.0	399.0				153.9	150.4	172.0	122.0	91.0	83.3	231.5	264.6	1.03
90	655.0	657.5				178.0	176.2	198.8	139.8	112.8	105.3	251.9	306.3	1.05
110	960.0	955.0				198.6	193.7	224.0	157.3	133.0	126.0	270.8	313.7	1.05
130	1360.0	1350.0				220.0	212.2	251.5	172.3	151.0	144.5	293.9	323.8	1.05
150	1810.0	1800.0				245.7	239.5	276.0	195.8	172.3	166.8	310.5	342.5	1.05
170	2340.0	2340.0				260.9	255.3	300.0	207.5	191.0	188.8	339.2	362.4	1.05

Geometric properties:

D =	39.5 mm
L_p =	276 mm
z_A =	0.0 mm
z_B =	0.6 mm
z_C =	4.1 mm
z_D =	4.7 mm

CALCULATIONS:

FLOW DEPTHS

h_{man_avg}	Q_{calc}	Q [l/s]	0 m y_0	1 m y_1	2 m y_2	3 m y_3	4 m y_4	UE upstream end y_{UE}	US upstream side y_{US}	DS downstream side y_{DS}	DE downstream end y_{DE}	6 m y_6	7 m y_7	B	B-b_p	v_c = $2g(y_{US}-y_{DS})^{0.5}$	Q_{meas}		Fr_4m	Fr_DS	Fr_DE
10.3	0.011266	11.3	NOT MEASURABLE			46.9	43.9	59.0	64.1	27.8	20.9	51.5	46.2	0.609	0.569	0.83	0.013115	0.86	0.64	1.38	1.96
75.5	0.030831	30.6	NOT MEASURABLE			84.9	82.0	104.5	71.6	50.1	45.9	60.1	78.0	0.609	0.569	1.07	0.030551	1.00	0.68	1.53	1.63
202.0	0.050104	50.1				114.8	112.8	141.0	101.8	71.8	69.4	67.0	104.0	0.609	0.569	1.20	0.049335	1.02	0.69	1.47	1.44
398.0	0.070329	70.3				140.4	134.9	172.0	122.6	95.1	87.9	84.0	117.6	0.609	0.569	1.28	0.069228	1.03	0.74	1.35	1.41
656.3	0.090308	90.3				164.5	160.7	198.8	140.3	116.9	109.9	104.4	159.3	0.609	0.569	1.30	0.089378	1.05	0.73	1.27	1.30
957.5	0.109084	109.1				185.1	178.2	224.0	157.8	137.1	130.7	123.3	166.7	0.609	0.569	1.34	0.104250	1.05	0.76	1.21	1.21
1355.0	0.129767	129.8				206.5	196.7	251.5	172.8	155.1	149.2	146.4	176.8	0.609	0.569	1.40	0.123938	1.05	0.78	1.16	1.18
1805.0	0.149772	149.8				232.2	224.0	276.0	196.3	176.4	171.4	163.0	195.5	0.609	0.569	1.43	0.143177	1.05	0.74	1.13	1.11
2340.0	0.17053	170.5				247.4	239.8	300.0	208.1	195.1	193.4	191.7	215.4	0.609	0.569	1.46	0.162357	1.05	0.76	1.11	1.05
																		1.04			

MODEL PIER, bp = 40 mm_LONG_DROWNED Q's

DATA: *Tuesday, 1 August 2000*

h_{man_1}	h_{man_2}	4 m	UE upstream end	US upstream side	DS downstream side	DE downstream end	6 m	7 m
		15.5					***147.5***	***147.0***
660.0	650.0	179.6	201.8	143.3	120.8	117.0	311.2	310.3
660.0	650.0	194.3	210.5	164.8	156.3	155.5	348.2	345.6
660.0	650.0	213.7	225.3	187.8	185.5	187.0	354.4	365.5
660.0	650.0	232.6	238.8	208.0	209.5	209.8	370.3	370.7
660.0	650.0	251.0	256.3	229.3	231.5	232.5	401.3	398.5

h_{man_1}	h_{man_2}	4 m	UE upstream end	US upstream side	DS downstream side	DE downstream end	6 m	7 m
		15.5					***147.5***	***147.0***
980.0	990.0	215.9	237.8	187.0	173.3	171.0	355.5	350.5
980.0	990.0	232.3	246.5	202.5	198.0	195.0	385.9	381.9
980.0	990.0	251.7	264.0	224.5	221.8	220.5	392.4	394.3
980.0	990.0	267.3	278.3	243.3	243.3	243.3	403.5	409.3
980.0	990.0	285.7	292.0	263.0	264.0	264.5	439.6	433.5

h_{man_1}	h_{man_2}	4 m	UE upstream end	US upstream side	DS downstream side	DE downstream end	6 m	7 m

		15.5					147.5	147.0
1355.0	1345.0	244.0	267.0	236.3	200.0	198.8	381.0	381.6
1355.0	1345.0	260.4	278.5	226.8	224.5	222.8	407.8	409.0
1355.0	1345.0	278.5	294.0	251.0	248.8	247.0	432.4	435.8
1355.0	1345.0	293.5	305.0	267.5	267.5	267.0	438.0	438.7
1355.0	1345.0	310.6	319.8	286.0	286.0	286.8	448.0	457.3

h_{main_1}	h_{main_2}	4 m	UE upstream end	US upstream side	DS downstream side	DE downstream end	6 m	7 m
		15.5					147.5	147.0
1830.0	1800.0	262.8	263.0	226.8	216.3	215.5	393.2	415.0
1830.0	1800.0	281.6	305.0	248.3	246.0	242.5	417.5	417.8
1830.0	1800.0	304.4	322.5	273.8	273.5	270.8	453.5	457.8
1830.0	1800.0	327.2	343.0	300.5	300.5	299.0	477.3	466.8
1830.0	1800.0	348.0	359.0	321.8	322.6	322.0	485.6	497.3

h_{main_1}	h_{main_2}	4 m	UE upstream end	US upstream side	DS downstream side	DE downstream end	6 m	7 m
		15.5					147.5	147.0
2305.0	2300.0	256.6	325.3	264.3	256.0	256.5	431.7	451.3
2305.0	2300.0	316.6	338.8	283.0	280.8	279.3	452.6	453.3
2305.0	2300.0	336.4	353.3	305.0	303.0	301.0	484.2	479.4
2305.0	2300.0	352.6	369.5	325.8	325.5	323.5	505.6	496.3
2305.0	2300.0	375.8	389.8	350.3	350.8	350.0	516.5	529.2

CALCULATIONS

FLOW DEPTHS

h_{main_avg}	Q_{uns}	Q [l/s]	4 m y_4	UE upstream end y_{ue}	US upstream side y_{us}	DS downstream side y_{ds}	DE downstream end y_{de}	6 m y_6	7 m y_7	B	B-b_y	v_c = $\sqrt{2g(y_{ue}-y_{ds})^{4/3}}$	Q_{theory}	[redacted]	$Fr_{...ue}$	$Fr_{...ds}$	$Fr_{...us}$
655.0	0.090222	90.2	164.1	201.8	143.5	124.9	121.7	163.7	172.3	0.609	0.569	1.26	0.090668	1.01	0.71	1.07	0.71
655.0	0.090222	90.2	178.8	210.5	165.3	160.4	160.2	200.7	198.6	0.609	0.569	1.03	0.094141	0.96	0.63	0.74	0.53
655.0	0.090222	90.2	198.2	225.3	188.3	189.6	191.7	206.9	218.5	0.609	0.569	0.88	0.095281	0.95	0.54	0.57	0.50
655.0	0.090222	90.2	217.1	238.8	208.6	213.6	214.4	222.8	232.7	0.609	0.569	0.76	0.092079	0.98	0.47	0.48	0.45
655.0	0.090222	90.2	235.5	256.3	226.8	235.6	237.2	253.8	251.5	0.609	0.569	0.70	0.093424	0.97	0.41	0.41	0.37

h_{main_avg}	Q_{uns}	Q [l/s]	4 m y_4	UE upstream end y_{ue}	US upstream side y_{us}	DS downstream side y_{ds}	DE downstream end y_{de}	6 m y_6	7 m y_7	B	B-b_y	v_c = $\sqrt{2g(y_{ue}-y_{ds})^{4/3}}$	Q_{theory}	[redacted]	$Fr_{...ue}$	$Fr_{...ds}$	$Fr_{...us}$
685.0	0.110643	110.6	200.4	237.8	187.6	177.4	175.7	208.0	203.5	0.609	0.569	1.12	0.113531	0.97	0.65	0.78	0.61
685.0	0.110643	110.6	216.8	246.5	203.1	202.1	199.7	238.4	234.9	0.609	0.569	0.98	0.112185	0.99	0.57	0.64	0.50
685.0	0.110643	110.6	236.2	264.0	225.1	225.9	225.2	244.9	247.3	0.609	0.569	0.91	0.117012	0.95	0.51	0.54	0.48
685.0	0.110643	110.6	251.8	276.3	243.8	247.4	247.5	256.9	262.3	0.609	0.569	0.80	0.113256	0.98	0.46	0.47	0.45
685.0	0.110643	110.6	270.2	292.0	263.6	268.1	268.2	292.1	286.5	0.609	0.569	0.74	0.113075	0.98	0.41	0.42	0.37

h_{main_avg}	Q_{uns}	Q [l/s]	4 m y_4	UE upstream end y_{ue}	US upstream side y_{us}	DS downstream side y_{ds}	DE downstream end y_{de}	6 m y_6	7 m y_7	B	B-b_y	v_c = $\sqrt{2g(y_{ue}-y_{ds})^{4/3}}$	Q_{theory}	[redacted]	$Fr_{...ue}$	$Fr_{...ds}$	$Fr_{...us}$
1350.0	0.126527	129.5	228.5	267.0	208.8	204.1	203.4	233.5	234.6	0.609	0.547	1.15	0.128913	1.01	0.62	0.74	0.60
1350.0	0.126527	129.5	244.6	278.5	227.3	228.8	227.4	260.3	262.0	0.609	0.547	1.03	0.128719	1.01	0.56	0.62	0.51
1350.0	0.126527	129.5	264.0	294.0	251.6	252.9	251.7	264.9	271.8	0.609	0.547	0.94	0.130328	0.99	0.50	0.53	0.45
1350.0	0.126527	129.5	278.0	305.0	268.1	271.6	271.7	290.5	291.7	0.609	0.547	0.86	0.127441	1.02	0.46	0.48	0.43
1350.0	0.126527	129.5	295.1	319.8	286.6	292.1	291.4	300.5	310.3	0.609	0.547	0.79	0.126115	1.03	0.42	0.43	0.41

			UE upstream	US upstream	DS downstream	DE downstream

h_{mer_avg}	Q_{vol}	Q [l/s]	4 m y_4	end y_{US}	side y_{US}	side y_{DS}	end y_{DE}	6 m y_6	7 m y_7	B	B-b_y	v_c = $2g'(y_{US}-y_{DS})^{1.5}$	Q_{theory}	[redacted]	Fr_{-4m}	Fr_{-US}	Fr_{-DS}
1815.0	0.150187	150.2	247.3	293.0	227.3	223.4	220.2	245.7	268.0	0.609	0.547	1.20	0.149973	1.02	0.64	0.75	0.65
1815.0	0.150187	150.2	266.1	305.0	248.8	250.1	247.2	270.0	270.5	0.609	0.547	1.08	0.147200	1.02	0.57	0.63	0.56
1815.0	0.150187	150.2	288.9	322.5	274.3	277.6	275.4	306.0	310.5	0.609	0.547	0.98	0.148895	1.01	0.51	0.54	0.47
1815.0	0.150187	150.2	311.7	343.0	301.1	304.6	303.7	329.8	310.5	0.609	0.547	0.91	0.152155	0.99	0.45	0.47	0.42
1815.0	0.150187	150.2	332.5	359.0	322.3	326.9	326.7	338.3	350.3	0.609	0.547	0.84	0.150786	1.00	0.41	0.42	0.40

h_{mer_avg}	Q_{vol}	Q [l/s]	4 m y_4	UE upstream end y_{US}	US upstream side y_{US}	DS downstream side y_{DS}	DE downstream end y_{DE}	6 m y_6	7 m y_7	B	B-b_y	v_c = $2g'(y_{US}-y_{DS})^{1.5}$	Q_{theory}	[redacted]	Fr_{-4m}	Fr_{-US}	Fr_{-DS}
2302.5	0.169158	169.2	283.3	325.3	264.8	262.1	261.2	284.2	304.3	0.609	0.547	1.15	0.164994	1.03	0.59	0.69	0.59
2302.5	0.169158	169.2	304.1	338.8	283.6	284.9	283.9	305.1	306.3	0.609	0.547	1.07	0.166224	1.02	0.54	0.58	0.53
2302.5	0.169158	169.2	326.9	353.3	305.6	307.1	305.7	326.7	332.4	0.609	0.547	0.99	0.166805	1.01	0.49	0.52	0.46
2302.5	0.169158	169.2	337.1	369.5	326.3	329.6	328.2	358.3	349.3	0.609	0.547	0.93	0.167523	1.01	0.45	0.47	0.41
2302.5	0.169158	169.2	360.3	389.8	350.5	354.9	354.7	369.0	373.2	0.609	0.547	0.87	0.169799	1.00	0.41	0.42	0.40
														0.99			

MODEL PIER, bp = 49 mm_SHORT_NORMAL Q's

OK

DATA *Monday, 30 July 2000*

Q	h_{man_1}	h_{man_2}	0 m	1 m	2 m	3 m	4 m	UE upstream end	US upstream side	DS downstream side	DE downstream end	6 m	7 m
bed levels			12.5	10.5	15.0	13.5	15.5					147.5	147.0
10	8.5	8.0	NOT MEASURABLE			55.9	55.2	54.5	23.6	21.3	16.0	184.6	189.7
30	73.0	73.5				99.7	98.2	105.0	72.0	47.8	37.0	195.0	232.5
50	200.0	200.5				130.7	129.4	141.5	101.3	75.0	60.3	208.8	254.3
70	397.5	395.0				155.9	153.1	174.0	123.3	101.0	84.8	229.6	253.8
90	655.0	660.0				180.8	178.5	202.0	142.3	124.3	112.5	249.7	307.6
110	970.0	973.0				201.9	197.5	226.5	159.3	144.8	135.5	269.2	321.5
130	1350.0	1350.0				220.9	214.2	251.3	173.0	161.5	155.8	290.4	325.8
150	1840.0	1830.0				247.5	240.2	278.0	196.0	182.5	178.3	307.9	342.0
170	2340.0	2350.0				263.4	257.1	301.8	207.3	200.0	200.0	334.1	361.1

Geometric properties:

D =	49 mm
L_p =	205 mm
z_A =	0 mm
z_B =	0.7 mm
z_C =	2.8 mm
z_D =	3.5 mm

CALCULATIONS

			FLOW DEPTHS																	
			Distance measured downstream within the flume					UE upstream end	US upstream side	DS downstream side	DE downstream end									
h_{man_avg}	Q_{calc}	Q [l/s]	0 m y_0	1 m y_1	2 m y_2	3 m y_3	4 m y_4	y_{ue}	y_{us}	y_{ds}	y_{de}	6 m y_6	7 m y_7	B	B-b_p	v_c = $2g(y_{us}-y_{ds})^{0.5}$	Q_{theory}		Fr_4m	Fr_DS	Fr_DE
8.3	0.003126	10.1				42.4	39.7	54.5	24.4	24.1	19.5	37.1	42.7	0.609	0.560	0.81	0.010882	0.93	0.67	1.55	1.95
73.3	0.030171	30.2				86.2	83.7	105.0	72.7	50.6	40.5	47.5	85.5	0.609	0.560	1.06	0.030007	1.01	0.65	1.51	1.94
200.3	0.049388	49.9				117.2	113.9	141.5	101.9	78.8	63.7	61.3	107.3	0.609	0.560	1.13	0.050030	1.00	0.68	1.29	1.63
398.3	0.070174	70.2				142.4	137.8	174.0	123.9	103.8	88.2	82.1	106.8	0.609	0.560	1.20	0.069572	1.01	0.72	1.20	1.40
657.5	0.090394	90.4				167.3	163.0	202.0	142.9	127.1	116.9	102.2	160.6	0.609	0.560	1.24	0.087880	1.03	0.72	1.14	1.20
970.0	0.109794	109.8				188.4	182.0	226.5	159.9	147.6	139.0	121.7	174.5	0.609	0.560	1.27	0.104651	1.05	0.74	1.10	1.11
1350.0	0.129527	129.5				207.4	198.7	251.3	173.7	164.3	159.2	142.9	178.8	0.609	0.560	1.33	0.122100	1.06	0.77	1.11	1.07
1835.0	0.151912	151.9				234.0	224.7	278.0	195.7	185.3	181.7	160.4	185.0	0.609	0.560	1.37	0.142048	1.06	0.74	1.08	1.02
2345.9	0.170712	170.7				249.9	241.8	301.8	207.9	202.8	203.5	188.6	214.1	0.609	0.560	1.41	0.160480	1.06	0.75	1.07	0.97
																		1.03			

MODEL PIER, bp = 49 mm_MEDIUM_DROWNED Q's

DATA *Monday, 30 July 2000*

h_{man_1}	h_{man_2}	4 m	UE upstream end	US upstream side	DS downstream side	DE downstream end	6 m	7 m
		15.5					147.5	147.0
655.0	640.0	183.6	205.0	147.3	132.8	122.5	316.5	317.3
655.0	640.0	201.2	215.0	172.5	155.0	158.5	342.2	346.0
655.0	640.0	216.9	227.0	190.0	187.0	185.5	359.2	362.6
655.0	640.0	234.2	240.5	211.5	219.3	210.0	383.6	380.5
655.0	640.0	251.9	256.3	230.3	230.6	229.0	395.4	398.7

h_{man_1}	h_{man_2}	4 m	UE upstream end	US upstream side	DS downstream side	DE downstream end	6 m	7 m
		15.5					147.5	147.0
975.0	970.0	221.8	241.3	187.0	178.5	160.5	364.8	362.3
975.0	970.0	233.8	248.5	203.5	198.5	181.5	383.6	377.0
975.0	970.0	251.1	262.0	224.5	220.3	217.3	394.5	397.5
975.0	970.0	268.2	276.8	243.3	241.5	240.0	403.9	414.5
975.0	970.0	284.5	288.5	261.3	263.8	258.5	433.2	430.2

h_{man_1}	h_{man_2}	4 m	UE upstream end	US upstream side	DS downstream side	DE downstream end	6 m	7 m

		f3.5					f47.5	f47.0
1385.0	1380.0	244.2	266.0	206.0	199.0	194.5	384.0	382.1
1385.0	1380.0	260.1	278.3	228.5	224.3	217.5	405.5	402.1
1385.0	1380.0	277.5	292.3	249.5	245.8	241.5	425.0	422.8
1385.0	1380.0	295.4	305.8	269.5	266.8	264.0	439.1	441.5
1385.0	1380.0	314.0	322.0	288.3	287.0	285.3	457.5	456.5

h_{man_1}	h_{man_2}	4 m	UE upstream end	US upstream side	DS downstream side	DE downstream end	6 m	7 m
		f3.5					f47.5	f47.0
1640.0	1615.0	271.5	297.3	235.8	229.5	226.0	415.1	419.9
1640.0	1615.0	287.2	309.3	253.0	249.0	244.0	432.3	427.3
1640.0	1615.0	305.6	323.0	276.3	273.0	269.0	455.5	451.8
1640.0	1615.0	324.0	338.0	297.0	295.5	292.8	469.8	469.8
1640.0	1615.0	343.6	353.0	319.5	315.0	312.5	487.8	488.2

h_{man_1}	h_{man_2}	4 m	UE upstream end	US upstream side	DS downstream side	DE downstream end	6 m	7 m
		f3.5					f47.5	f47.0
2310.0	2320.0	298.0	324.5	269.0	255.8	252.0	432.8	448.0
2310.0	2320.0	314.5	336.0	279.8	276.0	271.3	456.2	454.5
2310.0	2320.0	333.5	354.0	302.3	299.0	296.0	483.0	477.8
2310.0	2320.0	351.1	367.5	323.3	320.8	318.0	497.7	496.5
2310.0	2320.0	369.5	383.8	341.8	340.8	338.8	513.4	513.2

CALCULATIONS

FLOW DEPTHS

h_{man_avg}	Q_{calc}	Q [l/s]	4 m y_4	UE upstream end y_{UE}	US upstream side y_{US}	DS downstream side y_{DS}	DE downstream end y_{DE}	6 m y_6	7 m y_7	B	B-b_y	v_c = $2g(y_{UE}-y_{DS})^{0.5}$	Q_{theory}	[illegible]	$Fr_{...4m}$	$Fr_{...DS}$	$Fr_{...6m}$
647.5	0.089704	89.7	165.3	205.0	147.9	135.6	126.0	169.0	170.3	0.609	0.560	1.19	0.093382	0.99	0.68	0.94	0.68
647.5	0.089704	89.7	185.7	215.0	173.2	167.8	162.0	199.7	199.0	0.609	0.560	0.99	0.093078	0.96	0.59	0.68	0.53
647.5	0.089704	89.7	201.4	227.0	190.7	189.8	189.0	212.7	215.6	0.609	0.560	0.89	0.094164	0.95	0.52	0.57	0.48
647.5	0.089704	89.7	218.7	240.5	212.2	213.1	213.5	236.1	233.5	0.609	0.560	0.77	0.091918	0.96	0.46	0.48	0.41
647.5	0.089704	89.7	235.4	256.3	230.9	232.8	232.5	247.9	251.7	0.609	0.560	0.72	0.093562	0.96	0.41	0.42	0.38

h_{man_avg}	Q_{calc}	Q [l/s]	4 m y_4	UE upstream end y_{UE}	US upstream side y_{US}	DS downstream side y_{DS}	DE downstream end y_{DE}	6 m y_6	7 m y_7	B	B-b_y	v_c = $2g(y_{UE}-y_{DS})^{0.5}$	Q_{theory}	[illegible]	$Fr_{...4m}$	$Fr_{...DS}$	$Fr_{...6m}$
972.5	0.109935	109.9	206.3	241.3	187.7	181.3	173.0	217.3	215.3	0.639	0.590	1.11	0.112658	0.98	0.62	0.75	0.57
972.5	0.109935	109.9	218.3	248.5	204.2	201.3	195.0	235.1	230.0	0.639	0.590	0.99	0.111657	0.98	0.57	0.64	0.50
972.5	0.109935	109.9	235.6	262.0	225.2	223.1	220.7	247.0	250.5	0.639	0.590	0.91	0.113054	0.97	0.50	0.55	0.47
972.5	0.109935	109.9	252.7	276.8	243.6	244.3	243.5	256.4	267.5	0.639	0.590	0.83	0.113777	0.97	0.45	0.48	0.44
972.5	0.109935	109.9	269.0	288.5	261.9	263.6	262.0	285.7	283.2	0.639	0.590	0.74	0.108905	1.01	0.41	0.43	0.38

h_{man_avg}	Q_{calc}	Q [l/s]	4 m y_4	UE upstream end y_{UE}	US upstream side y_{US}	DS downstream side y_{DS}	DE downstream end y_{DE}	6 m y_6	7 m y_7	B	B-b_y	v_c = $2g(y_{UE}-y_{DS})^{0.5}$	Q_{theory}	[illegible]	$Fr_{...4m}$	$Fr_{...DS}$	$Fr_{...6m}$
1382.5	0.131077	131.1	228.7	269.0	206.7	201.5	198.0	236.5	235.1	0.609	0.560	1.17	0.132442	0.99	0.63	0.76	0.60
1382.5	0.131077	131.1	244.6	278.3	229.2	227.1	221.0	258.0	255.1	0.609	0.560	1.03	0.130880	1.00	0.57	0.64	0.52
1382.5	0.131077	131.1	262.0	292.3	249.2	248.6	245.0	277.5	275.8	0.609	0.560	0.96	0.132951	0.99	0.51	0.55	0.47
1382.5	0.131077	131.1	279.9	305.8	270.2	269.6	267.5	291.6	294.8	0.609	0.560	0.87	0.132045	0.99	0.46	0.49	0.44
1382.5	0.131077	131.1	298.5	322.0	288.9	289.6	288.7	310.0	311.5	0.609	0.560	0.83	0.134488	0.97	0.42	0.44	0.40

			UE upstream	US upstream	DS downstream	DE downstream

h_{mean_avg}	Q_{calc}	Q [l/s]	4 m y_4	end y_{US}	side y_{DS}	side y_{DE}	end y_{UE}	6 m y_6	7 m y_7	B	B-b_p	v_C = $2g(y_{UE}-y_{DE})^{1/2}$	Q_{theory}	[illegible]	Fr_{-4m}	Fr_{-DS}	Fr_{-6m}
1827.5	0.150703	150.7	258.0	297.3	238.4	232.3	229.5	267.6	272.9	0.609	0.560	1.15	0.349689	1.00	0.67	0.71	0.57
1827.5	0.150703	150.7	271.7	309.3	253.7	251.8	247.5	284.8	280.3	0.609	0.560	1.09	0.153316	0.98	0.56	0.63	0.52
1827.5	0.150703	150.7	290.1	323.0	276.9	275.8	272.5	308.0	304.8	0.609	0.560	0.99	0.152978	0.99	0.51	0.55	0.48
1827.5	0.150703	150.7	308.5	338.0	297.7	298.3	296.2	322.3	322.8	0.609	0.560	0.91	0.152545	0.99	0.46	0.48	0.43
1827.5	0.150703	150.7	328.1	353.0	317.2	317.8	316.0	343.3	341.2	0.609	0.560	0.85	0.153572	0.98	0.42	0.44	0.40

h_{mean_avg}	Q_{calc}	Q [l/s]	4 m y_4	UE upstream end y_{UE}	US upstream side y_{US}	DS downstream side y_{DS}	DE downstream end y_{DE}	6 m y_6	7 m y_7	B	B-b_p	v_C = $2g(y_{UE}-y_{DE})^{1/2}$	Q_{theory}	[illegible]	Fr_{-4m}	Fr_{-DS}	Fr_{-6m}
2315.0	0.169617	169.6	282.5	324.5	260.7	258.6	255.5	285.3	301.0	0.609	0.560	1.10	0.168164	1.01	0.59	0.65	0.56
2315.0	0.169617	169.6	299.0	336.0	280.4	278.8	274.7	308.7	307.5	0.609	0.560	1.06	0.169402	1.00	0.54	0.60	0.52
2315.0	0.169617	169.6	318.0	354.0	302.9	301.8	299.5	335.5	330.8	0.609	0.560	1.04	0.175570	0.97	0.50	0.54	0.48
2315.0	0.169617	169.6	335.6	367.5	323.9	323.6	321.5	350.2	349.5	0.609	0.560	0.96	0.173533	0.98	0.46	0.48	0.43
2315.0	0.169617	169.6	354.0	383.8	342.4	343.6	342.2	365.9	366.2	0.609	0.560	0.92	0.176715	0.96	0.42	0.44	0.40
														0.98			

MODEL PIER, bp = 49 mm_MEDIUM_NORMAL Q's

OK

DATA: *Friday, 28 July 2000*

Q	h_{man_1}	h_{man_2}	0 m	1 m	2 m	3 m	4 m	UE upstream end	US upstream side	DS downstream side	DE downstream end	6 m	7 m
bed levels			*12.5*	*10.5*	*13.0*	*12.5*	*15.5*					*147.5*	*147.0*
10	10.5	10.0	NOT MEASURABLE			60.8	60.3	60.0	32.0	24.6	15.3	195.5	192.7
30	72.5	72.5				100.0	99.5	105.0	73.3	45.0	38.0	199.2	221.5
50	201.0	199.0				132.1	130.8	142.5	104.3	67.0	60.3	210.0	226.5
70	391.0	390.0				156.6	155.2	173.5	127.0	90.0	82.5	227.5	259.4
90	650.0	650.0				182.8	181.2	203.8	147.5	113.0	104.8	246.9	319.2
110	975.0	960.0				205.8	204.5	233.0	167.8	134.0	126.5	267.2	323.5
130	1360.0	1360.0				225.3	221.5	253.5	184.3	150.0	146.3	289.0	327.2
150	1800.0	1810.0				248.3	240.6	279.0	198.8	170.5	166.0	304.8	351.7
170	2350.0	2370.0				270.0	265.5	299.5	219.3	192.8	191.3	321.3	372.3

Geometric properties:

D =	49 mm
L_p =	278 mm
z_A =	0 mm
z_B =	0.7 mm
z_C =	4.0 mm
z_D =	4.7 mm

CALCULATIONS:

FLOW DEPTHS

h_{man_avg}	Q_{calc}	Q [l/s]	Distance measured downstream within the flume: 0 m y_0	1 m y_1	2 m y_2	3 m y_3	4 m y_4	UE upstream end y_{UE}	US upstream side y_{US}	DS downstream side y_{DS}	DE downstream end y_{DE}	6 m y_6	7 m y_7	B	$B-b_p$	$y_C = 2g(h_{up}-y_{DS})^{2/3}$	Q_{theory}	$C_d = Q_{calc}/Q_{theory}$	Fr_4m	Fr_DS	Fr_DE
10.3	0.011286	11.3				47.3	44.8	60.0	32.7	28.0	19.9	48.0	45.7	0.609	0.560	0.84	0.013171	0.86	0.62	1.37	2.10
72.5	0.030017	30.0				88.5	84.0	105.0	73.9	49.0	42.7	42.7	74.5	0.609	0.560	1.08	0.029763	1.01	0.65	1.58	1.79
230.0	0.049855	49.9				118.6	115.3	142.5	104.9	71.0	64.9	62.5	79.5	0.609	0.560	1.22	0.048381	1.03	0.67	1.50	1.58
390.5	0.069663	69.7				143.1	139.7	173.5	127.7	94.0	87.2	80.0	112.4	0.609	0.560	1.28	0.067365	1.03	0.70	1.38	1.42
650.0	0.089877	89.9				169.3	165.7	203.8	148.2	117.0	109.4	99.4	172.2	0.609	0.560	1.33	0.087418	1.03	0.70	1.28	1.30
967.5	0.109653	109.7				192.3	189.0	233.0	168.4	138.0	131.2	119.7	176.5	0.609	0.560	1.39	0.107692	1.02	0.70	1.22	1.21
1360.0	0.133006	130.0				211.8	208.0	253.5	184.9	154.0	152.9	138.5	183.2	0.609	0.560	1.43	0.122881	1.06	0.73	1.23	1.14
1805.0	0.149772	149.8				234.8	225.1	279.0	199.4	174.5	170.7	157.3	204.7	0.609	0.560	1.46	0.142564	1.05	0.74	1.17	1.11
2360.0	0.171257	171.3				257.4	250.0	299.5	219.9	196.7	195.9	173.8	225.3	0.609	0.560	1.45	0.159442	1.07	0.72	1.12	1.04
																		1.04			

MODEL PIER, bp = 49 mm_MEDIUM_DROWNED Q's

DATA: *Saturday, 29 July 2000*

h_{man_1}	h_{man_2}	4 m	UE upstream end	US upstream side	DS downstream side	DE downstream end	6 m	7 m
		15.5					*147.5*	*147.0*
655.0	640.0	190.2	210.8	158.3	135.0	130.3	330.5	329.3
655.0	640.0	209.0	221.8	180.0	173.3	174.0	351.5	347.2
655.0	640.0	225.4	233.0	199.5	198.8	200.5	365.8	358.5
655.0	640.0	242.9	248.5	220.5	221.8	221.5	395.1	388.9
655.0	640.0	261.8	263.5	240.3	242.5	242.5	409.1	408.7

h_{man_1}	h_{man_2}	4 m	UE upstream end	US upstream side	DS downstream side	DE downstream end	6 m	7 m
		15.5					*147.5*	*147.0*
950.0	970.0	228.9	242.5	195.3	181.0	175.5	376.5	373.2
950.0	970.0	239.4	255.5	212.5	206.5	204.5	390.0	382.6
950.0	970.0	258.4	267.0	233.3	230.5	229.8	397.6	407.0
950.0	970.0	277.4	284.5	253.3	253.5	253.5	415.5	420.9
950.0	970.0	295.5	299.5	274.0	274.8	274.5	443.1	439.1

h_{man_1}	h_{man_2}	4 m	UE upstream end	US upstream side	DS downstream side	DE downstream end	6 m	7 m

		15.5					147.5	147.0
1350.0	1350.0	263.2	282.5	232.5	222.8	220.5	412.2	406.6
1350.0	1350.0	277.7	293.5	246.5	244.5	242.5	426.3	421.7
1350.0	1350.0	296.1	307.0	270.5	268.8	267.5	437.2	442.1
1350.0	1350.0	314.9	324.0	296.5	293.5	288.5	451.7	456.2
1350.0	1350.0	333.0	340.0	311.0	311.0	311.0	483.4	481.2

h_{nom_1}	h_{nom_2}	4 m	UE upstream end	US upstream side	DS downstream side	DE downstream end	6 m	7 m
		15.5					147.5	147.0
1830.0	1830.0	291.5	312.8	259.0	250.5	246.5	430.8	431.0
1830.0	1830.0	307.5	323.5	276.3	271.0	270.0	456.8	453.2
1830.0	1830.0	324.5	339.5	298.0	295.5	293.3	473.2	465.5
1830.0	1830.0	344.3	357.9	319.0	317.5	317.5	484.8	492.0
1830.0	1830.0	362.6	371.5	338.5	338.3	338.0	501.5	502.8

h_{nom_1}	h_{nom_2}	4 m	UE upstream end	US upstream side	DS downstream side	DE downstream end	6 m	7 m
		15.5					147.5	147.0
2310.0	2310.0	322.0	346.3	291.0	284.8	281.0	466.9	463.3
2310.0	2310.0	337.9	356.3	308.0	303.0	300.0	486.5	482.5
2310.0	2310.0	356.6	371.5	329.5	326.0	323.5	503.6	496.5
2310.0	2310.0	374.5	389.0	349.0	347.3	345.5	516.6	520.5
2310.0	2310.0	392.5	403.8	369.0	368.0	366.0	529.0	537.9

CALCULATIONS

FLOW DEPTHS

h_{nom_avg}	Q_{calc}	Q [l/s]	4 m y_4	UE upstream end y_{UE}	US upstream side y_{US}	DS downstream side y_{DS}	DE downstream end y_{DE}	6 m y_6	7 m y_7	B	B-b_p	v_c = $2g(y_{UE}-y_{DS})^{0.5}$	Q_{theory}		Fr_{4m}	Fr_{US}	Fr_{6m}
647.5	0.089704	89.7	174.7	253.8	158.9	139.0	134.9	183.0	182.3	0.609	0.560	1.22	0.094884	0.95	0.64	0.91	0.60
647.5	0.089704	89.7	193.5	221.8	180.7	177.2	176.7	204.0	200.2	0.609	0.560	0.98	0.096818	0.93	0.55	0.63	0.51
647.5	0.089704	89.7	209.9	233.0	200.2	202.7	205.2	218.3	221.5	0.609	0.560	0.82	0.093067	0.96	0.49	0.52	0.46
647.5	0.089704	89.7	227.4	248.5	221.2	225.7	226.2	247.6	241.9	0.609	0.560	0.72	0.091570	0.98	0.43	0.44	0.38
647.5	0.089704	89.7	246.3	263.5	240.9	246.5	247.2	261.6	261.7	0.609	0.560	0.64	0.088801	1.01	0.38	0.38	0.35

h_{nom_avg}	Q_{calc}	Q [l/s]	4 m y_4	UE upstream end y_{UE}	US upstream side y_{US}	DS downstream side y_{DS}	DE downstream end y_{DE}	6 m y_6	7 m y_7	B	B-b_p	v_c = $2g(y_{UE}-y_{DS})^{0.5}$	Q_{theory}		Fr_{4m}	Fr_{US}	Fr_{6m}
960.0	0.109227	109.2	211.4	242.5	195.9	185.0	183.2	229.0	226.2	0.609	0.560	1.10	0.113792	0.96	0.56	0.72	0.52
960.0	0.109227	109.2	223.9	255.5	213.2	210.5	209.2	242.5	235.6	0.609	0.560	0.98	0.115573	0.95	0.54	0.58	0.48
960.0	0.109227	109.2	242.9	267.0	233.9	234.5	234.4	250.1	250.0	0.609	0.560	0.85	0.111121	0.98	0.48	0.50	0.46
960.0	0.109227	109.2	261.9	284.5	253.9	257.5	258.2	272.0	273.9	0.609	0.560	0.78	0.112453	0.97	0.43	0.44	0.40
960.0	0.109227	109.2	280.0	299.5	274.7	278.7	279.2	295.6	292.1	0.609	0.560	0.70	0.108772	1.00	0.39	0.39	0.36

h_{nom_avg}	Q_{calc}	Q [l/s]	4 m y_4	UE upstream end y_{UE}	US upstream side y_{US}	DS downstream side y_{DS}	DE downstream end y_{DE}	6 m y_6	7 m y_7	B	B-b_p	v_c = $2g(y_{UE}-y_{DS})^{0.5}$	Q_{theory}		Fr_{4m}	Fr_{US}	Fr_{6m}
1355.0	0.129787	129.8	247.7	282.5	233.2	226.7	225.2	264.7	260.6	0.609	0.560	1.06	0.137475	0.94	0.55	0.63	0.50
1355.0	0.129787	129.8	262.2	290.5	250.2	248.5	247.2	281.8	274.7	0.609	0.560	0.95	0.132105	0.98	0.51	0.55	0.45
1355.0	0.129787	129.8	280.6	307.0	271.2	272.7	272.2	289.7	295.1	0.609	0.560	0.87	0.132310	0.98	0.46	0.48	0.44
1355.0	0.129787	129.8	299.4	324.0	291.2	293.5	293.2	304.2	311.2	0.609	0.560	0.82	0.135217	0.96	0.42	0.43	0.41
1355.0	0.129787	129.8	317.5	340.0	311.7	315.0	315.7	335.9	334.2	0.609	0.560	0.75	0.133053	0.98	0.38	0.38	0.35

				UE upstream	US upstream	DS downstream	DE downstream

h_{mean_avg}	Q_{calc}	Q [l/s]	4 m y_4	end y_{UE}	side y_{US}	side y_{DS}	end y_{DE}	6 m y_6	7 m y_7	B	B-b_p	y_C * $2g(y_{UE}-y_{DS})^{1/3}$	Q_{theory}		Fr_{4m}	Fr_{DS}	Fr_{4m}
1815.0	0.150187	150.2	276.0	312.8	288.7	254.5	251.2	283.3	284.0	0.609	0.560	1.11	0.157496	0.95	0.54	0.61	0.52
1815.0	0.150187	150.2	292.0	323.5	278.9	275.0	274.7	309.3	306.2	0.609	0.560	1.01	0.156288	0.96	0.50	0.55	0.46
1815.0	0.150187	150.2	309.0	339.5	298.7	299.5	297.9	325.7	318.5	0.609	0.560	0.93	0.155825	0.96	0.46	0.49	0.42
1815.0	0.150187	150.2	328.8	357.0	319.7	321.5	322.2	337.3	345.0	0.609	0.560	0.88	0.158488	0.95	0.42	0.43	0.40
1815.0	0.150187	150.2	347.1	371.5	339.2	342.2	342.7	354.3	355.8	0.609	0.560	0.81	0.154795	0.97	0.39	0.39	0.37

h_{mean_avg}	Q_{calc}	Q [l/s]	4 m y_4	UE upstream end y_{UE}	US upstream side y_{US}	DS downstream side y_{DS}	DE downstream end y_{DE}	6 m y_6	7 m y_7	B	B-b_p	y_C * $2g(y_{UE}-y_{DS})^{1/3}$	Q_{theory}		Fr_{4m}	Fr_{DS}	Fr_{4m}
2310.0	0.169433	169.4	306.5	346.3	291.7	288.7	285.7	319.4	316.3	0.609	0.560	1.10	0.177613	0.95	0.52	0.57	0.49
2310.0	0.169433	169.4	322.4	356.3	308.7	307.0	304.7	339.0	335.5	0.609	0.560	1.02	0.175717	0.96	0.49	0.52	0.45
2310.0	0.169433	169.4	341.1	371.5	330.2	330.0	328.2	356.1	351.5	0.609	0.560	0.94	0.174597	0.97	0.45	0.47	0.42
2310.0	0.169433	169.4	359.0	389.0	349.7	351.2	350.2	369.1	373.5	0.609	0.560	0.91	0.178018	0.95	0.41	0.43	0.40
2310.0	0.169433	169.4	377.0	403.8	369.7	372.0	370.7	381.5	390.9	0.609	0.560	0.84	0.174462	0.97	0.38	0.39	0.38
														0.97			

MODEL PIER, bp = 49 mm_LONG_NORMAL Q's

OK

DATA: *Wednesday, 26 July 2000*

Q	h_{man_1}	h_{man_2}	0 m	1 m	2 m	3 m	4 m	UE upstream end	US upstream side	DS downstream side	DE downstream end	6 m	7 m
bed levels			12.5	10.5	15.0	13.5	15.5					147.5	147.0
10	9.0	8.5	NOT MEASURABLE			57.8	56.6	56.3	25.5	24.0	14.0	188.2	190.4
30	75.5	74.0				100.9	99.5	105.8	73.0	48.5	40.0	192.0	220.8
50	208.0	206.5				133.6	131.9	146.0	104.5	68.5	61.8	211.5	236.5
70	408.0	408.0				160.6	158.2	177.0	129.0	91.0	85.0	230.9	308.0
90	665.0	665.0				186.3	184.5	204.0	150.5	112.3	103.8	250.3	246.3
110	990.0	985.0				208.9	208.3	233.5	171.0	132.3	122.3	269.6	274.6
130	1340.0	1345.0				227.8	224.8	256.0	187.8	151.5	141.0	285.2	302.1
150	1830.0	1830.0				250.0	243.0	280.5	202.8	170.0	159.0	303.8	331.2
170	2310.0	2320.0				273.0	267.9	301.5	222.5	187.8	179.0	318.5	347.5

Geometric properties:

D =	49 mm
L_p =	345 mm
z_A =	0 mm
z_B =	0.7 mm
z_C =	5.2 mm
z_D =	5.5 mm

CALCULATIONS:

FLOW DEPTHS

Distance measured downstream within the flume

h_{man_avg}	Q_{man}	Q [l/s]	0 m y_0	1 m y_1	2 m y_2	3 m y_3	4 m y_4	UE upstream end y_{ue}	US upstream side y_{us}	DS downstream side y_{ds}	DE downstream end y_{de}	6 m y_6	7 m y_7	B	B-b_p	v_0 = $2g(y_{us}-y_{ds})^{0.5}$	$Q_{manning}$	C_d	Fr_{4m}	Fr_{DS}	Fr_{DE}
8.0	0.010428	10.4				44.3	41.1	56.3	25.2	25.2	19.8	40.7		0.609	0.560	0.80	0.012990	0.80	0.66	1.19	1.06
74.8	0.030479	30.5				87.4	84.9	105.8	73.7	53.7	45.8	44.5		0.609	0.560	1.06	0.031848	0.96	0.66	1.43	1.63
207.3	0.050751	50.8				120.1	116.4	146.0	105.2	73.7	67.8	64.0		0.609	0.560	1.23	0.050865	1.00	0.67	1.45	1.51
408.0	0.071207	71.2				147.1	142.7	177.0	129.7	96.2	90.8	83.4		0.609	0.560	1.30	0.069949	1.02	0.69	1.38	1.38
665.0	0.090908	90.9				172.8	169.0	204.0	151.2	117.4	109.6	102.8	99.3	0.609	0.560	1.34	0.089216	1.03	0.69	1.29	1.31
987.5	0.110780	110.8				195.4	192.8	233.5	171.7	137.4	128.1	122.1	127.6	0.609	0.560	1.41	0.109456	1.02	0.69	1.24	1.27
1342.5	0.126167	126.2				214.3	209.3	256.0	188.4	156.7	146.8	137.7	165.1	0.609	0.560	1.43	0.125619	1.03	0.71	1.19	1.29
1830.0	0.150806	150.8				236.5	227.5	280.5	203.4	175.2	164.8	156.3	184.2	0.609	0.560	1.47	0.144429	1.04	0.73	1.17	1.18
2315.0	0.169617	169.6				256.5	252.4	301.5	223.2	192.9	184.8	171.0	200.5	0.609	0.560	1.49	0.161387	1.05	0.70	1.14	1.12
																		0.99			

MODEL PIER, bp = 49 mm_LONG_DROWNED Q's

DATA: *Wednesday, 26 July 2000*

h_{man_1}	h_{man_2}	4 m	UE upstream end	US upstream side	DS downstream side	DE downstream end	6 m	7 m
		15.5					147.5	147.0
645.0	635.0	191.0	209.0	160.0	138.5	138.5	331.3	328.5
645.0	635.0	210.0	220.5	181.8	179.8	180.8	356.2	353.3
645.0	635.0	226.1	232.5	201.5	203.3	204.3	361.0	358.2
645.0	635.0	244.4	248.0	223.0	224.8	224.0	368.7	393.2
645.0	635.0	262.5	264.0	242.0	243.0	241.0	400.7	407.9

h_{man_1}	h_{man_2}	4 m	UE upstream end	US upstream side	DS downstream side	DE downstream end	6 m	7 m
		15.5					147.5	147.0
960.0	965.0	225.0	245.5	192.3	178.3	172.5	362.5	359.8
960.0	965.0	237.5	253.0	209.0	202.5	203.5	393.1	391.5
960.0	965.0	256.6	264.5	230.5	230.3	230.0	394.8	403.9
960.0	965.0	274.9	282.5	251.0	252.8	253.5	416.4	419.4
960.0	965.0	293.1	297.5	270.8	272.8	272.0	436.4	439.5

h_{man_1}	h_{man_2}	4 m	UE upstream end	US upstream side	DS downstream side	DE downstream end	6 m	7 m

		15.5					147.5	147.0
1350.0	1350.0	251.3	270.0	217.3	203.0	197.0	383.0	386.7
1350.0	1350.0	265.8	284.0	234.3	227.0	223.8	415.4	411.0
1350.0	1350.0	281.3	295.5	255.5	252.5	250.5	435.3	422.1
1350.0	1350.0	300.5	310.0	274.8	276.0	275.0	440.5	450.0
1350.0	1350.0	319.4	327.3	296.3	297.8	296.5	459.5	465.0

h_{main_1}	h_{main_2}	4 m	UE upstream end	US upstream side	DS downstream side	DE downstream end	6 m	7 m
		15.5					147.5	147.0
1800.0	1780.0	276.0	300.0	241.0	227.5	222.0	410.6	417.6
1800.0	1780.0	289.3	311.5	259.0	253.0	248.5	427.4	430.9
1800.0	1780.0	308.8	324.0	280.8	277.8	274.5	461.5	454.4
1800.0	1780.0	328.1	340.5	301.5	301.3	298.0	480.8	494.6
1800.0	1780.0	345.5	356.5	322.0	322.3	321.3	483.7	492.9

h_{main_1}	h_{main_2}	4 m	UE upstream end	US upstream side	DS downstream side	DE downstream end	6 m	7 m
		15.5					147.5	147.0
2320.0	2325.0	301.3	327.5	267.3	254.5	248.5	434.7	446.5
2320.0	2325.0	317.4	341.3	285.5	278.5	274.5	453.3	458.2
2320.0	2325.0	338.9	356.0	309.0	305.5	300.5	484.6	479.8
2320.0	2325.0	354.5	372.8	328.3	326.8	324.5	511.2	503.5
2320.0	2325.0	372.8	386.0	347.3	347.0	345.5	515.3	512.8

CALCULATIONS

FLOW DEPTHS

h_{main_avg}	Q_{calc}	Q [l/s]	4 m y_4	UE upstream end y_{UE}	US upstream side y_{US}	DS downstream side y_{DS}	DE downstream end y_{DE}	6 m y_6	7 m y_7	B	B-b_y	v_c = $2g(y_{US}-y_{DS})^{0.5}$	Q_{theory}		$Fr_{...4m}$	$Fr_{...DS}$	$Fr_{...6m}$
640.0	0.089183	89.2	175.5	209.0	160.7	143.7	144.3	183.5	181.5	0.609	0.560	1.16	0.094617	0.94	0.54	0.66	0.59
640.0	0.089183	89.2	194.5	220.5	182.4	164.9	166.6	206.7	206.3	0.609	0.560	0.85	0.092590	0.96	0.55	0.59	0.49
640.0	0.089183	89.2	210.6	232.5	202.2	206.4	210.1	213.5	221.2	0.609	0.560	0.76	0.088414	1.01	0.48	0.49	0.47
640.0	0.089183	89.2	228.9	248.0	223.7	229.9	229.8	241.2	246.2	0.609	0.560	0.68	0.089958	1.03	0.43	0.42	0.39
640.0	0.089183	89.2	247.0	264.0	242.7	246.2	246.8	261.2	260.9	0.609	0.560	0.64	0.089233	1.00	0.38	0.38	0.35

h_{main_avg}	Q_{calc}	Q [l/s]	4 m y_4	UE upstream end y_{UE}	US upstream side y_{US}	DS downstream side y_{DS}	DE downstream end y_{DE}	6 m y_6	7 m y_7	B	B-b_y	v_c = $2g(y_{US}-y_{DS})^{0.5}$	Q_{theory}		$Fr_{...4m}$	$Fr_{...DS}$	$Fr_{...6m}$
962.5	0.909369	909.4	209.5	245.5	192.9	183.4	178.3	215.0	212.8	0.609	0.560	1.15	0.117980	0.93	0.60	0.73	0.58
962.5	0.909369	909.4	222.0	253.0	209.7	207.7	209.3	245.6	234.5	0.609	0.560	1.00	0.115754	0.94	0.55	0.61	0.47
962.5	0.909369	909.4	241.1	264.5	231.2	235.4	235.8	247.3	256.9	0.609	0.560	0.82	0.108067	1.01	0.48	0.50	0.47
962.5	0.909369	909.4	259.4	282.5	251.7	257.9	258.3	268.9	272.4	0.609	0.560	0.78	0.110344	0.99	0.43	0.44	0.41
962.5	0.909369	909.4	277.6	297.5	271.4	277.9	277.8	288.9	292.5	0.609	0.560	0.70	0.108450	1.01	0.39	0.39	0.37

h_{main_avg}	Q_{calc}	Q [l/s]	4 m y_4	UE upstream end y_{UE}	US upstream side y_{US}	DS downstream side y_{DS}	DE downstream end y_{DE}	6 m y_6	7 m y_7	B	B-b_y	v_c = $2g(y_{US}-y_{DS})^{0.5}$	Q_{theory}		$Fr_{...4m}$	$Fr_{...DS}$	$Fr_{...6m}$
1350.0	0.129527	129.5	235.8	270.0	217.9	208.2	202.8	241.5	241.7	0.609	0.560	1.15	0.133651	0.97	0.59	0.72	0.57
1350.0	0.129527	129.5	250.3	284.0	234.9	232.2	229.6	267.9	264.9	0.609	0.560	1.06	0.137487	0.94	0.54	0.61	0.49
1350.0	0.129527	129.5	265.8	295.5	256.2	257.7	256.3	287.8	275.1	0.609	0.560	0.92	0.132532	0.98	0.50	0.52	0.44
1350.0	0.129527	129.5	285.0	310.0	275.4	281.2	280.8	293.0	303.0	0.609	0.560	0.82	0.128597	1.01	0.45	0.46	0.43
1350.0	0.129527	129.5	303.9	327.3	296.9	302.9	302.3	312.3	318.0	0.609	0.560	0.78	0.129051	1.00	0.41	0.41	0.39

			UE upstream	US upstream	DS downstream	DE downstream

h_{mon_avg}	Q_{Lab}	Q [l/s]	4 m y_4	end y_{UE}	side y_{US}	side y_{DS}	end y_{DE}	6 m y_6	7 m y_7	B	B-b_p	v_C = $2g(y_{UE}-y_{DS})^{1/2}$	Q_{theory}	C_d = Q_{Lab}/Q_{theory}	Fr_{-4m}	Fr_{-DS}	Fr_{-6m}
1790.0	0.149149	149.1	261.4	300.0	241.7	232.7	227.8	263.1	270.6	0.609	0.560	1.19	0.155392	0.96	0.59	0.70	0.58
1790.0	0.149149	149.1	273.8	311.5	256.7	258.2	252.3	279.9	283.9	0.609	0.560	1.07	0.154883	0.96	0.55	0.60	0.53
1790.0	0.149149	149.1	293.3	324.0	281.4	282.9	280.3	314.0	307.4	0.609	0.560	0.95	0.150918	0.99	0.49	0.52	0.44
1790.0	0.149149	149.1	312.6	340.5	302.2	306.4	303.8	333.3	317.6	0.609	0.560	0.88	0.150578	0.99	0.45	0.46	0.41
1790.0	0.149149	149.1	330.0	356.5	322.7	327.4	327.1	338.2	345.9	0.609	0.560	0.82	0.150300	0.99	0.41	0.42	0.40

h_{mon_avg}	Q_{Lab}	Q [l/s]	4 m y_4	UE upstream end y_{UE}	US upstream side y_{US}	DS downstream side y_{DS}	DE downstream end y_{DE}	6 m y_6	7 m y_7	B	B-b_p	v_C = $2g(y_{UE}-y_{DS})^{1/2}$	Q_{theory}	C_d = Q_{Lab}/Q_{theory}	Fr_{-4m}	Fr_{-DS}	Fr_{-6m}
2322.5	0.169891	169.9	285.8	327.5	267.9	259.7	252.3	287.2	299.5	0.609	0.560	1.29	0.174022	0.98	0.58	0.67	0.58
2322.5	0.169891	169.9	301.9	341.3	286.2	283.7	280.3	305.8	311.2	0.609	0.560	1.11	0.176256	0.96	0.54	0.59	0.53
2322.5	0.169891	169.9	323.4	358.0	305.7	310.7	306.3	332.1	332.8	0.609	0.560	1.01	0.176564	0.96	0.48	0.51	0.46
2322.5	0.169891	169.9	339.0	372.8	328.9	331.9	330.3	363.7	356.5	0.609	0.560	0.95	0.176578	0.96	0.45	0.47	0.41
2322.5	0.169891	169.9	357.3	386.0	347.9	352.2	351.3	367.8	365.8	0.609	0.560	0.87	0.172508	0.98	0.42	0.43	0.40
														0.98			

MODEL PIER, bp = 62 mm_SHORT_NORMAL Q's

OK

DATA *Wednesday, 26 July 2000*

Q	h_{man_1}	h_{man_2}	0 m	1 m	2 m	3 m	4 m	UE upstream end	US upstream side	DS downstream side	DE downstream end	6 m	7 m
bed levels			12.5	10.5	15.0	12.5	15.5					147.5	147.0
10	9.0	9.5	NOT MEASURABLE			58.5	58.0	56.5	23.0	23.5	15.0	187.0	191.5
30	73.0	72.0				102.4	101.4	107.5	73.0	48.0	35.0	189.0	250.5
50	202.5	203.0				136.8	135.8	147.0	104.0	73.3	58.8	208.3	205.5
70	385.0	385.0				165.4	164.1	176.5	130.0	97.8	79.3	225.4	223.4
90	645.0	650.0				190.8	189.5	209.5	153.3	122.8	101.8	243.8	237.2
110	965.0	950.0				212.8	211.5	235.5	179.8	143.5	126.0	261.5	256.1
130	1340.0	1330.0				235.0	232.2	259.5	198.5	164.0	148.3	280.5	280.9
150	1820.0	1860.0				254.2	249.6	285.5	204.5	184.0	172.0	298.8	323.5
170	2300.0	2290.0				275.7	269.0	303.5	218.0	198.0	188.8	315.0	356.2

Geometric properties:

D =	62 mm
L_p =	263 mm
z_A =	0 mm
z_B =	0.9 mm
z_C =	3.6 mm
z_D =	4.4 mm

CALCULATIONS

FLOW DEPTHS

Distance measured downstream within the flume

h_{man_avg}	Q_{vol}	Q [l/s]	0 m y_0	1 m y_1	2 m y_2	3 m y_3	4 m y_4	UE upstream end y_{UE}	US upstream side y_{US}	DS downstream side y_{DS}	DE downstream end y_{DE}	6 m y_6	7 m y_7	B	B-b_p	v_c = $2g(y_{UE}-y_{DS})^{0.5}$	Q_{theory}	Cv = Q_{act}/Q_{theory}	Fr_4m	Fr_DS	Fr_DE
9.3	0.010722	10.7				45.0	42.5	56.5	23.9	27.1	19.4	39.5	44.5	0.609	0.547	0.80	0.011906	0.90	0.64	1.41	2.08
72.5	0.030017	30.0				88.9	85.9	107.5	73.9	51.6	39.4	41.5	103.5	0.609	0.547	1.08	0.030467	0.99	0.83	1.50	2.01
202.8	0.050197	50.2				123.3	120.3	147.0	104.9	76.8	63.2	60.8	58.5	0.609	0.547	1.20	0.050534	0.99	0.83	1.38	1.66
385.0	0.069171	69.2				151.9	148.6	176.5	130.9	101.3	83.7	77.9	76.4	0.609	0.547	1.24	0.068877	1.00	0.83	1.25	1.50
647.5	0.089704	89.7				177.3	174.0	209.5	154.1	126.3	106.2	95.3	90.2	0.609	0.547	1.30	0.090131	1.00	0.85	1.17	1.35
957.5	0.109084	109.1				199.3	196.0	235.5	171.5	147.1	130.4	114.0	112.1	0.609	0.547	1.34	0.108068	1.01	0.86	1.13	1.21
1335.0	0.128805	128.8				221.5	216.7	259.5	189.4	167.6	152.7	133.0	142.9	0.609	0.547	1.37	0.125454	1.03	0.87	1.10	1.13
1810.0	0.149680	150.0				240.7	234.1	285.5	205.4	187.6	176.4	151.3	176.5	0.609	0.547	1.41	0.144773	1.04	0.89	1.08	1.06
2295.0	0.168882	168.9				262.2	253.5	303.5	215.9	201.6	193.2	167.5	209.2	0.609	0.547	1.44	0.158616	1.06	0.89	1.09	1.04
																		1.01			

MODEL PIER, bp = 62 mm_SHORT_DROWNED Q's

DATA *Wednesday, 26 July 2000*

h_{man_1}	h_{man_2}	4 m	UE upstream end	US upstream side	DS downstream side	DE downstream end	6 m	7 m
		15.5					147.5	147.0
650.0	650.0	192.7	211.3	156.3	132.8	116.8	328.3	326.9
650.0	650.0	209.3	221.0	177.0	170.0	167.5	350.5	354.1
650.0	650.0	223.8	231.0	195.0	194.3	193.8	364.8	369.2
650.0	650.0	240.0	246.5	214.3	216.3	216.5	390.1	394.5
650.0	650.0	262.0	264.5	239.0	241.8	241.8	405.4	406.9

h_{man_1}	h_{man_2}	4 m	UE upstream end	US upstream side	DS downstream side	DE downstream end	6 m	7 m
		15.5					147.5	147.0
970.0	975.0	224.2	242.5	184.8	165.8	151.0	358.5	355.3
970.0	975.0	235.0	251.5	200.0	192.0	184.5	379.5	376.2
970.0	975.0	252.1	263.0	220.0	218.5	215.5	392.0	396.2
970.0	975.0	268.1	278.0	238.5	239.8	238.0	410.1	409.1
970.0	975.0	285.8	290.5	259.8	261.5	261.0	432.7	432.2

h_{man_1}	h_{man_2}	4 m	UE upstream end	US upstream side	DS downstream side	DE downstream end	6 m	7 m

		15.5					147.5	147.0
1355.0	1355.0	240.8	272.5	208.5	193.5	181.0	379.9	380.2
1355.0	1355.0	261.8	281.5	226.0	218.3	209.0	404.6	403.2
1355.0	1355.0	280.0	295.5	246.3	243.3	237.0	423.8	419.1
1355.0	1355.0	293.4	305.5	263.0	262.0	258.5	434.5	436.2
1355.0	1355.0	311.3	321.0	283.0	283.8	282.0	452.4	453.3

h_{nor_1}	h_{nor_2}	4 m	UE upstream end	US upstream side	DS downstream side	DE downstream end	6 m	7 m
		15.5					147.5	147.0
1835.0	1810.0	272.7	299.0	231.3	217.8	206.0	403.0	406.5
1835.0	1810.0	288.5	310.0	249.0	241.0	232.5	425.9	425.0
1835.0	1810.0	306.5	325.0	270.8	268.8	261.3	449.8	448.0
1835.0	1810.0	323.9	339.3	291.0	290.3	286.5	466.3	466.8
1835.0	1810.0	341.4	353.5	310.3	310.0	308.8	481.5	484.0

h_{nor_1}	h_{nor_2}	4 m	UE upstream end	US upstream side	DS downstream side	DE downstream end	6 m	7 m
		15.5					147.5	147.0
2320.0	2325.0	297.8	325.5	264.3	243.3	232.3	427.8	436.5
2320.0	2325.0	314.2	335.5	271.8	264.8	257.5	447.8	449.2
2320.0	2325.0	330.5	350.5	291.8	288.0	280.8	470.7	468.1
2320.0	2325.0	345.8	363.5	311.8	310.0	306.0	489.0	487.8
2320.0	2325.0	364.1	377.0	332.5	331.8	329.5	505.2	505.6

CALCULATIONS

FLOW DEPTHS

h_{nor_avg}	Q_{calc}	Q [l/s]	4 m y_4	UE upstream end y_{UE}	US upstream side y_{US}	DS downstream side y_{DS}	DE downstream end y_{DE}	6 m y_6	7 m y_7	B	B-b_p	x_U = $2g(y_{US}-y_{DS})^{1.5}$	Q_{theory}		Fr_{4m}	Fr_{DS}	Fr_{6m}
650.0	0.089877	89.9	177.2	211.3	187.1	136.3	121.2	180.8	179.9	0.609	0.547	1.24	0.092527	0.97	0.63	0.54	0.61
650.0	0.089877	89.9	193.8	221.0	177.9	173.6	171.9	203.0	207.1	0.609	0.547	1.00	0.094961	0.95	0.55	0.65	0.52
650.0	0.089877	89.9	208.3	231.0	195.9	197.8	198.2	217.3	222.2	0.609	0.547	0.85	0.091574	0.98	0.50	0.54	0.47
650.0	0.089877	89.9	224.5	246.5	215.1	219.8	220.9	242.6	237.5	0.609	0.547	0.77	0.092625	0.97	0.44	0.46	0.39
650.0	0.089877	89.9	246.5	264.5	239.9	245.3	246.2	257.9	259.9	0.609	0.547	0.67	0.089645	1.00	0.39	0.39	0.36

h_{nor_avg}	Q_{calc}	Q [l/s]	4 m y_4	UE upstream end y_{UE}	US upstream side y_{US}	DS downstream side y_{DS}	DE downstream end y_{DE}	6 m y_6	7 m y_7	B	B-b_p	x_U = $2g(y_{US}-y_{DS})^{1.5}$	Q_{theory}		Fr_{4m}	Fr_{DS}	Fr_{6m}
972.5	0.108835	108.9	208.7	242.5	185.6	169.3	155.4	211.0	208.3	0.609	0.547	1.23	0.113641	0.97	0.60	0.53	0.59
972.5	0.108835	108.9	210.5	251.5	200.9	195.6	188.9	232.0	229.2	0.609	0.547	1.08	0.115572	0.95	0.56	0.67	0.52
972.5	0.108835	108.9	236.6	263.0	220.9	222.1	219.9	244.5	249.2	0.609	0.547	0.93	0.113493	0.97	0.50	0.55	0.48
972.5	0.108835	108.9	252.5	278.0	239.4	243.3	242.4	262.6	262.1	0.609	0.547	0.87	0.115291	0.95	0.45	0.48	0.43
972.5	0.108835	108.9	270.3	290.5	260.6	265.1	265.4	285.2	285.2	0.609	0.547	0.75	0.109361	1.01	0.41	0.42	0.38

h_{nor_avg}	Q_{calc}	Q [l/s]	4 m y_4	UE upstream end y_{UE}	US upstream side y_{US}	DS downstream side y_{DS}	DE downstream end y_{DE}	6 m y_6	7 m y_7	B	B-b_p	x_U = $2g(y_{US}-y_{DS})^{1.5}$	Q_{theory}		Fr_{4m}	Fr_{DS}	Fr_{6m}
1355.0	0.129767	129.8	234.3	272.5	209.4	197.1	185.4	232.4	233.2	0.609	0.547	1.24	0.134192	0.97	0.60	0.78	0.61
1355.0	0.129767	129.8	246.3	281.5	226.9	221.8	213.4	257.1	256.2	0.609	0.547	1.11	0.135154	0.96	0.56	0.65	0.52
1355.0	0.129767	129.8	264.5	295.5	247.1	246.8	241.4	276.3	272.1	0.609	0.547	1.01	0.136687	0.95	0.50	0.55	0.47
1355.0	0.129767	129.8	277.9	305.5	263.9	265.6	262.0	287.0	289.2	0.609	0.547	0.92	0.134193	0.97	0.46	0.50	0.44
1355.0	0.129767	129.8	295.8	321.0	283.9	287.3	286.4	304.9	306.3	0.609	0.547	0.85	0.134350	0.97	0.42	0.44	0.40

			UE upstream	US upstream	DS downstream	DE downstream

h_{mean_avg}	Q_{calc}	Q [l/s]	4 m y_4	end y_{UE}	side y_{US}	side y_{DS}	end y_{DE}	6 m y_6	7 m y_7	B	$B-b_D$	$v_C = \sqrt{2g(y_{UE}-y_{DE})^{1.1}}$	Q_{theory}		Fr_{-4m}	Fr_{-DS}	Fr_{-6m}
1822.5	0.150497	150.5	257.2	299.0	232.1	221.3	210.4	255.5	262.5	0.609	0.547	1.26	0.152838	0.98	0.60	0.76	0.61
1822.5	0.150497	150.5	273.0	310.0	249.9	244.6	236.9	270.4	276.0	0.609	0.547	1.16	0.155643	0.97	0.55	0.65	0.53
1822.5	0.150497	150.5	291.0	325.0	271.6	270.3	265.7	302.3	305.0	0.609	0.547	1.07	0.158063	0.95	0.50	0.56	0.47
1822.5	0.150497	150.5	308.4	339.3	291.9	293.5	293.9	318.5	319.8	0.609	0.547	0.98	0.157575	0.96	0.46	0.50	0.44
1822.5	0.150497	150.5	325.9	353.5	311.1	313.6	313.2	334.0	337.0	0.609	0.547	0.92	0.158449	0.95	0.42	0.45	0.41

h_{mean_avg}	Q_{calc}	Q [l/s]	4 m y_4	UE upstream end y_{UE}	US upstream side y_{US}	DS downstream side y_{DS}	DE downstream end y_{DE}	6 m y_6	7 m y_7	B	$B-b_D$	$v_C = \sqrt{2g(y_{UE}-y_{DE})^{1.1}}$	Q_{theory}		Fr_{-4m}	Fr_{-DS}	Fr_{-6m}
2322.5	0.169891	169.9	282.3	325.5	255.1	246.8	236.7	280.3	291.5	0.609	0.547	1.27	0.171495	0.99	0.59	0.73	0.60
2322.5	0.169891	169.9	298.7	335.5	272.6	268.3	261.9	300.3	302.2	0.609	0.547	1.18	0.172911	0.98	0.55	0.64	0.54
2322.5	0.169891	169.9	315.0	350.5	292.6	291.6	285.2	323.2	321.1	0.609	0.547	1.11	0.176600	0.96	0.50	0.57	0.48
2322.5	0.169891	169.9	330.3	363.5	312.5	313.6	310.4	341.5	340.8	0.609	0.547	1.02	0.175720	0.97	0.47	0.51	0.45
2322.5	0.169891	169.9	346.6	377.0	333.4	335.3	333.9	357.7	358.5	0.609	0.547	0.94	0.172815	0.98	0.43	0.46	0.42
														0.97			

MODEL PIER, bp = 62 mm_MEDIUM_NORMAL Q's

OK

DATA: *Tuesday, 25 July 2000*

Q	$h_{man,1}$	$h_{man,2}$	0 m	1 m	2 m	3 m	4 m	UE upstream end	US upstream side	DS downstream side	DE downstream end	6 m	7 m
bed levels			**12.5**	**10.5**	**15.0**	**13.5**	**15.5**					**147.5**	**147.0**
10	11.0	11.0	NOT MEASURABLE			61.1	61.5	59.8	25.8	26.0	15.5	199.5	192.1
30	75.0	75.0				103.4	103.0	109.0	74.9	49.5	36.0	192.0	226.5
50	202.6	203.0				138.4	137.5	146.3	104.3	68.3	56.8	210.0	226.9
70	385.0	385.0				167.7	166.6	179.3	130.5	88.0	77.8	226.6	226.1
90	650.0	650.0				194.3	192.5	210.0	155.0	111.0	100.3	245.5	244.0
110	1000.0	1000.0				219.4	218.0	237.0	176.0	134.0	123.3	265.6	269.9
130	1350.0	1350.0				241.2	238.3	265.3	193.0	152.0	141.3	283.1	295.3
150	1815.0	1820.0				260.4	258.3	286.5	210.0	173.0	161.5	300.7	323.6
170	2320.0	2300.0				280.6	274.2	308.5	224.0	189.0	179.3	319.8	346.6

Geometric properties:

D =	62 mm
L_p =	351 mm
z_A =	0 mm
z_B =	0.9 mm
z_C =	5.0 mm
z_D =	5.9 mm

CALCULATIONS:

FLOW DEPTHS

$h_{man,avg}$	Q_{corr}	Q [l/s]	Distance measured downstream within the flume: 0 m y_0	1 m y_1	2 m y_2	3 m y_3	4 m y_4	UE upstream end y_{UE}	US upstream side y_{US}	DS downstream side y_{DS}	DE downstream end y_{DE}	6 m y_6	7 m y_7	B	B-b_p	v_c = $\sqrt{2g(y_{UE}-y_{DE})^{0.1}}$	Q_{theory}	Cd	Fr 4m	Fr DS	Fr DE
11.0	0.011692	11.7				47.6	46.0	59.8	26.6	31.0	21.4	52.0	45.1	0.639	0.547	0.81	0.013811	0.85	0.62	1.25	1.96
75.0	0.030530	30.5				89.9	87.5	109.0	74.9	54.5	41.9	44.5	78.5	0.639	0.547	1.08	0.032227	0.95	0.62	1.40	1.87
202.5	0.050166	50.2				124.9	122.0	146.3	105.1	73.3	62.6	62.5	79.9	0.639	0.547	1.24	0.049586	1.01	0.62	1.46	1.68
385.0	0.069171	69.2				154.2	151.1	179.3	131.4	93.0	83.6	79.1	79.1	0.639	0.547	1.34	0.068068	1.02	0.62	1.42	1.59
650.0	0.089877	89.9				180.8	177.0	210.0	155.9	116.0	106.1	96.0	97.0	0.639	0.547	1.39	0.089455	1.02	0.63	1.33	1.36
1000.0	0.111479	111.5				205.9	202.5	237.0	178.9	139.6	129.1	118.1	122.9	0.639	0.547	1.42	0.108109	1.03	0.64	1.26	1.26
1350.0	0.129527	129.5				227.7	222.8	265.3	193.9	157.6	147.1	135.6	148.3	0.639	0.547	1.49	0.128037	1.01	0.65	1.21	1.20
1817.5	0.150290	150.3				246.9	242.8	286.5	210.9	178.0	167.4	153.2	176.6	0.639	0.547	1.49	0.145320	1.03	0.66	1.17	1.15
2310.0	0.169433	169.4				267.1	258.7	308.5	224.9	194.0	185.1	172.3	199.6	0.639	0.547	1.53	0.162513	1.04	0.68	1.16	1.11
																		1.01			

MODEL PIER, bp = 62 mm_MEDIUM_DROWNED Q's

DATA: *Tuesday, 25 July 2000*

$h_{man,1}$	$h_{man,2}$	4 m	UE upstream end	US upstream side	DS downstream side	DE downstream end	6 m	7 m
		15.5					**147.5**	**147.0**
665.0	660.0	195.0	210.5	158.5	121.0	113.8	322.2	323.6
665.0	660.0	206.3	220.8	171.3	161.5	167.0	354.4	346.3
665.0	660.0	223.3	232.0	191.5	194.0	197.8	360.0	357.9
665.0	660.0	240.5	245.0	211.0	217.5	219.5	389.0	385.6
665.0	660.0	257.6	260.0	230.8	235.3	235.5	401.3	404.9

$h_{man,1}$	$h_{man,2}$	4 m	UE upstream end	US upstream side	DS downstream side	DE downstream end	6 m	7 m
		15.5					**147.5**	**147.0**
980.0	985.0	225.0	241.5	184.5	161.5	158.5	358.3	360.5
980.0	985.0	239.5	251.5	202.8	197.5	199.5	385.3	394.2
980.0	985.0	255.0	266.5	222.3	223.8	225.8	390.0	400.0
980.0	985.0	274.0	281.0	243.6	247.3	249.5	411.7	416.5
980.0	985.0	289.5	295.0	261.0	266.5	267.5	434.0	431.6

$h_{man,1}$	$h_{man,2}$	4 m	UE upstream end	US upstream side	DS downstream side	DE downstream end	6 m	7 m

		15.5					147.5	147.0
1360.0	1360.0	260.6	279.5	219.0	212.0	208.5	399.5	398.4
1360.0	1360.0	274.0	290.0	238.3	234.8	238.0	420.1	419.2
1360.0	1360.0	291.3	302.8	257.0	257.0	260.5	437.0	433.0
1360.0	1360.0	306.5	317.0	274.8	279.0	281.8	444.4	452.3
1360.0	1360.0	322.5	330.5	294.5	298.8	300.8	494.6	467.0

h_{man_1}	h_{man_2}	4 m	UE upstream end	US upstream side	DS downstream side	DE downstream end	6 m	7 m
		15.5					147.5	147.0
1820.0	1800.0	293.6	312.0	253.3	246.0	244.5	430.3	429.5
1820.0	1800.0	305.4	326.3	268.5	267.0	267.0	451.7	454.0
1820.0	1800.0	324.3	337.8	288.3	290.5	290.5	472.0	470.5
1820.0	1800.0	341.1	352.5	309.0	312.0	313.5	490.1	482.1
1820.0	1800.0	357.6	367.8	327.0	332.0	333.0	496.3	505.2

h_{man_1}	h_{man_2}	4 m	UE upstream end	US upstream side	DS downstream side	DE downstream end	6 m	7 m
		15.5					147.5	147.0
2310.0	2330.0	319.1	343.5	276.5	270.3	269.0	455.8	459.2
2310.0	2330.0	332.5	353.0	292.8	290.0	290.5	475.1	475.0
2310.0	2330.0	346.9	362.5	310.0	310.0	310.0	491.6	491.4
2310.0	2330.0	364.0	377.5	328.0	330.0	330.3	510.0	506.1
2310.0	2330.0	378.2	390.0	345.0	348.8	349.0	521.1	516.2

CALCULATIONS

FLOW DEPTHS

h_{man_avg}	Q_{calc}	Q [l/s]	4 m y_4	UE upstream end y_{UE}	US upstream side y_{US}	DS downstream side y_{DS}	DE downstream end y_{DE}	6 m y_6	7 m y_7	B	B-b_y	v_c = $\sqrt{2g(y_{UE}-y_{DS})}$	Q_{theory}	[illegible]	Fr_{-4m}	Fr_{-DS}	Fr_{-6m}
662.5	0.090737	90.7	179.5	210.5	159.4	126.0	119.6	174.7	176.5	0.609	0.547	1.33	0.091352	0.99	0.63	1.06	0.65
662.5	0.090737	90.7	190.8	220.8	172.1	166.5	172.9	206.9	199.3	0.609	0.547	1.08	0.098213	0.92	0.57	0.70	0.51
662.5	0.090737	90.7	207.8	232.0	192.4	199.0	203.8	212.5	220.9	0.609	0.547	0.86	0.094304	0.97	0.50	0.54	0.49
662.5	0.090737	90.7	225.0	245.0	211.9	222.5	225.4	241.5	238.5	0.609	0.547	0.73	0.089411	1.01	0.45	0.45	0.40
662.5	0.090737	90.7	242.1	260.0	231.6	240.3	241.4	253.8	257.9	0.609	0.547	0.70	0.091588	0.99	0.40	0.40	0.37

h_{man_avg}	Q_{calc}	Q [l/s]	4 m y_4	UE upstream end y_{UE}	US upstream side y_{US}	DS downstream side y_{DS}	DE downstream end y_{DE}	6 m y_6	7 m y_7	B	B-b_y	v_c = $\sqrt{2g(y_{UE}-y_{DS})}$	Q_{theory}	[illegible]	Fr_{-4m}	Fr_{-DS}	Fr_{-6m}
982.5	0.110499	110.5	209.5	241.5	185.4	166.5	164.4	210.8	213.5	0.609	0.547	1.25	0.114122	0.97	0.60	0.65	0.60
982.5	0.110499	110.5	224.0	251.5	203.6	202.5	205.4	237.8	237.2	0.609	0.547	1.03	0.114033	0.97	0.55	0.54	0.50
982.5	0.110499	110.5	239.5	266.5	223.1	228.8	231.6	242.5	253.0	0.609	0.547	0.92	0.114610	0.96	0.49	0.53	0.49
982.5	0.110499	110.5	256.5	281.0	243.9	252.3	255.4	264.2	269.5	0.609	0.547	0.81	0.112293	0.98	0.44	0.46	0.43
982.5	0.110499	110.5	274.0	295.0	261.9	271.5	273.4	286.5	284.6	0.609	0.547	0.75	0.111064	0.99	0.40	0.41	0.38

h_{man_avg}	Q_{calc}	Q [l/s]	4 m y_4	UE upstream end y_{UE}	US upstream side y_{US}	DS downstream side y_{DS}	DE downstream end y_{DE}	6 m y_6	7 m y_7	B	B-b_y	v_c = $\sqrt{2g(y_{UE}-y_{DS})}$	Q_{theory}	[illegible]	Fr_{-4m}	Fr_{-DS}	Fr_{-6m}
1360.0	0.130006	130.0	245.1	279.5	219.9	217.0	214.4	252.0	251.4	0.609	0.547	1.15	0.136617	0.95	0.56	0.57	0.54
1360.0	0.130006	130.0	258.5	290.0	239.1	239.8	243.9	272.6	272.2	0.609	0.547	1.04	0.136557	0.95	0.52	0.58	0.48
1360.0	0.130006	130.0	275.8	302.8	257.9	262.0	266.4	289.5	286.0	0.609	0.547	0.95	0.135794	0.96	0.47	0.51	0.44
1360.0	0.130006	130.0	291.0	317.0	275.6	284.0	287.6	296.9	305.3	0.609	0.547	0.86	0.134150	0.97	0.43	0.45	0.42
1360.0	0.130006	130.0	307.0	330.5	295.4	303.8	306.6	317.1	320.0	0.609	0.547	0.79	0.131149	0.99	0.40	0.41	0.38

				UE upstream	US upstream	DS downstream	DE downstream

h_{mer_avg}	Q_{calc}	Q [l/s]	4 m y_4	end y_{UE}	side y_{US}	side y_{DS}	end y_{DE}	6 m y_6	7 m y_7	B	B-b_p	v_C = $2g(y_{UE}-y_{US})^{0.5}$	Q_{theory}	[illegible]	Fr_{4m}	Fr_{DS}	Fr_{6m}
1810.0	0.149680	150.0	278.1	312.0	254.1	251.0	250.4	282.8	282.5	0.609	0.547	1.14	0.156254	0.96	0.54	0.63	0.52
1810.0	0.149680	150.0	290.9	326.3	269.4	272.0	272.9	304.2	307.9	0.609	0.547	1.08	0.160434	0.93	0.50	0.55	0.47
1810.0	0.149680	150.0	308.8	337.8	289.1	295.5	296.4	324.5	323.8	0.609	0.547	0.96	0.155648	0.96	0.46	0.49	0.43
1810.0	0.149680	150.0	325.6	352.5	309.9	317.0	319.4	332.6	335.1	0.609	0.547	0.89	0.154583	0.97	0.42	0.44	0.41
1810.0	0.149680	150.0	342.1	367.8	327.9	337.0	338.9	348.8	358.2	0.609	0.547	0.84	0.154398	0.97	0.39	0.40	0.38

h_{mer_avg}	Q_{calc}	Q [l/s]	4 m y_4	UE upstream end y_{UE}	US upstream side y_{US}	DS downstream side y_{DS}	DE downstream end y_{DE}	6 m y_6	7 m y_7	B	B-b_p	v_C = $2g(y_{UE}-y_{US})^{0.5}$	Q_{theory}	[illegible]	Fr_{4m}	Fr_{DS}	Fr_{6m}
2320.0	0.169800	169.8	303.8	343.5	277.4	275.3	274.9	308.3	312.2	0.609	0.547	1.20	0.160515	0.94	0.53	0.62	0.52
2320.0	0.169800	169.8	317.0	353.0	293.6	295.0	296.4	327.6	328.9	0.609	0.547	1.11	0.170420	0.95	0.50	0.56	0.47
2320.0	0.169800	169.8	331.4	362.5	310.9	315.0	315.9	344.1	344.4	0.609	0.547	1.01	0.174691	0.97	0.47	0.50	0.44
2320.0	0.169800	169.8	348.5	377.5	328.9	335.0	336.1	362.5	359.1	0.609	0.547	0.97	0.178915	0.96	0.43	0.46	0.41
2320.0	0.169800	169.8	362.7	390.0	345.9	353.8	354.9	373.6	369.2	0.609	0.547	0.90	0.174093	0.98	0.41	0.42	0.39
														0.97			

MODEL PIER, bp = 62 mm_LONG_NORMAL Q's

OK

DATA: *Friday, 28 July 2000*

Q	h_{mon_1}	h_{mon_2}	0 m	1 m	2 m	3 m	4 m	UE upstream end	US upstream side	DS downstream side	DE downstream end	6 m	7 m
bed levels			12.5	10.5	15.0	13.5	15.5					147.5	147.0
10	8.0	7.5	NOT MEASURABLE			57.5	57.2	56.0	22.3	23.5	14.5	184.9	189.2
30	69.5	70.0	NOT MEASURABLE			101.5	100.9	105.8	73.0	48.8	32.0	193.8	213.0
50	202.0	200.0				137.1	137.2	147.0	107.0	65.0	56.0	213.5	227.5
70	391.0	389.0				167.6	166.0	179.5	133.8	85.0	77.3	227.8	234.6
90	665.0	655.0				195.6	194.0	213.0	160.0	106.3	99.0	248.2	250.8
110	970.0	970.0				220.3	218.5	240.5	186.3	126.0	120.3	266.4	270.9
130	1370.0	1370.0				243.2	242.1	269.0	206.0	145.0	137.5	286.0	297.2
150	1800.0	1820.0				263.7	261.6	291.0	218.5	164.0	153.3	303.3	318.0
170	2340.0	2320.0				283.0	279.7	314.0	234.5	183.0	173.0	321.5	338.6

Geometric properties:

D =	62 mm
L_p =	437 mm
z_A =	0.0 mm
z_B =	0.9 mm
z_C =	6.5 mm
z_D =	7.3 mm

CALCULATIONS:

FLOW DEPTHS

h_{mon_avg}	Q_{calc}	Q [l/s]	Distance measured downstream within the flume: 0 m y_0	1 m y_1	2 m y_2	3 m y_3	4 m y_4	UE upstream end y_{UE}	US upstream side y_{US}	DS downstream side y_{DS}	DE downstream end y_{DE}	6 m y_6	7 m y_7	B	B-b_p	v_C = $\sqrt{2g(y_{UE}-y_{DE})}^{0.5}$	Q_{theory}	Cd = Q_{calc}/Q_{theory}	Fr_4m	Fr_DS	Fr_DE
7.8	0.009814	9.8		NOT MEASURABLE		44.0	41.7	56.0	23.1	30.0	21.8	37.4	42.2	0.609	0.547	0.80	0.013092	0.75	0.63	1.10	1.59
69.8	0.029442	29.4		NOT MEASURABLE		88.0	85.4	105.8	73.9	55.2	39.3	46.3	66.9	0.609	0.547	1.06	0.031945	0.92	0.62	1.32	1.98
201.0	0.049079	50.0				123.8	121.7	147.0	107.9	74.5	63.3	63.0	80.5	0.609	0.547	1.24	0.050717	0.99	0.62	1.44	1.64
390.0	0.069619	69.6				154.1	150.5	179.5	134.6	91.5	84.6	86.3	87.6	0.609	0.547	1.36	0.068132	1.02	0.63	1.47	1.48
660.0	0.090566	90.6				182.1	178.5	213.0	160.9	112.7	106.3	100.7	103.8	0.609	0.547	1.45	0.089235	1.01	0.63	1.40	1.37
970.0	0.109704	109.8				206.8	203.0	240.5	181.1	132.5	127.6	116.9	123.9	0.609	0.547	1.50	0.108610	1.01	0.63	1.33	1.28
1370.0	0.130485	130.5				229.7	226.6	269.0	200.9	151.5	144.8	136.5	150.2	0.609	0.547	1.56	0.129238	1.01	0.63	1.29	1.24
1810.0	0.14998	150.0				250.2	248.1	291.0	219.4	170.5	160.6	155.8	171.0	0.609	0.547	1.58	0.147199	1.02	0.64	1.24	1.22
2330.0	0.170165	170.2				269.5	264.2	314.0	235.4	189.5	180.3	174.0	191.6	0.609	0.547	1.60	0.166158	1.02	0.66	1.20	1.16
																		1.01			

MODEL PIER, bp = 62 mm_LONG_DROWNED Q's

DATA: *Friday, 28 July 2000*

h_{mon_1}	h_{mon_2}	4 m	UE upstream end	US upstream side	DS downstream side	DE downstream end	6 m	7 m
		15.5					147.5	147.0
665.0	655.0	200.1	215.0	166.3	148.0	153.8	335.9	338.6
665.0	655.0	217.4	229.5	186.0	190.3	193.5	360.3	369.3
665.0	655.0	233.2	241.5	205.0	209.5	210.0	378.7	380.4
665.0	655.0	249.3	253.8	223.5	226.8	225.0	393.3	395.1
665.0	655.0	264.0	267.0	241.5	243.3	241.8	407.5	411.2

h_{mon_1}	h_{mon_2}	4 m	UE upstream end	US upstream side	DS downstream side	DE downstream end	6 m	7 m
		15.8					147.5	147.0
990.0	975.0	226.9	248.0	190.0	166.0	170.0	359.6	361.2
990.0	975.0	241.2	256.9	207.3	204.8	209.5	385.1	386.2
990.0	975.0	260.7	269.0	229.3	233.3	236.3	397.7	406.0
990.0	975.0	277.1	285.5	249.3	253.0	253.5	423.9	422.2
990.0	975.0	295.0	300.0	270.0	272.0	271.0	438.4	439.8

h_{mon_1}	h_{mon_2}	4 m	UE upstream end	US upstream side	DS downstream side	DE downstream end	6 m	7 m

		f5.5					**147.5**	**147.0**
1360.0	1355.0	260.2	278.5	222.3	207.8	206.0	395.0	394.5
1360.0	1355.0	271.9	288.8	237.3	233.5	237.5	414.6	416.4
1360.0	1355.0	289.8	302.5	257.5	260.5	263.8	441.5	432.0
1360.0	1355.0	304.5	316.0	275.0	280.0	281.5	443.6	459.5
1360.0	1355.0	327.6	330.0	294.5	297.8	296.8	470.3	469.8

h_{man_1}	h_{man_2}	4 m	UE upstream end	US upstream side	DS downstream side	DE downstream end	6 m	7 m
		f5.5					**147.5**	**147.0**
1810.0	1820.0	283.5	306.0	243.0	224.8	224.0	417.5	419.5
1810.0	1820.0	296.4	317.8	258.3	251.0	255.0	430.5	432.5
1810.0	1820.0	313.7	329.6	280.0	279.8	281.0	464.1	456.5
1810.0	1820.0	330.0	345.5	298.0	301.3	303.5	479.9	472.8
1810.0	1820.0	347.4	359.8	318.3	322.0	323.0	487.2	497.6

h_{man_1}	h_{man_2}	4 m	UE upstream end	US upstream side	DS downstream side	DE downstream end	6 m	7 m
		f5.5					**147.5**	**147.0**
2300.0	2310.0	310.0	334.5	270.0	252.0	251.5	446.3	448.5
2300.0	2310.0	322.5	345.0	284.0	276.0	275.5	457.5	460.9
2300.0	2310.0	338.8	358.8	304.0	300.8	301.0	478.1	481.6
2300.0	2310.0	355.5	373.0	324.8	326.0	327.8	511.1	499.5
2300.0	2310.0	374.0	388.8	344.0	348.0	349.0	518.5	520.6

CALCULATIONS

FLOW DEPTHS

h_{man_avg}	Q_{usb}	Q [l/s]	4 m y_4	UE upstream end y_{UE}	US upstream side y_{US}	DS downstream side y_{DS}	DE downstream end y_{DE}	6 m y_6	7 m y_7	B	B-b_2	v_c = $2g(y_{US}-y_{DS})^{1/3}$	Q_{theory}		$Fr_{...4m}$	$Fr_{...DS}$	$Fr_{...6m}$
660.0	0.060566	90.6	184.6	215.0	187.1	154.5	161.1	187.5	191.8	0.939	0.547	1.15	0.066579	0.93	0.60	0.78	0.58
660.0	0.060566	90.6	201.9	229.5	186.9	196.7	200.8	212.8	222.3	0.939	0.547	0.88	0.064431	0.96	0.52	0.54	0.48
660.0	0.060566	90.6	217.7	241.5	205.9	216.0	217.3	231.2	233.4	0.939	0.547	0.79	0.063608	0.97	0.47	0.47	0.43
660.0	0.060566	90.6	233.8	253.8	224.4	233.2	232.3	245.8	248.1	0.939	0.547	0.73	0.062852	0.98	0.42	0.42	0.39
660.0	0.060566	90.6	249.4	267.0	242.4	249.7	249.1	260.0	264.2	0.939	0.547	0.68	0.063246	0.97	0.38	0.35	0.36

h_{man_avg}	Q_{usb}	Q [l/s]	4 m y_4	UE upstream end y_{UE}	US upstream side y_{US}	DS downstream side y_{DS}	DE downstream end y_{DE}	6 m y_6	7 m y_7	B	B-b_2	v_c = $2g(y_{US}-y_{DS})^{1/3}$	Q_{theory}		$Fr_{...4m}$	$Fr_{...DS}$	$Fr_{...6m}$
682.5	0.110499	110.5	211.4	248.0	190.9	172.5	177.3	212.1	214.2	0.939	0.547	1.27	0.119465	0.92	0.60	0.81	0.59
682.5	0.110499	110.5	225.7	256.0	208.1	211.2	216.8	241.6	239.2	0.939	0.547	1.00	0.115858	0.95	0.54	0.60	0.49
682.5	0.110499	110.5	245.2	269.0	230.1	239.7	243.6	250.2	256.0	0.939	0.547	0.84	0.109821	1.01	0.48	0.49	0.46
682.5	0.110499	110.5	261.6	285.5	250.1	259.5	260.8	276.4	275.2	0.939	0.547	0.80	0.113337	0.97	0.43	0.44	0.40
682.5	0.110499	110.5	279.5	303.0	270.9	278.5	278.3	290.9	292.8	0.939	0.547	0.74	0.112902	0.98	0.39	0.39	0.37

h_{man_avg}	Q_{usb}	Q [l/s]	4 m y_4	UE upstream end y_{UE}	US upstream side y_{US}	DS downstream side y_{DS}	DE downstream end y_{DE}	6 m y_6	7 m y_7	B	B-b_2	v_c = $2g(y_{US}-y_{DS})^{1/3}$	Q_{theory}		$Fr_{...4m}$	$Fr_{...DS}$	$Fr_{...6m}$
1357.5	0.129886	129.9	244.7	278.5	223.1	214.2	216.3	247.5	247.5	0.939	0.547	1.18	0.135060	0.94	0.56	0.69	0.55
1357.5	0.129886	129.9	256.4	288.8	238.1	243.0	244.8	267.1	269.4	0.939	0.547	1.04	0.136668	0.95	0.52	0.58	0.49
1357.5	0.129886	129.9	274.3	302.5	258.4	267.0	271.1	294.0	285.0	0.939	0.547	0.91	0.132565	0.98	0.47	0.49	0.43
1357.5	0.129886	129.9	280.0	316.0	275.9	286.5	288.8	296.1	303.5	0.939	0.547	0.84	0.131696	0.99	0.44	0.44	0.42
1357.5	0.129886	129.9	312.1	330.0	295.4	304.2	304.1	322.8	322.8	0.939	0.547	0.80	0.132372	0.99	0.39	0.41	0.37

		UE upstream	US upstream	DS downstream	DE downstream

h_{weir_org}	Q_{calc}	Q [l/s]	4 m y_4	end y_{UE}	side y_{US}	side y_{DS}	end y_{DE}	6 m y_6	7 m y_7	B	B-b_y	v_c = $2g(y_{US}{\cdot}y_{DS})^{0.5}$	Q_{theory}	[illegible]	Fr_{-4m}	Fr_{-DS}	Fr_{-6m}
1815.0	0.150187	150.2	268.0	306.0	243.9	231.2	231.3	270.0	272.5	0.609	0.547	1.26	0.159691	0.94	0.57	0.71	0.56
1815.0	0.150187	150.2	280.9	317.8	259.1	257.5	262.3	283.0	285.5	0.609	0.547	1.14	0.161174	0.93	0.53	0.66	0.52
1815.0	0.150187	150.2	298.2	329.8	280.9	286.2	289.3	316.6	309.5	0.609	0.547	0.99	0.155070	0.97	0.48	0.51	0.44
1815.0	0.150187	150.2	314.5	345.5	298.9	307.7	310.8	332.4	325.6	0.609	0.547	0.93	0.156839	0.96	0.45	0.46	0.41
1815.0	0.150187	150.2	331.9	359.8	319.1	328.5	330.3	339.7	353.6	0.609	0.547	0.86	0.154831	0.97	0.41	0.42	0.40

h_{weir_org}	Q_{calc}	Q [l/s]	4 m y_4	UE upstream end y_{UE}	US upstream side y_{US}	DS downstream side y_{DS}	DE downstream end y_{DE}	6 m y_6	7 m y_7	B	B-b_y	v_c = $2g(y_{US}{\cdot}y_{DS})^{0.5}$	Q_{theory}	[illegible]	Fr_{-4m}	Fr_{-DS}	Fr_{-6m}
2305.0	0.169250	169.2	294.5	334.5	270.9	258.5	258.8	298.8	301.5	0.609	0.547	1.27	0.179879	0.94	0.56	0.68	0.54
2305.0	0.169250	169.2	307.0	345.0	284.9	282.5	282.8	310.0	313.9	0.609	0.547	1.16	0.179779	0.94	0.52	0.59	0.51
2305.0	0.169250	169.2	323.3	358.8	304.9	307.2	308.3	330.6	334.6	0.609	0.547	1.07	0.179299	0.94	0.48	0.52	0.47
2305.0	0.169250	169.2	340.0	373.0	325.8	332.5	335.1	353.6	352.5	0.609	0.547	0.96	0.174540	0.97	0.45	0.46	0.40
2305.0	0.169250	169.2	358.5	388.8	344.9	354.5	356.3	371.0	373.6	0.609	0.547	0.89	0.173374	0.98	0.41	0.42	0.39
														0.96			

MODEL PIER, bp = 32 mm_SHORT_5Degrees_NORMAL Q's OK

DATA: *Tuesday, 15 August 2000*

Q	$h_{man,1}$	$h_{man,2}$	0 m	1 m	2 m	3 m	4 m	UE upstream end	US upstream side	DS downstream side	DE downstream end	6 m	7 m
Bed levels			12.5	10.5	15.0	13.5	15.5					147.5	147.0
10	12.0	12.0				59.0	57.2	58.9	39.1	27.4	15.8	195.2	195.2
30	73.0	73.0				93.3	91.9	98.9	79.1	55.3	40.9	228.1	204.8
50	205.0	206.0				120.2	115.9	134.9	99.1	83.1	72.4	275.3	232.1
70	395.0	390.0				145.6	142.4	162.1	116.0	104.4	91.1	296.5	254.6
90	665.0	650.0				170.2	162.7	193.8	138.5	125.8	120.5	306.5	280.4
110	970.0	970.0				192.0	182.4	215.9	161.9	147.8	143.3	333.8	305.8
130	1340.0	1345.0				215.4	207.8	241.9	170.5	158.9	156.3	306.5	
150	1800.0	1810.0				233.4	225.0	262.4	190.0	177.1	174.1	337.1	
170	2320.0	2310.0				249.2	243.7	290.1	209.1	192.6	188.5	360.4	

Geometric properties:

D =	31.5 mm
L_p =	132 mm
z_A =	1.4 mm
z_B =	1.8 mm
z_C =	3.1 mm
z_D =	3.6 mm
Theta =	5 degrees

CALCULATIONS:

FLOW DEPTHS

Distance measured downstream within the flume

$h_{man,avg}$	Q_{man}	Q [l/s]	0 m y_0	1 m y_1	2 m y_2	3 m y_3	4 m y_4	UE upstream end y_{UE}	US upstream side y_{US}	DS downstream side y_{DS}	DE downstream end y_{DE}	6 m y_6	7 m y_7	B	B-b_p	v_c = $\sqrt{2g(y_{UE}-y_{DS})}$ *	Q_{theory}	Q_{man}/Q_{th}	Fr_4m	Fr_DS	Fr_DE
12.0	0.012212	12.2				45.5	41.7	58.9	43.9	30.5	19.3	47.7	48.2	0.609	0.569	0.77	0.013356	0.91	0.75	1.29	2.38
73.0	0.030120	30.1				79.8	76.4	98.9	71.9	58.4	44.4	80.6	57.8	0.609	0.569	0.91	0.030263	1.00	0.75	1.20	1.69
205.5	0.050536	50.5				106.7	100.4	134.9	97.9	86.3	75.9	127.8	85.1	0.609	0.569	0.99	0.048781	1.04	0.83	1.12	1.27
392.5	0.069841	69.8				132.1	125.9	162.1	117.8	107.5	94.7	149.0	107.6	0.609	0.569	1.05	0.064316	1.09	0.81	1.11	1.26
657.5	0.090394	90.4				156.7	147.2	193.8	140.3	128.9	124.1	159.0	133.4	0.609	0.569	1.14	0.083818	1.08	0.84	1.10	1.08
970.0	0.109794	109.8				178.5	166.9	215.9	163.7	150.9	146.8	186.3	158.8	0.609	0.569	1.14	0.098218	1.12	0.84	1.05	1.02
1342.5	0.129167	129.2				201.9	192.3	241.9	172.3	162.0	155.8	159.0	-147.0	0.609	0.569	1.27	0.116617	1.11	0.80	1.11	1.06
1805.0	0.149772	149.8				219.9	209.5	262.4	254.0	180.3	177.7	189.6	-147.0	0.609	0.569	1.28	0.131579	1.14	0.82	1.10	1.05
2315.0	0.166617	166.6				235.7	228.2	290.1	296.0	195.8	192.1	212.9	-147.0	0.609	0.569	1.37	0.152913	1.11	0.82	1.10	1.06
																		1.06			

MODEL PIER, bp = 32 mm_SHORT_5Degrees_DROWNED Q's

DATA: *Tuesday, 15 August 2000*

$h_{man,1}$	$h_{man,2}$	4 m	UE upstream end	US upstream side	DS downstream side	DE downstream end	6 m	7 m
		15.5					147.5	147.0
640.0	635.0	170.5	195.1	149.1	137.6	131.1	305.0	
640.0	635.0	190.1	204.9	177.8	168.4	161.3	345.3	
640.0	635.0	211.1	219.7	198.6	191.1	187.4	356.0	
640.0	635.0	229.9	237.3	217.6	213.9	208.5	375.1	
640.0	635.0	248.2	249.1	235.9	230.9	229.1	394.3	

$h_{man,1}$	$h_{man,2}$	4 m	UE upstream end	US upstream side	DS downstream side	DE downstream end	6 m	7 m
		15.5					147.5	147.0
0.0	0.0							
0.0	0.0							
0.0	0.0							
0.0	0.0							
0.0	0.0							

$h_{man,1}$	$h_{man,2}$	4 m	UE upstream end	US upstream side	DS downstream side	DE downstream end	6 m	7 m

		15.5					147.5	147.0
1375.0	1375.0	216.1	247.9	199.9	188.6	180.6	372.2	
1375.0	1375.0	240.8	262.1	227.1	214.9	211.3	375.5	
1375.0	1375.0	262.2	278.5	249.9	241.8	236.0	415.1	
1375.0	1375.0	284.0	295.0	272.0	263.8	259.8	431.1	
1375.0	1375.0	307.2	313.9	295.0	288.3	284.3	450.9	

h_{man_1}	h_{man_2}	4 m	UE upstream end	US upstream side	DS downstream side	DE downstream end	6 m	7 m
		15.5					147.5	147.0
0.0	0.0							
0.0	0.0							
0.0	0.0							
0.0	0.0							
0.0	0.0							

h_{man_1}	h_{man_2}	4 m	UE upstream end	US upstream side	DS downstream side	DE downstream end	6 m	7 m
		15.5					147.5	147.0
2350.0	2335.0	262.9	295.6	243.0	230.1	226.0	421.3	
2350.0	2335.0	284.5	314.6	272.9	260.9	251.4	428.5	
2350.0	2335.0	314.2	332.6	301.0	288.8	282.6	450.2	
2350.0	2335.0	334.0	348.1	321.5	312.9	308.3	486.6	
2350.0	2335.0	356.5	368.6	345.9	337.1	333.8	504.3	

CALCULATIONS:

FLOW DEPTHS

h_{man_avg}	Q_{calc}	Q [l/s]	4 m y_4	UE upstream end y_{UE}	US upstream side y_{US}	DS downstream side y_{DS}	DE downstream end y_{DE}	6 m y_6	7 m y_7	B	$B-b_p$	$v_C = 2g(y_{UE}-y_{DS})^{0.5}$	Q_{theory}	[illegible]	Fr_{4m}	Fr_{DS}	Fr_{6m}
637.5	0.089009	89.0	155.0	195.1	150.9	140.8	134.7	157.5	-147.0	0.609	0.569	1.05	0.084022	1.06	0.76	0.88	0.75
637.5	0.089009	89.0	174.6	204.9	179.5	171.5	164.8	197.8	-147.0	0.609	0.569	0.83	0.081001	1.10	0.64	0.66	0.53
637.5	0.089009	89.0	195.6	219.7	200.4	194.3	190.9	208.5	-147.0	0.609	0.569	0.73	0.080725	1.10	0.54	0.55	0.49
637.5	0.089009	89.0	214.4	237.3	219.4	216.1	212.1	227.6	-147.0	0.609	0.569	0.67	0.082392	1.08	0.47	0.46	0.43
637.5	0.089009	89.0	232.7	249.1	237.7	233.1	232.7	246.8	-147.0	0.609	0.569	0.59	0.078299	1.14	0.42	0.41	0.38

h_{man_avg}	Q_{calc}	Q [l/s]	4 m y_4	UE upstream end y_{UE}	US upstream side y_{US}	DS downstream side y_{DS}	DE downstream end y_{DE}	6 m y_6	7 m y_7	B	$B-b_p$	$v_C = 2g(y_{UE}-y_{DS})^{0.5}$	Q_{theory}	[illegible]	Fr_{4m}	Fr_{DS}	Fr_{6m}
0.0	0.000000	0.0	-15.5	0.0	1.8	3.1	3.6	-147.5	-147.0	0.609	0.569	#NUM!	#NUM!	#NUM!	#NUM!	0.00	#NUM!
0.0	0.000000	0.0	-15.5	0.0	1.8	3.1	3.6	-147.5	-147.0	0.609	0.569	#NUM!	#NUM!	#NUM!	#NUM!	0.00	#NUM!
0.0	0.000000	0.0	-15.5	0.0	1.8	3.1	3.6	-147.5	-147.0	0.609	0.569	#NUM!	#NUM!	#NUM!	#NUM!	0.00	#NUM!
0.0	0.000000	0.0	-15.5	0.0	1.8	3.1	3.6	-147.5	-147.0	0.609	0.569	#NUM!	#NUM!	#NUM!	#NUM!	0.00	#NUM!
0.0	0.000000	0.0	-15.5	0.0	1.8	3.1	3.6	-147.5	-147.0	0.609	0.569	#NUM!	#NUM!	#NUM!	#NUM!	0.00	#NUM!

h_{man_avg}	Q_{calc}	Q [l/s]	4 m y_4	UE upstream end y_{UE}	US upstream side y_{US}	DS downstream side y_{DS}	DE downstream end y_{DE}	6 m y_6	7 m y_7	B	$B-b_p$	$v_C = 2g(y_{UE}-y_{DS})^{0.5}$	Q_{theory}	[illegible]	Fr_{4m}	Fr_{DS}	Fr_{6m}
1375.0	0.130721	130.7	200.6	247.9	201.7	191.8	184.2	224.7	-147.0	0.609	0.569	1.07	0.116238	1.12	0.76	0.82	0.64
1375.0	0.130721	130.7	225.3	262.1	228.9	218.0	214.8	228.0	-147.0	0.609	0.569	0.95	0.117580	1.11	0.64	0.67	0.63
1375.0	0.130721	130.7	246.7	278.5	251.7	244.9	239.6	267.6	-147.0	0.609	0.569	0.83	0.116067	1.13	0.56	0.57	0.50
1375.0	0.130721	130.7	268.5	295.0	273.8	266.9	263.3	283.6	-147.0	0.609	0.569	0.77	0.116254	1.12	0.45	0.50	0.45
1375.0	0.130721	130.7	291.7	313.9	296.8	291.4	287.8	303.4	-147.0	0.609	0.569	0.69	0.114512	1.14	0.43	0.44	0.41

UE	US	DS	DE
upstream	upstream	downstream	downstream

			4 m	end	side	side	end	6 m	7 m			v_c =					
h_{man_avg}	Q_{calc}	Q [l/s]	y_4	y_{ue}	y_{us}	y_{ds}	y_{de}	y_6	y_7	B	B-b_p	$2g(y_{ue}-y_{ds})^{0.5}$	Q_{theory}	[illegible]	Fr_4m	Fr_cs	Fr_6m
0.0	0.000000	0.0	-15.5	0.0	1.8	3.1	3.6	-147.5	-147.0	0.609	0.569	#NUM!	#NUM!	#NUM!	#NUM!	0.00	#NUM!
0.0	0.000000	0.0	-15.5	0.0	1.8	3.1	3.6	-147.5	-147.0	0.609	0.569	#NUM!	#NUM!	#NUM!	#NUM!	0.00	#NUM!
0.0	0.000000	0.0	-15.5	0.0	1.8	3.1	3.6	-147.5	-147.0	0.609	0.569	#NUM!	#NUM!	#NUM!	#NUM!	0.00	#NUM!
0.0	0.000000	0.0	-15.5	0.0	1.8	3.1	3.6	-147.5	-147.0	0.609	0.569	#NUM!	#NUM!	#NUM!	#NUM!	0.00	#NUM!
0.0	0.000000	0.0	-15.5	0.0	1.8	3.1	3.6	-147.5	-147.0	0.609	0.569	#NUM!	#NUM!	#NUM!	#NUM!	0.00	#NUM!

			4 m	UE upstream end	US upstream side	DS downstream side	DE downstream end	6 m	7 m			v_c =					
h_{man_avg}	Q_{calc}	Q [l/s]	y_4	y_{ue}	y_{us}	y_{ds}	y_{de}	y_6	y_7	B	B-b_p	$2g(y_{ue}-y_{ds})^{0.5}$	Q_{theory}	[illegible]	Fr_4m	Fr_cs	Fr_6m
2342.5	0.170621	170.6	247.4	295.6	244.8	233.3	229.6	273.8	-147.0	0.609	0.569	1.12	0.148828	1.15	0.73	0.79	0.62
2342.5	0.170621	170.6	269.0	314.6	274.7	264.0	254.9	281.0	-147.0	0.609	0.569	1.01	0.152242	1.12	0.64	0.66	0.60
2342.5	0.170621	170.6	298.7	332.6	302.8	291.9	286.2	302.7	-147.0	0.609	0.569	0.91	0.151629	1.13	0.55	0.57	0.54
2342.5	0.170621	170.6	318.5	348.1	323.3	316.0	311.8	339.1	-147.0	0.609	0.569	0.82	0.146572	1.16	0.50	0.50	0.45
2342.5	0.170621	170.6	341.0	368.6	347.7	340.3	337.3	356.8	-147.0	0.609	0.569	0.77	0.148835	1.15	0.45	0.45	0.42
														1.12			

MODEL PIER, bp = 32 mm_SHORT_10Degrees_NORMAL Q's OK

DATA: *Monday, 14 August 2000*

Q	h_{man_1}	h_{man_2}	0 m	1 m	2 m	3 m	4 m	UE upstream end	US upstream side	DS downstream side	DE downstream end	6 m	7 m
bed levels			*12.5*	*10.5*	*15.0*	*13.5*	*15.5*					*147.5*	*147.0*
10	10.0	10.0				56.8	55.3	56.8	39.5	27.9	15.5	188.7	
30	75.0	75.0				94.2	92.6	100.6	73.9	58.8	40.4	226.5	
50	202.0	203.5				120.8	117.1	134.8	102.6	87.8	71.5	277.5	
70	390.0	393.0				146.2	144.0	159.6	124.3	108.0	96.5	294.5	
90	665.0	665.0				171.8	166.0	189.9	150.0	132.0	120.5	305.3	
110	960.0	950.0				192.3	184.5	211.6	170.5	150.6	138.4	332.5	
130	1370.0	1375.0				219.4	210.4	236.4	196.1	174.6	154.8	305.8	
150	1810.0	1820.0				237.1	229.2	259.4	208.0	186.8	177.9	336.2	
170	2300.0	2310.0				251.7	246.2	280.0	230.4	264.9	195.9	360.2	

Geometric properties:

D =	31.5 mm
L_p =	132 mm
r_A =	1.4 mm
r_B =	1.8 mm
r_C =	3.1 mm
r_D =	3.6 mm
Theta =	10 degrees

CALCULATIONS:

FLOW DEPTHS

h_{man_avg}	Q_{man}	Q [l/s]	Distance measured downstream within the flume: 0 m y_0	1 m y_1	2 m y_2	3 m y_3	4 m y_4	UE upstream end y_{UE}	US upstream side y_{US}	DS downstream side y_{DS}	DE downstream end y_{DE}	6 m y_6	7 m y_7	B	B-b_p	v_C = $\sqrt{2g(y_{UE}-y_{DS})}^{0.5}$	Q_{theory}	Q/Q_{theory}	Fr_4m	Fr_DS	Fr_DE
10.0	0.011148	11.1				43.3	39.8	56.8	41.3	31.0	19.1	41.2	-147.0	0.609	0.569	0.73	0.012759	0.87	0.74	1.16	2.22
75.0	0.030530	30.5				80.7	77.1	100.6	75.7	61.9	43.9	79.0	-147.0	0.609	0.569	0.89	0.030877	0.99	0.75	1.13	1.74
202.8	0.050197	50.2				107.3	101.6	134.8	104.4	90.9	75.1	130.0	-147.0	0.609	0.569	0.95	0.046200	1.04	0.81	1.04	1.28
391.5	0.069752	69.8				132.7	128.5	159.6	126.0	111.1	100.1	147.0	-147.0	0.609	0.569	0.99	0.061773	1.13	0.79	1.07	1.86
665.0	0.090908	90.9				158.3	150.5	189.9	151.8	135.1	124.1	157.8	-147.0	0.609	0.569	1.05	0.079695	1.14	0.82	1.04	1.09
955.0	0.108642	108.9				178.8	169.0	211.6	172.3	153.8	141.9	165.0	-147.0	0.609	0.569	1.08	0.093154	1.17	0.82	1.03	1.07
1372.5	0.130602	130.6				205.9	194.9	236.4	197.9	177.8	168.3	156.3	-147.0	0.609	0.569	1.09	0.108369	1.21	0.80	0.99	0.99
1815.0	0.150187	150.2				223.6	213.7	259.4	254.0	189.5	181.4	188.7	-147.0	0.609	0.569	1.18	0.125752	1.19	0.80	1.03	1.02
2305.0	0.169250	169.2				238.2	230.7	283.0	296.0	208.0	199.4	212.7	-147.0	0.609	0.569	1.20	0.140151	1.21	0.80	1.02	1.00
																		1.11			

MODEL PIER, bp = 32 mm_SHORT_10Degrees_DROWNED Q's

DATA: *Monday, 14 August 2000*

h_{man_1}	h_{man_2}	4 m	UE upstream end	US upstream side	DS downstream side	DE downstream end	6 m	7 m
		15.5					*147.5*	*147.0*
650.0	635.0	181.6	195.5	171.4	155.3	149.4	326.4	
650.0	635.0	203.7	210.0	194.8	182.4	176.6	348.8	
650.0	635.0	221.4	222.9	214.1	203.6	200.3	368.5	
650.0	635.0	240.5	240.7	232.4	223.8	220.3	384.5	
650.0	635.0	256.5	258.7	247.4	242.0	240.8	404.2	

h_{man_1}	h_{man_2}	4 m	UE upstream end	US upstream side	DS downstream side	DE downstream end	6 m	7 m
		15.5					*147.5*	*147.0*
0.0	0.0							
0.0	0.0							
0.0	0.0							
0.0	0.0							
0.0	0.0							

h_{man_1}	h_{man_2}	4 m	UE upstream end	US upstream side	DS downstream side	DE downstream end	6 m	7 m

		15.5					147.5	147.0
1370.0	1370.0	228.6	249.6	219.0	203.5	194.5	366.9	
1370.0	1370.0	251.9	263.0	244.3	228.9	221.4	397.2	
1370.0	1370.0	268.8	277.0	261.3	249.9	243.3	419.1	
1370.0	1370.0	289.2	293.0	280.0	267.5	261.1	433.9	
1370.0	1370.0	307.7	312.4	297.6	288.5	283.9	453.9	

h_{man_1}	h_{man_2}	4 m	UE upstream end	US upstream side	DS downstream side	DE downstream end	6 m	7 m
		15.5					147.5	147.0
0.0	0.0							
0.0	0.0							
0.0	0.0							
0.0	0.0							
0.0	0.0							

h_{man_1}	h_{man_2}	4 m	UE upstream end	US upstream side	DS downstream side	DE downstream end	6 m	7 m
		15.5					147.5	147.0
2360.0	2390.0	275.2	293.6	268.3	245.9	236.8	423.9	
2360.0	2390.0	297.8	314.3	291.9	273.4	266.9	431.8	
2360.0	2390.0	317.0	328.9	309.5	292.9	286.3	452.8	
2360.0	2390.0	336.7	348.0	348.0	312.4	304.8	487.5	
2360.0	2390.0	353.0	364.5	346.0	333.1	324.8	502.1	

CALCULATIONS

FLOW DEPTHS

h_{man_avg}	Q_{calc}	Q [l/s]	4 m y_4	UE upstream end y_{UE}	US upstream side y_{US}	DS downstream side y_{DS}	DE downstream end y_{DE}	6 m y_6	7 m y_7	B	$B\text{-}b_2$	$v_C = 2g(y_{UE}-y_{DS})^{0.5}$	Q_{theory}	[illegible]	Fr_{4m}	Fr_{DS}	Fr_{6m}
642.5	0.089357	89.4	166.1	195.8	173.2	158.4	151.9	178.9	-147.0	0.609	0.560	0.89	0.077737	1.15	0.69	0.74	0.62
642.5	0.089357	89.4	188.2	210.0	196.5	185.5	180.2	201.3	-147.0	0.609	0.560	0.72	0.074592	1.20	0.57	0.59	0.52
642.5	0.089357	89.4	205.9	222.9	215.9	206.8	203.8	221.0	-147.0	0.609	0.560	0.59	0.068619	1.30	0.50	0.50	0.45
642.5	0.089357	89.4	225.0	240.7	234.2	226.9	223.8	237.0	-147.0	0.609	0.560	0.55	0.070266	1.27	0.44	0.43	0.41
642.5	0.089357	89.4	241.0	258.7	249.2	245.1	244.3	256.7	-147.0	0.609	0.560	0.55	0.075307	1.19	0.40	0.39	0.36

h_{man_avg}	Q_{calc}	Q [l/s]	4 m y_4	UE upstream end y_{UE}	US upstream side y_{US}	DS downstream side y_{DS}	DE downstream end y_{DE}	6 m y_6	7 m y_7	B	$B\text{-}b_2$	$v_C = 2g(y_{UE}-y_{DS})^{0.5}$	Q_{theory}	[illegible]	Fr_{4m}	Fr_{DS}	Fr_{6m}
0.0	0.000000	0.0	-15.5	0.0	1.8	3.1	3.6	-147.5	-147.0	0.609	0.560	#NUM!	#NUM!	#NUM!	#NUM!	0.00	#NUM!
0.0	0.000000	0.0	-15.5	0.0	1.8	3.1	3.6	-147.5	-147.0	0.609	0.560	#NUM!	#NUM!	#NUM!	#NUM!	0.00	#NUM!
0.0	0.000000	0.0	-15.5	0.0	1.8	3.1	3.6	-147.5	-147.0	0.609	0.560	#NUM!	#NUM!	#NUM!	#NUM!	0.00	#NUM!
0.0	0.000000	0.0	-15.5	0.0	1.8	3.1	3.6	-147.5	-147.0	0.609	0.560	#NUM!	#NUM!	#NUM!	#NUM!	0.00	#NUM!
0.0	0.000000	0.0	-15.5	0.0	1.8	3.1	3.6	-147.5	-147.0	0.609	0.560	#NUM!	#NUM!	#NUM!	#NUM!	0.00	#NUM!

h_{man_avg}	Q_{calc}	Q [l/s]	4 m y_4	UE upstream end y_{UE}	US upstream side y_{US}	DS downstream side y_{DS}	DE downstream end y_{DE}	6 m y_6	7 m y_7	B	$B\text{-}b_2$	$v_C = 2g(y_{UE}-y_{DS})^{0.5}$	Q_{theory}	[illegible]	Fr_{4m}	Fr_{DS}	Fr_{6m}
1370.0	0.130483	130.5	213.1	249.6	220.8	206.6	198.1	219.4	-147.0	0.609	0.560	0.94	0.108462	1.20	0.70	0.73	0.67
1370.0	0.130483	130.5	236.4	263.0	246.0	232.0	224.9	249.7	-147.0	0.609	0.560	0.80	0.104192	1.25	0.60	0.61	0.55
1370.0	0.130483	130.5	253.3	277.0	263.0	253.0	246.8	271.6	-147.0	0.609	0.560	0.71	0.100761	1.29	0.54	0.54	0.48
1370.0	0.130483	130.5	273.7	293.0	281.8	270.6	264.7	286.4	-147.0	0.609	0.560	0.69	0.104328	1.25	0.48	0.49	0.45
1370.0	0.130483	130.5	292.2	312.4	299.4	291.6	287.4	306.4	-147.0	0.609	0.560	0.66	0.108575	1.20	0.43	0.43	0.40

				UE upstream	US upstream	DS downstream	DE downstream		

			4 m	end	side	side	end	6 m	7 m			v_c =					
h_{man_avg}	Q_{calc}	Q [l/s]	y_4	y_{UE}	y_{US}	y_{DS}	y_{DE}	y_6	y_7	B	$B-b_p$	$2g(y_{UE}-y_{DS})^{0.5}$	Q_{theory}	[illegible]	$Fr_{\_4m}$	$Fr_{\_DS}$	$Fr_{\_6m}$
0.0	0.000000	0.0	-15.5	0.0	1.8	3.1	3.6	-147.5	-147.0	0.809	0.560	#NUM!	#NUM!	#NUM!	#NUM!	0.00	#NUM!
0.0	0.000000	0.0	-15.5	0.0	1.8	3.1	3.6	-147.5	-147.0	0.809	0.560	#NUM!	#NUM!	#NUM!	#NUM!	0.00	#NUM!
0.0	0.000000	0.0	-15.5	0.0	1.8	3.1	3.6	-147.5	-147.0	0.809	0.560	#NUM!	#NUM!	#NUM!	#NUM!	0.00	#NUM!
0.0	0.000000	0.0	-15.5	0.0	1.8	3.1	3.6	-147.5	-147.0	0.809	0.560	#NUM!	#NUM!	#NUM!	#NUM!	0.00	#NUM!
0.0	0.000000	0.0	-15.5	0.0	1.8	3.1	3.6	-147.5	-147.0	0.809	0.560	#NUM!	#NUM!	#NUM!	#NUM!	0.00	#NUM!

				UE	US	DS	DE										
				upstream	upstream	downstream	downstream										
			4 m	end	side	side	end	6 m	7 m			v_c =					
h_{man_avg}	Q_{calc}	Q [l/s]	y_4	y_{UE}	y_{US}	y_{DS}	y_{DE}	y_6	y_7	B	$B-b_p$	$2g(y_{UE}-y_{DS})^{0.5}$	Q_{theory}	[illegible]	$Fr_{\_4m}$	$Fr_{\_DS}$	$Fr_{\_6m}$
2375.0	0.171801	171.8	259.7	293.6	270.0	250.0	240.3	276.4	-147.0	0.809	0.560	0.94	0.132143	1.30	0.68	0.72	0.62
2375.0	0.171801	171.8	262.3	314.3	293.7	276.5	270.4	284.3	-147.0	0.809	0.560	0.88	0.136366	1.26	0.60	0.62	0.59
2375.0	0.171801	171.8	301.5	328.5	311.3	296.0	289.8	305.3	-147.0	0.809	0.560	0.82	0.136684	1.26	0.54	0.56	0.53
2375.0	0.171801	171.8	321.2	348.0	340.8	315.5	308.3	343.0	-147.0	0.809	0.560	0.82	0.144898	1.19	0.49	0.51	0.45
2375.0	0.171801	171.8	337.5	364.5	347.8	336.3	328.3	354.8	-147.0	0.809	0.560	0.77	0.144536	1.19	0.46	0.46	0.43
														1.23			

MODEL PIER, bp = 32 mm_SHORT_15Degrees_NORMAL Q's OK

DATA *Sunday, 13 August 2000*

Q	h_{man_1}	h_{man_2}	0 m	1 m	2 m	3 m	4 m	UE upstream end	US upstream side	DS downstream side	DE downstream end	6 m	7 m
Bed levels			12.5	10.5	15.0	13.5	15.5					147.5	147.0
10	11.0	10.5				58.5	57.0	57.8	44.6	31.8	15.0	197.7	
30	71.5	71.0				93.7	92.2	96.6	82.0	53.1	41.5	232.8	
50	208.0	207.5				125.0	122.1	125.1	118.5	94.9	74.5	257.5	
70	395.0	397.0				149.3	147.8	150.2	142.3	119.3	102.9	293.5	
90	660.0	645.0				173.9	172.7	171.3	168.6	141.3	125.5	286.9	
110	965.0	960.0				197.3	191.2	199.3	185.9	162.1	147.3	320.5	
130	1350.0	1353.0				219.2	210.5	225.1	209.1	178.1	160.8	302.4	
150	1820.0	1830.0				246.2	239.4	246.5	238.4	201.8	182.3	322.3	
170	2300.0	2300.0				261.6	256.8	268.4	252.9	215.4	194.8	341.8	

Geometric properties:

D =	31.5 mm
L_y =	132 mm
z_a =	1.4 mm
z_b =	1.8 mm
z_c =	3.1 mm
z_d =	3.6 mm
Theta =	15 degrees

CALCULATIONS

FLOW DEPTHS

h_{man_avg}	Q_{calc}	Q [l/s]	Distance measured downstream within the flume: 0 m y_0	1 m y_1	2 m y_2	3 m y_3	4 m y_4	UE upstream end y_{UE}	US upstream side y_{US}	DS downstream side y_{DS}	DE downstream end y_{DE}	6 m y_6	7 m y_7	B	B-b_0	x_L = $2g(y_{UE}-y_{DS})^{1.5}$	Q_{man_2}	Q_{calc}/Q_{man_2}	Fr_4m	Fr_DS	Fr_DE
10.8	0.011558	11.6				45.0	41.5	57.8	46.4	34.9	18.6	50.2	-147.0	0.609	0.551	0.70	0.013378	0.86	0.72	1.03	2.39
71.3	0.029757	29.8				80.2	76.7	96.6	83.6	66.3	45.1	85.3	-147.0	0.609	0.551	0.79	0.025990	1.03	0.73	1.01	1.63
207.8	0.050812	50.8				111.5	106.6	125.1	120.5	98.0	78.1	70.0	-147.0	0.609	0.551	0.75	0.043653	1.25	0.77	0.99	1.22
396.0	0.070152	70.2				135.8	132.3	153.2	144.0	122.4	106.4	146.0	-147.0	0.609	0.551	0.76	0.051421	1.36	0.76	0.95	1.06
652.5	0.090050	90.0				160.4	157.2	171.3	170.4	144.4	129.1	139.4	-147.0	0.609	0.551	0.75	0.059696	1.51	0.76	0.95	1.02
962.5	0.109389	109.4				183.8	175.7	199.3	191.7	165.3	150.8	173.0	-147.0	0.609	0.551	0.84	0.070419	1.43	0.78	0.94	0.98
1350.0	0.129527	129.5				205.7	195.0	225.1	210.9	181.3	164.3	154.9	-147.0	0.609	0.551	0.95	0.094599	1.37	0.79	0.97	1.02
1825.0	0.150600	150.6				232.7	223.5	246.5	254.0	204.9	185.8	174.8	-147.0	0.609	0.551	0.92	0.104261	1.44	0.75	0.94	0.99
2300.0	0.169066	169.1				248.1	241.3	268.4	296.0	218.5	198.3	194.3	-147.0	0.609	0.551	1.01	0.121304	1.39	0.75	0.96	1.00
																		1.29			

MODEL PIER, bp = 32 mm_SHORT_15Degrees_DROWNED Q's

DATA *Sunday, 13 August 2000*

h_{man_1}	h_{man_2}	4 m	UE upstream end	US upstream side	DS downstream side	DE downstream end	6 m	7 m
		15.5					147.5	147.0
633.0	660.5	151.2	188.6	191.8	170.0	158.9	339.5	
633.0	660.0	212.5	209.6	210.5	193.3	182.4	357.8	
633.0	660.0	230.9	232.1	225.6	211.5	202.9	375.0	
633.0	660.0	248.2	247.1	243.9	228.8	220.4	392.5	
633.0	660.0	264.9	263.9	254.6	245.4	240.0	408.9	

h_{man_1}	h_{man_2}	4 m	UE upstream end	US upstream side	DS downstream side	DE downstream end	6 m	7 m
		15.5					147.5	147.0
0.0	0.0							
0.0	0.0							
0.0	0.0							
0.0	0.0							
0.0	0.0							

h_{man_1}	h_{man_2}	4 m	UE upstream end	US upstream side	DS downstream side	DE downstream end	6 m	7 m

		15.5					147.5	147.0
1365.0	1360.0	243.4	245.5	239.6	213.1	197.0	372.5	
1365.0	1360.0	264.9	267.5	261.0	237.5	219.8	410.3	
1365.0	1360.0	279.8	278.5	275.0	256.0	242.3	424.5	
1365.0	1360.0	298.3	298.5	291.6	274.1	264.5	443.2	
1365.0	1360.0	317.1	317.4	336.6	293.5	283.1	459.8	

h_{man_1}	h_{man_2}	4 m	UE upstream end	US upstream side	DS downstream side	DE downstream end	6 m	7 m
		15.5					147.5	147.0
0.0	0.0							
0.0	0.0							
0.0	0.0							
0.0	0.0							
0.0	0.0							

h_{man_1}	h_{man_2}	4 m	UE upstream end	US upstream side	DS downstream side	DE downstream end	6 m	7 m
		15.5					147.5	147.0
2330.0	2320.0	277.9	281.3	274.5	241.8	222.4	452.2	
2330.0	2320.0	298.0	303.8	294.3	265.1	244.5	424.5	
2330.0	2320.0	318.1	323.8	311.8	285.8	268.4	455.3	
2330.0	2320.0	337.8	341.3	331.8	307.5	291.1	482.9	
2330.0	2320.0	357.0	360.4	351.3	329.6	317.9	500.9	

CALCULATIONS

FLOW DEPTHS

h_{man_avg}	Q_{calc}	Q [l/s]	4 m y_4	UE upstream end y_{UE}	US upstream side y_{US}	DS downstream side y_{DS}	DE downstream end y_{DE}	6 m y_6	7 m y_7	B	$B-b_0$	$v_c = 2g(y_{UE}-y_{DS})^{0.5}$	Q_{theory}	[illegible]	Fr_{4m}	Fr_{DS}	Fr_{6m}
645.0	0.089531	89.5	175.7	188.6	193.5	173.1	162.4	192.0	-147.0	0.609	0.551	0.58	0.055584	1.61	0.64	0.65	0.56
645.0	0.089531	89.5	197.0	209.8	212.3	196.4	185.9	210.3	-147.0	0.609	0.551	0.55	0.059044	1.52	0.54	0.54	0.49
645.0	0.089531	89.5	215.4	232.1	227.4	214.6	206.4	227.5	-147.0	0.609	0.551	0.61	0.072788	1.23	0.47	0.47	0.43
645.0	0.089531	89.5	232.7	247.1	242.7	231.9	223.9	245.0	-147.0	0.609	0.551	0.58	0.073906	1.21	0.42	0.42	0.39
645.0	0.089531	89.5	249.4	263.9	256.4	248.5	243.6	262.4	-147.0	0.609	0.551	0.58	0.079495	1.13	0.38	0.38	0.35

h_{man_avg}	Q_{calc}	Q [l/s]	4 m y_4	UE upstream end y_{UE}	US upstream side y_{US}	DS downstream side y_{DS}	DE downstream end y_{DE}	6 m y_6	7 m y_7	B	$B-b_0$	$v_c = 2g(y_{UE}-y_{DS})^{0.5}$	Q_{theory}	[illegible]	Fr_{4m}	Fr_{DS}	Fr_{6m}
0.0	0.000000	0.0	-15.5	0.0	1.8	3.1	3.6	-147.5	-147.0	0.609	0.551	#NUM!	#NUM!	#NUM!	#NUM!	0.00	#NUM!
0.0	0.000000	0.0	-15.5	0.0	1.8	3.1	3.6	-147.5	-147.0	0.609	0.551	#NUM!	#NUM!	#NUM!	#NUM!	0.00	#NUM!
0.0	0.000000	0.0	-15.5	0.0	1.8	3.1	3.6	-147.5	-147.0	0.609	0.551	#NUM!	#NUM!	#NUM!	#NUM!	0.00	#NUM!
0.0	0.000000	0.0	-15.5	0.0	1.8	3.1	3.6	-147.5	-147.0	0.609	0.551	#NUM!	#NUM!	#NUM!	#NUM!	0.00	#NUM!
0.0	0.000000	0.0	-15.5	0.0	1.8	3.1	3.6	-147.5	-147.0	0.609	0.551	#NUM!	#NUM!	#NUM!	#NUM!	0.00	#NUM!

h_{man_avg}	Q_{calc}	Q [l/s]	4 m y_4	UE upstream end y_{UE}	US upstream side y_{US}	DS downstream side y_{DS}	DE downstream end y_{DE}	6 m y_6	7 m y_7	B	$B-b_0$	$v_c = 2g(y_{UE}-y_{DS})^{0.5}$	Q_{theory}	[illegible]	Fr_{4m}	Fr_{DS}	Fr_{6m}
1362.5	0.130125	130.1	227.9	245.5	241.4	216.3	200.6	225.0	-147.0	0.609	0.551	0.78	0.093046	1.40	0.63	0.68	0.64
1362.5	0.130125	130.1	249.4	267.5	262.8	240.6	223.3	262.8	-147.0	0.609	0.551	0.75	0.099492	1.31	0.55	0.58	0.51
1362.5	0.130125	130.1	264.3	278.5	276.8	259.1	245.8	277.0	-147.0	0.609	0.551	0.64	0.092055	1.41	0.50	0.52	0.47
1362.5	0.130125	130.1	282.8	298.5	293.4	277.3	268.1	295.7	-147.0	0.609	0.551	0.67	0.102767	1.27	0.45	0.47	0.42
1362.5	0.130125	130.1	301.6	317.4	310.4	296.6	286.7	312.3	-147.0	0.609	0.551	0.67	0.108869	1.19	0.41	0.42	0.39

UE	US	DS	DE
upstream	upstream	downstream	downstream

			4 m	end	side	side	end	6 m	7 m			$v_C =$					
h_{man_avg}	Q_{calc}	Q [l/s]	y_4	y_{UE}	y_{US}	y_{DS}	y_{DE}	y_6	y_7	B	$B\text{-}b_p$	$2g(y_{UE}-y_{DS})^{0.5}$	Q_{theory}	[illegible]	$Fr_{\_4m}$	$Fr_{\_DS}$	$Fr_{\_6m}$
0.0	0.000000	0.0	-15.5	0.0	1.8	3.1	3.6	-147.5	-147.0	0.609	0.551	#NUM!	#NUM!	#NUM!	#NUM!	0.00	#NUM!
0.0	0.000000	0.0	-15.5	0.0	1.8	3.1	3.6	-147.5	-147.0	0.609	0.551	#NUM!	#NUM!	#NUM!	#NUM!	0.00	#NUM!
0.0	0.000000	0.0	-15.5	0.0	1.8	3.1	3.6	-147.5	-147.0	0.609	0.551	#NUM!	#NUM!	#NUM!	#NUM!	0.00	#NUM!
0.0	0.000000	0.0	-15.5	0.0	1.8	3.1	3.6	-147.5	-147.0	0.609	0.551	#NUM!	#NUM!	#NUM!	#NUM!	0.00	#NUM!
0.0	0.000000	0.0	-15.5	0.0	1.8	3.1	3.6	-147.5	-147.0	0.609	0.551	#NUM!	#NUM!	#NUM!	#NUM!	0.00	#NUM!

				UE upstream	US upstream	DS downstream	DE downstream										
			4 m	end	side	side	end	6 m	7 m			$v_C =$					
h_{man_avg}	Q_{calc}	Q [l/s]	y_4	y_{UE}	y_{US}	y_{DS}	y_{DE}	y_6	y_7	B	$B\text{-}b_p$	$2g(y_{UE}-y_{DS})^{0.5}$	Q_{theory}	[illegible]	$Fr_{\_4m}$	$Fr_{\_DS}$	$Fr_{\_6m}$
2325.0	0.169683	170.0	262.4	281.3	276.3	244.9	225.9	304.7	-147.0	0.606	0.551	0.87	0.116836	1.45	0.66	0.74	0.53
2325.0	0.169683	170.0	282.5	303.8	296.0	268.3	248.1	277.0	-147.0	0.609	0.551	0.86	0.126513	1.34	0.59	0.64	0.61
2325.0	0.169683	170.0	302.6	323.8	313.5	288.9	271.9	307.8	-147.0	0.606	0.551	0.85	0.135093	1.26	0.54	0.57	0.52
2325.0	0.169683	170.0	322.3	341.3	333.5	310.6	294.7	335.4	-147.0	0.609	0.551	0.80	0.136582	1.24	0.49	0.51	0.46
2325.0	0.169683	170.0	341.5	360.4	353.0	332.8	321.4	353.4	-147.0	0.609	0.551	0.76	0.139372	1.22	0.45	0.46	0.42
														1.32			

MODEL PIER, bp = 32 mm_MEDIUM_5Degrees_NORMAL Q's OK

DATA Sunday, 13 August 2000

Q	h_{man_1}	h_{man_2}	0 m	1 m	2 m	3 m	4 m	UE upstream end	US upstream side	DS downstream side	DE downstream end	6 m	7 m
bed levels			12.5	10.5	15.0	13.5	15.5					147.5	147.0
10	12.0	12.5				59.2	57.3	59.1	38.5	26.3	16.8	195.7	
30	79.0	78.0				95.3	94.5	103.1	72.4	53.0	42.0	236.0	204.5
50	209.0	208.5				122.3	118.9	138.8	99.8	81.3	67.9	277.1	231.0
70	406.0	405.0				148.1	145.4	166.6	120.4	103.3	93.0	297.2	257.0
90	640.0	650.0				165.2	165.1	194.5	140.9	124.5	115.9	299.1	274.0
110	955.0	960.0				191.7	183.6	216.1	162.5	143.8	134.4	277.6	
130	1350.0	1350.0				215.9	209.0	242.5	178.0	163.6	157.3	333.5	
150	1840.0	1825.0				234.6	227.3	269.9	195.0	178.8	173.5	328.9	
170	2360.0	2315.0				251.5	246.6	291.6	212.6	197.0	192.0	356.4	

Geometric properties:

D =	31.5 mm
L_0 =	178 mm
z_A =	0.6 mm
z_B =	1.3 mm
z_C =	3.4 mm
z_D =	3.8 mm

CALCULATIONS

FLOW DEPTHS

h_{man_avg}	Q_{corr}	Q [l/s]	Distance measured downstream within the flume: 0 m y_0	1 m y_1	2 m y_2	3 m y_3	4 m y_4	UE upstream end y_{UE}	US upstream side y_{US}	DS downstream side y_{DS}	DE downstream end y_{DE}	6 m y_6	7 m y_7	B	$B-b_0$	$v_c = \sqrt{2g(h_{up}-y_{cr})^{1.5}}$	Q_{theory}	[illegible]	Fr_4m	Fr_DS	Fr_DE
12.3	0.012338	12.3				45.7	41.8	59.1	39.8	29.6	20.6	48.2	-147.0	0.609	0.564	0.79	0.313261	0.93	0.76	1.37	2.19
78.5	0.031234	31.2				81.8	79.0	103.1	73.7	56.4	45.8	88.5	57.5	0.609	0.564	0.98	0.331252	1.00	0.74	1.32	1.87
208.8	0.050534	50.9				108.8	103.4	138.8	101.0	84.8	71.7	129.6	84.0	0.609	0.564	1.05	0.053059	1.01	0.80	1.17	1.39
405.5	0.070989	71.0				134.6	129.9	166.8	121.7	106.8	96.8	149.7	110.0	0.609	0.564	1.11	0.066823	1.07	0.79	1.15	1.24
645.0	0.089531	89.5				155.7	149.6	194.5	142.2	127.9	119.5	151.6	127.0	0.609	0.564	1.16	0.084367	1.07	0.81	1.11	1.14
957.5	0.109084	109.1				178.2	168.1	216.1	163.6	147.1	138.2	130.1	-147.0	0.609	0.564	1.20	0.099732	1.09	0.83	1.09	1.11
1350.0	0.129527	129.5				202.4	193.5	242.5	179.3	167.0	161.1	156.0	-147.0	0.609	0.564	1.24	0.116918	1.11	0.80	1.07	1.05
1832.5	0.150909	150.9				221.1	211.8	269.9	264.0	182.1	177.3	181.4	-147.0	0.609	0.564	1.33	0.135795	1.10	0.81	1.10	1.06
2337.5	0.170439	170.4				238.0	231.1	291.6	296.0	200.4	195.8	268.9	-147.0	0.609	0.564	1.36	0.153391	1.11	0.80	1.07	1.03
																		1.05			

MODEL PIER, bp = 32 mm_MEDIUM_5Degrees_DROWNED Q's

DATA Sunday, 13 August 2000

h_{man_1}	h_{man_2}	4 m	UE upstream end	US upstream side	DS downstream side	DE downstream end	6 m	7 m	
		15.5					147.5	147.0	
640.0	645.0	193.4	205.8	174.9	163.3	154.6	342.1		1.05
640.0	645.0	206.1	218.9	194.1	183.1	128.1	354.0		1.03
640.0	645.0	222.5	229.4	212.4	204.0	199.3	370.5		1.10
640.0	645.0	242.2	245.4	231.6	225.3	222.4	389.2		1.12
640.0	645.0	262.1	263.4	251.1	246.5	244.1	407.0		1.13

h_{man_1}	h_{man_2}	4 m	UE upstream end	US upstream side	DS downstream side	DE downstream end	6 m	7 m
		15.5					147.5	147.0
0.0	0.0							
0.0	0.0							
0.0	0.0							
0.0	0.0							
0.0	0.0							

h_{man_1}	h_{man_2}	4 m	UE upstream end	US upstream side	DS downstream side	DE downstream end	6 m	7 m

		15.5					147.5	147.0	
1365.0	1375.0	234.5	261.6	219.5	207.5	200.9	371.7		1.07
1365.0	1375.0	254.8	273.4	245.1	230.9	224.4	403.1		1.09
1365.0	1375.0	272.5	286.9	261.9	250.3	246.0	422.1		1.09
1365.0	1375.0	291.9	300.8	279.9	273.0	269.0	437.6		1.15
1365.0	1375.0	312.3	319.3	300.5	293.0	290.9	457.5		1.11

$h_{man,1}$	$h_{man,2}$	4 m	UE upstream end	US upstream side	DS downstream side	DE downstream end	6 m	7 m
		15.5					147.5	147.0
0.0	0.0							
0.0	0.0							
0.0	0.0							
0.0	0.0							
0.0	0.0							

$h_{man,1}$	$h_{man,2}$	4 m	UE upstream end	US upstream side	DS downstream side	DE downstream end	6 m	7 m	
		15.5					147.5	147.0	
2350.0	2350.0	272.4	306.3	254.6	240.4	234.1	416.5		1.10
2350.0	2350.0	290.0	314.6	276.0	264.3	258.8	424.2		1.15
2350.0	2350.0	313.1	333.0	300.8	286.3	281.5	453.0		1.10
2350.0	2350.0	335.3	348.5	321.3	310.8	304.4	481.3		1.13
2350.0	2350.0	352.6	368.1	342.3	331.3	326.8	502.1		1.08

CALCULATIONS

FLOW DEPTHS

$h_{man,avg}$	Q_{calc}	Q [l/s]	4 m y_4	UE upstream end y_{UE}	US upstream side y_{US}	DS downstream side y_{DS}	DE downstream end y_{DE}	6 m y_6	7 m y_7	B	$B-b_p$	$v_c = 2g(y_{US}-y_{DS})^{0.5}$	Q_{theory}	[illegible]	Fr_ue	Fr_us	Fr_de
642.5	0.089357	89.4	173.9	205.8	176.2	166.6	158.5	194.6	-147.0	0.609	0.564	0.90	0.085012	1.05	0.65	0.69	0.55
642.5	0.089357	89.4	190.6	218.9	195.4	186.5	132.0	206.5	-147.0	0.609	0.564	0.83	0.087101	1.03	0.56	0.58	0.50
642.5	0.089357	89.4	207.0	229.4	213.7	207.4	203.1	223.0	-147.0	0.609	0.564	0.69	0.081190	1.10	0.50	0.50	0.44
642.5	0.089357	89.4	226.7	245.4	232.9	228.6	226.2	241.7	-147.0	0.609	0.564	0.62	0.079483	1.12	0.43	0.43	0.39
642.5	0.089357	89.4	246.6	263.4	252.4	249.9	248.0	259.5	-147.0	0.609	0.564	0.56	0.079082	1.13	0.38	0.38	0.35

$h_{man,avg}$	Q_{calc}	Q [l/s]	4 m y_4	UE upstream end y_{UE}	US upstream side y_{US}	DS downstream side y_{DS}	DE downstream end y_{DE}	6 m y_6	7 m y_7	B	$B-b_p$	$v_c = 2g(y_{US}-y_{DS})^{0.5}$	Q_{theory}	[illegible]	Fr_ue	Fr_us	Fr_de
0.0	0.000000	0.0	-15.5	0.0	1.3	3.4	3.8	-147.5	-147.0	0.609	0.564	#NUM!	#NUM!	#NUM!	#NUM!	0.00	#NUM!
0.0	0.000000	0.0	-15.5	0.0	1.3	3.4	3.8	-147.5	-147.0	0.609	0.564	#NUM!	#NUM!	#NUM!	#NUM!	0.00	#NUM!
0.0	0.000000	0.0	-15.5	0.0	1.3	3.4	3.8	-147.5	-147.0	0.609	0.564	#NUM!	#NUM!	#NUM!	#NUM!	0.00	#NUM!
0.0	0.000000	0.0	-15.5	0.0	1.3	3.4	3.8	-147.5	-147.0	0.609	0.564	#NUM!	#NUM!	#NUM!	#NUM!	0.00	#NUM!
0.0	0.000000	0.0	-15.5	0.0	1.3	3.4	3.8	-147.5	-147.0	0.609	0.564	#NUM!	#NUM!	#NUM!	#NUM!	0.00	#NUM!

$h_{man,avg}$	Q_{calc}	Q [l/s]	4 m y_4	UE upstream end y_{UE}	US upstream side y_{US}	DS downstream side y_{DS}	DE downstream end y_{DE}	6 m y_6	7 m y_7	B	$B-b_p$	$v_c = 2g(y_{US}-y_{DS})^{0.5}$	Q_{theory}	[illegible]	Fr_ue	Fr_us	Fr_de
1370.0	0.133483	130.5	219.0	261.6	220.8	210.9	204.7	224.2	-147.0	0.609	0.564	1.02	0.121676	1.07	0.67	0.71	0.64
1370.0	0.133483	130.5	239.3	273.4	246.4	234.3	228.2	255.6	-147.0	0.609	0.564	0.90	0.119511	1.09	0.58	0.60	0.53
1370.0	0.133483	130.5	257.0	286.9	263.2	253.6	249.8	274.6	-147.0	0.609	0.564	0.84	0.120028	1.09	0.53	0.54	0.48
1370.0	0.133483	130.5	276.4	300.8	281.2	276.4	272.8	290.1	-147.0	0.609	0.564	0.73	0.113319	1.15	0.47	0.47	0.44
1370.0	0.133483	130.5	296.8	319.3	301.8	296.4	294.7	310.0	-147.0	0.609	0.564	0.71	0.118083	1.11	0.42	0.42	0.40

UE upstream	US upstream	DS downstream	DE downstream

h_{man_avg}	Q_{calc}	Q [l/s]	4 m y_4	end y_{UE}	side y_{US}	side y_{DS}	end y_{DE}	6 m y_6	7 m y_7	B	$B-b_y$	$v_C = 2g(y_{UE}-y_{DE})^{0.5}$	Q_{theory}	[illegible]	$Fr_{\_4m}$	$Fr_{\_DS}$	$Fr_{\_6m}$
0.0	0.000000	0.0	-15.5	0.0	1.3	3.4	3.8	-147.5	-147.0	0.609	0.564	#NUM!	#NUM!	#NUM!	#NUM!	0.00	#NUM!
0.0	0.000000	0.0	-15.5	0.0	1.3	3.4	3.8	-147.5	-147.0	0.609	0.564	#NUM!	#NUM!	#NUM!	#NUM!	0.00	#NUM!
0.0	0.000000	0.0	-15.5	0.0	1.3	3.4	3.8	-147.5	-147.0	0.609	0.564	#NUM!	#NUM!	#NUM!	#NUM!	0.00	#NUM!
0.0	0.000000	0.0	-15.5	0.0	1.3	3.4	3.8	-147.5	-147.0	0.609	0.564	#NUM!	#NUM!	#NUM!	#NUM!	0.00	#NUM!
0.0	0.000000	0.0	-15.5	0.0	1.3	3.4	3.8	-147.5	-147.0	0.609	0.564	#NUM!	#NUM!	#NUM!	#NUM!	0.00	#NUM!

h_{man_avg}	Q_{calc}	Q [l/s]	4 m y_4	UE upstream end y_{UE}	US upstream side y_{US}	DS downstream side y_{DS}	DE downstream end y_{DE}	6 m y_6	7 m y_7	B	$B-b_y$	$v_C = 2g(y_{UE}-y_{DE})^{0.5}$	Q_{theory}	[illegible]	$Fr_{\_4m}$	$Fr_{\_DS}$	$Fr_{\_6m}$
2350.0	0.170894	170.9	256.3	306.3	255.9	243.8	238.0	269.0	-147.0	0.609	0.564	1.13	0.155380	1.10	0.69	0.74	0.64
2350.0	0.170894	170.9	274.5	314.6	277.3	267.6	262.6	276.7	-147.0	0.609	0.564	0.99	0.148885	1.15	0.62	0.65	0.62
2350.0	0.170894	170.9	297.6	333.0	302.0	289.6	285.3	305.5	-147.0	0.609	0.564	0.95	0.155115	1.10	0.55	0.57	0.53
2350.0	0.170894	170.9	319.8	348.5	322.5	314.1	308.2	333.8	-147.0	0.609	0.564	0.85	0.150844	1.13	0.50	0.51	0.48
2350.0	0.170894	170.9	337.1	368.1	343.5	334.6	333.6	354.6	-147.0	0.609	0.564	0.84	0.158772	1.08	0.45	0.46	0.42
														1.10			

MODEL PIER, bp = 32 mm_MEDIUM_10Degrees_NORMAL Q's

OK

DATA *Saturday, 12 August 2000*

Q	h_{man_1}	h_{man_2}	0 m	1 m	2 m	3 m	4 m	UE upstream end	US upstream side	DS downstream side	DE downstream end	6 m	7 m
bed levels			12.5	10.5	10.0	13.5	15.5					147.5	147.0
10	13.0	13.5				80.4	59.0	61.1	43.9	30.3	15.8	201.5	
30	78.0	78.5				96.2	94.5	102.9	81.0	58.0	41.5	227.1	
50	212.5	212.5				125.9	123.8	134.4	114.6	88.0	69.0	243.3	
70	405.0	405.0				150.3	149.2	161.9	138.3	111.9	96.4	295.0	
90	660.0	650.0				175.4	174.4	189.8	163.1	133.9	120.0	255.7	
110	970.0	970.0				197.1	190.7	215.1	184.5	152.9	139.5	278.0	
130	1385.0	1385.0				221.2	212.4	237.3	207.3	173.0	159.5	301.3	
150	1810.0	1830.0				244.3	237.8	255.6	230.5	196.1	182.9	324.4	
170	2350.0	2380.0				259.5	254.2	275.1	250.1	214.0	201.5	354.4	

Geometric properties:

D =	31.5 mm
L_p =	178 mm
r_A =	0.8 mm
A_B =	1.3 mm
A_C =	3.4 mm
A_D =	3.8 mm

CALCULATIONS

FLOW DEPTHS

h_{man_avg}	Q_{corr}	Q [l/s]	0 m y_0	1 m y_1	2 m y_2	3 m y_3	4 m y_4	UE upstream end y_{UE}	US upstream side y_{US}	DS downstream side y_{DS}	DE downstream end y_{DE}	6 m y_6	7 m y_7	B	B-b_p	v_C = $2g(y_{US}-y_{DS})^{2.5}$	Q_{theory}	$\frac{Q_{corr}}{Q_{theory}}$	Fr_4m	Fr_DS	Fr_DE
13.3	0.012832	12.8				46.9	43.5	61.1	45.2	33.6	19.6	54.0	-147.0	0.609	0.552	0.77	0.014290	0.90	0.74	1.20	2.45
78.3	0.031184	31.2				82.7	79.0	102.9	82.3	61.4	45.3	79.6	-147.0	0.609	0.552	0.93	0.031498	0.99	0.74	1.19	1.69
212.5	0.051389	51.4				112.4	108.3	134.4	115.9	91.4	72.8	95.8	-147.0	0.609	0.552	0.95	0.047648	1.08	0.76	1.08	1.37
405.0	0.070545	70.9				136.8	133.7	161.9	139.5	115.3	100.2	147.5	-147.0	0.609	0.552	0.98	0.062441	1.14	0.78	1.05	1.17
655.0	0.090222	90.2				161.9	158.9	189.8	164.4	137.3	123.6	108.2	-147.0	0.609	0.552	1.04	0.078677	1.15	0.75	1.03	1.03
970.0	0.109794	109.8				183.6	175.2	215.1	185.8	156.3	143.3	130.5	-147.0	0.609	0.552	1.10	0.094613	1.16	0.78	1.03	1.06
1385.0	0.131195	131.2				207.7	196.9	237.3	208.5	178.4	163.3	153.8	-147.0	0.609	0.552	1.12	0.108523	1.21	0.79	1.03	1.04
1820.0	0.150393	150.4				230.8	222.1	255.6	254.0	199.5	186.7	176.9	-147.0	0.609	0.552	1.07	0.118062	1.27	0.75	0.98	0.98
2365.0	0.171439	171.4				246.0	238.7	275.1	296.0	217.4	205.3	206.9	-147.0	0.609	0.552	1.09	0.130400	1.31	0.77	0.98	0.97
																		1.13			

MODEL PIER, bp = 32 mm_MEDIUM_10Degrees_DROWNED Q's

DATA *Saturday, 12 August 2000*

h_{man_1}	h_{man_2}	4 m	UE upstream end	US upstream side	DS downstream side	DE downstream end	6 m	7 m	
		15.5					147.5	147.0	
650.0	645.0	199.3	204.5	195.1	174.4	166.4	347.1		1.20
650.0	645.0	215.8	217.0	209.9	194.1	187.8	360.6		1.25
650.0	645.0	232.9	232.4	227.1	214.6	211.3	377.4		1.30
650.0	645.0	250.0	249.3	242.6	233.3	230.1	395.4		1.26
650.0	645.0	267.4	266.3	258.8	252.1	250.8	413.5		1.24

h_{man_1}	h_{man_2}	4 m	UE upstream end	US upstream side	DS downstream side	DE downstream end	6 m	7 m
		15.5					147.5	147.0
0.0	0.0							
0.0	0.0							
0.0	0.0							
0.0	0.0							
0.0	0.0							

h_{man_1}	h_{man_2}	4 m	UE upstream end	US upstream side	DS downstream side	DE downstream end	6 m	7 m

		15.5					147.5	147.0	
1340.0	1320.0	251.0	257.5	244.0	222.3	214.6	389.2		1.26
1340.0	1320.0	265.7	269.1	261.5	242.4	235.1	412.3		1.33
1340.0	1320.0	283.8	286.5	279.6	263.4	259.1	430.8		1.32
1340.0	1320.0	303.3	302.5	297.9	282.4	276.6	446.2		1.33
1340.0	1320.0	319.5	319.1	313.5	301.0	297.5	463.5		1.32

h_{man_1}	h_{man_2}	4 m	UE upstream end	US upstream side	DS downstream side	DE downstream end	6 m	7 m
		15.5					147.5	147.0
0.0	0.0							
0.0	0.0							
0.0	0.0							
0.0	0.0							
0.0	0.0							

h_{man_1}	h_{man_2}	4 m	UE upstream end	US upstream side	DS downstream side	DE downstream end	6 m	7 m	
		15.5					147.5	147.0	
2320.0	2310.0	291.6	302.5	293.1	265.3	256.9	424.8		1.35
2320.0	2310.0	312.4	321.0	311.3	285.4	278.4	449.1		1.29
2320.0	2310.0	331.0	337.5	328.3	305.9	297.9	475.4		1.28
2320.0	2310.0	349.2	351.9	347.0	325.8	322.5	494.2		1.33
2320.0	2310.0	367.8	370.0	363.8	345.5	340.5	513.0		1.29

CALCULATIONS:

FLOW DEPTHS

h_{man_avg}	Q_{calc}	Q [l/s]	4 m y_4	UE upstream end y_{UE}	US upstream side y_{US}	DS downstream side y_{DS}	DE downstream end y_{DE}	6 m y_6	7 m y_7	B	$B-b_0$	$v_C = 2g(y_{UE}-y_{DS})^{0.5}$	Q_{theory}	[illegible]	Fr_{4m}	Fr_{DS}	Fr_{6m}
647.5	0.089704	89.7	183.8	204.6	196.4	177.8	170.2	199.6	-147.0	0.609	0.552	0.76	0.074480	1.20	0.60	0.63	0.53
647.5	0.089704	89.7	200.3	217.0	211.2	197.5	191.6	213.1	-147.0	0.609	0.552	0.66	0.071629	1.25	0.52	0.54	0.48
647.5	0.089704	89.7	217.4	232.4	228.4	218.0	215.1	229.9	-147.0	0.609	0.552	0.58	0.069258	1.30	0.46	0.46	0.43
647.5	0.089704	89.7	234.5	249.3	243.9	236.6	234.0	247.9	-147.0	0.609	0.552	0.55	0.071177	1.26	0.41	0.41	0.38
647.5	0.089704	89.7	251.9	266.3	261.0	255.5	254.6	266.0	-147.0	0.609	0.552	0.51	0.072112	1.24	0.37	0.36	0.34

h_{man_avg}	Q_{calc}	Q [l/s]	4 m y_4	UE upstream end y_{UE}	US upstream side y_{US}	DS downstream side y_{DS}	DE downstream end y_{DE}	6 m y_6	7 m y_7	B	$B-b_0$	$v_C = 2g(y_{UE}-y_{DS})^{0.5}$	Q_{theory}	[illegible]	Fr_{4m}	Fr_{DS}	Fr_{6m}
0.0	0.000000	0.0	-15.5	0.0	1.3	3.4	3.8	-147.5	-147.0	0.609	0.552	#NUM!	#NUM!	#NUM!	#NUM!	0.00	#NUM!
0.0	0.000000	0.0	-15.5	0.0	1.3	3.4	3.8	-147.5	-147.0	0.609	0.552	#NUM!	#NUM!	#NUM!	#NUM!	0.00	#NUM!
0.0	0.000000	0.0	-15.5	0.0	1.3	3.4	3.8	-147.5	-147.0	0.609	0.552	#NUM!	#NUM!	#NUM!	#NUM!	0.00	#NUM!
0.0	0.000000	0.0	-15.5	0.0	1.3	3.4	3.8	-147.5	-147.0	0.609	0.552	#NUM!	#NUM!	#NUM!	#NUM!	0.00	#NUM!
0.0	0.000000	0.0	-15.5	0.0	1.3	3.4	3.8	-147.5	-147.0	0.609	0.552	#NUM!	#NUM!	#NUM!	#NUM!	0.00	#NUM!

h_{man_avg}	Q_{calc}	Q [l/s]	4 m y_4	UE upstream end y_{UE}	US upstream side y_{US}	DS downstream side y_{DS}	DE downstream end y_{DE}	6 m y_6	7 m y_7	B	$B-b_0$	$v_C = 2g(y_{UE}-y_{DS})^{0.5}$	Q_{theory}	[illegible]	Fr_{4m}	Fr_{DS}	Fr_{6m}
1330.0	0.128564	128.6	235.5	257.5	245.3	225.6	218.5	241.7	-147.0	0.609	0.552	0.82	0.102260	1.26	0.59	0.63	0.57
1330.0	0.128564	128.6	250.2	269.1	262.8	245.8	239.0	264.8	-147.0	0.609	0.552	0.71	0.096647	1.33	0.54	0.55	0.49
1330.0	0.128564	128.6	268.3	286.5	280.9	266.8	263.0	283.3	-147.0	0.609	0.552	0.66	0.097289	1.32	0.48	0.49	0.45
1330.0	0.128564	128.6	287.8	302.5	299.2	285.8	280.5	298.7	-147.0	0.609	0.552	0.62	0.096948	1.33	0.44	0.44	0.41
1330.0	0.128564	128.6	304.0	319.1	314.8	304.4	301.3	316.0	-147.0	0.609	0.552	0.58	0.097764	1.32	0.40	0.40	0.38

UE	US	DS	DE
upstream	upstream	downstream	downstream

			4 m	end	side	side	end	6 m	7 m			v_c =					
h_{man_avg}	Q_{calc}	Q [l/s]	y_4	y_{UE}	y_{US}	y_{DS}	y_{DE}	y_6	y_7	B	$B\text{-}b_p$	$2g(y_{UE}\text{-}y_{DS})^{0.5}$	Q_{theory}	[illegible]	$Fr_{\_ds}$	$Fr_{\_ps}$	$Fr_{\_as}$
0.0	0.000000	0.0	-15.5	0.0	1.3	3.4	3.8	-147.5	-147.0	0.609	0.552	#NUM!	#NUM!	#NUM!	#NUM!	0.00	#NUM!
0.0	0.000000	0.0	-15.5	0.0	1.3	3.4	3.8	-147.5	-147.0	0.609	0.552	#NUM!	#NUM!	#NUM!	#NUM!	0.00	#NUM!
0.0	0.000000	0.0	-15.5	0.0	1.3	3.4	3.8	-147.5	-147.0	0.609	0.552	#NUM!	#NUM!	#NUM!	#NUM!	0.00	#NUM!
0.0	0.000000	0.0	-15.5	0.0	1.3	3.4	3.8	-147.5	-147.0	0.609	0.552	#NUM!	#NUM!	#NUM!	#NUM!	0.00	#NUM!
0.0	0.000000	0.0	-15.5	0.0	1.3	3.4	3.8	-147.5	-147.0	0.609	0.552	#NUM!	#NUM!	#NUM!	#NUM!	0.00	#NUM!

				UE	US	DS	DE										
				upstream	upstream	downstream	downstream										
			4 m	end	side	side	end	6 m	7 m			v_c =					
h_{man_avg}	Q_{calc}	Q [l/s]	y_4	y_{UE}	y_{US}	y_{DS}	y_{DE}	y_6	y_7	B	$B\text{-}b_p$	$2g(y_{UE}\text{-}y_{DS})^{0.5}$	Q_{theory}	[illegible]	$Fr_{\_ds}$	$Fr_{\_ps}$	$Fr_{\_as}$
2315.0	0.169617	169.6	276.1	302.5	294.4	268.6	260.7	277.3	-147.0	0.609	0.552	0.85	0.125236	1.35	0.61	0.64	0.61
2315.0	0.169617	169.6	296.9	321.0	312.5	288.8	282.2	301.6	-147.0	0.609	0.552	0.83	0.131579	1.29	0.55	0.57	0.54
2315.0	0.169617	169.6	315.5	337.5	329.5	309.3	301.7	327.9	-147.0	0.609	0.552	0.78	0.132569	1.28	0.50	0.52	0.47
2315.0	0.169617	169.6	333.7	351.9	348.3	329.1	326.3	346.7	-147.0	0.609	0.552	0.70	0.127863	1.33	0.46	0.47	0.44
2315.0	0.169617	169.6	352.3	370.0	365.0	348.9	344.3	365.5	-147.0	0.609	0.552	0.68	0.131107	1.29	0.43	0.43	0.43

1.29

MODEL PIER, bp = 32 mm_MEDIUM_15Degrees_NORMAL Q's OK

DATA: *Friday, 11 August 2000*

Q	h_{main_1}	h_{main_2}	0 m	1 m	2 m	3 m	4 m	UE upstream end	US upstream side	DS downstream side	DE downstream end	6 m	7 m
bed levels			12.5	10.5	15.0	13.5	15.5					147.5	147.0
10	14.5	14.5				61.3	60.7	61.3	48.4	34.0	15.0	206.5	
30	73.0	73.0				97.4	95.6	96.1	57.8	61.5	40.5	217.6	
50	205.0	210.0				130.0	129.9	126.4	126.4	91.0	65.0	215.0	
70	397.9	392.0				154.4	150.6	149.6	152.8	115.8	92.4	232.0	
90	650.0	650.0				180.6	179.1	174.0	180.9	141.5	121.5	250.8	
110	970.0	965.0				204.6	202.2	197.3	205.5	165.3	146.1	272.2	
130	1350.0	1330.9				225.0	221.3	210.5	229.3	185.4	166.8	295.3	
150	1830.0	1830.0				249.5	242.2	238.9	251.0	204.5	185.1	323.8	
170	2300.0	2310.0				271.3	265.0	248.0	273.9	224.5	205.5	341.7	

Geometric properties:

D =	31.5 mm
L_p =	178 mm
z_A =	0.8 mm
z_B =	1.3 mm
z_C =	3.4 mm
z_D =	3.8 mm

CALCULATIONS:

FLOW DEPTHS

Distance measured downstream within the flume

h_{main_avg}	Q_{calc}	Q [l/s]	0 m y_0	1 m y_1	2 m y_2	3 m y_3	4 m y_4	UE upstream end y_{UE}	US upstream side y_{US}	DS downstream side y_{DS}	DE downstream end y_{DE}	6 m y_6	7 m y_7	B	B-δ_y	$v_c = \sqrt{2g(y_{UE}-y_{DS})}^{1.1}$	Q_{theory}		Fr_4m	Fr_DS	Fr_DE
14.5	0.013424	13.4				47.8	46.2	61.3	49.7	37.4	18.8	59.0	-147.0	0.639	0.535	0.54	0.010871	1.23	0.73	1.10	2.72
73.0	0.030120	30.1				83.9	80.1	96.1	89.0	64.9	44.6	70.1	-147.0	0.639	0.535	0.72	0.025322	1.19	0.70	1.06	1.68
206.5	0.051025	51.0				116.5	114.4	126.4	127.7	95.3	71.8	67.5	-147.0	0.639	0.535	0.83	0.042533	1.20	0.69	1.03	1.39
384.5	0.070019	70.0				140.9	135.1	149.6	154.0	119.1	96.2	84.5	-147.0	0.639	0.535	0.88	0.055062	1.27	0.74	1.01	1.23
650.0	0.089877	89.9				167.1	163.6	174.0	182.2	144.9	125.3	103.3	-147.0	0.639	0.535	0.89	0.069053	1.30	0.71	0.96	1.06
967.5	0.109653	109.7				191.1	186.7	197.3	206.8	168.6	150.0	124.7	-147.0	0.639	0.535	0.89	0.081250	1.35	0.71	0.94	0.99
1340.0	0.129046	129.0				211.5	205.8	210.5	230.5	188.8	170.6	147.8	-147.0	0.639	0.535	0.93	0.094910	1.36	0.72	0.93	0.96
1830.0	0.150806	150.8				235.0	226.7	238.9	254.0	207.9	189.0	176.3	-147.0	0.639	0.535	0.98	0.109523	1.38	0.73	0.94	0.96
2305.0	0.169250	169.2				257.8	249.5	248.0	296.0	227.9	209.3	194.2	-147.0	0.639	0.535	1.18	0.144678	1.17	0.71	0.92	0.93
																		1.27			

MODEL PIER, bp = 32 mm_MEDIUM_15Degrees_DROWNED Q's

DATA: *Friday, 11 August 2000*

h_{main_1}	h_{main_2}	4 m	UE upstream end	US upstream side	DS downstream side	DE downstream end	6 m	7 m
		15.5					147.5	147.0
655.0	630.0	196.5	187.9	202.1	172.9	158.9	341.5	
655.0	630.0	213.9	205.1	214.5	191.0	183.8	358.3	
655.0	630.0	232.5	226.0	228.9	211.1	264.6	376.5	
655.0	630.0	249.9	244.0	244.6	230.3	224.4	394.5	
655.0	630.0	267.1	262.7	261.0	248.6	243.3	411.3	

h_{main_1}	h_{main_2}	4 m	UE upstream end	US upstream side	DS downstream side	DE downstream end	6 m	7 m
		15.5					147.5	147.0
0.0	0.0							
0.0	0.0							
0.0	0.0							
0.0	0.0							
0.0	0.0							

h_{main_1}	h_{main_2}	4 m	UE upstream end	US upstream side	DS downstream side	DE downstream end	6 m	7 m

		15.5					147.5	147.0
1360.0	1375.0	249.2	231.3	253.8	218.8	204.4	380.5	
1360.0	1375.0	265.8	255.1	269.3	236.6	225.9	408.1	
1360.0	1375.0	284.4	276.3	284.8	258.8	247.0	426.2	
1360.0	1375.0	301.5	297.6	300.6	278.5	267.8	445.8	
1360.0	1375.0	321.2	316.4	317.5	295.5	286.9	462.8	

h_{man_1}	h_{man_2}	4 m	UE upstream end	US upstream side	DS downstream side	DE downstream end	6 m	7 m
		15.5					147.5	147.0
0.0	0.0							
0.0	0.0							
0.0	0.0							
0.0	0.0							
0.0	0.0							

h_{man_1}	h_{man_2}	4 m	UE upstream end	US upstream side	DS downstream side	DE downstream end	6 m	7 m
		15.5					147.5	147.0
2320.0	2330.0	294.6	281.3	303.0	260.6	243.0	424.3	
2320.0	2330.0	310.5	304.1	315.5	278.6	264.3	444.8	
2320.0	2330.0	332.8	328.0	333.1	299.8	285.5	470.3	
2320.0	2330.0	347.7	343.5	349.5	318.8	305.3	491.2	
2320.0	2330.0	366.2	362.3	365.8	337.3	324.6	508.4	

CALCULATIONS

FLOW DEPTHS

h_{man_avg}	Q_{ven}	Q [l/s]	4 m y_4	UE upstream end y_{UE}	US upstream side y_{US}	DS downstream side y_{DS}	DE downstream end y_{DE}	6 m y_6	7 m y_7	B	B-b_y	$v_c = 2g(y_{UE}-y_{DE})^{0.5}$	Q_{theory}	[illegible]	Fr_um	Fr_us	Fr_dm
642.5	0.089357	89.4	183.0	187.9	203.4	176.3	162.7	194.0	-147.0	0.609	0.539	0.76	0.072542	1.23	0.60	0.63	0.55
642.5	0.089357	89.4	198.4	205.1	215.8	194.4	187.6	210.8	-147.0	0.609	0.539	0.69	0.071838	1.24	0.53	0.55	0.48
642.5	0.089357	89.4	217.0	226.0	230.2	214.5	208.5	229.0	-147.0	0.609	0.539	0.60	0.069103	1.29	0.46	0.47	0.43
642.5	0.089357	89.4	234.4	244.0	245.9	233.6	228.2	247.0	-147.0	0.609	0.539	0.54	0.067924	1.32	0.41	0.41	0.38
642.5	0.089357	89.4	251.6	262.7	262.3	252.0	247.1	263.8	-147.0	0.609	0.539	0.50	0.068141	1.31	0.37	0.37	0.35

h_{man_avg}	Q_{ven}	Q [l/s]	4 m y_4	UE upstream end y_{UE}	US upstream side y_{US}	DS downstream side y_{DS}	DE downstream end y_{DE}	6 m y_6	7 m y_7	B	B-b_y	$v_c = 2g(y_{UE}-y_{DE})^{0.5}$	Q_{theory}	[illegible]	Fr_um	Fr_us	Fr_dm
0.0	0.000000	0.0	-15.5	0.0	1.3	3.4	3.8	-147.5	-147.0	0.609	0.539	#NUM!	#NUM!	#NUM!	#NUM!	0.00	#NUM!
0.0	0.000000	0.0	-15.5	0.0	1.3	3.4	3.8	-147.5	-147.0	0.609	0.539	#NUM!	#NUM!	#NUM!	#NUM!	0.00	#NUM!
0.0	0.000000	0.0	-15.5	0.0	1.3	3.4	3.8	-147.5	-147.0	0.609	0.539	#NUM!	#NUM!	#NUM!	#NUM!	0.00	#NUM!
0.0	0.000000	0.0	-15.5	0.0	1.3	3.4	3.8	-147.5	-147.0	0.609	0.539	#NUM!	#NUM!	#NUM!	#NUM!	0.00	#NUM!
0.0	0.000000	0.0	-15.5	0.0	1.3	3.4	3.8	-147.5	-147.0	0.609	0.539	#NUM!	#NUM!	#NUM!	#NUM!	0.00	#NUM!

h_{man_avg}	Q_{ven}	Q [l/s]	4 m y_4	UE upstream end y_{UE}	US upstream side y_{US}	DS downstream side y_{DS}	DE downstream end y_{DE}	6 m y_6	7 m y_7	B	B-b_y	$v_c = 2g(y_{UE}-y_{DE})^{0.5}$	Q_{theory}	[illegible]	Fr_um	Fr_us	Fr_dm
1367.5	0.130364	130.4	233.7	231.3	255.0	222.1	208.2	233.0	-147.0	0.609	0.539	0.83	0.099882	1.31	0.60	0.65	0.61
1367.5	0.130364	130.4	250.3	255.1	270.5	243.0	229.7	260.6	-147.0	0.609	0.539	0.77	0.100642	1.30	0.55	0.57	0.51
1367.5	0.130364	130.4	268.9	276.3	286.0	262.1	250.8	276.7	-147.0	0.609	0.536	0.72	0.101807	1.28	0.49	0.51	0.46
1367.5	0.130364	130.4	286.0	297.6	301.9	281.9	271.6	298.3	-147.0	0.609	0.536	0.67	0.101138	1.29	0.45	0.46	0.42
1367.5	0.130364	130.4	305.7	316.4	318.8	298.9	290.7	315.3	-147.0	0.609	0.539	0.66	0.106940	1.22	0.40	0.42	0.39

UE	US	DS	DE
upstream	upstream	downstream	downstream

h_{man_avg}	Q_{sen}	Q [l/s]	4 m y_4	end y_{UE}	side y_{US}	side y_{DS}	end y_{DE}	6 m y_6	7 m y_7	B	$B-b_s$	$v_c = 2g(y_{US}-y_{DS})^{0.5}$	Q_{theory}	[illegible]	Fr_{4m}	Fr_{US}	Fr_{6m}
0.0	0.000000	0.0	-15.5	0.0	1.3	3.4	3.8	-147.5	-147.0	0.609	0.539	#NUM!	#NUM!	#NUM!	#NUM!	0.00	#NUM!
0.0	0.000000	0.0	-15.5	0.0	1.3	3.4	3.8	-147.5	-147.0	0.609	0.539	#NUM!	#NUM!	#NUM!	#NUM!	0.00	#NUM!
0.0	0.000000	0.0	-15.5	0.0	1.3	3.4	3.8	-147.5	-147.0	0.609	0.539	#NUM!	#NUM!	#NUM!	#NUM!	0.00	#NUM!
0.0	0.000000	0.0	-15.5	0.0	1.3	3.4	3.8	-147.5	-147.0	0.609	0.539	#NUM!	#NUM!	#NUM!	#NUM!	0.00	#NUM!
0.0	0.000000	0.0	-15.5	0.0	1.3	3.4	3.8	-147.5	-147.0	0.609	0.539	#NUM!	#NUM!	#NUM!	#NUM!	0.00	#NUM!

h_{man_avg}	Q_{sen}	Q [l/s]	4 m y_4	UE upstream end y_{UE}	US upstream side y_{US}	DS downstream side y_{DS}	DE downstream end y_{DE}	6 m y_6	7 m y_7	B	$B-b_s$	$v_c = 2g(y_{US}-y_{DS})^{0.5}$	Q_{theory}	[illegible]	Fr_{4m}	Fr_{US}	Fr_{6m}
2325.0	0.169983	170.0	279.1	281.3	304.3	264.0	246.8	276.8	-147.0	0.609	0.539	0.92	0.130479	1.30	0.60	0.66	0.61
2325.0	0.169983	170.0	295.6	304.1	316.8	282.0	268.1	297.3	-147.0	0.609	0.539	0.86	0.130115	1.31	0.56	0.60	0.55
2325.0	0.169983	170.0	317.3	328.0	334.4	303.1	289.3	322.8	-147.0	0.609	0.539	0.81	0.133141	1.28	0.50	0.53	0.49
2325.0	0.169983	170.0	332.2	343.5	350.8	322.1	309.1	343.7	-147.0	0.609	0.539	0.78	0.135883	1.25	0.47	0.49	0.44
2325.0	0.169983	170.0	350.7	362.3	367.0	340.6	328.5	360.9	-147.0	0.609	0.539	0.75	0.138407	1.23	0.43	0.45	0.41
														1.28			

MODEL PIER, bp = 32 mm_LONG_5Degrees_NORMAL Q's OK

DATA: *Friday, 11 August 2000*

Q	h_{man_1}	h_{man_2}	0 m	1 m	2 m	3 m	4 m	UE upstream end	US upstream side	DS downstream side	DE downstream end	6 m	7 m
Bed levels			12.5	10.5	15.0	13.5	15.5					147.5	147.0
10	12.0	12.0				57.1	56.1	57.6	37.750	22.625	16.250	593.500	
30	74.0	73.0				94.3	92.8	102.3	74.080	44.250	42.125	243.800	
50	199.0	200.0				122.6	120.3	135.5	105.500	70.250	63.500	239.300	
70	400.0	402.5				148.5	147.5	168.0	125.000	91.750	88.750	291.500	
90	655.0	660.0				172.8	170.9	198.0	150.000	114.250	111.625	255.300	
110	955.0	960.0				194.1	187.0	220.6	168.750	132.125	130.125	276.400	
130	1360.0	1360.0				219.2	209.6	245.3	190.375	151.625	151.000	297.900	
150	1825.0	1830.0				238.8	231.9	267.4	203.000	170.500	173.250	326.700	
170	2350.0	2350.0				254.2	249.5	288.0	222.375	186.250	191.000	351.300	

Geometric properties:

D =	31.5 mm
L_p =	222 mm
z_A =	0.4 mm
z_B =	0.8 mm
z_C =	3.7 mm
z_D =	4.1 mm

CALCULATIONS:

FLOW DEPTHS

Distance measured downstream within the flume

h_{man_avg}	Q_{corr}	Q [l/s]	0 m y_A	1 m y_1	2 m y_2	3 m y_3	4 m y_4	UE upstream end y_{UE}	US upstream side y_{US}	DS downstream side y_{DS}	DE downstream end y_{DE}	6 m y_6	7 m y_7	B	B-b_p	v_C = $\sqrt{2g(y_{US}-y_{DS})^{0.5}}$	Q_{theory}	$\frac{Q_{corr}}{Q_{theory}}$	Fr 4m	Fr_DS	Fr_DE
12.0	0.012212	12.2				43.6	40.6	57.6	38.6	26.3	20.3	46.0	-147.0	0.609	0.560	0.92	0.012139	1.01	0.75	1.63	2.21
73.5	0.030223	30.2				80.8	77.3	102.3	74.9	47.9	46.2	96.3	-147.0	0.609	0.560	1.06	0.028546	1.06	0.74	1.64	1.56
199.5	0.049753	49.8				109.1	104.8	135.5	106.3	73.9	67.6	91.8	-147.0	0.609	0.560	1.13	0.046728	1.07	0.77	1.41	1.49
401.3	0.070616	70.6				135.0	132.0	168.0	125.8	95.4	92.8	144.0	-147.0	0.609	0.560	1.22	0.065236	1.08	0.77	1.37	1.31
657.5	0.090354	90.4				159.3	155.4	198.0	150.8	117.9	115.7	107.8	-147.0	0.609	0.560	1.28	0.084511	1.07	0.77	1.27	1.20
957.5	0.109084	109.1				180.6	171.5	220.6	169.6	135.8	134.2	128.6	-147.0	0.609	0.560	1.32	0.100058	1.09	0.81	1.24	1.16
1360.0	0.130006	130.0				205.7	194.1	245.3	191.2	155.3	155.1	150.4	-147.0	0.609	0.560	1.35	0.117708	1.10	0.80	1.21	1.12
1827.5	0.150703	150.7				225.3	216.4	267.4	203.8	174.2	177.3	179.2	-147.0	0.609	0.560	1.38	0.134297	1.12	0.78	1.18	1.06
2350.0	0.170854	170.9				240.7	233.0	288.0	296.0	189.9	195.1	203.8	-147.0	0.609	0.560	1.41	0.150055	1.14	0.80	1.18	1.04
																		1.08			

MODEL PIER, bp = 32 mm_LONG_5Degrees_DROWNED Q's

DATA: *Friday, 11 August 2000*

h_{man_1}	h_{man_2}	4 m	UE upstream end	US upstream side	DS downstream side	DE downstream end	6 m	7 m
		15.5					147.5	147.0
630.0	620.0	184.9	213.3	169.8	143.8	142.1	333.6	
630.0	620.0	203.3	214.4	192.8	174.1	172.3	352.1	
630.0	620.0	221.3	225.3	213.1	199.9	199.1	367.0	
630.0	620.0	240.2	243.8	231.1	222.0	222.5	389.9	
630.0	620.0	259.8	263.6	246.6	242.1	242.8	406.2	

h_{man_1}	h_{man_2}	4 m	UE upstream end	US upstream side	DS downstream side	DE downstream end	6 m	7 m
		15.5					147.5	147.0
0.0	0.0							
0.0	0.0							
0.0	0.0							
0.0	0.0							
0.0	0.0							

h_{man_1}	h_{man_2}	4 m	UE upstream end	US upstream side	DS downstream side	DE downstream end	6 m	7 m

		15.5					147.5	147.0
1375.0	1380.0	229.2	256.3	215.6	189.5	191.6	384.5	
1375.0	1380.0	250.7	268.6	237.6	218.4	216.9	393.8	
1375.0	1380.0	270.0	279.8	250.3	241.1	241.6	418.2	
1375.0	1380.0	289.0	298.1	279.9	265.1	264.6	436.1	
1375.0	1380.0	307.9	314.3	299.8	296.8	266.5	452.6	

h_{man_1}	h_{man_2}	4 m	UE upstream end	US upstream side	DS downstream side	DE downstream end	6 m	7 m
		15.5					147.5	147.0
0.0	0.0							
0.0	0.0							
0.0	0.0							
0.0	0.0							
0.0	0.0							

h_{max_1}	h_{max_2}	4 m	UE upstream end	US upstream side	DS downstream side	DE downstream end	6 m	7 m
		15.5					147.5	147.0
2325.0	2330.0	270.0	335.5	253.8	217.8	223.4	423.8	
2325.0	2330.0	286.0	309.5	271.5	245.5	247.3	421.8	
2325.0	2330.0	309.4	325.1	300.3	274.1	274.9	450.6	
2325.0	2330.0	328.2	345.1	318.5	298.1	298.9	474.9	
2325.0	2330.0	349.2	336.5	341.0	323.5	324.6	496.9	

CALCULATIONS

FLOW DEPTHS

h_{man_avg}	Q_{calc}	Q [l/s]	4 m y_4	UE upstream end y_{UE}	US upstream side y_{US}	DS downstream side y_{DS}	DE downstream end y_{DE}	6 m y_6	7 m y_7	B	$B-b_p$	$v_c = 2g(y_{UE}-y_{DS})^{0.5}$	Q_{theory}	[illegible]	Fr [illegible]	Fr [illegible]	Fr [illegible]
625.0	0.088132	88.1	169.4	213.3	170.6	147.4	146.2	166.1	-147.0	0.609	0.560	1.16	0.096207	0.92	0.66	0.82	0.58
625.0	0.088132	88.1	187.8	214.4	193.6	177.8	176.3	204.6	-147.0	0.609	0.560	0.89	0.088202	1.00	0.57	0.62	0.50
625.0	0.088132	88.1	205.8	225.3	213.9	203.5	203.2	219.5	-147.0	0.609	0.560	0.70	0.080000	1.10	0.49	0.50	0.45
625.0	0.088132	88.1	224.7	243.8	231.9	225.7	226.6	242.4	-147.0	0.609	0.560	0.65	0.081916	1.08	0.43	0.43	0.39
625.0	0.088132	88.1	244.3	260.6	250.4	245.8	246.8	258.7	-147.0	0.609	0.560	0.60	0.082022	1.07	0.38	0.38	0.35

h_{man_avg}	Q_{calc}	Q [l/s]	4 m y_4	UE upstream end y_{UE}	US upstream side y_{US}	DS downstream side y_{DS}	DE downstream end y_{DE}	5 m y_6	7 m y_7	B	$B-b_p$	$v_c = 2g(y_{UE}-y_{DS})^{0.5}$	Q_{theory}	[illegible]	Fr [illegible]	Fr [illegible]	Fr [illegible]
0.0	0.000000	0.0	-15.5	0.0	0.8	3.7	4.1	-147.5	-147.0	0.609	0.560	#NUM!	#NUM!	#NUM!	#NUM!	0.00	#NUM!
0.0	0.000000	0.0	-15.5	0.0	0.8	3.7	4.1	-147.5	-147.0	0.609	0.560	#NUM!	#NUM!	#NUM!	#NUM!	0.00	#NUM!
0.0	0.000000	0.0	-15.5	0.0	0.8	3.7	4.1	-147.5	-147.0	0.609	0.560	#NUM!	#NUM!	#NUM!	#NUM!	0.00	#NUM!
0.0	0.000000	0.0	-15.5	0.0	0.8	3.7	4.1	-147.5	-147.0	0.609	0.560	#NUM!	#NUM!	#NUM!	#NUM!	0.00	#NUM!
0.0	0.000000	0.0	-15.5	0.0	0.8	3.7	4.1	-147.5	-147.0	0.609	0.560	#NUM!	#NUM!	#NUM!	#NUM!	0.00	#NUM!

h_{man_avg}	Q_{calc}	Q [l/s]	4 m y_4	UE upstream end y_{UE}	US upstream side y_{US}	DS downstream side y_{DS}	DE downstream end y_{DE}	5 m y_6	7 m y_7	B	$B-b_p$	$v_c = 2g(y_{UE}-y_{DS})^{0.5}$	Q_{theory}	[illegible]	Fr [illegible]	Fr [illegible]	Fr [illegible]
1377.5	0.130839	130.8	213.7	256.3	216.4	193.2	195.7	217.0	-147.0	0.609	0.560	1.14	0.123534	1.06	0.69	0.81	0.65
1377.5	0.130839	130.8	235.2	268.6	238.4	222.0	221.0	246.3	-147.0	0.609	0.560	0.99	0.123097	1.06	0.60	0.66	0.56
1377.5	0.130839	130.8	254.5	279.8	260.1	244.8	245.7	270.7	-147.0	0.609	0.560	0.87	0.118948	1.10	0.53	0.57	0.49
1377.5	0.130839	130.8	273.5	298.1	280.7	268.6	268.7	288.6	-147.0	0.609	0.560	0.80	0.120415	1.09	0.48	0.49	0.44
1377.5	0.130839	130.8	292.4	314.3	300.6	290.4	290.8	305.1	-147.0	0.609	0.560	0.73	0.118749	1.10	0.43	0.44	0.41

UE upstream	US upstream	DS downstream	DE downstream

			4 m	end	side	side	end	6 m	7 m			v_c =					
h_{man_avg}	Q_{calc}	Q [l/s]	y_4	y_{UE}	y_{US}	y_{DS}	y_{DE}	y_6	y_7	B	B-b_y	$2g(y_{UE}-y_{DE})^{0.5}$	Q_{theory}	[illegible]	Fr_{UE}	Fr_{DS}	Fr_{DE}
0.0	0.000000	0.0	-15.5	0.0	0.8	3.7	4.1	-147.5	-147.0	0.609	0.560	#NUM!	#NUM!	#NUM!	#NUM!	0.00	#NUM!
0.0	0.000000	0.0	-15.5	0.0	0.8	3.7	4.1	-147.5	-147.0	0.609	0.560	#NUM!	#NUM!	#NUM!	#NUM!	0.00	#NUM!
0.0	0.000000	0.0	-15.5	0.0	0.8	3.7	4.1	-147.5	-147.0	0.609	0.560	#NUM!	#NUM!	#NUM!	#NUM!	0.00	#NUM!
0.0	0.000000	0.0	-15.5	0.0	0.8	3.7	4.1	-147.5	-147.0	0.609	0.560	#NUM!	#NUM!	#NUM!	#NUM!	0.00	#NUM!
0.0	0.000000	0.0	-15.5	0.0	0.8	3.7	4.1	-147.5	-147.0	0.609	0.560	#NUM!	#NUM!	#NUM!	#NUM!	0.00	#NUM!

				UE upstream	US upstream	DS downstream	DE downstream										
			4 m	end	side	side	end	6 m	7 m			v_c =					
h_{man_avg}	Q_{calc}	Q [l/s]	y_4	y_{UE}	y_{US}	y_{DS}	y_{DE}	y_6	y_7	B	B-b_y	$2g(y_{UE}-y_{DE})^{0.5}$	Q_{theory}	[illegible]	Fr_{UE}	Fr_{DS}	Fr_{DE}
2327.5	0.170074	170.1	254.5	305.5	254.6	221.4	227.5	276.3	-147.0	0.609	0.560	1.31	0.162462	1.05	0.69	0.86	0.61
2327.5	0.170074	170.1	270.5	309.5	272.3	249.2	251.3	274.3	-147.0	0.609	0.560	1.12	0.156015	1.09	0.63	0.72	0.62
2327.5	0.170074	170.1	293.9	325.1	301.1	277.8	279.6	303.1	-147.0	0.609	0.560	1.05	0.155160	1.10	0.56	0.61	0.53
2327.5	0.170074	170.1	312.7	345.1	319.3	301.8	303.0	327.4	-147.0	0.609	0.560	0.96	0.161771	1.05	0.51	0.54	0.48
2327.5	0.170074	170.1	333.7	336.5	341.8	327.2	328.7	349.4	-147.0	0.609	0.560	0.50	0.091291	1.86	0.46	0.48	0.43
														1.12			

MODEL PIER, bp = 32 mm_LONG_10Degrees_NORMAL Q's OK

DATA *Thursday, 10 August 2000*

Q	h_{mar_1}	h_{mar_2}	0 m	1 m	2 m	3 m	4 m	UE upstream end	US upstream side	DS downstream side	DE downstream end	6 m	7 m
bed levels			12.5	10.5	15.0	13.5	15.5					147.5	147.0
10	9.0	9.0				56.1	54.6	44.4	39.3	28.5	16.0	191.5	
30	75.5	77.0				97.9	97.1	101.0	85.8	57.5	43.0	225.0	
50	202.5	202.5				127.7	127.3	132.4	130.4	83.3	63.8	213.2	
70	390.0	391.0				154.1	150.5	160.5	149.8	108.8	87.3	230.8	
90	660.0	665.0				181.8	179.7	188.8	175.9	135.0	115.8	252.0	
110	970.0	965.0				203.9	200.5	210.1	197.9	157.0	139.8	271.5	
130	1375.0	1370.0				225.1	219.5	232.8	222.1	177.5	160.5	293.8	
150	1820.0	1800.0				247.8	240.5	251.6	242.9	193.5	177.0	315.0	
170	2360.0	2350.0				270.1	264.5	265.1	267.4	216.3	201.5	335.8	

Geometric properties:

D =	31.5 mm
L_p =	222 mm
z_A =	0.4 mm
z_B =	0.8 mm
z_C =	3.7 mm
z_D =	4.1 mm

CALCULATIONS

FLOW DEPTHS

h_{mar_avg}	Q_{calc}	Q [l/s]	Distance measured downstream within the flume: 0 m y_0	1 m y_1	2 m y_2	3 m y_3	4 m y_4	UE upstream end y_{UE}	US upstream side y_{US}	DS downstream side y_{DS}	DE downstream end y_{DE}	6 m y_6	7 m y_7	B	B-b_p	v_C = $2g(y_{US}-y_{DS})^{1/2}$	Q_{mars}	Q [l/s]	Fr_4m	Fr_DS	Fr_DE
9.0	0.010576	10.6				42.6	39.1	44.4	40.1	32.2	20.1	44.0	-147.0	0.609	0.544	0.47	0.009196	1.29	0.72	1.08	1.95
76.3	0.030783	30.8				84.4	81.6	101.0	86.6	61.2	47.1	77.5	-147.0	0.609	0.544	0.75	0.024959	1.23	0.69	1.19	1.58
202.5	0.050166	50.2				114.2	111.8	132.4	131.2	85.9	67.8	65.7	-147.0	0.609	0.544	0.97	0.045669	1.10	0.73	1.15	1.49
390.5	0.069663	69.7				140.6	135.0	160.5	149.6	112.4	91.3	83.1	-147.0	0.609	0.544	0.83	0.054466	1.28	0.74	1.08	1.32
662.5	0.090737	90.7				168.3	164.2	188.8	176.7	138.7	119.8	104.5	-147.0	0.609	0.544	0.90	0.067909	1.34	0.78	1.03	1.15
967.5	0.109653	109.7				190.4	185.0	210.1	198.7	160.7	142.8	124.0	-147.0	0.609	0.544	0.90	0.079585	1.39	0.72	1.00	1.06
1372.5	0.130602	130.6				211.6	204.0	232.8	222.0	181.2	164.6	146.3	-147.0	0.609	0.544	0.94	0.092565	1.41	0.74	0.99	1.03
1810.0	0.149680	150.0				234.3	225.0	251.0	242.8	197.2	181.1	167.5	-147.0	0.609	0.544	0.98	0.105095	1.43	0.74	1.01	1.02
2325.0	0.169983	170.0				256.6	249.0	265.1	296.0	219.9	205.6	188.3	-147.0	0.609	0.544	1.25	0.149297	1.14	0.72	0.97	0.96
																		1.29			

MODEL PIER, bp = 32 mm_LONG_10Degrees_DROWNED Q's

DATA *Thursday, 10 August 2000*

h_{mar_1}	h_{mar_2}	4 m	UE upstream end	US upstream side	DS downstream side	DE downstream end	6 m	7 m
		15.5					147.5	147.0
645.0	645.0	196.6	193.6	197.3	168.3	152.8	342.5	
645.0	645.0	212.9	205.2	211.3	187.5	170.0	358.6	
645.0	645.0	229.3	227.5	226.0	208.5	204.0	374.5	
645.0	645.0	248.1	244.4	241.8	228.8	225.0	392.0	
645.0	645.0	264.3	263.1	257.9	247.5	245.0	410.0	

h_{mar_1}	h_{mar_2}	4 m	UE upstream end	US upstream side	DS downstream side	DE downstream end	6 m	7 m
		15.5					147.5	147.0
0.0	0.0							
0.0	0.0							
0.0	0.0							
0.0	0.0							
0.0	0.0							

h_{mar_1}	h_{mar_2}	4 m	UE upstream end	US upstream side	DS downstream side	DE downstream end	6 m	7 m

		15.5					147.5	147.0
1360.0	1370.0	256.2	248.3	256.8	224.5	214.0	392.2	
1360.0	1370.0	269.4	263.3	269.9	243.8	233.4	412.2	
1360.0	1370.0	287.8	279.0	286.5	264.5	259.5	429.4	
1360.0	1370.0	304.8	298.4	302.5	284.5	279.0	449.3	
1360.0	1370.0	322.9	319.3	318.5	301.5	299.5	466.8	

h_{man_1}	h_{man_2}	4 m	UE upstream end	US upstream side	DS downstream side	DE downstream end	6 m	7 m
		15.5					147.5	147.0
0.0	0.0							
0.0	0.0							
0.0	0.0							
0.0	0.0							
0.0	0.0							

h_{man_1}	h_{man_2}	4 m	UE upstream end	US upstream side	DS downstream side	DE downstream end	6 m	7 m
		15.5					147.5	147.0
2310.0	2310.0	298.8	290.0	304.0	265.5	255.5	424.8	
2310.0	2310.0	316.8	311.3	320.5	290.3	282.0	451.5	
2310.0	2310.0	335.8	320.6	337.8	308.9	302.8	475.8	
2310.0	2310.0	353.2	350.4	354.5	331.0	324.9	495.4	
2310.0	2310.0	370.3	368.0	370.4	348.3	343.6	516.5	

CALCULATIONS

FLOW DEPTHS

h_{man_avg}	Q_{calc}	Q [l/s]	4 m y_4	UE upstream end y_{UE}	US upstream side y_{US}	DS downstream side y_{DS}	DE downstream end y_{DE}	6 m y_6	7 m y_7	B	$B-b_y$	$v_c = 2g(y_{UE}-y_{DS})^{0.5}$	Q_{theory}	[illegible]	$Fr_{\_an}$	$Fr_{\_pe}$	$Fr_{\_an}$
645.0	0.089531	89.5	181.3	193.8	198.1	171.9	156.8	195.0	-147.0	0.609	0.544	0.76	0.071073	1.26	0.61	0.66	0.55
645.0	0.089531	89.5	197.4	205.2	212.1	191.2	183.1	211.1	-147.0	0.609	0.544	0.69	0.071639	1.25	0.54	0.56	0.48
645.0	0.089531	89.5	213.8	227.5	226.8	212.5	208.1	227.4	-147.0	0.609	0.544	0.59	0.067873	1.32	0.47	0.48	0.43
645.0	0.089531	89.5	232.6	244.4	242.6	232.4	229.1	244.5	-147.0	0.609	0.544	0.51	0.064924	1.38	0.42	0.42	0.39
645.0	0.089531	89.5	248.8	263.1	258.7	251.2	249.1	262.5	-147.0	0.609	0.544	0.46	0.062939	1.42	0.38	0.37	0.35

h_{man_avg}	Q_{calc}	Q [l/s]	4 m y_4	UE upstream end y_{UE}	US upstream side y_{US}	DS downstream side y_{DS}	DE downstream end y_{DE}	6 m y_6	7 m y_7	B	$B-b_y$	$v_c = 2g(y_{UE}-y_{DS})^{0.5}$	Q_{theory}	[illegible]	$Fr_{\_an}$	$Fr_{\_pe}$	$Fr_{\_an}$
0.0	0.000000	0.0	-15.5	0.0	0.8	3.7	4.1	-147.5	-147.0	0.609	0.544	#NUM!	#NUM!	#NUM!	#NUM!	0.00	#NUM!
0.0	0.000000	0.0	-15.5	0.0	0.8	3.7	4.1	-147.5	-147.0	0.609	0.544	#NUM!	#NUM!	#NUM!	#NUM!	0.00	#NUM!
0.0	0.000000	0.0	-15.5	0.0	0.8	3.7	4.1	-147.5	-147.0	0.609	0.544	#NUM!	#NUM!	#NUM!	#NUM!	0.00	#NUM!
0.0	0.000000	0.0	-15.5	0.0	0.8	3.7	4.1	-147.5	-147.0	0.609	0.544	#NUM!	#NUM!	#NUM!	#NUM!	0.00	#NUM!
0.0	0.000000	0.0	-15.5	0.0	0.8	3.7	4.1	-147.5	-147.0	0.609	0.544	#NUM!	#NUM!	#NUM!	#NUM!	0.00	#NUM!

h_{man_avg}	Q_{calc}	Q [l/s]	4 m y_4	UE upstream end y_{UE}	US upstream side y_{US}	DS downstream side y_{DS}	DE downstream end y_{DE}	6 m y_6	7 m y_7	B	$B-b_y$	$v_c = 2g(y_{UE}-y_{DS})^{0.5}$	Q_{theory}	[illegible]	$Fr_{\_an}$	$Fr_{\_pe}$	$Fr_{\_an}$
1365.0	0.130244	130.2	240.7	248.3	257.6	226.2	218.1	244.7	-147.0	0.609	0.544	0.80	0.099400	1.31	0.58	0.63	0.56
1365.0	0.130244	130.2	253.9	263.3	270.7	247.4	237.5	264.7	-147.0	0.609	0.544	0.72	0.097166	1.34	0.53	0.55	0.50
1365.0	0.130244	130.2	272.3	279.0	287.3	268.2	263.6	281.9	-147.0	0.609	0.544	0.66	0.096794	1.35	0.48	0.49	0.46
1365.0	0.130244	130.2	289.3	298.4	303.3	288.2	283.1	301.8	-147.0	0.609	0.544	0.60	0.094289	1.38	0.44	0.44	0.41
1365.0	0.130244	130.2	307.4	319.3	319.3	305.2	303.6	319.3	-147.0	0.609	0.544	0.56	0.097107	1.34	0.40	0.41	0.38

UE	US	DS	DE
upstream	upstream	downstream	downstream

h_{man_avg}	Q_{ain}	Q [l/s]	4 m y_4	end y_{UE}	side y_{US}	side y_{DS}	end y_{DE}	6 m y_6	7 m y_7	B	$B-b_s$	$v_c = 2g(y_{US}-y_{DS})^{0.5}$	Q_{theory}	[illegible]	$Fr_{\_4m}$	$Fr_{\_DS}$	$Fr_{\_6m}$
0.0	0.000000	0.0	-15.5	0.0	0.8	3.7	4.1	-147.5	-147.0	0.609	0.544	#NUM!	#NUM!	#NUM!	#NUM!	0.00	#NUM!
0.0	0.000000	0.0	-15.5	0.0	0.8	3.7	4.1	-147.5	-147.0	0.609	0.544	#NUM!	#NUM!	#NUM!	#NUM!	0.00	#NUM!
0.0	0.000000	0.0	-15.5	0.0	0.8	3.7	4.1	-147.5	-147.0	0.609	0.544	#NUM!	#NUM!	#NUM!	#NUM!	0.00	#NUM!
0.0	0.000000	0.0	-15.5	0.0	0.8	3.7	4.1	-147.5	-147.0	0.609	0.544	#NUM!	#NUM!	#NUM!	#NUM!	0.00	#NUM!
0.0	0.000000	0.0	-15.5	0.0	0.8	3.7	4.1	-147.5	-147.0	0.609	0.544	#NUM!	#NUM!	#NUM!	#NUM!	0.00	#NUM!

h_{man_avg}	Q_{calc}	Q [l/s]	4 m y_4	UE upstream end y_{UE}	US upstream side y_{US}	DS downstream side y_{DS}	DE downstream end y_{DE}	6 m y_6	7 m y_7	B	$B-b_s$	$v_c = 2g(y_{US}-y_{DS})^{0.5}$	Q_{theory}	[illegible]	$Fr_{\_4m}$	$Fr_{\_DS}$	$Fr_{\_6m}$
2310.0	0.169433	169.4	283.3	290.0	304.8	270.2	259.6	277.3	-147.0	0.609	0.544	0.86	0.126707	1.34	0.59	0.63	0.61
2310.0	0.169433	169.4	301.3	311.3	321.3	293.9	286.1	304.0	-147.0	0.609	0.544	0.78	0.124067	1.37	0.54	0.56	0.53
2310.0	0.169433	169.4	320.3	329.6	338.6	312.5	306.8	328.3	-147.0	0.609	0.544	0.76	0.129050	1.31	0.49	0.51	0.47
2310.0	0.169433	169.4	337.7	350.4	355.3	334.7	329.0	347.9	-147.0	0.609	0.544	0.69	0.124770	1.36	0.45	0.46	0.43
2310.0	0.169433	169.4	354.8	368.0	371.2	351.9	347.7	369.0	-147.0	0.609	0.544	0.67	0.127379	1.33	0.42	0.43	0.40
														1.34			

MODEL PIER, bp = 32 mm_LONG_15Degrees_NORMAL Q's OK

DATA: *Tuesday, 8 August 2000*

Q	h_{man_1}	h_{man_2}	0 m	1 m	2 m	3 m	4 m	UE upstream end	US upstream side	DS downstream side	DE downstream end	6 m	7 m
bed levels			*12.5*	*10.5*	*15.0*	*13.8*	*15.5*					*147.5*	*147.0*
10	11.0	11.0				59.7	59.2	57.6	47.3	34.8	16.0	205.8	
30	68.5	68.5				98.2	97.8	93.4	90.8	61.3	38.3	205.2	
50	200.0	200.0				133.5	132.5	122.3	130.8	90.0	64.5	211.5	
70	405.0	410.0				163.4	163.2	141.5	166.0	117.8	89.8	231.2	
90	650.0	645.0				189.1	188.5	162.1	193.8	142.3	114.8	246.8	
110	975.0	970.0				213.6	213.2	178.0	217.8	167.0	140.5	268.9	
130	1360.0	1360.0				237.0	234.2	190.5	244.0	188.8	163.8	289.5	
150	1840.0	1840.0				258.2	255.9	204.3	271.5	211.8	187.5	312.2	
170	2350.0	2400.0				282.5	276.2	217.1	296.5	232.8	208.0	335.6	

Geometric properties:

D =	31.5 mm
L_p =	222 mm
z_a =	0.4 mm
z_b =	0.8 mm
z_c =	3.7 mm
z_d =	4.1 mm

CALCULATIONS:

FLOW DEPTHS

Distance measured downstream within the flume

h_{man_avg}	Q_{corr}	Q [l/s]	0 m y_0	1 m y_1	2 m y_2	3 m y_3	4 m y_4	UE upstream end y_{UE}	US upstream side y_{US}	DS downstream side y_{DS}	DE downstream end y_{DE}	6 m y_6	7 m y_7	B	B-b_p	x_c = $2g(y_{UE}-y_{DE})^{2/3}$	Q_{theory}	y_4/y_c	Fr_4m	Fr_DS	Fr_DE
11.0	0.011092	11.7				46.2	43.7	57.6	45.1	38.4	20.1	58.3	-147.0	0.639	0.528	0.50	0.010213	1.14	0.67	0.64	2.15
68.5	0.029177	29.2				84.7	82.3	93.4	91.6	64.9	42.3	57.7	-147.0	0.639	0.528	0.77	0.026254	1.11	0.65	1.07	1.76
200.0	0.069855	69.6				120.0	117.0	122.3	131.6	93.7	68.6	64.0	-147.0	0.639	0.528	0.90	0.044436	1.12	0.65	1.05	1.45
407.5	0.071163	71.2				149.9	147.7	141.5	166.8	121.4	93.8	83.7	-147.0	0.639	0.528	0.95	0.062628	1.14	0.66	1.02	1.30
647.5	0.099704	99.7				175.6	173.0	162.1	194.6	145.9	118.8	99.3	-147.0	0.639	0.528	1.01	0.077738	1.15	0.65	0.97	1.15
972.5	0.109935	109.9				200.1	197.7	178.0	218.6	170.7	144.6	121.4	-147.0	0.639	0.528	1.00	0.080266	1.22	0.66	0.94	1.05
1360.0	0.130006	130.0				223.5	218.7	190.5	244.8	192.4	167.8	142.0	-147.0	0.639	0.528	1.05	0.106150	1.22	0.67	0.93	0.99
1840.0	0.151217	151.2				244.7	240.4	204.3	272.3	215.4	191.6	164.7	-147.0	0.639	0.528	1.09	0.123547	1.22	0.67	0.92	0.95
2375.0	0.171803	171.8				269.0	260.7	217.1	296.0	236.4	212.1	188.1	-147.0	0.639	0.528	1.11	0.138596	1.24	0.68	0.90	0.92
																		1.17			

MODEL PIER, bp = 32 mm_LONG_15Degrees_DROWNED Q's

DATA: *Tuesday, 8 August 2000*

h_{man_1}	h_{man_2}	4 m	UE upstream end	US upstream side	DS downstream side	DE downstream end	6 m	7 m
		15.5					*147.5*	*147.0*
650.0	645.0	205.8	173.0	208.5	172.3	154.8	343.5	343.6
650.0	645.0	222.9	202.0	221.8	196.0	186.3	365.0	363.0
650.0	645.0	240.8	224.8	237.5	216.8	210.0	382.5	382.1
650.0	645.0	257.1	245.3	253.5	236.3	230.3	399.8	398.9
650.0	645.0	274.5	262.6	269.3	253.5	249.5	417.8	418.0

h_{man_1}	h_{man_2}	4 m	UE upstream end	US upstream side	DS downstream side	DE downstream end	6 m	7 m
		15.5					*147.5*	*147.0*
0.0	0.0							
0.0	0.0							
0.0	0.0							
0.0	0.0							
0.0	0.0							

h_{man_1}	h_{man_2}	4 m	UE upstream end	US upstream side	DS downstream side	DE downstream end	6 m	7 m

		15.5					147.5	147.0
1385.0	1375.0	264.9	218.1	270.8	229.8	215.3	395.6	397.2
1385.0	1375.0	277.2	240.1	282.8	247.0	234.5	414.1	411.5
1385.0	1375.0	295.2	274.0	296.5	266.3	255.5	433.4	433.0
1385.0	1375.0	312.9	297.8	312.3	284.3	276.0	452.1	451.5
1385.0	1375.0	329.5	320.4	326.5	302.5	293.5	471.0	471.3

h_{man_1}	h_{man_2}	4 m	UE upstream end	US upstream side	DS downstream side	DE downstream end	6 m	7 m
		15.5					147.5	147.0
0.0	0.0							
0.0	0.0							
0.0	0.0							
0.0	0.0							
0.0	0.0							

h_{man_1}	h_{man_2}	4 m	UE upstream end	US upstream side	DS downstream side	DE downstream end	6 m	7 m
		15.5					147.5	147.0
2320.0	2330.0	309.8	254.3	320.3	272.5	255.0	430.6	441.0
2320.0	2330.0	324.3	279.3	334.0	289.8	273.5	453.9	461.4
2320.0	2330.0	342.1	312.3	348.8	309.0	294.5	477.8	475.8
2320.0	2330.0	359.4	338.8	364.3	328.8	314.5	498.0	500.0
2320.0	2330.0	378.1	363.9	380.0	345.5	336.5	519.0	516.8

CALCULATIONS:

FLOW DEPTHS

h_{man_avg}	Q_{calc}	Q [l/s]	4 m y_4	UE upstream end y_{UE}	US upstream side y_{US}	DS downstream side y_{DS}	DE downstream end y_{DE}	6 m y_6	7 m y_7	B	$B-b_0$	$v_c = 2g(y_{UE}-y_{DE})^{0.5}$	Q_{theory}	[illegible]	Fr_{um}	Fr_{us}	Fr_{dm}
647.5	0.089704	89.7	190.3	173.0	209.3	175.9	158.8	196.1	196.6	0.609	0.528	0.85	0.078771	1.14	0.57	0.64	0.54
647.5	0.089704	89.7	207.4	202.0	222.6	199.7	190.3	217.5	216.0	0.609	0.528	0.72	0.075538	1.19	0.50	0.53	0.46
647.5	0.089704	89.7	225.3	224.8	238.3	220.4	214.1	235.0	235.1	0.609	0.528	0.64	0.075008	1.20	0.44	0.45	0.41
647.5	0.089704	89.7	241.6	245.3	254.3	239.9	234.3	252.3	251.9	0.609	0.528	0.59	0.074598	1.20	0.40	0.40	0.37
647.5	0.089704	89.7	259.0	262.6	270.1	257.2	253.6	270.3	271.0	0.609	0.528	0.56	0.076497	1.17	0.36	0.36	0.33

h_{man_avg}	Q_{calc}	Q [l/s]	4 m y_4	UE upstream end y_{UE}	US upstream side y_{US}	DS downstream side y_{DS}	DE downstream end y_{DE}	6 m y_6	7 m y_7	B	$B-b_0$	$v_c = 2g(y_{UE}-y_{DE})^{0.5}$	Q_{theory}	[illegible]	Fr_{um}	Fr_{us}	Fr_{dm}
0.0	0.000000	0.0	-15.5	0.0	0.8	3.7	4.1	-147.5	-147.0	0.609	0.578	#NUM!	#NUM!	#NUM!	#NUM!	0.00	#NUM!
0.0	0.000000	0.0	-15.5	0.0	0.8	3.7	4.1	-147.5	-147.0	0.609	0.578	#NUM!	#NUM!	#NUM!	#NUM!	0.00	#NUM!
0.0	0.000000	0.0	-15.5	0.0	0.8	3.7	4.1	-147.5	-147.0	0.609	0.578	#NUM!	#NUM!	#NUM!	#NUM!	0.00	#NUM!
0.0	0.000000	0.0	-15.5	0.0	0.8	3.7	4.1	-147.5	-147.0	0.609	0.578	#NUM!	#NUM!	#NUM!	#NUM!	0.00	#NUM!
0.0	0.000000	0.0	-15.5	0.0	0.8	3.7	4.1	-147.5	-147.0	0.609	0.578	#NUM!	#NUM!	#NUM!	#NUM!	0.00	#NUM!

h_{man_avg}	Q_{calc}	Q [l/s]	4 m y_4	UE upstream end y_{UE}	US upstream side y_{US}	DS downstream side y_{DS}	DE downstream end y_{DE}	6 m y_6	7 m y_7	B	$B-b_0$	$v_c = 2g(y_{UE}-y_{DE})^{0.5}$	Q_{theory}	[illegible]	Fr_{um}	Fr_{us}	Fr_{dm}
1380.0	0.130958	131.0	249.4	218.1	271.6	233.4	219.3	248.1	250.2	0.609	0.528	0.90	0.111080	1.18	0.55	0.61	0.59
1380.0	0.130958	131.0	261.7	243.1	283.6	250.7	238.6	266.6	264.5	0.609	0.528	0.84	0.111478	1.17	0.51	0.55	0.50
1380.0	0.130958	131.0	279.7	274.0	297.3	269.9	259.6	285.9	286.0	0.609	0.528	0.78	0.110542	1.18	0.46	0.49	0.45
1380.0	0.130958	131.0	297.4	297.8	313.1	287.9	280.1	304.6	304.5	0.609	0.528	0.75	0.113510	1.15	0.42	0.44	0.41
1380.0	0.130958	131.0	314.0	320.4	327.3	306.2	297.6	323.5	324.3	0.609	0.528	0.69	0.111806	1.17	0.39	0.41	0.37

UE	US	DS	DE
upstream	upstream	downstream	downstream

			4 m	end	side	side	end	6 m	7 m			$v_c =$					
h_{man_avg}	Q_{calc}	Q [l/s]	y_4	y_{UE}	y_{US}	y_{DS}	y_{DE}	y_6	y_7	B	$B\text{-}b_2$	$2g(y_{UE}-y_{DS})^{0.5}$	Q_{theory}	[illegible]	$Fr_{\_4m}$	$Fr_{\_DS}$	$Fr_{\_6m}$
0.0	0.000000	0.0	-15.5	0.0	0.8	3.7	4.1	-147.5	-147.0	0.609	0.528	#NUM!	#NUM!	#NUM!	#NUM!	0.00	#NUM!
0.0	0.000000	0.0	-15.5	0.0	0.8	3.7	4.1	-147.5	-147.0	0.609	0.528	#NUM!	#NUM!	#NUM!	#NUM!	0.00	#NUM!
0.0	0.000000	0.0	-15.5	0.0	0.8	3.7	4.1	-147.5	-147.0	0.609	0.528	#NUM!	#NUM!	#NUM!	#NUM!	0.00	#NUM!
0.0	0.000000	0.0	-15.5	0.0	0.8	3.7	4.1	-147.5	-147.0	0.609	0.528	#NUM!	#NUM!	#NUM!	#NUM!	0.00	#NUM!
0.0	0.000000	0.0	-15.5	0.0	0.8	3.7	4.1	-147.5	-147.0	0.609	0.528	#NUM!	#NUM!	#NUM!	#NUM!	0.00	#NUM!

				UE	US	DS	DE										
				upstream	upstream	downstream	downstream										
			4 m	end	side	side	end	6 m	7 m			$v_c =$					
h_{man_avg}	Q_{calc}	Q [l/s]	y_4	y_{UE}	y_{US}	y_{DS}	y_{DE}	y_6	y_7	B	$B\text{-}b_2$	$2g(y_{UE}-y_{DS})^{0.5}$	Q_{theory}	[illegible]	$Fr_{\_4m}$	$Fr_{\_DS}$	$Fr_{\_6m}$
2325.0	0.169983	170.0	294.3	254.3	321.1	276.2	258.1	289.1	294.0	0.609	0.528	0.97	0.141726	1.20	0.56	0.61	0.57
2325.0	0.169983	170.0	308.8	279.3	334.8	293.4	277.6	306.4	314.4	0.609	0.528	0.94	0.145007	1.17	0.52	0.56	0.53
2325.0	0.169983	170.0	326.6	312.3	349.6	312.7	298.6	330.3	328.8	0.609	0.528	0.89	0.146536	1.16	0.48	0.51	0.47
2325.0	0.169983	170.0	343.9	338.8	365.1	332.4	318.6	350.5	353.0	0.609	0.528	0.84	0.147325	1.15	0.44	0.47	0.43
2325.0	0.169983	170.0	362.6	363.9	380.8	349.2	340.6	371.5	369.8	0.609	0.528	0.83	0.152581	1.11	0.41	0.43	0.39
														1.17			

APPENDIX C

FIELD TESTS

C1. INTRODUCTION

Following on the promising results of laboratory studies on discharge measurements in terms of pressure differences at bridge piers, it was decided to perform full-scale field tests on a real bridge during the year 2000. These tests were undertaken primarily by Mr GC Cloete, as a final year civil engineering student at Stellenbosch University, who also is and was an employee of the Department of Water Affairs and Forestry (DWAF). The tests were made possible by the generous support received from the provision of measuring instruments and manpower. This test contains an abbreviated summary of the contents of Mr Cloete's unpublished final year thesis report titled "Hoogvloeimeting in Riviere met behulp van Drukmeting by Brugpylers.

C2. BRIDGE SELECTION

In order to be able to perform prototype tests, a suitable bridge had to be identified. The following requirements were set:

- Flow velocities at the bridge had to be greater than 2 m/s in order to generate large enough pressure differences for accurate measurement.
- A pier was to be selected within the main river channel where the highest flow velocities occur.
- For comparing with model results a pier with parallel sides and rounded ends, both upstream and downstream was preferable.
- Uniform flow conditions should prevail both upstream and downstream of the bridge with flow lines parallel to the pier direction.
- High flow discharges, which were independently determined, were required for comparison.

- A number of bridges in the proximity of Worcester were considered and the "White Bridge" across the Breede River near Ceres was eventually selected as being the most suitable for testing purposes. This bridge was far from ideal, it was believed that if the approach could work here, it should be applicable on a large number of other bridges.

C3. PRESSURE DIFFERENCES AND DISCHARGE CALCULATIONS

STS pressure gauges, which are presently being used by DWAF, were installed at 4 positions on a pier of the "White Bridge"

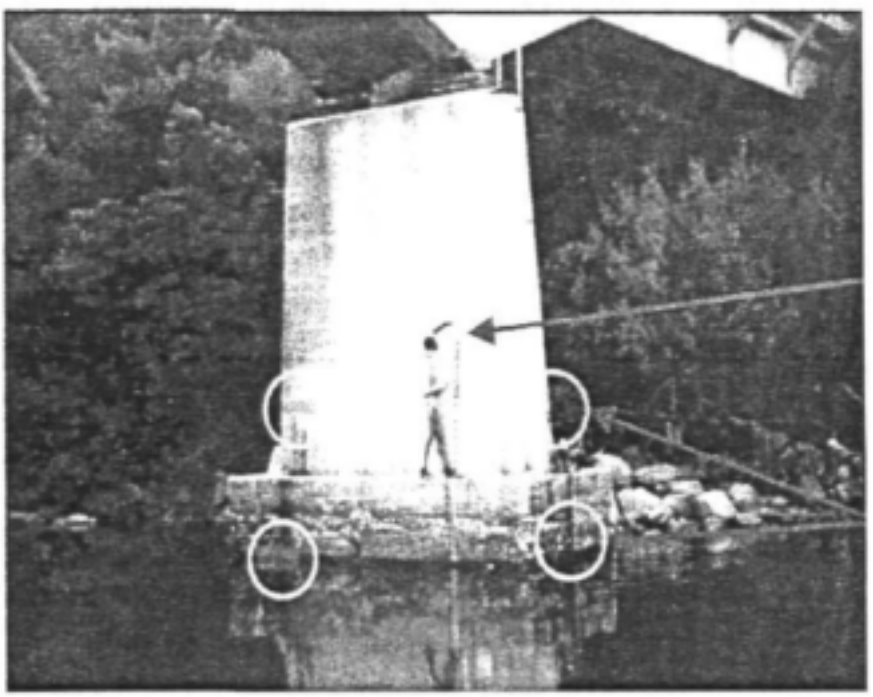

***Photo 3.1**: White Bridge : Positions of pressure gauges*

The pressure differences, which were recorded, were translated into approach velocities by means of the Pitot principle. However allowance had to be made for the particular shape of the pier. This was done by building a model of the pier and determining a correction factor (C_D) which represents the ratio:

$$\frac{\textit{True Discharge}}{\textit{Apparent Discharge}}$$

With the apparent discharges being calculated from the pressure difference without allowance for the particular pier shape. For non-drowned flow conditions, the value of C_D varied from about 0,90 to about 0,98, indicating that even without a correction factor, the discharge may be calculated with an accuracy of at least 10%.

In the case of drowned flow conditions, the C_D value varied more, from about 0,75 to about 0,93. The steady pattern and the limited variability found in C_D values indicate that once these values are determined it will be possible to determine oncoming flow velocities at piers with a high degree of accuracy.

Velocities do however vary across river sections and velocities measured at individual piers therefore have to be converted into local values for the section as a whole for the calculation of discharges.

In the case of the "White Bridge" stream flow measurements had been undertaken which reflected the variations in velocity across the section. The velocity variations were also analysed in terms of techniques used in backwater calculations. Fair agreement was obtained.

C4. FINAL RESULTS

Peak discharges which were measured at the gauging station just upstream of the "White Bridge" were compared with values calculated from pressure differences measured at the pier and pier discharge coefficients determined in the laboratory.

The following discharges (m^3/s) were obtained:

Date (2000)	Lower Gauges	Upper Gauges	DWAF Gauging Station
14-07	57	-	43,3
15-07	62	-	47,4
18-07	208	207	202

02-08	56	-	42
31-08	65	-	54
02-09	119	128	118
02-09	204	215	202
03-09	202	213	200
03-09	174	181	170

The results are very encouraging. There is good agreement between the discharges measured at the gauging station and those calculated from pressure differences. What is also important is that the results for the two pairs of pressure gauges agree so well given the complicated shape of the bridge pier.

C5. CONCLUSIONS AND RECOMMENDATIONS

The combined results of model studies and field tests prove that differences in pressures measured against bridge piers can be used to measure discharges in rivers. Given the limited costs involved, even if laboratory calibration is involved, as opposed to the high costs of measuring weirs capable of measuring high flows, this method deserves serious consideration for application and further development.

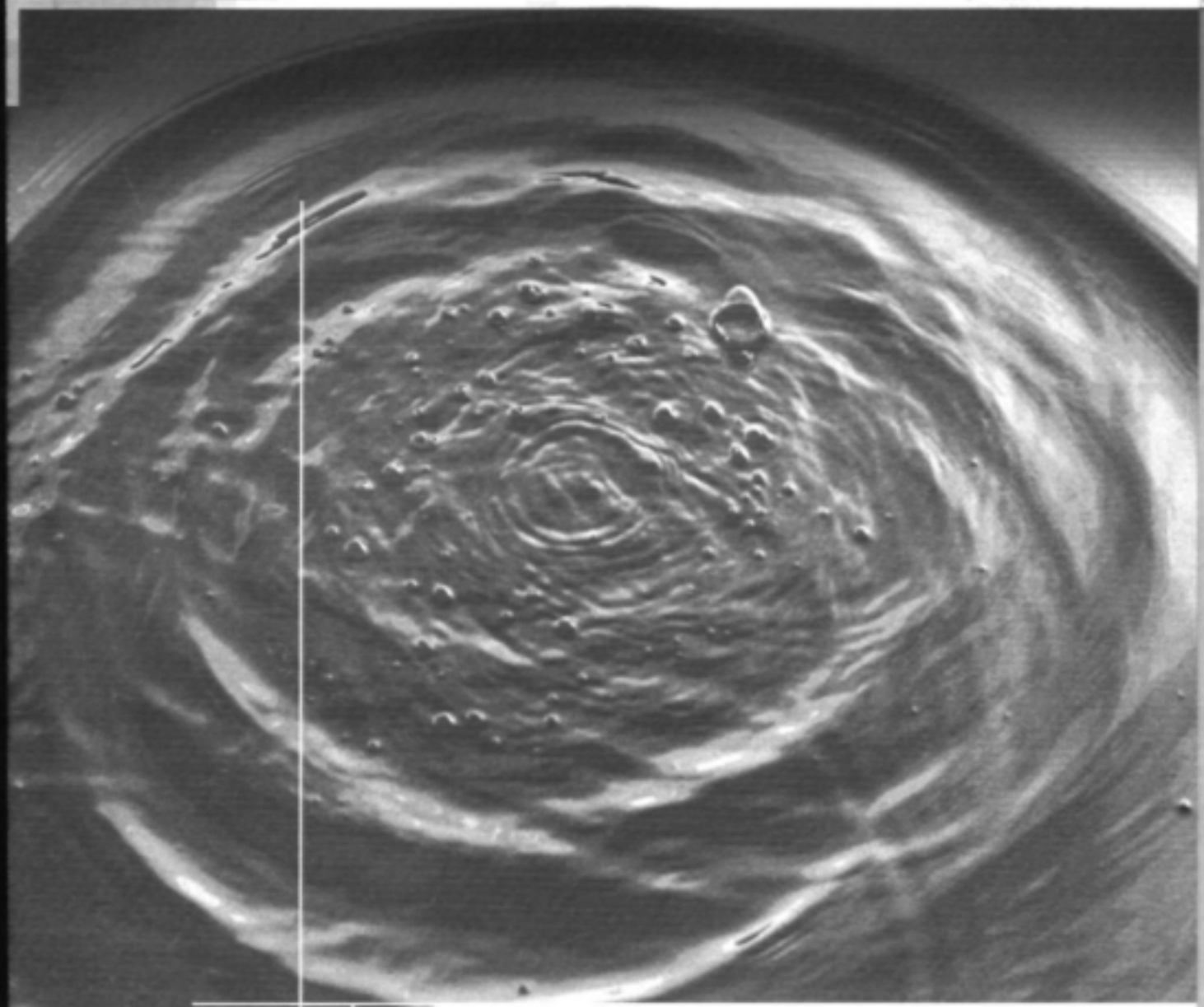

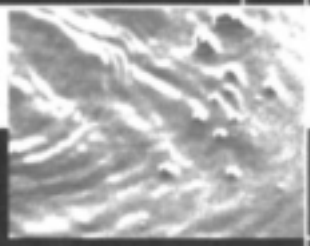

Water Research Commission
PO Box 824, Pretoria, 0001, South Africa
Tel: +27 12 330 0340, Fax: +27 12 331 2565
Web: http://www.wrc.org.za

1868456655X